Severe Acute Respiratory Syndrome Coronavirus 2:

Susceptibility, Immunoprophylaxis, and Variant Characterization in Animal Models

Von Lorenz Ulrich

Inaugural-Dissertation zur Erlangung der Doktorwürde der Tierärztlichen Fakultät der

Ludwig-Maximilians-Universität München

Severe Acute Respiratory Syndrome Coronavirus 2:

Susceptibility, Immunoprophylaxis, and Variant Characterization in Animal Models

Von Lorenz Ulrich

aus Tübingen

München 2022

Aus dem Veterinärwissenschaftlichen Department der Tierärztlichen Fakultät der

Ludwig-Maximilians-Universität München

Lehrstuhl für Virologie

Arbeit angefertigt unter der Leitung von Univ.-Prof. Dr. Dr. h.c. Gerd Sutter

Angefertigt am Institut für Virusdiagnostik

des Friedrich-Loeffler-Instituts,

Bundesforschungsinstitut für Tiergesundheit, Insel Riems

Mentor: Prof. Dr. Martin Beer

Dekan:	Univ.-Prof. Dr. Reinhard K. Straubinger, Ph.D.
Berichterstatter:	Univ.-Prof. Dr. Dr. h.c. Gerd Sutter
Korreferent/en:	Priv.-Doz. Dr. Roswitha Dorsch
	Univ.-Prof. Dr. Markus Meißner
	Univ.-Prof. Dr. Heidrun Potschka
	Univ.-Prof. Dr. Michael H. Erhard

Tag der Promotion: 12. Februar 2022

Meiner lieben Familie.

Die vorliegende Arbeit wurde gemäß § 6 Abs. 2 der Promotionsordnung für die Tierärztliche Fakultät der Ludwig-Maximilians-Universität München in kumulativer Form verfasst.

Die folgenden wissenschaftlichen Arbeiten sind in dieser Dissertationsschrift enthalten:

1. Review article: Michelitsch A, Wernike K, Ulrich L, Mettenleiter TC, Beer M: **„SARS-CoV-2 in animals: From potential hosts to animal models."**, erschienen in Advances in Virus Research, 2021, online verfügbar unter doi: 10.1016/bs.aivir.2021.03.004.

2. Publication I: Ulrich L, Wernike K, Hoffmann D, Mettenleiter TC, Beer M: **„Experimental Infection of Cattle with SARS-CoV-2."**, erschienen in Emerging Infectious Diseases, 2020, online verfügbar unter doi: 10.3201/eid2612.203799.

3. Publication II: Ulrich L, Michelitsch A, Halwe N, Wernike K, Hoffmann D, Beer M: **„Experimental SARS-CoV-2 Infection of Bank Voles."**, erschienen in Emerging Infectious Diseases, 2021, online verfügbar unter doi: 10.3201/eid2704.204945.

4. Publication III: Zhou B, Thao TTN, Hoffmann D, Taddeo A, Ebert N, Labroussaa F, Pohlmann A, King J, Steiner S, Kelly JN, Portmann J, Halwe NJ, Ulrich L, Trüeb BS, Fan X, Hoffmann B, Wang L, Thomann L, Lin X, Stalder H, Pozzi B, de Brot S, Jiang N, Cui D, Hossain J, Wilson MM, Keller MW, Stark TJ, Barnes JR, Dijkman R, Jores J, Benarafa C, Wentworth DE, Thiel V, Beer M: **„SARS-CoV-2 spike D614G change enhances replication and transmission."**, erschienen in Nature, 2021, online verfügbar unter doi: 10.1038/s41586-021-03361-1.

5. Publication IV: <u>Ulrich L</u>, Halwe N, Taddeo A, Ebert N, Schön J, Devisme C, Trüeb B, Hoffmann B, Wider M, Fan X, Bekliz M, Essaidi-Laziosi M, Schmidt M, Niemeyer D, Corman V, Kraft A, Godel A, Laloli L, Kelly J, Calderon B, Breithaupt A, Wylezich C, Veiga I, Gultom M, Osman S, Zhou B, Adea K, Meyer B, Eberhardt C, Thomann L, Gsell M, Labroussaa F, Jores J, Summerfield A, Drosten C, Eckerle I, Wentworth D, Dijkman R, Hoffmann D, Thiel V, Beer M, Benarafa C: **„Enhanced fitness of SARS-CoV-2 variant of concern Alpha but not Beta.“**, erschienen in Nature, 2021, online verfügbar unter doi: 10.1038/s41586-021-04342-0.

6. Publication V: Hoffmann D, Corleis B, Rauch S, Roth N, Mühe J, Halwe N, <u>Ulrich L</u>, Fricke C, Schön J, Kraft A, Breithaupt A, Wernike K, Michelitsch A, Sick F, Wylezich C, Hoffmann B, Thran M, Thess A, Mueller S, Mettenleiter TC, Petsch B, Dorhoi A, Beer M: **„CVnCoV and CV2CoV protect human ACE2 transgenic mice from ancestral B BavPat1 and emerging B.1.351 SARS-CoV-2.“**, erschienen in Nature Communications, 2021, online verfügbar unter doi: 10.1038/s41467-021-24339-7.

Weitere wissenschaftliche Arbeiten, die nicht Teil dieser Dissertationsschrift sind:

Koethe S, <u>Ulrich L</u>, Ulrich R, Amler S, Graaf A, Harder TC, Grund C, Mettenleiter TC, Conraths FJ, Beer M, Globig A: **„Modulation of lethal HPAIV H5N8 clade 2.3.4.4B infection in AIV pre-exposed mallards.“**, erschienen in Emerging Microbes & Infections, 2020, online verfügbar unter doi: 10.1080/22221751.2020.1713706.

Wernike K, Aebischer A, Michelitsch A, Hoffmann D, Freuling C, Balkema-Buschmann A, Graaf A, Müller T, Osterrieder N, Rissmann M, Rubbenstroth D, Schön J, Schulz C, Trimpert J, <u>Ulrich L</u>, Volz A, Mettenleiter T, Beer M: **„Multi-species ELISA for the detection of antibodies against SARS-CoV-2 in animals.“**, erschienen in Transboundary and Emerging Diseases, 2021, online verfügbar unter doi: 10.1111/tbed.13926.

CONTENTS

CHAPTER I: INTRODUCTION

I.   INTRODUCTION

Evolution of live has always been accompanied by pandemics affecting susceptible populations more or less dramatically (Morens et al., 2020). Just within the last century, mankind and animal populations have faced numerous (re-)emerging pandemics with a viral etiology: Influenza A viruses (1918, 1957, 1968, 2009), human immunodeficiency virus (1981-ongoing), African swine fever virus genotype II in Europe (2007-ongoing), and coronaviruses (2002, 2012, 2019-ongoing) are among those with highest fatality numbers (Woolhouse and Gaunt, 2007, Bean et al., 2013). The latter being the youngest in a long history of pandemics, but certainly one of the most sweeping: only within months following its first description a novel coronavirus, which was named severe acute respiratory syndrome coronavirus-2 (SARS-CoV-2), has caused a pandemic with worldwide consequences (Dong et al., 2020a, Pak et al., 2020).

Humans are affected at varying degrees by the SARS-CoV-2-provoked coronavirus disease 2019 (COVID-19); symptoms range from asymptomatic to mild up to severe disease progression, which may even lead to fatal outcomes in some cases or cause long-term consequences (Gandhi et al., 2020, Zhu et al., 2020, Carfi et al., 2020, Nalbandian et al., 2021, Jin et al., 2020). While disease pathogenesis in humans and its consequences for clinical outcomes are still just about to be understood, it was already early suspected, that the emerging SARS-CoV-2 originates from an animal host and found its way into human population via either a putative intermediate host or was directly transmitted to an index patient (Zhang and Holmes, 2020, WHO, 2020c, Mallapaty, 2021a, Andersen et al., 2020).

Cross-linking between geographic regions and ethnicities living far apart has contributed to the rapid pan-global spread of SARS-CoV-2 (Bontempi and Coccia, 2021). Contemporaneously the habitat of wildlife and humans coalesce, which enlarges the wildlife-animal-human interface boosting the chance for viruses, e.g. SARS-CoV-2, to find their way into a new species (Jones et al., 2013).

WHO, FAO, and OIE have introduced the concept of One Health, to unite human health, animal health, and health of the ecosystems in one view (OIE, 2021). They also accept, that these fields are closely entangled and account for each other.

Under these assumptions, the distinct contribution of animals in the current COVID-19 pandemic needs to be illuminated on one hand, but also their special suitability to serve as animal models in research.

In this light, the animal studies presented in this work contribute to an improved understanding of SARS-CoV-2 by bridging from (i) analyzing and identifying potential animal hosts for SARS-CoV-2, to (ii) characterizing significant VOCs, and (iii) vaccine-precursor testing in an animal model.

CHAPTER II: REVIEW OF LITERATURE

II. REVIEW OF LITERATURE

Coronaviridae is a family within the order *Nidovirales* consisting of two subfamilies: *orthocoronavirinae* and *letovirinae*. Within the *orthocoronavirinae* four genera are defined: *alpha-, beta-, delta-,* and *gammacoronavirus*. *Orthocoronavirinae* from all four distinct genera are associated with acute to chronic disease in a broad variety of *Vertebralia* (ICTV, 2021). Virus spread between hosts is either due to direct or indirect transmission, e.g. by contaminated matter or environment (WHO, 2020a, Pusterla et al., 2016, Saif, 2010, Addie et al., 2003). Disease severity is ranging from subclinical to acute and fatal disease, and can vary depending on host factors or the virus itself (Nikolai et al., 2020, Su et al., 2016). However, coronavirus outbreaks have regularly been associated with quite serious epidemics causing grievous losses among affected animals and humans (Fan et al., 2019).

Although only the genera *alpha-* and *betacoronavirus* bear yet known species, that are pathogenic for humans, relevant vertebrate-harming species are found among all genera; e.g. *alphacoronavirus* with *feline infectious peritonitis virus* and various porcine coronaviruses e.g. *porcine epidemic diarrhea virus* (Jung et al., 2020, Tekes and Thiel, 2016, Saif et al., 1994), *betacoronavirus* with *bovine coronavirus* (Clark, 1993, Vlasova and Saif, 2021), *gammacoronavirus* with the *infectious bronchitis avian coronavirus* of mainly gallinaceous birds (Jackwood, 2012, Cavanagh, 2007, Fadhilah et al., 2020), and the recently described *deltacoronavirus* HKU-15, a porcine coronavirus (Woo et al., 2012, Wang et al., 2014). Despite seven pathogenic human coronaviruses are described (Human coronavirus HCoV-229E, HCoV-HKU1, HCoV-NL63, HCoV-OC43, SARS-CoV, MERS-CoV, SARS-CoV-2), a particular broad attention has been put in three of them: the two *severe acute respiratory syndrome coronaviruses* (SARS-CoV and SARS-CoV-2), and the *middle east respiratory syndrome-related coronavirus* (MERS-CoV) (Ye et al., 2020, Corman et al., 2018, Yang et al., 2020).

Coronaviruses were first identified in the 1960s by group members of a common cold research unit and named according to their characteristic brink appearance in electron microscopy and the pleomorphic to round shaping resembling the solar corona (Coronaviruses, 1968). This morphology is due to embedded membrane proteins in the envelope of the 60 to 220 nanometer virion (Siddell et al., 1982). A wide range of different host and reservoir species for members of the subfamily *Orthocoronavirinae* are described, as well as repeatedly the

overcoming of species barriers and introduction into a new and naïve population (Graham and Baric, 2010, Fan et al., 2019).

With a size of about 27,000 to approximately 32,000 nucleotides they have the largest known viral RNA genome; the positive sensed, single stranded genome is non-segmented (Weiss and Leibowitz, 2011, Brian and Baric, 2005). This quite impressive genome size and the high fidelity in genome replication and hence low mutational rate is associated with a feature within the replication complex of coronaviruses, which acts as a "proof-reading" 3'→ 5' exoribonuclease in RNA-replication (Minskaia et al., 2006, Gorbalenya et al., 2006, Drake and Holland, 1999).

1. SEVERE ACUTE RESPIRATORY SYNDROME CORONAVIRUS – 2 (SARS-COV-2)

The World Health Organization has officially named the still ongoing pandemic disease COVID-19 (coronavirus disease-19) (WHO, 2020b). Causing fatal disease in humans, the etiologic agent, SARS-CoV-2, queues with the 2003-2005 SARS-CoV and the 2012 MERS-CoV as a highly pathogenic human coronavirus (Coronaviridae Study Group of the International Committee on Taxonomy of Viruses, 2020).

Together with the two other human coronaviruses of high impact, SARS-CoV-2 belongs to the genus *betacoronavirus*; SARS-CoV and SARS-CoV-2 are found within the subgenus of *SARS-related betacoronavirus*, *sarbecovirus* (Coronaviridae Study Group of the International Committee on Taxonomy of Viruses, 2020). However, emergence of both *sarbecoviruses* has occurred independently, and SARS-CoV-2 is not a direct descendant of SARS-CoV (Dong et al., 2020b). Bat populations, mainly in southern Asia are considered the reservoir species for *sarbecoviruses* and for a great diversity of other coronaviruses (Gouilh et al., 2011, Drexler et al., 2014, Wong et al., 2019, Latinne et al., 2020).

1.1. VIRION MORPHOLOGY

The pleomorphic to spherical shape of the SARS-CoV-2 lipid envelope measures approximately 90-100 nanometers in diameter (Ke et al., 2020). Each particle carries about 40 characteristic trimeric spike proteins (S) in its surrounding lipid bilayer, which are eponymous for coronaviruses; they are found randomly allotted in the membrane and jut out by approximately 20 nanometers (Turonova et al., 2020). Two other proteins can be found in the

envelope: the membrane glycoprotein (M) and the envelope (E) protein (Mittal et al., 2020, Bianchi et al., 2020) (also see Figure 1). The lipid membrane itself is a residue of the cellular endoplasmic reticulum – Golgi intermediate compartment with embedded viral proteins, which forms prior to viral budding (Fehr and Perlman, 2015, Plescia et al., 2021). Encapsulated within the envelope, and in steric contact to its proteins, the nucleocapsid protein or core domain is found in a bead-on-a-string formation (Fehr and Perlman, 2015) (also see Figure 1). The embedded genome has a size of around 29.8 to 29.9 kilobases (Khailany et al., 2020, Naqvi et al., 2020, Lu et al., 2020).
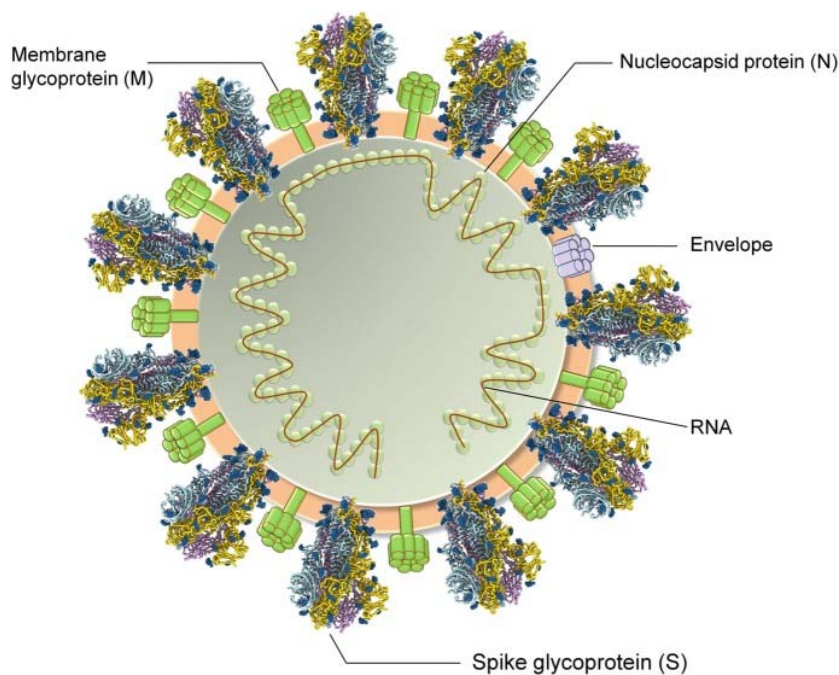

Figure 1. Virion structure of SARS-CoV-2. (Kumar S. et al., 2020).

STRUCTURAL PROTEINS

Attachment and internalization in cells are mediated by the trimeric SARS-CoV-2 spike protein (S), a class I fusion glycoprotein (Walls et al., 2020). Two conformations, "pre-" and "post-fusion", are described for S (Turonova et al., 2020). It consists of two subunits (S1 and S2) and a transmembrane domain; with the S1 subunit carrying the receptor binding domain (RBD) and the N-terminal domain (NTD), and S2 carrying the actual fusion subunit (Duan et al., 2020, Huang et al., 2020b). The S1 RBD has two prefusion conformations: in the open conformation RBD sits exposed at the tip of the fusion core, whereas RBD accessibility is hidden in the closed conformation (Ke et al., 2020). Conformational changes in the S architecture mediate merging of the viral envelope and the cell membrane (Luchini et al., 2021). After binding to the cellular

ACE2 receptor (angiotensin-converting enzyme), S1 and S2 are proteolytically cleaved from each other and thereby activated (Hoffmann et al., 2020). A furin convertase cleaves at the furin-like S1-S2 and the transmembrane serin-protease TMPRSS2 at the S2' cleavage site (Bestle et al., 2020).

Two S1 subunit domains, RBD and NTD, are major epitopes recognized by the vertebrate immune system and targeted by neutralizing antibodies (Liu et al., 2020). Therefore, many efforts in vaccine development and in the search for therapeutic substances have focused on S itself or its domains and combinations of both (Polack et al., 2020, Yang and Du, 2021, Samrat et al., 2020). Antibodies against S domains have also proven to be of importance for diagnostic approaches in the aftermath of a SARS-CoV-2 infection (Wernike et al., 2021, Freeman et al., 2020, Roy et al., 2020, Krahling et al., 2021, MacMullan et al., 2020).

The M glycoprotein integrated in large numbers into the viral envelope is equipped with three transmembrane domains (EA and Jones, 2019). It is found in two conformational stages, "Mcompact" and "Mlong" (Neuman et al., 2011), and in dimers; interactions in between M form a truss, which ultimately shapes the virion and serves as lattice for S and E in the viral membrane (Neuman and Buchmeier, 2016, Ujike and Taguchi, 2015). M is presumably also involved in downregulation of cellular inflammatory responses after viral infection and is considered a driver of apoptosis, by indirectly fostering the release of caspases 8 and 9 (Fang et al., 2007, Tsoi et al., 2014).

The viral envelope protein (E) is a rather small protein, additionally modified by posttranscriptional processes (Liao et al., 2006, Fung and Liu, 2018). The transmembrane domains of E form so called viroporins, that carry ion channel traits; E also oligomerizes to pentameric structures (Gupta et al., 2021, Fung and Liu, 2018). Coronavirus' virulence, pathogenesis, and membrane formation is associated with the channel activity of viroporins, and E might therefore be a target to attenuate SARS-CoV-2 (Ye and Hogue, 2007, Nieto-Torres et al., 2014, To et al., 2017). Interaction of E and cellular tight junction proteins, which can contribute to increased pathology, has also been observed (Shepley-McTaggart et al., 2021).

Both of these proteins, and especially their interplay, are important in spatial organization, virion assembly and budding at intracellular organelles and membranes, and release (Kumar S. et al., 2020, EA and Jones, 2019, Satarker and Nampoothiri, 2020, Schoeman and Fielding, 2019).

A nucleocapsid protein, the fourth structural, and most abundant protein, possesses five functional domains and interacts with viral RNA (Cubuk et al., 2021). It also critically interacts with the membrane structural proteins in virion formation; the constitution of a ribonucleoprotein complex with viral RNA, induces packaging of the very same and fits the quite large 30 kb genome in a characteristic 3D pattern into the limited space of the virion (Cubuk et al., 2021, Lu et al., 2011, McBride et al., 2014, Yao et al., 2020). N is also suspected to impede cell cycle progression, cellular degradation of external proteins, modulate the host immune-response, and directly activate inflammatory pathways by upregulation of COX-2 gene expression in lungs (Wang et al., 2010, Zeng et al., 2008, Yan et al., 2006). Serologic response against N is also used as a diagnostic tool (CDC, 2021a, Houlihan and Beale, 2020, Okba et al., 2020). However, both the sensitivity and specificity of N-specific tests in animal samples is insufficient (Berguido et al., 2021).

NON-STRUCTURAL PROTEINS

Besides the four structural proteins, an ambiguous number (up to 27 or even more) of non-structural proteins (nsp) and accessory proteins has been described for SARS-CoV-2 (Finkel et al., 2021, Redondo et al., 2021, Yoshimoto, 2020). The suspected number of proteins is derived from data for related coronaviruses, and conventional genome and transcriptome analysis, as experimental data towards SARS-CoV-2 open reading frame's (ORF) expression is still limited; of course, knowledge about SARS-CoV-2 proteins will increase with the ongoing pandemic (Yoshimoto, 2021, Kim et al., 2020). Non-structural proteins are considered to be obligatory involved in viral replication, or to act as accessory proteins, which contribute to pathogenesis and virulence, but are not essential in the cellular life cycle of the virus; however, they are specific for *sarbecoviruses* and involved in virus-host interactions, and viral evolution (Hodgson et al., 2006, Liu et al., 2014, Redondo et al., 2021).

Nsps are derived from ORF1a and ORF1b polypeptides (see Figure 2), which encode for the replicative and transcriptional machinery, and are cleaved into a certain number of smaller proteins; cleaving of this large peptide is mediated by a viral protease-activity of nsp3 and nsp5 (Imbert et al., 2008, Kim et al., 2020). Nsps have acquired a wide variety of functions contributing to efficient viral replication in the host cell. The leader protein nsp1 is among the first to become active and for instance interferes with ribosomal subunits and hinders host translational processes (Yoshimoto, 2020, Clark et al., 2021, Arya et al., 2021). Nsp 2 is known for its ability to perturb host cellular pathways (Yoshimoto, 2020). Together with others, nsp3,

the largest coronavirus protein, is involved in the viral replication-transcription complex (Imbert et al., 2008), and it is a viral cysteine-protease, just as nsp5, which, after a self-cleaving step, cleaves essential proteins from the ORF1ab polyprotein (Lei et al., 2018, Yadav et al., 2021). Nsps 4, 6, 7, 8, 9, 10, 12, 13 are also involved in the replication machinery, all having specific functions, such as RNA processing or elongation (nsp 7, 8, 12), or hindering cellular antiviral mechanisms, such as autophagy (Cottam et al., 2014, Subissi et al., 2014). The 5'-3' helicase function during RNA plus-strand synthesis is confirmed for nsp13, which becomes essential during replication; helicase activity is increased by the cooperative binding of nsp13 to other nsp-complexes; nsp13 is therefore of great interest as a target of direct antiviral treatment and drug development (Jang et al., 2020, Spratt et al., 2021). Among these proteins nsp14 is certainly salient. Exoribonuclease activity is associated with this protein, which contributes to the large coding capacity of SARS-CoV-2 and high fidelity in genome reproduction (Gorbalenya et al., 2006, Ma et al., 2015). The function of nsp15 and 16 consists in preventing viral RNA from destruction through host responses, either by masking it or protecting it by adding RNA-modifications (Decroly et al., 2011, Hackbart et al., 2020). According to Yoshimoto, nsp enzyme functions can be assigned to the following major categories: (i) proteases, (ii) RNA capping enzymes, (iii) replication, and (iv) other RNA modifications, one category (v) should also be added: enzymes targeting host cellular pathways (Yoshimoto, 2021).

ACCESSORY PROTEINS

The total number of exact ORFs in SARS-CoV-2 coding for accessory proteins is unknown and needs to be experimentally determined (Mariano et al., 2020). Furthermore, these are highly diverse in coronaviruses and ORF presence alters even between closely related coronaviruses; they are considered to be responsible for the observed differences in virulence of related betacoronaviruses (Gordon et al., 2020, Wu et al., 2020a) (see Figure 2). ORFs are defined as the regions between a start and stop codon, independently from potential translation (Jungreis et al., 2021). SARS-CoV-2 possesses a set of nine accessory proteins (Wu et al., 2020b, Gordon et al., 2020). Like E, ORF3a, the largest accessory protein, oligomerizes to a viroporin (Azad and Khan, 2021, Hassan et al., 2020). For ORF3a a pro-apoptotic activity has been determined; in direct comparison to SARS-CoV, however, it is reduced, which might favor the strategy of the virus to spread relatively well and undetected from cell-to-cell in an early infection stage (Ren et al., 2020). Mutations in ORF3a and subsequent non-synonymous amino

acid exchanges might contribute to differences in pathogenicity of SARS-CoV-2 strains (Azad and Khan, 2021). As an initiator of necrosis, ORF3a also contributes to cytopathologic effects (Yue et al., 2018). Finally, this protein also interacts with cellular pathogen defense mechanisms, such as phagolysosome formation (Miao et al., 2021a). The potency of ORF3b to act as an interferon antagonist is influenced by its length (Konno et al., 2020). ORF6 is also involved in suppressing the interferon response and additionally impairs nuclear host-mRNA transport mechanisms (Kato et al., 2021, Miorin et al., 2020). The ORF7a protein is associated with suppression of antigen presentation on monocytes and with firing a cytokine storm (Zhou et al., 2021c). Also, for ORF8, 9b, and 9c downregulating activities of host immune responses have been described, partially by targeting mitochondrial processes (Shi et al., 2014, Dominguez Andres et al., 2020, Wong et al., 2018). The functions of ORF3c, d, and ORF7b in the life-cycle of SARS-CoV-2 are still unknown; nonetheless, ORF3d provokes a solid antibody response and the ORF7b leucine zipper might be involved in loss of taste and olfaction (Fogeron et al., 2021, Hachim et al., 2020, Redondo et al., 2021). While the role of ORF10 as coding region is up for discussion, it was demonstrated that absence of ORF10 in the genome of SARS-CoV-2 does not attenuate human disease (Pancer et al., 2020).

Recently, Jungreis and colleagues defined a reference gene panel of functional protein-coding genes for SARS-CoV-2 consisting of the ORFs 1a, 1ab, S, 3a, 3c, E, M, 6, 7a, 7b, 8, N, and 9b (Jungreis et al., 2021). In summary, functions of accessory proteins can be abstracted in sharing one aim: to subdue infected cells in manifold ways to enable unobstructed viral growth and replication. Hence both, nsps and accessory proteins, are of great interest as potential drug targets or for creation of live, attenuated SARS-CoV-2 strains lacking certain ORFs (Silvas et al., 2021, Habtemariam et al., 2020).

1.2. GENOME CHARACTERISTICS

The SARS-CoV-2 genome ranges in size between 29.8 to 29.9 kilobases and encodes for about 9860 amino acids; it is a single stranded, positive sensed RNA genome, meaning viral RNA can directly be translated by cellular ribosomes, just like mRNA (Pfefferle et al., 2020, Chan et al., 2020, Khailany et al., 2020, Masters, 2006). The vast genome organization does not differ between SARS-CoV and SARS-CoV-2, but individual disparity between both viruses is prominent in S, ORF3b, and ORF8 genes specifically (Chan et al., 2020). Towards the 5' genome end two large genes encoding for nonstructural proteins are allocated (ORF1a and ORF1b) and they engross about two thirds of the entire genome; the much smaller genes for the four

structural proteins are found with orientation towards the 3' genome end (Masters, 2006). They are arranged discontinuously between those encoding for accessory proteins (ORF3a-ORF10) (Khailany et al., 2020). The hemagglutinin-esterase gene is not present in the SARS-CoV-2 genome (Zandi and Soltani, 2021, Chan et al., 2020). An overview on the genome organization is given in Figure 2.

Either genomic end is flanked by an untranslated region (UTR) of variable lengths (Chan et al., 2020, Khailany et al., 2020). UTRs carry specific modifications, such as a 3' poly a-tail, a 5' cap, and structural adaptations (Miao et al., 2021b). Secondary RNA-structures, as stem loops, long-range RNA-RNA interactions, and double-stranded regions are known and some of these are involved in modulating transcription efficiency (Vandelli et al., 2020, Rangan et al., 2020, Plant et al., 2005, Cao et al., 2021, Chan et al., 2020). A well-described structure is the three stemmed pseudoknot in ORF1ab. It is essential for frame-shifting, as it enables translation of polyprotein (pp) 1 and pp2 from the ORF1ab by circumnavigating ribosomes around the ORF1a stop codon to allow for translation of the downstream ORF1ab proteins (Huston et al., 2020).
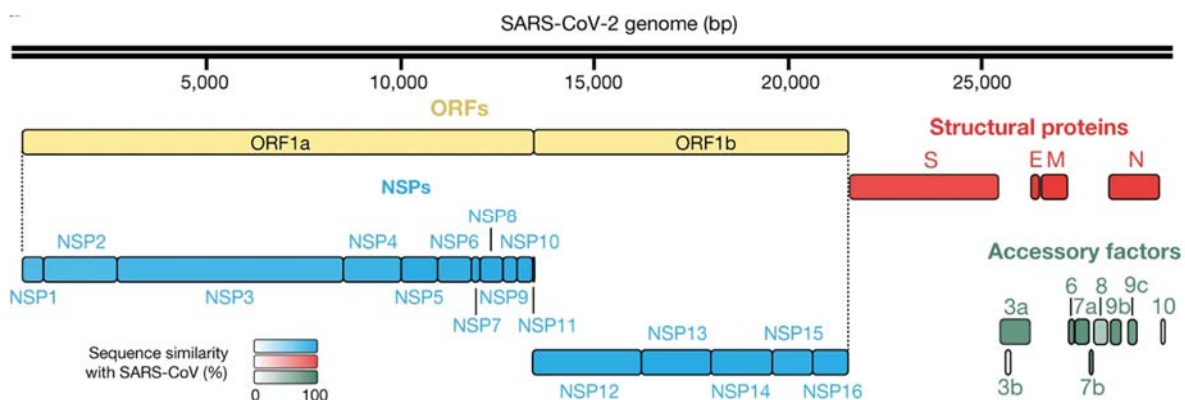

Figure 2. SARS-CoV-2 genome organization and annotation of ORFs. Modified after Gordon et al., 2020.

Viral RNA is stowed in the virion in a globular, slightly helical spatial arrangement (Cao et al., 2021). RNA packaging is mediated by packaging signals and dependent on interactions of N and M terminal regions (Masters, 2006).

Characteristic for Nidovirales is also the production of a set of nested 3' subgenomic RNAs (Fehr and Perlman, 2015). The underlying mechanisms are intricate and likely the consequence of halted negative RNA strand synthesis (Alexandersen et al., 2020). The subgenomic RNAs also serve as templates for translation of the 3' orientated genes, including the structural genes (Kim et al., 2020, Sola et al., 2015). However, subgenomic RNAs are not

included in virions, as they do not have any packaging signals (Alexandersen et al., 2020). The set of subgenomic RNAs is illustrated in Figure 3.

A major driver in both CoV' evolution and host-switch are genome recombination events, which occur during RNA-synthesis due to template switch; recombination can result in the generation of defective viral genomes, or altered subgenomic RNAs, or novel full genomes (Graham and Baric, 2010, Sola et al., 2015, Gribble et al., 2021). Recombination frequency and preciseness is depending on the activity of the nsp14 exonuclease (Gribble et al., 2021). Both, intermolecular trans-recombination events between two co-infecting RNA molecules, which may result in chimeric viruses, as well as intramolecular cis-recombination events at transcription-regulating sequences are described (J. G. Keck, 1988, Sola et al., 2015). In addition to recombination, coronaviruses evolve within new hosts or if forced from hosts with partial immunity, through genomic drift. Accumulation of such drift mutations resulted in a divergence of SARS-CoV-2 variants and is still in progress.
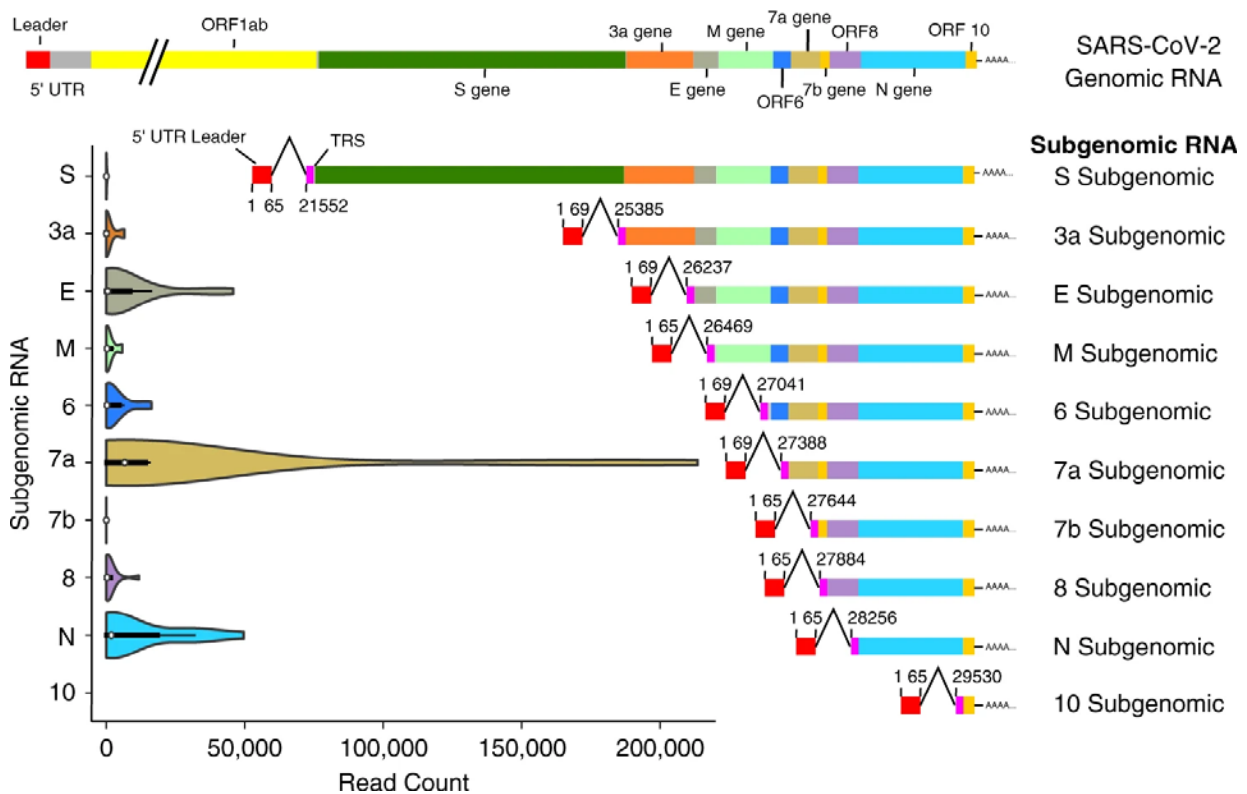

Figure 3. Illustration of the set of sub-genomic RNAs in a SARS-CoV-2 diagnostic sample and their frequency. Modified after Alexandersen et al., 2020.

2. SARS-CoV-2 Life Cycle

For replication, SARS-CoV-2 virions critically depend on the intracellular milieu and machinery of eukaryotic cells. First steps in viral infection and hence the viral life cycle are attachment to and internalization into host cells. With its RBD located in the spike protein the virus particle attaches to the ACE2 cellular receptor (Wang et al., 2020b). Further uptake of the virion occurs only after proteolytic activation of the S1 and S2 subunit by cellular proteases (furin and TMPRSS2) (Jaimes et al., 2020, Ord et al., 2020, Hoffmann et al., 2020). Upon activation, the S2 domain catalyzes the fusion of viral and cellular membranes by ionic changes, after its self-insertion into the cell membrane (Millet and Whittaker, 2018, Murgolo et al., 2021). ACE2 receptors and relevant proteases are found on many cell types in mammals, e.g. in lung or bronchial tree tissues (Lukassen et al., 2020). Internalization may also be achieved by an alternative, less-favored pathway: endocytic-endosomal intake, and cathepsin L-mediated fusion of endosomal and viral membranes (Simmons et al., 2013, Yang and Shen, 2020). Besides, also other cellular proteins, as Neuropilin-1, are known to alleviate cell entry (Zhang et al., 2020b, Cantuti-Castelvetri et al., 2020).

Subsequently, the nucleocapsid-complex is released into the cytoplasm (Kirtipal et al., 2020). The viral RNA acts similar to host mRNA, hence direct translation of 5' terminal genes at cellular ribosomes under the influence of frame-shifting events commences, and polyprotein 1 and 2 (pp) are released (Fehr and Perlman, 2015). After auto-cleavage of the papain-proteases nsp3 and nsp5 from the pp, these in turn cleave the remnant-pp and allow formation of the viral replication and transcription complex (RTC); RTC is allocated near the rough endoplasmic reticulum (rER), and nsp1 and others subsequently conquer the host-transcription processes at the rER (Schubert et al., 2020). RTC core units are the RNA-dependent RNA polymerase with its cofactors, the proof-reading machinery, and RNA modifying subunits (Romano et al., 2020, Gao et al., 2020).

The following steps, which include synthesis of the initially produced minus-strand RNA, subgenomic RNAs, and the ultimate viral positive-strand RNA, require the formation of characteristic, endoplasmic reticulum-derived membrane structures: so-called double membrane vesicles (DMV) (V'Kovski et al., 2021, Knoops et al., 2008, Perlman and Netland, 2009). Formation of DMV and anchoring of RTC is induced by several nsps (Zhang et al., 2020a). The DMV are beneficial for viral replication, as they can protect viral RNA, especially double-stranded intermediates from degradation, they concentrate necessary substrates and

spatially organize enzyme-systems; hence they are also designated as SARS-CoV-2 replication factories (Du Toit, 2020, Wolff et al., 2020b, Snijder et al., 2020). Then, positive-strand RNA is disguised by RNA-capping modifications, to veil its non-cellular origin (Romano et al., 2020). For egress of newly synthesized RNA, pores are coined in the DMV (Wolff et al., 2020a).

After the RNA-synthesis steps in the DMV microenvironment, viral proteins are produced: structural and accessory proteins are translated from the subgenomic RNA at the rER, where they are internalized under synthesis for posttranslational modifications - with one exception: N is directly released into the cytoplasm following translation, to allow formation of the ribonuclein-complex and nucleocapsid-formation with the positive RNA strand (V'Kovski et al., 2021, Hopfer et al., 2021, Khade et al., 2021). Encapsidation is driven by RNA packaging signals, which effectuate accumulation of numerous N proteins and self-organization processes (Masters, 2019, de Haan CA, 2005). Following translation, the proteins are delivered via the ER-to-Golgi intermediate compartment ERGIC to finally bud with the nucleocapsid, to form new virions; these processes are initiated and coordinated by activity of mainly M, but also E, and N protein (Caldas et al., 2020, de Haan CA, 2005, Plescia et al., 2021, Fehr and Perlman, 2015, Kirtipal et al., 2020, V'Kovski et al., 2021). Structural proteins are sent on their way to ERGIC by expression of intracellular trafficking signals (Boson et al., 2021), and morphologically distinct membrane vesicles act as a transport receptacle for different types of proteins; finally these vesicles fuse to allow viral budding and the eventual release (Ulasli et al., 2010, Mendonca et al., 2021).

In infected cells, the assembly sites are characterized by proximity of membrane structures resembling ER and Golgi apparatus and high vesicle densities (Klein et al., 2020).

SARS-CoV-2 has several strategies for egress: along with bio-secretion also egress via lysosomal pathways occurs (Ghosh et al., 2020, Zhang and Zhang, 2021). SARS-CoV-2 manages to impair normal lysosomal functions: enzymes are inactivated, antigen-presentation is hindered and the pH is increased, so ultimately virions are released via lysosomal trafficking (V'Kovski et al., 2021, Ghosh et al., 2020, Miao et al., 2021a).

A schematic overview about the steps in the cellular SARS-CoV-2 replication cycle is given in Figure 4.
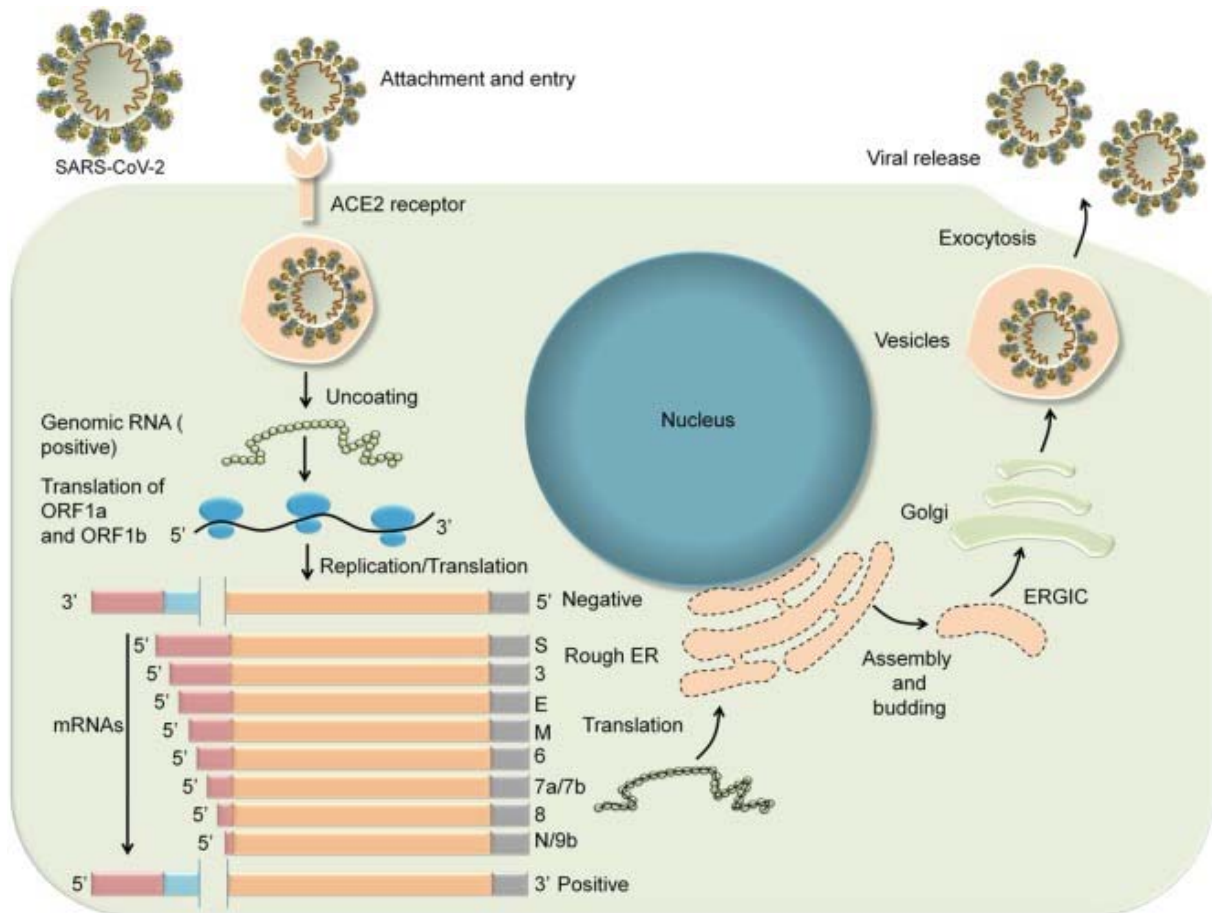
Figure 4. Overview of SARS-CoV-2 cellular entry, replication, and egress. (Kumar S. et al., 2020).

3. ORIGIN AND HISTORY

SARS-CoV-2 was first identified in late 2019 from swab and bronchoalveolar lavage samples collected from a diseased person in China (Zhou et al., 2020, Wu et al., 2020b). The majority of first COVID-19 cases were epidemiologically linked to a seafood market in Wuhan, Hubei Province, China (Li et al., 2020a, Zhu et al., 2020). Although many theories on the origin of SARS-CoV-2 exist, the most plausible ones – similar to other coronaviruses - include transmission of a SARS-CoV-2 ancestral virus from a bat species as reservoir host to an intermediate host and finally to humans, where it further adapted to maximum replication and transmission capacity; most likely, trade and consumption of wildlife animals were involved in the gateway of the pandemic (Holmes et al., 2021, Lam et al., 2020, Dong et al., 2020b, Cui et al., 2019, Wong et al., 2019, Lundstrom et al., 2020, Andersen et al., 2020, Ge et al., 2013, Bloom, 2021, Temmam et al., 2021). For the respective seafood market, the sale of species, which have proved to be highly susceptible for SARS-CoV-2, has been documented

until November 2019 (Xiao et al., 2021). What is more, just recently the finding of a close SARS-CoV-2 relative in Chinese bats was reported (Li et al., 2021b).

A more detailed discussion of reservoir and host species is included in the enclosed Review Article `SARS-CoV-2 in animals: From potential hosts to animal models´.

Although knowledge about contagiousness, transmissibility, and pathogenesis of SARS-CoV-2 was little in the beginning, reports from China indicate that the initial infection wave could be controlled quickly (Zhu et al., 2020, Kong et al., 2021, Shi et al., 2021). Yet, the virus spread world-wide and among others, Italy, France, Spain, the United Kingdom, and the United States faced an enormous first pandemic wave with a critically high number of patients requiring intensive treatment (Davis et al., 2021, Zeller et al., 2021, Yang et al., 2021, Nadeau et al., 2021, Dong et al., 2020a). In response to the rapid spread and dramatic scenarios, many countries have launched disease control measures and lock-downs (Fokas and Kastis, 2021).

March 11, 2020, the Director-General of WHO, finally announced a global SARS-CoV-2 pandemic (WHO, 2020e).

Simultaneously, the SARS-CoV-2 pandemic has been driven by the emergence of new viral variants. The first to become important, was the so-called variant "D614G". One nucleotide exchange in the coding sequence of S resulted in an altered primary structure of the protein and overtook disease dynamics only shortly after its detection (Korber et al., 2020). In the aftermath of this first dominant variant also others emerged: the Alpha B.1.1.7 variant and Delta B.1.617.2 variant, which have both achieved preferred spreading in comparison to the strains endemic beforehand, and the Beta B 1.351 variant, which is associated with immune-escape properties (Li et al., 2021a, Reardon, 2021, Kraemer et al., 2021, Wibmer et al., 2021).

To keep track with the rapid viral evolution a classification system was proposed, with the categories variant of concern (VOC), variant of interest (VOI), and variants of high interest (WHO, 2021b, CDC, 2021c). First, naming of the variants referred to the country, they were initially reported from (e.g. the British, South African, Brazilian, Indian variant) (Callaway, 2021). Also, a naming system respecting phylogenetic relatedness was proposed (Rambaut et al., 2020). In order to simplify and harmonize nomenclature, WHO announced in May 2021 a new classification system, referring to Greek letters for distinct variants (WHO, 2021c). By end of August 2021 four variants of concern are defined, which have been, or are, dictating

epidemics in the past ten months: Alpha (B.1.1.7), Beta (B.1.351), Gamma (P.1), and Delta (B.1.617.2); they are defined by their specific genomic configuration at certain sites (WHO, 2021b).

4. SARS-CoV-2-related Disease

Certainly, SARS-CoV-2 is dreaded for its consequences for human health. Most frequently, SARS-CoV-2 is shed via respiratory droplets from infected patients; transmission occurs either by direct inhalation of these, or by droplet, or smear infection of mucous membranes (Zhou et al., 2021b, WHO, 2020d, CDC, 2021e). Upon infection with SARS-CoV-2, a patient may develop clinical symptoms at varying severity of Coronavirus Disease-19 (COVID-19). The spectrum of disease includes every stage between mild or even asymptomatic progression and severe to fatal clinical disease (Schonfeld et al., 2021, Huang et al., 2020a, Oran and Topol, 2020, Nogrady, 2020, Casas-Rojo et al., 2020, NIH, 2021).

Among the commonly reported symptoms are coughing, sore throat, fever, asthenia, headache, myalgia, loss of smell and taste, and shortness of breath (Tong et al., 2020, Aziz et al., 2020, Lechien et al., 2020, CDC, 2021d). These studies also show clearly that the subset of clinical symptoms varies from patient to patient and symptoms can be others than the mentioned most common signs, e.g. diarrhea or gastro-intestinal symptoms (Ghimire et al., 2021, Li et al., 2020b).

As disease progression continues, initially mild symptoms can rapidly gain in severity, which might afford aggressive therapy, e.g. intensive care, artificial ventilation, or even extracorporeal membrane oxygenation of venous blood (ECMO), that can still result in coma or death of the patient (Wongtangman et al., 2021, Richardson et al., 2020, Wang et al., 2020c, Wunsch, 2020, Dreier et al., 2021). Complications, symptoms, and diagnoses in these cases include pneumonia, lung failure, cyanosis, chest CT abnormalities, lymphopenia and leukopenia, reduced hemoglobin and platelets, aberrations in blood biochemistry, vasculitis and haemophagocytic lymphohistiocytosis, coagulopathy and thrombosis, cerebral infarction, encephalitis and myelitis, myocarditis, glomerulonephritis, cutaneous involvement, and death (Wang et al., 2020a, Andrikopoulou et al., 2020, Wollina et al., 2020, Ramos-Casals et al., 2021, Wang et al., 2021).

Time between infection and symptom onset adds up to about 7 days, but can vary depending on individual factors (Zaki and Mohamed, 2021, Elias et al., 2021, Quesada et al., 2021, Paul

and Lorin, 2021). Time from symptom onset to a stage, which makes treatment obligatory, amounts to about 8 days and patients may worsen within a very short period of time, even quite a while after the onset of symptoms (Wang et al., 2021). Unfortunately, it has to be noted, that patients are already infectious during the asymptomatic phase (Byambasuren et al., 2020, Sayampanathan et al., 2021, Wilmes et al., 2021, Johansson et al., 2021).

Most abundant risk-factors for severe disease and lethality include sex and age of the patients, obesity, diabetes, hypertension, and cardio-vascular diseases (CDC, 2021b, Venkatakrishnan et al., 2021, Nogueira et al., 2020, Wollenstein-Betech et al., 2020, Pawlowski et al., 2021, Ahrenfeldt et al., 2021, Green et al., 2021, Peckham et al., 2020).

As more and more patients recovered from SARS-CoV-2 infection, it became clear, that a certain fraction of patients, independent from disease severity, develops symptoms in the aftermath of the acute phase; this syndrome has been termed "post-COVID syndrome" or "Long-COVID" (Fan et al., 2021, Halpin et al., 2021, Wostyn, 2021, Carroll et al., 2020, Lancet, 2020, Nalbandian et al., 2021). However, both, case definition and the pathogenesis of this syndrome, are still unclear.

5. SARS-CoV-2 in Animals

Animals play a particular role in the SARS-CoV-2 pandemic. On the one hand SARS-CoV-2, and the ancestral virus respectively, originates from a reservoir bat species and was transmitted to humans via an intermediate host. Therefore, SARS-CoV-2 is a zoonotic pathogen, even if meanwhile most animal infections are of an anthropo-zoonotic origin. Furthermore, also other animal species, than originally infected, could reveal susceptible for SARS-CoV-2 infection and act as reservoirs or even as `recombination vessel´. Human existence is closely linked to large scale animal production systems – another possible reservoir pool. And, probably most important in the current phase of the pandemic, animals are irreplaceable as model species to picture human disease and illness, and to promote evidence in many research fields, e.g. in vaccine development.

A comprehensive summary embracing the named topics is presented in the following pages as a Review Article. Figure and table numbering are according to the published chapter and references are presented in the journal style and do not appear in the reference section of this thesis.

<u>Review article</u>

SARS-CoV-2 in animals: From potential hosts to animal models

Anna Michelitsch, Kerstin Wernike, Lorenz Ulrich, Thomas C. Mettenleiter, Martin Beer

> CHAPTER THREE

SARS-CoV-2 in animals: From potential hosts to animal models

Anna Michelitsch[†], Kerstin Wernike[†,*], Lorenz Ulrich, Thomas C. Mettenleiter, and Martin Beer

Friedrich-Loeffler-Institut, Greifswald – Insel Riems, Germany
*Corresponding author: e-mail address: kerstin.wernike@fli.de

Contents

Abstract

Within only one year after the first detection of severe acute respiratory syndrome coronavirus-2 (SARS-CoV-2), nearly 100 million infections were reported in the human population globally, with more than two million fatal cases. While SARS-CoV-2 most likely originated from a natural wildlife reservoir, neither the immediate viral precursor nor the reservoir or intermediate hosts have been identified conclusively. Due to its zoonotic origin, SARS-CoV-2 may also be relevant to animals. Thus, to evaluate the host range of the virus and to assess the risk to act as potential animal reservoir, a large number of different animal species were experimentally infected with SARS-CoV-2 or monitored in the field in the last months. In this review, we provide an update on studies describing permissive and resistant animal species. Using a scoring system based on viral genome detection subsequent to SARS-CoV-2 inoculation, seroconversion, the development of clinical signs and transmission to conspecifics or humans, the susceptibility of diverse animal species was classified on a semi-quantitative scale. While major livestock species such as pigs, cattle and poultry are mostly resistant, companion animals appear moderately susceptible, while several model animal species used in

---

[†] These authors contributed equally to this article.

59

research, including several *Cricetidae* species and non-human primates, are highly susceptible to SARS-CoV-2 infection. By natural infections, it became obvious that American minks (*Neovison vison*) in fur farms, e.g., in the Netherlands and Denmark are highly susceptible resulting in local epidemics in these animals.

1. Introduction

The World Health Organization (WHO) defines a pandemic as a global spread of a new disease (WHO, 2010) focusing on the human population. However, as it can be seen during the recent pandemic of severe acute respiratory syndrome coronavirus type 2 (SARS–CoV-2), not only humans but also a variety of other animal species can be affected by the spread of this novel pathogen (Abdel-Moneim and Abdelwhab, 2020; Kiros et al., 2020). From the origin of the virus from a yet unknown animal reservoir (Zhou et al., 2020) to the appearance of new viral variants in farmed minks (Elaswad et al., 2020), and the threat of the establishment of separate transmission cycles in nature (Kiros et al., 2020), animals are an epidemiological part of this pandemic. Thus, the susceptibility of different animal species needs to be assed in order to fully understand the epidemiology of the pandemic (Kiros et al., 2020), and to find suitable animal models (Muñoz-Fontela et al., 2020) to support the development and validation of efficient vaccines and therapeutics.

To date, seven human coronaviruses are known and all of them likely originate from an animal source (Cui et al., 2019). HCoV–OC43 and HCoV–HKU1, which induce only mild upper respiratory disease in immunocompetent humans, likely originated in rodents. Progenitor viruses of HCoV–229E and HCoV–NL63, which likewise usually cause only mild human infections, were recently found in African bats (Cui et al., 2019). The remaining three human coronaviruses, namely the Middle East respiratory syndrome coronavirus (MERS-CoV), the first severe acute respiratory syndrome coronavirus (SARS–CoV) and SARS–CoV-2 induce severe to fatal diseases in infected humans, and all three are suspected to originate from bats (Cui et al., 2019; WHO, 2003, 2019; Zhou et al., 2020). In addition, a variety of intermediate hosts is discussed. SARS–CoV was found, e.g., in four *Paguma larvata* (Himalayan palm civets) and a *Nyctereutes procyonoides* (raccoon dog) in a live-animal market (Guan et al., 2003) in the province Guangdong, China, which was the center of the SARS-CoV epidemic in 2002/03 (Zhong et al., 2003). This led to a mass killing of these animal species. The analysis of sampled civets

(n = 91) and raccoon dogs (n = 15) showed that all of them were positive for SARS-CoV. However, in civets from 12 other Chinese provinces (n = 1107) no SARS-CoV genomes were detected (Kan et al., 2005).

Further, a serological study found antibodies against SARS-CoV in civets in another market in Guangdong, but not in civets sampled from farms and markets outside of Guangdong (Tu et al., 2004). Both studies support the hypothesis that civets and raccoon dogs are not the original source of the ancestor virus, but rather a recipient in the local market, that acquired the virus from an original source and may have acted as an amplifier for virus spread (Kan et al., 2005; Tu et al., 2004). For MERS-CoV, the human–to–human transmission rate appears to be rather low. Therefore, an animal source for the numerous independent human infections was suspected (Breban et al., 2013). Initial analyses of the exposure history of the first human MERS-CoV cases showed that all patients had contact with livestock animals (WHO, 2013).

Serological studies were conducted in the affected regions of the Arabic peninsula. They found that *Camelus dromedarius* (dromedary camels), but not *Bos taurus* (cattle), *Ovis aries* (sheep) or *Capra aegagrus hircus* (goats) had high antibody prevalence against MERS-CoV (Hemida et al., 2013; Perera et al., 2013; Reusken et al., 2013). Furthermore, MERS-CoV was isolated from a camel farm owned by an infected person (Haagmans et al., 2014). Transmission from dromedary camels to humans also was subsequently demonstrated by RT–PCR-based genome detection and sequence analysis (Azhar et al., 2014). As of now, dromedary camels are seen as the central intermediate host for MERS-CoV (Cui et al., 2019) and are believed to be the source of constant re-introduction of MERS-CoV into the human population (Al-Ahmadi et al., 2020). Nevertheless, the most likely original hosts of a MERS-CoV ancestor virus are bats (Cui et al., 2019).

The most recent human-pathogenic coronavirus, SARS-CoV-2, also is suspected to originate from an animal reservoir, potentially through one or more intermediate hosts. In humans, the clinical presentation of the novel disease, called "Corona Virus Disease 2019 (COVID-19)," ranges from asymptomatic infections or mild respiratory symptoms to pneumonia with acute respiratory distress syndrome, cardiovascular failure, coagulopathy, multiple organ failure and death, with much higher fatality rates in the elderly or when certain underlying health conditions exist (Grasselli et al., 2020; WHO, 2020a; Wu and McGoogan, 2020). Until January 2021, which is only one year after the first cases of SARS-CoV-2 were reported to WHO, about 100 million human infections were reported from 224 countries, with more than 2 million fatal cases (Dong et al., 2020).

Since SARS-CoV-2 very likely has a zoonotic origin, it is important to identify the original animal reservoir to prevent future similar outbreaks. Therefore, during the last months, a significant number of different animal species were either sampled in the field or experimentally infected with SARS-CoV-2, in order to evaluate their susceptibility to infection and to assess their potential as animal reservoirs.
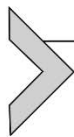
2. Reservoir and intermediate hosts

SARS-CoV-2, SARS-CoV and MERS-CoV very likely originate from an animal reservoir. However, it is not known how, where and when the ancestor virus transferred into the human population. Although highly important to prevent future similar spill-over transmissions of related viruses (Wong et al., 2020), neither SARS-CoV-2 nor an immediate precursor coronavirus in animals has been reported. Nevertheless, given the sequence similarity of about 96% between SARS-CoV-2 and the betacoronaviruses RaTG13 found in *Rinolophus affinus* (intermediate horseshoe bats) in China (Zhou et al., 2020), and the detection of a wide range of further coronaviruses in bats (order *Chiroptera*) (Colunga-Salas and Hernández-Canchola, 2020; Lacroix et al., 2020; Lau et al., 2005; Li et al., 2005; Wacharapluesadee et al., 2021; Yadav et al., 2020), bats are suspected to be the reservoir host for the progenitor virus of SARS-CoV-2 (Latinne et al., 2020; Lu et al., 2020a; Wacharapluesadee et al., 2021; Zhou et al., 2020).

Interestingly, antisera raised against the bat coronavirus RmYN02 were able to cross-neutralize SARS-CoV-2 (Wacharapluesadee et al., 2021). Whether the pandemic started by a direct spill-over of the SARS-CoV-2 ancestor from bats to humans followed by natural selection in humans, or via another intermediate mammalian host providing further adaptation to the human host, is still under debate (Andersen et al., 2020; Wacharapluesadee et al., 2021).

When assessing the relatedness of coronaviruses to identify potential hosts, the amino acid sequence and structure of the receptor-binding domain (RBD) within the spike (S) protein is relevant, as it mediates binding of the virus to the cellular surface protein angiotensin-converting enzyme 2 (ACE2) (Brooke and Prischi, 2020; Damas et al., 2020). The RBD of the RaTG13 bat coronavirus differs substantially from that of human coronaviruses, suggesting that it may not bind efficiently to the human ACE2 receptor (Andersen et al., 2020; Conceicao et al., 2020). Other bat

coronavirus RBDs are even less similar, making a direct spill-over to humans unlikely. Nevertheless, there could be other more closely related coronaviruses in bats that have not been detected yet, or an intermediate host. To assess whether bats support replication and transmission of SARS-CoV-2, *Rousettus aegyptiacus* (fruit bats) and *Eptesicus fuscus* (North American big brown bats) have been inoculated experimentally (Hall et al., 2020; Schlottau et al., 2020). Big brown bats appear to be resistant, since neither virus excretion, nor virus detection in tissues, signs of disease or transmission were found (Hall et al., 2020). In contrast, SARS-CoV-2 inoculation of fruit bats led to efficient replication in the upper respiratory tract followed by seroconversion in seven out of nine intranasally inoculated animals. Although no clinical signs were observed, immunohistochemical analyses detected the presence of rhinitis. Transmission to in-contact bats of the same species occurred in one out of three animals (Schlottau et al., 2020). Thus, fruit bats show characteristics of a reservoir host and could help to model the physiopathology of SARS-CoV-2 infection in a bat host.

Several candidates for potential intermediate hosts have been proposed. At the beginning of the pandemic, *Pholidota* spp. (pangolins) were implicated because of the identification of several SARS-CoV-2-related coronaviruses in these animals, including viruses with an RBD similar to that of SARS-CoV-2 (Lam et al., 2020b; Xiao et al., 2020; Zhang et al., 2020d). However, the pangolin theory is still up for debate, as it became clear that the pangolin viruses are even less related to SARS-CoV-2 than the currently known bat coronaviruses, meaning that the sequence similarity is not sufficient to either confirm or rule out a role of pangolins in the emergence of SARS-CoV-2 (Liu et al., 2020; Malaiyan et al., 2020; Wacharapluesadee et al., 2021; Wahba et al., 2020). In addition, experimental infection studies are missing.

A wide range of additional wild animals from *Murinae* (e.g., house mouse), *Cricetidae* (e.g., deer-mouse and bank voles) or *Sciuridae* species (e.g., squirrels) to *Serpentes* (snakes), *Feliformia* (cat-like carnivorans), *Caniformia* (dog-like carnivorans), *Viverridae* (e.g., civets), *Cervidae* (deer) and non–human primates including close relatives (e.g., Chinese tree shrew) were analyzed as potential missing links between bats and humans or potential animal reservoirs (Deng et al., 2020b; Zhao et al., 2020b). Some species could be quickly excluded, while others are still up for debate.

Computational analysis may assist in the prediction of a certain species as a potential host for a specific virus. However, this theoretical approach should be viewed with caution and verified by experimental studies.

Snakes, for example, were hypothesized to be a potential host for SARS-CoV-2 by comparison of the relative synonymous codon usage of virus and snake (Ji et al., 2020). However, bioinformatics approaches based on the analysis of their ACE2 receptor (Luan et al., 2020; Zhang et al., 2020b) argued against this assumption. Direct experimental evidence that determines whether snakes can be infected is still missing. By experimental inoculation *Sylvilagus* sp. (cottontail rabbits), *Sciurus niger* (fox squirrels), *Urocitellus elegans* (Wyoming ground squirrels), *Cynomys ludovicianus* (black-tailed prairie dogs), *Mus musculus* (house mice), and *Procyon lotor* (raccoons) were found to be not susceptible to SARS-CoV-2 (Bosco-Lauth et al., 2021).

Carnivora wildlife species that are wide-spread in North America and often live in close proximity to human dwellings are *Mephitis mephitis* (striped skunk) and raccoon. Both species were tested by experimental inoculation with SARS-CoV-2. Virus replication and seroconversion was detected in skunks, but not in raccoons. No clinical or gross pathological signs were observed for either species, but bronchiole associated lymphoid tissue was found in skunks (Bosco-Lauth et al., 2021).

Three species of Cervids show a high similarity in their ACE2 receptor to that of humans: *Odocoileus virginianus* (white-tailed deer), *Rangifer tarandus* (reindeer), and *Elaphurus davidianus* (Père David´s deer) (Damas et al., 2020). In addition, deer lung cells were found to be susceptible to SARS-CoV-2, and the virus replicates to similar titers as in African green monkey (Vero-E6) cells, although markedly delayed (Palmer et al., 2021). Upon intranasal inoculation of white-tailed deer all inoculated fawns shed infectious virus and seroconverted. Noteworthy, also in-contact fawns, separated by plexiglass, became productively infected, most likely by droplets. Virus was isolated from nasal and rectal swabs, and the viral genome was detected mainly in the upper respiratory tract and corresponding lymphatic organs of inoculated animals and deer infected by contact to virus-shedding conspecifics. Body temperature was transiently elevated in some cases, but gross lesions were not obvious. Histologically, acute alveolar damage-related lesions were detected, resembling human infection, but no viral RNA was detected, suggesting that the virus had already been cleared (Damas et al., 2020).

Rodentia (Rodents) is the largest order of mammals encompassing more than 2000 species. Rodents are notorious as hosts for zoonotic viruses. They occur worldwide and some species live in high numbers in close proximity

to humans in urban, suburban and rural setting. Moreover, parental viruses of two human coronaviruses, OC43 and HKU1, have already been found in rodents (Cui et al., 2019).

Based on comparative sequence and structural analyses of the SARS-CoV-2-binding receptor ACE2, some rodents were identified as in a high-risk group for susceptibility (Damas et al., 2020). Though house mice could be excluded as an amplifying host by experimental infection (Bosco-Lauth et al., 2021), some species of the family Cricetidae support virus replication. *Neotoma cinerea* (bushy tailed woodrats) shed virus from their oral cavity and developed specific antibodies subsequent to experimental infection, and during necropsy, mild signs indicative for inflammation were found (Bosco-Lauth et al., 2021). Further Cricetidae species that are susceptible to SARS-CoV-2 include *Peromyscus maniculatus* (North American deer mice), *Peromyscus leucopus* (white-footed mice), and *Myodes glareolus* (European bank vole) (Bosco-Lauth et al., 2021; Fagre et al., 2020; Griffin et al., 2020; Ulrich et al., 2020a). After experimental intranasal infection, deer mice carry high amounts of infectious virus in their respiratory organs and also in the intestine, whereas infectious virus is shed at significantly lower levels in a biphasic pattern from the mouth and nose (Bosco-Lauth et al., 2021;Fagre et al., 2020; Griffin et al., 2020). Transmission to contact animals was successful for deer mice (Fagre et al., 2020; Griffin et al., 2020) and antibodies were produced by the animals, in which viral replication took place. Although histopathology revealed signs of inflammation and pneumonia in the lungs as well as inflammatory alterations and presence of viral antigen in head ganglia and cerebral portions of the brain, clinical disease was not obvious (Bosco-Lauth et al., 2021; Fagre et al., 2020; Griffin et al., 2020). Expression of cytokines and inflammatory cells, resembling that of the human COVID-19 disease, have been described (Fagre et al., 2020; Griffin et al., 2020). Intranasal inoculation of bank voles with SARS-CoV-2 likewise led to viral replication in the respiratory tract without inducing any obvious clinical signs, detection of low amounts of viral genome in the central nervous and lymphatic systems, and seroconversion (Ulrich et al., 2020a). Intra-species transmission to direct in-contact animals was not observed (Ulrich et al., 2020a).

When SARS-CoV-2 was detected in a mink farm in the Netherlands (ProMED-mail, 2020b), fur-bearing animals kept for pelt production, particularly the three main species *Neovison vison* (mink), foxes (several genera of the family Canidae), and raccoon dogs, became a focus of interest.

These animals also are held in large numbers in China (ACT Asia, 2019) and raccoon dogs had already been considered as potential intermediate hosts for SARS-CoV. The Netherlands reported its first case of SARS-CoV-2 in a mink farm at the end of April 2020, which was amid the first wave of the pandemic. Shortly afterwards, the virus was detected in a second farm. Both farms reported respiratory symptoms and the latter an increase in mortality (OIE, 2021b). A first epidemiological investigation demonstrated that the virus was most likely introduced by infected farm workers on two separate occasions. In addition, the airborne inhalable dust on the farm was found positive for viral RNA and suspected to be the source of transmission within the farm to both mink and workers. On both farms the outbreak was reported to be self–limiting, as the symptoms disappeared together with the viral RNA in the dust. Seroconversion was found in nearly all sampled animals (Oreshkova et al., 2020) indicating a high infection rate. As of January 6, 2021, the number of infected farms had risen to 69 farms in the Netherlands alone, of which 29 (42%) reported respiratory clinical signs in their mink. An evaluation of these cases focusing on virus introduction and transmission is currently under way (OIE, 2021b). Besides the Netherlands, Denmark, Sweden, the USA, Canada, France, Spain, Greece, Lithuania and Poland (OIE, 2021b; Rabalski et al., 2020) reported SARS-CoV-2 infections in mink farms. SARS-CoV-2 positive workers could be identified in the vast majority of cases as the source of infection (OIE, 2021b). Like in the Netherlands, respiratory symptoms were reported in the animals for a subset of farms by the other countries as well, occasionally accompanied by an increase in mortality (OIE, 2021b). Pathological examination found an interstitial pneumonia in almost all sampled mink that supposedly died because of the SARS-CoV-2 infection (Molenaar et al., 2020; Oreshkova et al., 2020).

In Denmark, an intensive surveillance program was started after the first farms tested positive in June 2020, leading to the detection of 25 infected holdings until the 1st of October 2020 and 67 additional farms until the 16th of October (OIE, 2021b). By the 1st of December, this number had increased to 289 farms, which represents 20% of the Danish mink farms (WHO, 2020b). In about a third of the affected farms, no clinical signs were observed (Boklund et al., 2021). An extensive sampling of the environment and of numerous animals roaming around the farms did not lead to a conclusive explanation of the transmission mode between farms, except for direct transfer by infected humans (Boklund et al., 2021). Particularly worrying, mink to human transmission occurred in the affected farms

and pelting facilities, resulting in at least 982 mink-associated human infections by November 2020 (Oude Munnink et al., 2020; WHO, 2020b). Moreover, a new mutation within the viral genome was found in SARS-CoV-2 of mink-origin, comprising characteristic S-protein changes, subsequently referred to as cluster V mutations (Frutos and Devaux, 2020; Koopmans, 2020; Lassaunière et al., 2020; OIE, 2021b). Preliminary findings suggested decreased sensitivity of this variant toward neutralization by convalescent patient serum that could potentially interfere with vaccine efficiency (Lassaunière et al., 2020). Furthermore, the deletion of amino acids 69 and 70 within the S-coding region is likely to perturb detection by RT-PCR (ECDC, 2020). However, a broadly-based sequencing campaign of positive human patient samples revealed that the proportion of infection with the mink virus variant continuously decreased from June to mid-November (from 60% to 31%), and from the 20th of November onwards no new human cluster V infections were detected (WHO, 2020b). Hence, this mink-associated virus variant is believed to be extinct by now (Mallapaty, 2020; WHO, 2020c). Overall, mink in fur farms appear to be highly susceptible for SARS-CoV-2 outbreaks. A high proportion of mink in the infected premises were infected within a short period of time, with only a subset of animals, if any, developing clinical signs (Boklund et al., 2021; Hamer et al., 2020; OIE, 2021b). Both, the high susceptibility of mink as well as the lack of clinical signs imply a potential hazard for workers on mink farms and continuous re-emergence of SARS-CoV-2 variants (Koopmans, 2020). Furthermore, mink might play a potential role as an animal reservoir or intermediate host, especially since natural infection of wild free-ranging mink also has been reported (ProMED-mail, 2020d).

Another animal species kept for fur production is the raccoon dog (ACT Asia, 2019). In the aftermath of the first SARS outbreak in China, raccoon dogs sampled at a wet market were found to carry SARS-CoV and related viruses (Guan et al., 2003; Kan et al., 2005). Due to this finding and because of the high similarity of SARS-CoV sequences from raccoon dogs and humans (Bolles et al., 2011; Gautam et al., 2020; Graham and Baric, 2010; Lam et al., 2020a), raccoon dogs are considered to be one of the key amplifying hosts for SARS-CoV, with intra-species spread and transmission to humans. To investigate their susceptibility for SARS-CoV-2, raccoon dogs were experimentally infected and co-housed with uninfected controls (Freuling et al., 2020). Viral replication to relatively high titers without obvious clinical signs followed by seroconversion could be observed in six of nine intranasally inoculated animals and two of three

in-contact animals. Virus distribution and pathological changes resembled a transient subclinical infection, with a restriction of virus replication to the nasal cavities (Freuling et al., 2020). Because of the combination of rapid virus replication and shedding without clinical disease, raccoon dogs could represent a putative amplifying host and may have served as an intermediate host in the initial spread of SARS-CoV-2 from a presumed bat reservoir to humans.

To summarize the current knowledge about potential intermediate hosts, members of the Feliformia and Caniformia, the same subfamilies as involved in the SARS-CoV epidemic in 2002–2003, are the mammals that most likely play a role as intermediate hosts of SARS-CoV-2, since they are susceptible, replicate the virus to high titers and transmit to other animals and occasionally to humans. In addition, members of the Cricetidae family are susceptible to SARS-CoV-2 and shed the virus to an appreciable amount.
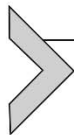
3. Pet animals and their non-domesticated counterparts

Pet animals live in close contact with humans and in most cases share a common living space. The close interaction between humans and pets poses a potential risk for the transmission of zoonotic pathogens (Chomel, 2014). Among companion animals, *Felis catus* (cats) and *Canis familiaris* (dogs) are at the center of attention, since they are the most common pet species and tend to have contact to humans outside of their own household (Overgaauw et al., 2020).

Both dogs and cats were shown to be susceptible to an experimental infection with SARS-CoV-2. In an initial animal trial, subadult dogs (3 months) showed a low susceptibility to infection, as only two of five animals seroconverted, and no transmission to uninoculated co-housed dogs was observed (Shi et al., 2020). Juvenile (<100 days old) and subadult (6–9 months old) cats, on the other hand, proved to be highly susceptible to a SARS-CoV-2 infection, since all inoculated animals became positive by RT-PCR in various organs, and developed antibodies. In addition, two of six in-contact cats became infected through intra-species transmission. They seroconverted and were positive by RT-PCR in organs of the upper respiratory tract and nasal washing (Shi et al., 2020). A subsequent experimental study confirmed these results for adult animals. Additionally, several of the infected cats were challenged with an additional inoculation of SARS-CoV-2 after 28 days. No shedding of virus was detected after the second

inoculation, indicating an effective protection against a secondary virus infection (Bosco-Lauth et al., 2020). None of the experimental studies to this date described clinical signs in any of the infected animals (Bosco-Lauth et al., 2020; Gaudreault et al., 2020; Halfmann et al., 2020; Shi et al., 2020). However, histopathological analyses revealed lesions in the nasal and tracheal mucosa epitheliums and lungs (Bosco-Lauth et al., 2020; Gaudreault et al., 2020; Shi et al., 2020).

The susceptibility of cats and dogs was further confirmed by serosurveillance studies. The first surveillance study was conducted in Wuhan during the initial outbreak. Out of 102 randomly sampled cat sera, antibodies against SARS-CoV-2 were found by ELISA in 15 sera (14.7%). In addition, 11 of the ELISA-positive sera tested positive in serum neutralization assays (Zhang et al., 2020a). In Italy, a similar survey was conducted during a time of frequent human infections. In that study, 11 out of 191 cats (5.8%) and 15 out of 451 (3.3%) dogs tested positive for neutralizing antibodies (Patterson et al., 2020). Another surveillance study performed in Germany during the first wave of the pandemic found 6 out of 920 randomly sampled cat sera positive for SARS-CoV-2 antibodies by ELISA. The prevalence of 0.7% in the sampled cat sera corresponded with the estimated prevalence of human infection of 0.85% during the sampling period. In two of the six positive sera, neutralizing antibodies could be detected (Michelitsch et al., 2020). In a study performed in France, two out of 13 dogs (15.4%) and eight out of 34 cats (23.5%) from households that were known to be infected with SARS-CoV-2 were found positive for SARS-CoV-2-specific antibodies. Another positive sample was found among 16 cats from households with an unknown infection status (Fritz et al., 2021). For details about seroprevalence studies performed in cats and dogs see Table 1. Overall, these initial surveillance studies show that infections of cats and dogs with SARS-CoV-2 occur frequently.

To assess the impact of inter-species transmission on the course of the pandemic, single case reports need to be investigated, in which transmission to co-housed pets and re-infection of humans might be observed. In six case studies, the course of infection was described for two dogs and a total of 14 cats (Barrs et al., 2020; Garigliany et al., 2020; Neira et al., 2020; Newman et al., 2020; Sailleau et al., 2020; Segalés et al., 2020; Sit et al., 2020). While the dogs remained free of clinical signs, six of the cats were described to have clinical signs similar to COVID-19 disease in humans. The cats were reported to show mild respiratory signs, sneezing and ocular discharge. In none of the studies was transmission from an infected pet to a

Table 1 Overview of the surveillance studies of SARS-CoV-2 in pets.

Sampling period	Species	Prevalence	Household	Neutral. AB	Country	References
January–March 2020	Cat	15/120 (14.7%)	Unknown	11/15	China	Zhang et al. (2020a)
March–May 2020	Cat	11/191 (5.8%)	Unknown	11/11	Italy	Patterson et al. (2020)
March–May 2020	Dog	15/451 (3.3%)	Unknown	15/15	Italy	Patterson et al. (2020)
April–September 2020	Cat	6/920 (0.7%)	Unknown	2/6	Germany	Michelitsch et al. (2020)
May–June 2020	Cat	8/34 (23.5%)	Infected	n.a.	France	Fritz et al. (2021)
May–June 2020	Dog	2/13 (15.4%)	Infected	n.a.	France	Fritz et al. (2021)

Testing was performed on serum samples. Prevalence gives the rate of positive samples in relation to all tested samples. Neutral. AB: number of positive samples that tested positive for neutralizing antibodies. n.a.: data is not available

human or a co-housed pet described (Barrs et al., 2020; Garigliany et al., 2020; Neira et al., 2020; Newman et al., 2020; Sailleau et al., 2020; Segalés et al., 2020). Further, additional cases are constantly reported to the world organization for animal health (OIE) and displayed on their official website (OIE, 2021b). The following analysis is based on the reports that were submitted until January 15, 2021. Seventeen countries had reported SARS-CoV-2 infection in a pet animal.

Altogether 103 SARS-CoV-2 infected animals, 57 cats and 46 dogs were reported to the OIE. The reports mentioned symptoms that could be linked to a SARS-CoV-2 infection in 26 cats (45.6%) and 21 dogs (45.7%), of which 7 cats (26.9%) and 2 dogs (9.5%) were reported to have preexisting comorbidities. Clinical signs in cats were mostly described as respiratory (13/26; 50.0%), of which 38.5% (5/13) were defined as very mild or mild, or as nasal (7/26, 26.9%) or ocular discharge (2/26, 7.7%). Dogs were also reported to show respiratory signs (9/21; 42.9%), of which 44.4% (4/9) were classified as mild, sneezing (8/21; 38.1%) and nasal discharge (5/21; 23.8%). The majority of cases were found through screening pet animals from households that were confirmed to be SARS-CoV-2 positive. In addition, the USA reported 53 pet animals that were found to be positive for antibodies against SARS-CoV-2 (OIE, 2021b). Although the reported cases hint at frequent inter-species transmission events, a study performed on SARS-CoV-2-infected veterinary students, that tracked their pet animals closely during the course of infection found no signs of infection in the studied nine cats and 12 dogs (Temmam et al., 2020).

In summary, the transmission of SARS-CoV-2 to animals from infected humans happens on a regular basis. Since clinical signs are mostly described as mild or in the context of severe comorbidities, and considering the experimental infection studies, the course of infections in cats and dogs seems to be mild. To date, no transmission of SARS-CoV-2 from an infected pet to its owner, to another house pet or a human was described (Barrs et al., 2020; Garigliany et al., 2020; Neira et al., 2020; Newman et al., 2020; Sailleau et al., 2020; Segalés et al., 2020). However, hygienic standards should be applied when interacting with a potentially infected animal and quarantine requirements should be extended to animals that had extensive contact with an infected human. Recommendations can be found from the various official institutions (ABCD (Advisory Board on Cat Diseases), 2021; CDC (Centers for Disease Control and Prevention), 2021; WSAVA (World Small Animal Veterinary Association), 2020).

Given the regular transmission of SARS-CoV-2 from infected owners to their pet cats and dogs, it was to be expected that the virus might also be spread to non-domesticated felines or canines. Infections of felines in zoos were indeed reported to the OIE (OIE, 2021b). Early in the pandemic, the Bronx Zoo in New York reported the infection of four *Panthera tigris* (tigers), and three *Panthera leo* (lions), which exhibited mild respiratory clinical signs for up to 2 weeks. A fifth tiger remained asymptomatic (Bartlett et al., 2020). Sequence analysis from samples of the affected animals showed that the tiger SARS-CoV-2 belonged to a different genotype than the lion viruses. Both genotypes were also found in the corresponding animal caretakers. Therefore, a transmission from the attending humans to the cared-for animals seems to have happened on two different occasions (McAloose et al., 2020). Three other zoos in the United States reported SARS-CoV-2 infections in large felids, three additional tigers and a *Panthera uncia* (snow leopard) with mild respiratory symptoms (OIE, 2021b). In South Africa, a *Puma concolor* (puma) acquired a SARS-CoV-2 infection from a zookeeper. No symptoms were reported, and the contact animals were negative by RT-PCR (OIE, 2021b). In addition, news outlets reported the infection of four additional lions in a zoo in Barcelona, Spain, and a tiger and four lions in a zoo in Sweden. They showed mild respiratory symptoms and were most likely infected by an asymptomatic zookeeper in whom an infection with SARS-CoV-2 was subsequently diagnosed (ProMED-mail, 2020a,c).

Tigers, snow leopards and lions are members of the genus *Panthera*, and pumas belong to the genus *Puma*. Both genera are part of the phylogenetic family Felidae, the same family to which the genus (*Felis*) of the domestic cat belongs. Keeping in mind the several reports of SARS-CoV-2 infections in cats (Barrs et al., 2020; Garigliany et al., 2020; Neira et al., 2020; Newman et al., 2020; Sailleau et al., 2020; Segalés et al., 2020), it is no surprise that large cats were also found to be infected in zoos. Although, reverse transmission from zoo animal to human has not been observed until know, strict hygiene rules should be implemented in the management of zoo animals.
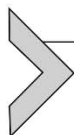
4. Livestock animals

As the SARS-CoV-2 outbreak evolved rapidly into a global pandemic and the zoonotic origin of the pathogen became obvious, there were apprehensions that farmed livestock species could be involved in virus

transmission. The world livestock population is by far larger than the human population (Tomley and Shirley, 2009) and livestock demand will continue to increase with human population growth and socio-economic trends (Alexandratos and Bruinsma, 2012; Herrero and Thornton, 2013). Furthermore, close connection between humans and farmed animals exists in small-scale agriculture as well as in intensified livestock-producing-systems. This close contact is considered to be a fundamental driver of emerging zoonotic diseases, of which viral diseases have become increasingly important (Gilbert et al., 2020; Klous et al., 2016; Wiethoelter et al., 2015). Although the origin of the SARS-CoV-2 pandemic was suspected to be traced to the Huanan Seafood Market (Huang et al., 2020), concerns were raised about the susceptibility of major mammalian livestock and poultry species, particularly as the first ever described coronavirus was infectious bronchitis virus (IBV) of chickens in 1931 (Schalk and Hawn, 1931). Besides IBV, many other livestock-affecting coronaviruses of different genera have been found (e.g., additional bird, bovine, and porcine coronaviruses) (Clark, 1993; Wang et al., 2019; Wille and Holmes, 2020). Of these livestock species, cattle with an estimated global population of 1.5 billion (FAO, 2020) were discovered to be the potential intermediate host for HCoV-OC43, one of the only two human coronaviruses that were known until SARS-CoV emerged in 2002/03 (Cui et al., 2019; Drexler et al., 2014; Forni et al., 2017). Because of the close relatedness of bovine coronaviruses and human HCoV-OC43 (Bidokhti et al., 2013; Vijgen et al., 2005; Vijgen et al., 2006), and also due to the similarity of the cattle ACE2 receptor to that of humans (Damas et al., 2020; Luan et al., 2020), concerns about the potential role of cattle in the SARS-CoV-2 pandemic were raised. Susceptibility of bovine tracheal and lung *ex vivo* organ cultures (EVOCs) toward SARS-CoV-2 was tested in an air–liquid interface system using two different SARS-CoV-2 isolates and viral titers were found to be higher in bovine lung EVOCs than tracheal EVOCs (Di Teodoro et al., 2020). In an *in vivo* study, experimental SARS-CoV-2 infection of 6-month-old Holstein-Friesian dairy calves resulted in a short virus replication in the upper respiratory tract in two out of six animals that subsequently seroconverted. One calf was found positive in a nasal swab on days two and three after infection, another one on day three only. Transmission to commingled cattle did not occur. Despite viral replication and seroconversion, clinical disease was not observed (Ulrich et al., 2020b). Furthermore, no serological cross-reactivity of antibodies against bovine coronavirus and SARS-CoV-2 was recorded (Ulrich et al., 2020b).

For *Sus scrofa* (pigs), another major livestock species (Gilbert et al., 2018), the susceptibility for SARS-CoV-2 was suspected, as they can be infected with MERS-CoV and were found to host several other coronaviruses (de Wit et al., 2017; Gong et al., 2017; Opriessnig and Huang, 2020; Pan et al., 2017; Vergara-Alert et al., 2017a,b; Wang et al., 2019; Widagdo et al., 2019a). In addition, computational analyses of the porcine ACE2 protein revealed that it shares significant identity with human ACE2 in residues contacting the viral spike protein (Wan et al., 2020). *In vitro*, SARS-CoV-2 bound to HeLa cells expressing the porcine ACE2 instead of the human orthologue (Zhou et al., 2020). Furthermore, SARS-CoV-2 replicated in porcine SK-6 and ST cell lines (Meekins et al., 2020; Schlottau et al., 2020), but not in swine tracheal and lung EVOCs (Di Teodoro et al., 2020). In experimental infections, the outcome seems to be dependent on the inoculation route and virus titer. Nevertheless, in general the susceptibility of pigs for SARS-CoV-2 appears very low. Intranasal application of 10^5 plaque forming units (PFU) or 10^5 tissue culture infectious dose 50% ($TCID_{50}$) of SARS-CoV-2 did not lead to virus replication or seroconversion in 40-day old Landrace × Large White pigs of both sexes or 9-week old German Landrace pigs, respectively (Schlottau et al., 2020; Shi et al., 2020). Clinical signs as well as pathological lesions were also absent and transmission to contact animals did not occur (Schlottau et al., 2020; Shi et al., 2020). Meekins et al. (2020) used younger piglets and simultaneously infected them intranasally, orally, and intratracheally with a higher $TCID_{50}$ of 10^6, while Vergara-Alert et al. (2020) investigated among other infection routes intramuscular and intravenous application using $10^{5.8}$ $TCID_{50}$ of culture-grown SARS-CoV-2. Seroconversion was reported for parenterally infected animals (Meekins et al., 2020; Vergara-Alert et al., 2020). Remarkably, one intranasally inoculated piglet was found positive for viral RNA in the proximal trachea on the day after inoculation (Vergara-Alert et al., 2020). In another *in vivo* study, inoculation of 10^6 PFU of SARS-CoV-2 simultaneously into the nostrils and the pharynx of 8-week-old American Yorkshire crossbred piglets resulted in mild clinical signs in at least 5 out of 19 animals (Pickering et al., 2021). Ocular discharge, nasal secretion and cough were observed within the first days after infection, but body temperature remained normal. Nasal, oral, and rectal swab samples tested negative for SARS-CoV-2 genome. Two pigs, however, tested weakly positive in a nasal wash sample collected 3 days after infection. In addition, infectious virus was isolated 13 days after infection from the submandibular lymph

node of a sacrificed pig. Two other pigs tested positive for serum antibodies and anti–SARS-CoV-2 antibodies were also detected in saliva recovered from chewing-ropes (Pickering et al., 2021).

Although mammals were identified as key players in SARS-CoV and MERS-CoV emergence and distribution (de Wit et al., 2016), SARS-CoV-2 susceptibility of different bird species was elucidated by several groups. Following oculo-oronasal inoculation of *Gallus gallus domesticus* (chickens) with high-titer virus preparations, neither virus replication nor seroconversion or transmission to in–contact chickens could be observed (Schlottau et al., 2020; Shi et al., 2020). *In vivo* experimental infection studies using *Anas platyrhynchos domesticus* (ducks) led to identical results, i.e., neither virus replication nor seroconversion occurred (Shi et al., 2020). Besides chicken and ducks, *Meleagris galloparvo* (turkey), *Coturnix japonica* (Japanese quail) and *Anser cygnoides* (Chinese goose) were experimentally infected. None of the tested poultry species showed any susceptibility toward SARS-CoV-2 infection (Berhane et al., 2020; Suarez et al., 2020). Further, the ability of SARS-CoV-2 to replicate in embryonated chicken eggs was evaluated. Inoculation into the yolk sac, the chorio-allantoic membrane or the chorio-allantoic sac did not lead to virus replication and embryogenesis was not impaired (Barr et al., 2020; Berhane et al., 2020; Schlottau et al., 2020; Suarez et al., 2020).

5. Animal models in SARS-CoV-2 research

Suitable animal models reflecting different aspects of SARS-CoV-2 pathogenesis are required to assist in development of antiviral vaccines and treatment options, and also to study the mechanistic basics of SARS-CoV-2 infections.

One of the most widely used laboratory animal in biomedical research is the mouse. For SARS-CoV-2, however, infection studies in wild-type mice are hampered by the lack of appropriate receptors to initiate viral infection, as murine ACE2 does not bind the viral spike protein effectively (Wan et al., 2020). This obstacle might be overcome by either virus adaptation to mice or by expression of human ACE2 in genetically modified mice. Both approaches were successful for the closely related MERS-CoV (Kim et al., 2020a; Li and McCray, 2020), in which the murine dipeptidyl peptidase 4 receptor failed to support MERS-CoV infection. For SARS-CoV-2, genetically modified mice were generated that express human ACE2, e.g., driven

by the mouse ACE2 promotor (ACE2-hACE2 mice), by the human keratin 18 promoter (K18-hACE2 mice), by the human lung ciliated epithelial cell-specific HFH4/FOXJ1 promoter (HFH4-hACE2 mice) or by the cytomegalovirus enhancer followed by the chicken β-actin promoter (Bao et al., 2020a,b; Jiang et al., 2020; Oladunni et al., 2020; Tseng et al., 2007; Winkler et al., 2020). Human ACE2 was also expressed by insertion into the endogenous mouse ACE2 gene locus via CRISPR/Cas9 technology (Sun et al., 2020b). Another approach to rapidly produce susceptible mice without additional breeding utilized the transduction of human ACE2 into cells of the respiratory tract through intranasal, intratracheal or oropharyngeal instillations of adenoviral vectors expressing human ACE2 (Han et al., 2020; Hassan et al., 2020; Israelow et al., 2020; Sun et al., 2020a). Independent of the protein expression approach, mouse breed and experimental design, all mice expressing the human ACE2 receptor instead of the mouse orthologue are susceptible to SARS-CoV-2 as demonstrated by a robust virus replication in the respiratory tract. However, varying degrees of disease were observed. Clinical signs ranged from weight loss and pneumonia to pathological alterations also found in human COVID-19 patients and, in some studies, brain infestation and differing numbers of fatalities (Golden et al., 2020; Han et al., 2020; Hassan et al., 2020; Israelow et al., 2020; Jiang et al., 2020; Rathnasinghe et al., 2020; Sun et al., 2020a,b; Yinda et al., 2021). Hence, human ACE2 expressing mice facilitate investigations of the pathogenesis of severe COVID-19 by, e.g., histopathological analyses at varying time points after infection, measuring the cytokine responses (Israelow et al., 2020; Oladunni et al., 2020) or analyzing the transcriptome of lungs of diseased mice (Han et al., 2020). However, this mouse model currently does not reflect all aspects of COVID-19, since unusual features such as the hyperinflammatory syndromes that are sometimes seen in children (Yasuhara et al., 2021) have not been observed in human ACE2 mice. Nevertheless, as human ACE2 expressing mice shed high viral titers and efficiently transmit SARS-CoV-2 to naïve in-contact animals (Bao et al., 2020b), they represent a useful model for transmission studies. In addition, human ACE2 expressing mice provide a suitable tool to evaluate vaccines and therapeutics, as has been demonstrated by research groups worldwide (e.g., Hassan et al., 2020; Ku et al., 2020; Li et al., 2020a,b; Seo and Jang, 2020; Sun et al., 2020a; Zheng et al., 2020a). A further approach to circumvent the lack of susceptibility of wild-type mice to SARS-CoV-2 is the use of mice displaying a humanized immune system induced by infusion of human hematopoietic stem cells, which leads to

severe COVID-19-like symptoms in the respective mouse line (Brumeanu et al., 2020). Besides the adaptations of mice to SARS-CoV-2, one could use a reverse approach and adapt the virus to mice (Dinnon et al., 2020; Gu et al., 2020; Wang et al., 2020). Mouse-adapted SARS-CoV-2 would allow the use of more readily available mouse strains. However, a major disadvantage is the limited suitability for pathogenesis studies, when new virus mutants that emerge in the field have to be rapidly tested for altered *in vivo* behavior. Nevertheless, this animal model of wild-type mouse/adapted virus is still applicable to test therapeutics and preventive measures (Dinnon et al., 2020; Wang et al., 2020).

Another widely used small animal model in research of human diseases is the hamster. *In silico* comparisons of the ACE2 receptor suggested that hamsters, in contrast to mice, might be susceptible to SARS-CoV-2 infection without any further adaptation (Damas et al., 2020). Consequently, *Mesocricetus auratus* (golden Syrian hamster), *Cricetulus griseus* (Chinese hamster), *Phodopus roborovskii* (Roborovski dwarf hamster), *Phodopus campbelli* (Campbell's dwarf hamster) and *Phodopus sungorus* (Djungarian hamster) have been explored regarding their suitability to support SARS-CoV-2 replication and to develop disease similar to human COVID-19 (Bertzbach et al., 2020; Imai et al., 2020; Osterrieder et al., 2020; Rosenke et al., 2020; Trimpert et al., 2020). All investigated hamster species are susceptible. However, the course of disease and the outcome of infection vary dramatically. While Campbell's or Djungarian dwarf hamsters show either no or only mild clinical signs, Roborovski dwarf hamsters develop a fulminant disease characterized by decrease of body temperature, weight loss, snuffling, dyspnea, ruffled hair and strongly reduced activity within the first three days following infection. By day four or five after infection, most individuals reached a pre-defined humane endpoint (Trimpert et al., 2020). In golden Syrian hamsters, experimental SARS-CoV-2 infection induced weight loss, ruffled fur, postural changes, labored breathing, damage of the olfactory epithelium and severe lung pathology mimicking that of COVID-19 in humans, associated with virus replication to high titers in the upper and lower respiratory and gastrointestinal tracts followed by a profound immune response (Bertzbach et al., 2020; Boudewijns et al., 2020; Bryche et al., 2020; Imai et al., 2020; Osterrieder et al., 2020; Rosenke et al., 2020; Sia et al., 2020; Tostanoski et al., 2020). Furthermore, microcomputed tomographic imaging of hamster lung samples revealed severe injury, with characteristics shared with COVID-19-diseased humans (Imai et al., 2020). Co-infection with influenza A virus led to a more severe course of disease

(Zhang et al., 2020c). Moreover, older hamsters exhibited more pronounced and consistent weight loss, while young animals launched an earlier and stronger immune cell influx into the lungs resulting in a faster recovery from the disease compared with aged hamster (Osterrieder et al., 2020). Hence, golden Syrian hamsters reflect the age-dependent disease progression seen in human patients, with the limitation that they do not develop the fatal course of disease that often occurs in elderly humans. This obstacle could be overcome by chemically induced immunosuppression or by using genetically modified animals, e.g., recombination activating gene 2-knockout hamster, which develop more pronounced clinical signs and fatalities (Brocato et al., 2020). Nevertheless, even wild-type golden Syrian hamsters might be used for comparative preclinical assessments of treatment options in young versus elderly individuals. As golden Syrian hamsters shed the virus to high titers and efficiently transmit SARS-CoV-2 by direct contact and via aerosols (Chan et al., 2020; Sia et al., 2020), they are also used as a model to study the mechanisms of intra-species transmission.

The third frequently used small model animal is rabbit. This species is used mainly for immunization, but also for implant research (Mapara et al., 2012) as well as a model for various human infectious diseases, among them norovirus infections, syphilis, tuberculosis, or human papillomavirus infections (Esteves et al., 2018). Important for SARS-CoV-2 research, rabbits were already proven to be susceptible for MERS-CoV (Haagmans et al., 2015; Houser et al., 2017; Widagdo et al., 2019b) and *in silico* analyses using different animal ACE2 receptors predicted rabbits to be also susceptible for SARS-CoV-2 (Damas et al., 2020). Further, it was shown that SARS-CoV-2 replicated in the rabbit derived cell-line RK-13 (Chu et al., 2020). Hence, experimental SARS-CoV-2 infection studies in rabbits seemed obvious. Surprisingly, to date only one study is published (Mykytyn et al., 2021). Three-month-old New Zealand white rabbits were intranasally inoculated, which resulted in virus replication and shedding from the nose and throat followed by seroconversion. Four days after infection, the olfactory epithelium showed hyperplasia and hypertrophy, along with multifocal eosinophilic and lymphoplasmacytic infiltration. Antigen was not detected in immunohistochemical stainings of the lungs. Alveolar macrophages and neutrophils, however, were increased. In the terminal region of the bronchioles, mildly thickened septa and inflammatory cells could be detected. Alveolar epithelium cells showed mild necrosis and peribronchiolar and peribronchial lymphoid tissue proliferation, and tracheo-bronchial lymph nodes were enlarged. Despite the histopathologic abnormalities, clinical disease was not present in rabbits.

An animal model used especially in studies that investigate the pathogenesis and transmission of human respiratory viruses such as influenza virus is ferrets (*Mustela putorius*), since their lungs share many similarities with that of humans. As previous studies have shown that ferrets are susceptible to SARS-CoV infection and readily transmit the virus to in-contact animals (Martina et al., 2003), this animal model was tested very early during the pandemic for susceptibility to SARS-CoV-2. After experimental infection with SARS-CoV-2, high level virus replication was observed in the upper respiratory tract associated with either no or only mild clinical signs such as transient loss of appetite or elevated body temperature (Kim et al., 2020b; Marsh et al., 2021; Ryan et al., 2021; Schlottau et al., 2020; Shi et al., 2020). Importantly, air-borne transmission via respiratory droplets and/or aerosols to in-contact animals could be demonstrated (Richard et al., 2020), making the ferret a highly suitable model for transmission studies and for testing (mucosal) vaccines and therapeutics for their effect on virus shedding (Cox et al., 2020; Proud et al., 2020). Moreover, a first natural infection of a ferret that was kept as a pet in a SARS-CoV-2 positive household was reported to the OIE at the end of November, further proving the high susceptibility of ferrets to SARS-CoV-2 infection (OIE, 2021b).

When a severe acute respiratory syndrome emerged as a novel human infectious disease in 2002 non-human primate models were used to demonstrate that SARS-CoV was the etiological agent (Fouchier et al., 2003). Based on these studies, non-human primates also were investigated regarding their suitability as animal models to study the pathogenesis of MERS-CoV-2 (de Wit et al., 2013; Falzarano et al., 2014) and recently also for SARS-CoV-2. So far *Macaca fascicularis* (Cynomolgus macaque), *Macaca mulatta* (rhesus macaque), *Chlorocebus aethiops* (African green monkey), *Callithrix jacchus* (common marmoset) and *Papio hamadryas* (baboon) have been experimentally infected with SARS-CoV-2 (Lu et al., 2020b; Rockx et al., 2020; Shan et al., 2020; Singh et al., 2021; Woolsey et al., 2020).

Although a certain variability in clinical manifestations was seen between "Old World" and "New World" monkeys with Old World monkeys developing a more severe disease, the virus replicated efficiently in the upper and lower respiratory tract of all investigated primate species, leading to pathological features of a viral pneumonia. The clinical course is either inapparent or mild to moderate, where the symptoms include rise in body temperature, weight loss, reduced appetite, hunched posture, dyspnea or increased respiration rate (Blair et al., 2020; Deng et al., 2020a; Ishigaki et al., 2020; Koo et al., 2020; Lu et al., 2020b; Munster et al., 2020;

Williamson et al., 2020). The high susceptibility of monkeys followed by the development of mild clinical signs is further supported by natural infections of *Gorilla gorilla* (gorillas) that are kept in human care in zoos and that had contact to infected animal keepers (OIE, 2021b). In some experimentally infected animals, besides direct clinical symptoms, increased inflammatory cytokine and chemokine expression, reduced pulse oxygen levels or alterations of the level of selected plasma proteins, e.g., the release of acute-phase-proteins like CRP, decreased serum albumin or hemoglobin and reduced white blood cell and lymphocyte counts could be observed (Chandrashekar et al., 2020; Deng et al., 2020a; Fahlberg et al., 2020; Lu et al., 2020b; Singh et al., 2021; Zheng et al., 2020b). Importantly, older animals were more likely to develop radiological and histopathological changes than young primates, recapitulating the clinical outcome seen in the human population. In addition, aged animals shed virus for longer periods of time, had higher viral loads in lung tissue and showed a delay in the immune response compared to young animals (Rockx et al., 2020; Song et al., 2020; Yu et al., 2020b). Notwithstanding, a profound humoral and cellular immune response that protects from re-infection is induced in the vast majority of infected non-human primates, independent of species and age (Chandrashekar et al., 2020; Deng et al., 2020a; Elizaldi et al., 2020; Ishigaki et al., 2020; McMahan et al., 2020). Therefore and because monkeys reflect the clinical picture seen in humans, non-human primates are used by numerous research groups and pharmaceutical companies to test candidate vaccines and therapeutics against COVID-19 (e.g., Baum et al., 2020; Corbett et al., 2020; Feng et al., 2020; Guebre-Xabier et al., 2020; Hoang et al., 2020; Kim et al., 2021; Maisonnasse et al., 2020; van Doremalen et al., 2020; Williamson et al., 2020; Yu et al., 2020a). However, the resources for those complex trials and the available animals are limited. Therefore, research and testing of therapeutics and vaccines with SARS-CoV-2 and non-human primates need to be well focused.

A species genetically closely related to non-human primates and recently increasingly used in pathogenesis studies for many human pathogens is *Tupaia belangeri chinensis* (Chinese tree shrew) (Li et al., 2018). Experimental SARS-CoV-2 infection of different age groups resulted in viral shedding from various sites (nose, oral cavity, rectum), with higher titers in the early phase after infection in young tree shrews, but longer-lasting in aged individuals (Zhao et al., 2020a). The highest viral loads were detectable in the lungs, again in younger animals in the early phase and in older animals at a later stage after infection, hinting at age-related effects. Clinical signs could

not be observed, except from an increase in body temperature in some animals (Zhao et al., 2020a). Evidence for inflammatory processes in the lungs were found in all age groups, and infiltrates resembled those observed in humans and monkeys (Xu et al., 2020).
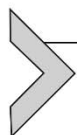
6. Concluding remarks

Within only a few months, the novel coronavirus SARS-CoV-2 spread around the globe, resulting in tens of millions of infections in the human population and about two million deaths. The pandemic has affected public and personal life in manifold spheres with an inconceivable impact. Unprecedented research efforts have been implemented to keep up with an exceedingly dynamic virus. To control the pandemic, but also to prevent future outbreaks that might be caused by similar pathogens, main objectives are the discovery of the SARS-CoV-2 ancestor virus, its animal host, as well as potential animal hosts and reservoirs. Moreover, adequate animal models are needed to understand the dynamics of virus infection and the human disease "COVID-19," as well as to test preventive measures and therapy options. In a global effort, an enormous number of research groups tested a plethora of animal species regarding their susceptibility to SARS-CoV-2 and suitability as a COVID-19 animal model resembling the human disease.

Here, we collected evidence from the literature to establish a scoring system considering the proportion of animals in which the viral genome was detectable subsequent to inoculation reflecting virus multiplication, the seroconversion rate, clinical signs and the ability to transmit the virus to conspecifics or humans. For each category zero to three points were awarded. In the category "genome detection" three points were given for the detection of viral RNA in all inoculated or tested animals of a certain species. Two points indicated a frequent detection and one point a sporadic event. The same gradation was applied in the category "seroconversion," but for the detection of antibodies instead of viral RNA. For the "transmission" category three points were awarded for an efficient transmission rate to conspecifics that indicates the potential to develop an independent transmission cycle. Two points were given for a regularly observed intraspecies transmission and one point for an occasional event. The category "clinical signs" was scored as follows: Three points stand for severe pan-respiratory or systemic symptoms that might end in death, two points for moderate respiratory or vascular symptoms and one point for mild,

nonspecific symptoms. The sum of all points was taken as a parameter for the overall susceptibility of each species for SARS-CoV-2. To provide an over-view about the susceptibility of diverse animal species and their ability to transmit the virus, we implemented this scoring system whose results are shown in Table 2 and visually summarized in Fig. 1. Fortunately, livestock animals that are kept in very high numbers worldwide appear not to play a

Table 2 Susceptibility of different animal species to SARS-CoV-2.

Animal	Genome detection	Seroconversion	Transmission to conspecifics	Clinics	Σ Awarded points
Chicken	0	0	0	0	0
Duck	0	0	0	0	0
Pig	0	1	0	0	1
Cattle	1	1	0	0	2
Dog	2	1	0	0	3
Rabbit	2	2	0	0	4
Fruit bat	2	1	2	0	5
Bank vole	3	3	0	0	6
Raccoon dog	2	2	2	0	6
Cat	2	2	1	1	6
Deer mouse	3	2	2	1	8
Ferret	3	3	2	0	8
White-tailed deer	3	3	3	0	9
Mink	2	3	3	1	9
Non-human primate	3	3	2	2	10
Hamster	3	3	3	3	12
hACE2 transgenic mouse	3	3	3	3	12

By a semi-quantitative scoring system zero to three points were awarded for each of the categories viral genome detection following SARS-CoV-2 inoculation, seroconversion, transmission to conspecifics and the development of clinical signs.
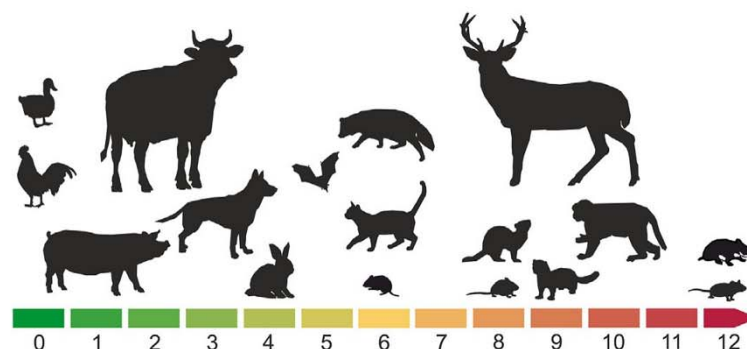
Fig. 1 Visual depiction of the scoring system for the susceptibility of different animal species for SARS-CoV-2. Three points each were awarded for the categories genome detection, seroconversion, transmission to conspecifics and clinical signs. Animal species were placed according to the sum of the awarded points. Zero points stand for no susceptibility and twelve points for a maximal susceptibility to SARS-CoV-2.

noteworthy role in the SARS–CoV–2 pandemics. Although viral replication was detectable in some of the investigated farm animal species (Table 2, Fig. 1), long-term virus shedding at relevant levels was not found, nor did transmission to contact-animals occur in any of these species, which would also make animal-to-human transmission unlikely. Besides some rodents, cervids, primates and related species, numerous Carnivora species have been found to be susceptible not only for experimental, but also for natural SARS–CoV–2 infection and intra–species transmission. In particular minks which are farmed in large numbers for fur production are at risk and mass outbreaks with subsequent culling measures have been seen, e.g., in the Netherlands and Denmark.

Finally, SARS–CoV–2 transmission from an animal reservoir, potentially via intermediate animals hosts, resulting in a global pandemic in the human population highlights the requirement of more holistic approaches in global health, considering the dependence and interaction between human health, animal health and environmental health as incorporated in the "One Health approach" (FAO, 2021; OIE, 2021a; WHO, 2021).

References

ABCD, 2021. SARS–Coronavirus (CoV)–2 and cats.

Abdel–Moneim, A.S., Abdelwhab, E.M., 2020. Evidence for SARS-CoV-2 infection of animal hosts. Pathogens 9, 529.

ACT Asia, 2019. China's fur trade and its position in the global fur industry. Online available: https://www.actasia.org/wp-content/uploads/2019/10/China-Fur-Report-7.4-DIGITAL-2.pdf. last accessed: 23 January 2021.

Anna Michelitsch et al.

Al-Ahmadi, K., Alahmadi, M., Al-Zahrani, A., 2020. Spatial association between primary Middle East respiratory syndrome coronavirus infection and exposure to dromedary camels in Saudi Arabia. Zoonoses Public Health 67, 382.

Alexandratos, N., Bruinsma, J., 2012. World Agriculture Towards 2030/2050: The 2012 Revision. Agricultural Development Economics Division, Food and Agriculture Organization of the United Nations (FAO). ESA Working Paper No. 12-03.

Andersen, K.G., Rambaut, A., Lipkin, W.I., Holmes, E.C., Garry, R.F., 2020. The proximal origin of SARS-CoV-2. Nat. Med. 26, 450.

Azhar, E.I., El-Kafrawy, S.A., Farraj, S.A., Hassan, A.M., Al-Saeed, M.S., Hashem, A.M., Madani, T.A., 2014. Evidence for camel-to-human transmission of MERS coronavirus. N. Engl. J. Med. 370, 2499.

Bao, L., Deng, W., Huang, B., Gao, H., Liu, J., Ren, L., Wei, Q., Yu, P., Xu, Y., Qi, F., Qu, Y., Li, F., Lv, Q., Wang, W., Xue, J., Gong, S., Liu, M., Wang, G., Wang, S., Song, Z., Zhao, L., Liu, P., Zhao, L., Ye, F., Wang, H., Zhou, W., Zhu, N., Zhen, W., Yu, H., Zhang, X., Guo, L., Chen, L., Wang, C., Wang, Y., Wang, X., Xiao, Y., Sun, Q., Liu, H., Zhu, F., Ma, C., Yan, L., Yang, M., Han, J., Xu, W., Tan, W., Peng, X., Jin, Q., Wu, G., Qin, C., 2020a. The pathogenicity of SARS-CoV-2 in hACE2 transgenic mice. Nature 583, 830.

Bao, L., Gao, H., Deng, W., Lv, Q., Yu, H., Liu, M., Yu, P., Liu, J., Qu, Y., Gong, S., Lin, K., Qi, F., Xu, Y., Li, F., Xiao, C., Xue, J., Song, Z., Xiang, Z., Wang, G., Wang, S., Liu, X., Zhao, W., Han, Y., Wei, Q., Qin, C., 2020b. Transmission of severe acute respiratory syndrome coronavirus 2 via close contact and respiratory droplets among human angiotensin-converting enzyme 2 mice. J. Infect. Dis. 222, 551.

Barr, I.G., Rynehart, C., Whitney, P., Druce, J., 2020. SARS-CoV-2 does not replicate in embryonated hen's eggs or in MDCK cell lines. Euro Surveill. 25, 2001122.

Barrs, V.R., Peiris, M., Tam, K.W.S., Law, P.Y.T., Brackman, C.J., To, E.M.W., Yu, V.Y.T., Chu, D.K.W., Perera, R., Sit, T.H.C., 2020. SARS-CoV-2 in quarantine domestic cats from COVID-19 households or close contacts, Hong Kong, China. Emerg. Infect. Dis. 26.

Bartlett, S.L., Diel, D.G., Wang, L., Zec, S., Laverack, M., Martins, M., Caserta, L.C., Killian, M.L., Terio, K., Olmstead, C., Delaney, M.A., Stokol, T., Ivančić, M., Jenkins-Moore, M., Ingerman, K., Teegan, T., McCann, C., Thomas, P., McAloose, D., Sykes, J.M., Calle, P.P., 2020. SARS-CoV-2 infection and longitudinal fecal screening in Malayan tigers (Panthera tigris jacksoni), Amur tigers (Panthera tigris altaica), and African lions (Panthera leo krugeri) at the Bronx Zoo, New York, USA. bioRxiv. 2020.08.14.250928.

Baum, A., Ajithdoss, D., Copin, R., Zhou, A., Lanza, K., Negron, N., Ni, M., Wei, Y., Mohammadi, K., Musser, B., Atwal, G.S., Oyejide, A., Goez-Gazi, Y., Dutton, J., Clemmons, E., Staples, H.M., Bartley, C., Klaffke, B., Alfson, K., Gazi, M., Gonzalez, O., Dick, E., Jr., Carrion, R., Jr., Pessaint, L., Porto, M., Cook, A., Brown, R., Ali, V., Greenhouse, J., Taylor, T., Andersen, H., Lewis, M.G., Stahl, N., Murphy, A.J., Yancopoulos, G.D., Kyratsous, C.A., 2020. REGN-COV2 antibodies prevent and treat SARS-CoV-2 infection in rhesus macaques and hamsters. Science 370, 1110.

Berhane, Y., Suderman, M., Babiuk, S., Pickering, B., 2020. Susceptibility of turkeys, chickens and chicken embryos to SARS-CoV-2. Transbound. Emerg. Dis.

Bertzbach, L.D., Vladimirova, D., Dietert, K., Abdelgawad, A., Gruber, A.D., Osterrieder, N., Trimpert, J., 2020. SARS-CoV-2 infection of Chinese hamsters (Cricetulus griseus) reproduces COVID-19 pneumonia in a well-established small animal model. Transbound. Emerg. Dis.

Bidokhti, M.R.M., Traven, M., Krishna, N.K., Munir, M., Belak, S., Alenius, S., Cortey, M., 2013. Evolutionary dynamics of bovine coronaviruses: natural selection pattern of the spike gene implies adaptive evolution of the strains. J. Gen. Virol. 94, 2036.

Blair, R.V., Vaccari, M., Doyle-Meyers, L.A., Roy, C.J., Russell-Lodrigue, K., Fahlberg, M., Monjure, C.J., Beddingfield, B., Plante, K.S., Plante, J.A., Weaver, S.C., Qin, X., Midkiff, C.C., Lehmicke, G., Golden, N., Threeton, B., Penney, T., Allers, C., Barnes, M.B., Pattison, M., Datta, P.K., Maness, N.J., Birnbaum, A., Fischer, T., Bohm, R.P., Rappaport, J., 2020. Acute respiratory distress in aged, SARS-CoV-2-infected African green monkeys but not rhesus macaques. Am. J. Pathol.

Boklund, A., Hammer, A.S., Quaade, M.L., Rasmussen, T.B., Lohse, L., Strandbygaard, B., Jørgensen, C.S., Olesen, A.S., Hjerpe, F.B., Petersen, H.H., Jensen, T.K., Mortensen, S., Calvo-Artavia, F.F., Lefèvre, S.K., Nielsen, S.S., Halasa, T., Belsham, G.J., Bøtner, A., 2021. SARS-CoV-2 in Danish mink farms: course of the epidemic and a descriptive analysis of the outbreaks in 2020. Animals (Basel) 11.

Bolles, M., Donaldson, E., Baric, R., 2011. SARS-CoV and emergent coronaviruses: viral determinants of interspecies transmission. Curr. Opin. Virol. 1, 624.

Bosco-Lauth, A.M., Hartwig, A.E., Porter, S.M., Gordy, P.W., Nehring, M., Byas, A.D., VandeWoude, S., Ragan, I.K., Maison, R.M., Bowen, R.A., 2020. Experimental infection of domestic dogs and cats with SARS-CoV-2: pathogenesis, transmission, and response to reexposure in cats. Proc. Natl. Acad. Sci. U. S. A. 117, 26382.

Bosco-Lauth, A., Root, J.J., Porter, S., Walker, A., Guilbert, L., Hawvermale, D., Pepper, A., Maison, R., Hartwig, A., Gordy, P., Bielefeldt-Ohmann, H., Bowen, R.A., 2021. Survey of peridomestic mammal susceptibility to SARS-CoV-2 infection. bioRxiv.

Boudewijns, R., Thibaut, H.J., Kaptein, S.J.F., Li, R., Vergote, V., Seldeslachts, L., Van Weyenbergh, J., De Keyzer, C., Bervoets, L., Sharma, S., Liesenborghs, L., Ma, J., Jansen, S., Van Looveren, D., Vercruysse, T., Wang, X., Jochmans, D., Martens, E., Roose, K., De Vlieger, D., Schepens, B., Van Buyten, T., Jacobs, S., Liu, Y., Martí-Carreras, J., Vanmechelen, B., Wawina-Bokalanga, T., Delang, L., Rocha-Pereira, J., Coelmont, L., Chiu, W., Leyssen, P., Heylen, E., Schols, D., Wang, L., Close, L., Matthijnssens, J., Van Ranst, M., Compernolle, V., Schramm, G., Van Laere, K., Saelens, X., Callewaert, N., Opdenakker, G., Maes, P., Weynand, B., Cawthorne, C., Vande Velde, G., Wang, Z., Neyts, J., Dallmeier, K., 2020. STAT2 signaling restricts viral dissemination but drives severe pneumonia in SARS-CoV-2 infected hamsters. Nat. Commun. 11, 5838.

Breban, R., Riou, J., Fontanet, A., 2013. Interhuman transmissibility of Middle East respiratory syndrome coronavirus: estimation of pandemic risk. The Lancet 382, 694.

Brocato, R.L., Principe, L.M., Kim, R.K., Zeng, X., Williams, J.A., Liu, Y., Li, R., Smith, J.M., Golden, J.W., Gangemi, D., Youssef, S., Wang, Z., Glanville, J., Hooper, J.W., 2020. Disruption of adaptive immunity enhances disease in SARS-CoV-2-infected Syrian hamsters. J. Virol. 94.

Brooke, G.N., Prischi, F., 2020. Structural and functional modelling of SARS-CoV-2 entry in animal models. Sci. Rep. 10, 15917.

Brumeanu, T.D., Vir, P., Shashikumar, S., Karim, A.F., Kar, S., Chung, K.K., Pratt, K.P., Casares, S., 2020. A human-immune-system mouse model for COVID-19 research (DRAGA mouse: HLA-A2.HLA-DR4.Rag1KO.IL-2Rγc KO.NOD). bioRxiv.

Bryche, B., St Albin, A., Murri, S., Lacôte, S., Pulido, C., Ar Gouilh, M., Lesellier, S., Servat, A., Wasniewski, M., Picard-Meyer, E., Monchatre-Leroy, E., Volmer, R., Rampin, O., Le Goffic, R., Marianneau, P., Meunier, N., 2020. Massive transient damage of the olfactory epithelium associated with infection of sustentacular cells by SARS-CoV-2 in golden Syrian hamsters. Brain Behav. Immun. 89, 579.

CDC, 2021. If You Have Pets.

Chan, J.F., Zhang, A.J., Yuan, S., Poon, V.K., Chan, C.C., Lee, A.C., Chan, W.M., Fan, Z., Tsoi, H.W., Wen, L., Liang, R., Cao, J., Chen, Y., Tang, K., Luo, C., Cai, J.P., Kok, K.H., Chu, H., Chan, K.H., Sridhar, S., Chen, Z., Chen, H., To, K.K.,

Anna Michelitsch et al.

Yuen, K.Y., 2020. Simulation of the clinical and pathological manifestations of corona-virus disease 2019 (COVID-19) in a golden Syrian hamster model: implications for disease pathogenesis and transmissibility. Clin. Infect. Dis. 71, 2428.

Chandrashekar, A., Liu, J., Martinot, A.J., McMahan, K., Mercado, N.B., Peter, L., Tostanoski, L.H., Yu, J., Maliga, Z., Nekorchuk, M., Busman-Sahay, K., Terry, M., Wrijil, L.M., Ducat, S., Martinez, D.R., Atyeo, C., Fischinger, S., Burke, J.S., Slein, M.D., Pessaint, L., Van Ry, A., Greenhouse, J., Taylor, T., Blade, K., Cook, A., Finneyfrock, B., Brown, R., Teow, E., Velasco, J., Zahn, R., Wegmann, F., Abbink, P., Bondzie, E.A., Dagotto, G., Gebre, M.S., He, X., Jacob-Dolan, C., Kordana, N., Li, Z., Lifton, M.A., Mahrokhian, S.H., Maxfield, L.F., Nityanandam, R., Nkolola, J.P., Schmidt, A.G., Miller, A.D., Baric, R.S., Alter, G., Sorger, P.K., Estes, J.D., Andersen, H., Lewis, M.G., Barouch, D.H., 2020. SARS-CoV-2 infection protects against rechallenge in rhesus macaques. Science 369, 812.

Chomel, B.B., 2014. Emerging and re-emerging zoonoses of dogs and cats. Animals 4, 434.

Chu, H., Chan, J.F., Yuen, T.T., Shuai, H., Yuan, S., Wang, Y., Hu, B., Yip, C.C., Tsang, J.O., Huang, X., Chai, Y., Yang, D., Hou, Y., Chik, K.K., Zhang, X., Fung, A.Y., Tsoi, H.W., Cai, J.P., Chan, W.M., Ip, J.D., Chu, A.W., Zhou, J., Lung, D.C., Kok, K.H., To, K.K., Tsang, O.T., Chan, K.H., Yuen, K.Y., 2020. Comparative tropism, replication kinetics, and cell damage profiling of SARS-CoV-2 and SARS-CoV with implications for clinical manifestations, transmissibility, and laboratory studies of COVID-19: an observational study. Lancet Microbe 1, e14.

Clark, M.A., 1993. Bovine coronavirus. Br. Vet. J. 149, 51.

Colunga-Salas, P., Hernández-Canchola, G., 2020. Bats and humans during the SARS-CoV-2 outbreak: the case of bat-coronaviruses from Mexico. Transbound. Emerg. Dis.

Conceicao, C., Thakur, N., Human, S., Kelly, J.T., Logan, L., Bialy, D., Bhat, S., Stevenson-Leggett, P., Zagrajek, A.K., Hollinghurst, P., Varga, M., Tsirigoti, C., Tully, M., Chiu, C., Moffat, K., Silesian, A.P., Hammond, J.A., Maier, H.J., Bickerton, E., Shelton, H., Dietrich, I., Graham, S.C., Bailey, D., 2020. The SARS-CoV-2 Spike protein has a broad tropism for mammalian ACE2 proteins. PLoS Biol. 18, e3001016.

Corbett, K.S., Flynn, B., Foulds, K.E., Francica, J.R., Boyoglu-Barnum, S., Werner, A.P., Flach, B., O'Connell, S., Bock, K.W., Minai, M., Nagata, B.M., Andersen, H., Martinez, D.R., Noe, A.T., Douek, N., Donaldson, M.M., Nji, N.N., Alvarado, G.S., Edwards, D.K., Flebbe, D.R., Lamb, E., Doria-Rose, N.A., Lin, B.C., Louder, M.K., O'Dell, S., Schmidt, S.D., Phung, E., Chang, L.A., Yap, C., Todd, J.M., Pessaint, L., Van Ry, A., Browne, S., Greenhouse, J., Putman-Taylor, T., Strasbaugh, A., Campbell, T.A., Cook, A., Dodson, A., Steingrebe, K., Shi, W., Zhang, Y., Abiona, O.M., Wang, L., Pegu, A., Yang, E.S., Leung, K., Zhou, T., Teng, I.T., Widge, A., Gordon, I., Novik, L., Gillespie, R.A., Loomis, R.J., Moliva, J.I., Stewart-Jones, G., Himansu, S., Kong, W.P., Nason, M.C., Morabito, K.M., Ruckwardt, T.J., Ledgerwood, J.E., Gaudinski, M.R., Kwong, P.D., Mascola, J.R., Carfi, A., Lewis, M.G., Baric, R.S., McDermott, A., Moore, I.N., Sullivan, N.J., Roederer, M., Seder, R.A., Graham, B.S., 2020. Evaluation of the mRNA-1273 vaccine against SARS-CoV-2 in nonhuman primates. N. Engl. J. Med. 383, 1544.

Cox, R.M., Wolf, J.D., Plemper, R.K., 2020. Therapeutically administered ribonucleoside analogue MK-4482/EIDD-2801 blocks SARS-CoV-2 transmission in ferrets. Nat. Microbiol.

Cui, J., Li, F., Shi, Z.L., 2019. Origin and evolution of pathogenic coronaviruses. Nat. Rev. Microbiol. 17, 181.

Damas, J., Hughes, G.M., Keough, K.C., Painter, C.A., Persky, N.S., Corbo, M., Hiller, M., Koepfli, K.P., Pfenning, A.R., Zhao, H., Genereux, D.P., Swofford, R., Pollard, K.S.,

Ryder, O.A., Nweeia, M.T., Lindblad-Toh, K., Teeling, E.C., Karlsson, E.K., Lewin, H.A., 2020. Broad host range of SARS-CoV-2 predicted by comparative and structural analysis of ACE2 in vertebrates. Proc. Natl. Acad. Sci. U. S. A.

de Wit, E., Rasmussen, A.L., Falzarano, D., Bushmaker, T., Feldmann, F., Brining, D.L., Fischer, E.R., Martellaro, C., Okumura, A., Chang, J., Scott, D., Benecke, A.G., Katze, M.G., Feldmann, H., Munster, V.J., 2013. Middle East respiratory syndrome coronavirus (MERS-CoV) causes transient lower respiratory tract infection in rhesus macaques. Proc. Natl. Acad. Sci. U. S. A. 110, 16598.

de Wit, E., van Doremalen, N., Falzarano, D., Munster, V.J., 2016. SARS and MERS: recent insights into emerging coronaviruses. Nat. Rev. Microbiol. 14, 523.

de Wit, E., Feldmann, F., Horne, E., Martellaro, C., Haddock, E., Bushmaker, T., Rosenke, K., Okumura, A., Rosenke, R., Saturday, G., Scott, D., Feldmann, H., 2017. Domestic pig unlikely reservoir for MERS-CoV. Emerg. Infect. Dis. 23, 985.

Deng, W., Bao, L., Liu, J., Xiao, C., Liu, J., Xue, J., Lv, Q., Qi, F., Gao, H., Yu, P., Xu, Y., Qu, Y., Li, F., Xiang, Z., Yu, H., Gong, S., Liu, M., Wang, G., Wang, S., Song, Z., Liu, Y., Zhao, W., Han, Y., Zhao, L., Liu, X., Wei, Q., Qin, C., 2020a. Primary exposure to SARS-CoV-2 protects against reinfection in rhesus macaques. Science 369, 818.

Deng, J., Jin, Y., Liu, Y., Sun, J., Hao, L., Bai, J., Huang, T., Lin, D., Jin, Y., Tian, K., 2020b. Serological survey of SARS-CoV-2 for experimental, domestic, companion and wild animals excludes intermediate hosts of 35 different species of animals. Transbound. Emerg. Dis. 67, 1745.

Di Teodoro, G., Valleriani, F., Puglia, I., Monaco, F., Di Pancrazio, C., Luciani, M., Krasteva, I., Petrini, A., Marcacci, M., D'Alterio, N., Curini, V., Iorio, M., Migliorati, G., Di Domenico, M., Morelli, D., Calistri, P., Savini, G., Decaro, N., Holmes, E.C., Lorusso, A., 2020. SARS-CoV-2 replicates in respiratory ex vivo organ cultures of domestic ruminant species. Vet. Microbiol. 252, 108933.

Dinnon, K.H., 3rd, Leist, S.R., Schäfer, A., Edwards, C.E., Martinez, D.R., Montgomery, S.A., West, A., Yount, B.L., Jr., Hou, Y.J., Adams, L.E., Gully, K.L., Brown, A.J., Huang, E., Bryant, M.D., Choong, I.C., Glenn, J.S., Gralinski, L.E., Sheahan, T.P., Baric, R.S., 2020. A mouse-adapted model of SARS-CoV-2 to test COVID-19 countermeasures. Nature 586, 560.

Dong, E., Du, H., Gardner, L., 2020. An interactive web-based dashboard to track COVID-19 in real time. Lancet Infect. Dis.

Drexler, J.F., Corman, V.M., Drosten, C., 2014. Ecology, evolution and classification of bat coronaviruses in the aftermath of SARS. Antiviral Res. 101, 45.

ECDC, 2020. Risk related to spread of new SARS-CoV-2 Variants of Concern in the EU/EEA, 29 December 2020. Online available: https://www.ecdc.europa.eu/sites/default/files/documents/COVID-19-risk-related-to-spread-of-new-SARS-CoV-2-variants-EU-EEA.pdf. last accessed: 26 January 2021.

Elaswad, A., Fawzy, M., Basiouni, S., Shehata, A.A., 2020. Mutational spectra of SARS-CoV-2 isolated from animals. PeerJ 8, e10609.

Elizaldi, S., Lakshmanappa, Y.S., Roh, J., Schmidt, B., Carroll, T., Weaver, K., Smith, J., Deere, J., Dutra, J., Stone, M., Franz, S., Sammak, R., Olstad, K., Reader, J.R., Ma, Z.M., Nguyen, N., Watanabe, J., Usachenko, J., Immareddy, R., Yee, J., Weiskopf, D., Sette, A., Hartigan-O'Connor, D., McSorley, S., Morrison, J., Tran, N., Simmons, G., Busch, M., Kozlowski, P., van Rompay, K., Miller, C., Iyer, S., 2020. SARS-CoV-2 infection induces robust germinal center CD4 T follicular helper cell responses in rhesus macaques. Res. Sq.

Esteves, P.J., Abrantes, J., Baldauf, H.M., BenMohamed, L., Chen, Y., Christensen, N., González-Gallego, J., Giacani, L., Hu, J., Kaplan, G., Keppler, O.T., Knight, K.L., Kong, X.P., Lanning, D.K., Le Pendu, J., de Matos, A.L., Liu, J., Liu, S., Lopes, A.M., Lu, S., Lukehart, S., Manabe, Y.C., Neves, F., McFadden, G., Pan, R.,

Peng, X., de Sousa-Pereira, P., Pinheiro, A., Rahman, M., Ruvoën-Clouet, N., Subbian, S., Tuñón, M.J., van der Loo, W., Vaine, M., Via, L.E., Wang, S., Mage, R., 2018. The wide utility of rabbits as models of human diseases. Exp. Mol. Med. 50, 1.

Fagre, A., Lewis, J., Eckley, M., Zhan, S., Rocha, S.M., Sexton, N.R., Burke, B., Geiss, B.J., Peersen, O., Kading, R., Rovnak, J., Ebel, G.D., Tjalkens, R.B., Aboellail, T., Schountz, T., 2020. SARS-CoV-2 infection, neuropathogenesis and transmission among deer mice: implications for reverse zoonosis to New World rodents. bioRxiv.

Fahlberg, M.D., Blair, R.V., Doyle-Meyers, L.A., Midkiff, C.C., Zenere, G., Russell-Lodrigue, K.E., Monjure, C.J., Haupt, E.H., Penney, T.P., Lehmicke, G., Threeton, B.M., Golden, N., Datta, P.K., Roy, C.J., Bohm, R.P., Maness, N.J., Fischer, T., Rappaport, J., Vaccari, M., 2020. Cellular events of acute, resolving or progressive COVID-19 in SARS-CoV-2 infected non-human primates. Nat. Commun. 11, 6078.

Falzarano, D., de Wit, E., Feldmann, F., Rasmussen, A.L., Okumura, A., Peng, X., Thomas, M.J., van Doremalen, N., Haddock, E., Nagy, L., LaCasse, R., Liu, T., Zhu, J., McLellan, J.S., Scott, D.P., Katze, M.G., Feldmann, H., Munster, V.J., 2014. Infection with MERS-CoV causes lethal pneumonia in the common marmoset. PLoS Pathog. 10, e1004250.

FAO, 2020. Livestock Systems, Cattle. Online available: http://www.fao.org/livestock-systems/global-distributions/cattle/en/. last accessed: 25 January 2021.

FAO, 2021. One Health. Online available: http://www.fao.org/one-health/en/;. last accessed: 25 January 2021.

Feng, L., Wang, Q., Shan, C., Yang, C., Feng, Y., Wu, J., Liu, X., Zhou, Y., Jiang, R., Hu, P., Liu, X., Zhang, F., Li, P., Niu, X., Liu, Y., Zheng, X., Luo, J., Sun, J., Gu, Y., Liu, B., Xu, Y., Li, C., Pan, W., Zhao, J., Ke, C., Chen, X., Xu, T., Zhong, N., Guan, S., Yuan, Z., Chen, L., 2020. An adenovirus-vectored COVID-19 vaccine confers protection from SARS-COV-2 challenge in rhesus macaques. Nat. Commun. 11, 4207.

Forni, D., Cagliani, R., Clerici, M., Sironi, M., 2017. Molecular evolution of human coronavirus genomes. Trends Microbiol. 25, 35.

Fouchier, R.A., Kuiken, T., Schutten, M., van Amerongen, G., van Doornum, G.J., van den Hoogen, B.G., Peiris, M., Lim, W., Stöhr, K., Osterhaus, A.D., 2003. Aetiology: Koch's postulates fulfilled for SARS virus. Nature 423, 240.

Freuling, C.M., Breithaupt, A., Müller, T., Sehl, J., Balkema-Buschmann, A., Rissmann, M., Klein, A., Wylezich, C., Höper, D., Wernike, K., Aebischer, A., Hoffmann, D., Friedrichs, V., Dorhoi, A., Groschup, M.H., Beer, M., Mettenleiter, T.C., 2020. Susceptibility of raccoon dogs for experimental SARS-CoV-2 infection. Emerg. Infect. Dis. 26.

Fritz, M., Rosolen, B., Krafft, E., Becquart, P., Elguero, E., Vratskikh, O., Denolly, S., Boson, B., Vanhomwegen, J., Gouilh, M.A., Kodjo, A., Chirouze, C., Rosolen, S.G., Legros, V., Leroy, E.M., 2021. High prevalence of SARS-CoV-2 antibodies in pets from COVID-19+ households. One Health 11, 100192.

Frutos, R., Devaux, C.A., 2020. Mass culling of minks to protect the COVID-19 vaccines: is it rational? New Microbes New Infect. 38, 100816.

Garigliany, M., Van Laere, A.-S., Clercx, C., Giet, D., Escriou, N., Huon, C., Van Der Werf, S., Eloit, M., Desmecht, D., 2020. SARS-CoV-2 natural transmission from human to cat, Belgium, March 2020. Emerg. Infect. Dis. 26, 3069.

Gaudreault, N.N., Trujillo, J.D., Carossino, M., Meekins, D.A., Morozov, I., Madden, D.W., Indran, S.V., Bold, D., Balaraman, V., Kwon, T., Artiaga, B.L., Cool, K., García-Sastre, A., Ma, W., Wilson, W.C., Henningson, J., Balasuriya, U.B.R., Richt, J.A., 2020. SARS-CoV-2 infection, disease and transmission in domestic cats. Emerg. Microbes Infect. 9, 2322.

Gautam, A., Kaphle, K., Shrestha, B., Phuyal, S., 2020. Susceptibility to SARS, MERS, and COVID-19 from animal health perspective. Open Vet. J. 10, 164.

Gilbert, M., Nicolas, G., Cinardi, G., Van Boeckel, T.P., Vanwambeke, S.O., Wint, G.R.W., Robinson, T.P., 2018. Global distribution data for cattle, buffaloes, horses, sheep, goats, pigs, chickens and ducks in 2010. Sci. Data 5, 180227.

Gilbert, W., Thomas, L., Coyne, L., Rushton, J., 2020. Review: mitigating the risks posed by intensification in livestock production: the examples of antimicrobial resistance and zoonoses. Animal.

Golden, J.W., Cline, C.R., Zeng, X., Garrison, A.R., Carey, B.D., Mucker, E.M., White, L.E., Shamblin, J.D., Brocato, R.L., Liu, J., Babka, A.M., Rauch, H.B., Smith, J.M., Hollidge, B.S., Fitzpatrick, C., Badger, C.V., Hooper, J.W., 2020. Human angiotensin-converting enzyme 2 transgenic mice infected with SARS-CoV-2 develop severe and fatal respiratory disease. JCI Insight 5.

Gong, L., Li, J., Zhou, Q., Xu, Z., Chen, L., Zhang, Y., Xue, C., Wen, Z., Cao, Y., 2017. A new Bat-HKU2-like coronavirus in swine, China, 2017. Emerg. Infect. Dis. 23.

Graham, R.L., Baric, R.S., 2010. Recombination, reservoirs, and the modular spike: mechanisms of coronavirus cross-species transmission. J. Virol. 84, 3134.

Grasselli, G., Zangrillo, A., Zanella, A., Antonelli, M., Cabrini, L., Castelli, A., Cereda, D., Coluccello, A., Foti, G., Fumagalli, R., Iotti, G., Latronico, N., Lorini, L., Merler, S., Natalini, G., Piatti, A., Ranieri, M.V., Scandroglio, A.M., Storti, E., Cecconi, M., Pesenti, A., 2020. Baseline characteristics and outcomes of 1591 patients infected with SARS-CoV-2 admitted to ICUs of the Lombardy region, Italy. JAMA 323, 1574.

Griffin, B.D., Chan, M., Tailor, N., Mendoza, E.J., Leung, A., Warner, B.M., Duggan, A.T., Moffat, E., He, S., Garnett, L., Tran, K.N., Banadyga, L., Albietz, A., Tierney, K., Audet, J., Bello, A., Vendramelli, R., Boese, A.S., Fernando, L., Lindsay, L.R., Jardine, C.M., Wood, H., Poliquin, G., Strong, J.E., Drebot, M., Safronetz, D., Embury-Hyatt, C., Kobasa, D., 2020. North American deer mice are susceptible to SARS-CoV-2. bioRxiv.

Gu, H., Chen, Q., Yang, G., He, L., Fan, H., Deng, Y.Q., Wang, Y., Teng, Y., Zhao, Z., Cui, Y., Li, Y., Li, X.F., Li, J., Zhang, N.N., Yang, X., Chen, S., Guo, Y., Zhao, G., Wang, X., Luo, D.Y., Wang, H., Yang, X., Li, Y., Han, G., He, Y., Zhou, X., Geng, S., Sheng, X., Jiang, S., Sun, S., Qin, C.F., Zhou, Y., 2020. Adaptation of SARS-CoV-2 in BALB/c mice for testing vaccine efficacy. Science 369, 1603.

Guan, Y., Zheng, B.J., He, Y.Q., Liu, X.L., Zhuang, Z.X., Cheung, C.L., Luo, S.W., Li, P.H., Zhang, L.J., Guan, Y.J., Butt, K.M., Wong, K.L., Chan, K.W., Lim, W., Shortridge, K.F., Yuen, K.Y., Peiris, J.S., Poon, L.L., 2003. Isolation and characterization of viruses related to the SARS coronavirus from animals in southern China. Science 302, 276.

Guebre-Xabier, M., Patel, N., Tian, J.H., Zhou, B., Maciejewski, S., Lam, K., Portnoff, A.D., Massare, M.J., Frieman, M.B., Piedra, P.A., Ellingsworth, L., Glenn, G., Smith, G., 2020. NVX-CoV2373 vaccine protects cynomolgus macaque upper and lower airways against SARS-CoV-2 challenge. Vaccine 38, 7892.

Haagmans, B.L., Al Dhahiry, S.H.S., Reusken, C.B.E.M., Raj, V.S., Galiano, M., Myers, R., Godeke, G.-J., Jonges, M., Farag, E., Diab, A., Ghobashy, H., Alhajri, F., Al-Thani, M., Al-Marri, S.A., Al Romaihi, H.E., Al Khal, A., Bermingham, A., Osterhaus, A.D.M.E., AlHajri, M.M., Koopmans, M.P.G., 2014. Middle East respiratory syndrome coronavirus in dromedary camels: an outbreak investigation. Lancet Infect. Dis. 14, 140.

Haagmans, B.L., van den Brand, J.M., Provacia, L.B., Raj, V.S., Stittelaar, K.J., Getu, S., de Waal, L., Bestebroer, T.M., van Amerongen, G., Verjans, G.M., Fouchier, R.A., Smits, S.L., Kuiken, T., Osterhaus, A.D., 2015. Asymptomatic Middle East respiratory syndrome coronavirus infection in rabbits. J. Virol. 89, 6131.

Anna Michelitsch et al.

Halfmann, P.J., Hatta, M., Chiba, S., Maemura, T., Fan, S., Takeda, M., Kinoshita, N., Hattori, S.I., Sakai-Tagawa, Y., Iwatsuki-Horimoto, K., Imai, M., Kawaoka, Y., 2020. Transmission of SARS-CoV-2 in domestic cats. N. Engl. J. Med. 383, 592.

Hall, J.S., Knowles, S., Nashold, S.W., Ip, H.S., Leon, A.E., Rocke, T., Keller, S., Carossino, M., Balasuriya, U., Hofmeister, E., 2020. Experimental challenge of a North American bat species, big brown bat (Eptesicus fuscus), with SARS-CoV-2. Transbound. Emerg. Dis.

Hamer, S.A., Pauvolid-Corrêa, A., Zecca, I.B., Davila, E., Auckland, L.D., Roundy, C.M., Tang, W., Torchetti, M., Killian, M.L., Jenkins-Moore, M., Mozingo, K., Akpalu, Y., Ghai, R.R., Spengler, J.R., Behravesh, C.B., Fischer, R.S.B., Hamer, G.L., 2020. Natural SARS-CoV-2 infections, including virus isolation, among serially tested cats and dogs in households with confirmed human COVID-19 cases in Texas, USA. bioRxiv.

Han, K., Blair, R.V., Iwanaga, N., Liu, F., Russell-Lodrigue, K.E., Qin, Z., Midkiff, C.C., Golden, N.A., Doyle-Meyers, L.A., Kabir, M.E., Chandler, K.E., Cutrera, K.L., Ren, M., Monjure, C.J., Lehmicke, G., Fischer, T., Beddingfield, B., Wanek, A.G., Birnbaum, A., Maness, N.J., Roy, C.J., Datta, P.K., Rappaport, J., Kolls, J.K., Qin, X., 2020. Lung expression of human ACE2 sensitizes the mouse to SARS-CoV-2 infection. Am. J. Respir. Cell Mol. Biol.

Hassan, A.O., Case, J.B., Winkler, E.S., Thackray, L.B., Kafai, N.M., Bailey, A.L., McCune, B.T., Fox, J.M., Chen, R.E., Alsoussi, W.B., Turner, J.S., Schmitz, A.J., Lei, T., Shrihari, S., Keeler, S.P., Fremont, D.H., Greco, S., McCray, P.B., Jr., Perlman, S., Holtzman, M.J., Ellebedy, A.H., Diamond, M.S., 2020. A SARS-CoV-2 infection model in mice demonstrates protection by neutralizing antibodies. Cell 182, 744.

Hemida, M.G., Perera, R.A., Wang, P., Alhammadi, M.A., Siu, L.Y., Li, M., Poon, L.L., Saif, L., Alnaeem, A., Peiris, M., 2013. Middle East Respiratory Syndrome (MERS) coronavirus seroprevalence in domestic livestock in Saudi Arabia, 2010 to 2013. Euro. Surveill. 18, 20659.

Herrero, M., Thornton, P.K., 2013. Livestock and global change: emerging issues for sustainable food systems. Proc. Natl. Acad. Sci. U. S. A. 110, 20878.

Hoang, T.N., Pino, M., Boddapati, A.K., Viox, E.G., Starke, C.E., Upadhyay, A.A., Gumber, S., Nekorchuk, M., Busman-Sahay, K., Strongin, Z., Harper, J.L., Tharp, G.K., Pellegrini, K.L., Kirejczyk, S., Zandi, K., Tao, S., Horton, T.R., Beagle, E.N., Mahar, E.A., Lee, M.Y.H., Cohen, J., Jean, S.M., Wood, J.S., Connor-Stroud, F., Stammen, R.L., Delmas, O.M., Wang, S., Cooney, K.A., Sayegh, M.N., Wang, L., Filev, P.D., Weiskopf, D., Silvestri, G., Waggoner, J., Piantadosi, A., Kasturi, S.P., Al-Shakhshir, H., Ribeiro, S.P., Sekaly, R.P., Levit, R.D., Estes, J.D., Vanderford, T.H., Schinazi, R.F., Bosinger, S.E., Paiardini, M., 2020. Baricitinib treatment resolves lower-airway macrophage inflammation and neutrophil recruitment in SARS-CoV-2-infected rhesus macaques. Cell.

Houser, K.V., Broadbent, A.J., Gretebeck, L., Vogel, L., Lamirande, E.W., Sutton, T., Bock, K.W., Minai, M., Orandle, M., Moore, I.N., Subbarao, K., 2017. Enhanced inflammation in New Zealand white rabbits when MERS-CoV reinfection occurs in the absence of neutralizing antibody. PLoS Pathog. 13, e1006565.

Huang, C., Wang, Y., Li, X., Ren, L., Zhao, J., Hu, Y., Zhang, L., Fan, G., Xu, J., Gu, X., Cheng, Z., Yu, T., Xia, J., Wei, Y., Wu, W., Xie, X., Yin, W., Li, H., Liu, M., Xiao, Y., Gao, H., Guo, L., Xie, J., Wang, G., Jiang, R., Gao, Z., Jin, Q., Wang, J., Cao, B., 2020. Clinical features of patients infected with 2019 novel coronavirus in Wuhan, China. The Lancet 395, 497.

Imai, M., Iwatsuki-Horimoto, K., Hatta, M., Loeber, S., Halfmann, P.J., Nakajima, N., Watanabe, T., Ujie, M., Takahashi, K., Ito, M., Yamada, S., Fan, S., Chiba, S.,

Kuroda, M., Guan, L., Takada, K., Armbrust, T., Balogh, A., Furusawa, Y., Okuda, M., Ueki, H., Yasuhara, A., Sakai-Tagawa, Y., Lopes, T.J.S., Kiso, M., Yamayoshi, S., Kinoshita, N., Ohmagari, N., Hattori, S.I., Takeda, M., Mitsuya, H., Krammer, F., Suzuki, T., Kawaoka, Y., 2020. Syrian hamsters as a small animal model for SARS-CoV-2 infection and countermeasure development. Proc. Natl. Acad. Sci. U. S. A. 117, 16587.

Ishigaki, H., Nakayama, M., Kitagawa, Y., Nguyen, C.T., Hayashi, K., Shiohara, M., Gotoh, B., Itoh, Y., 2020. Neutralizing antibody-dependent and –independent immune responses against SARS-CoV-2 in cynomolgus macaques. Virology 554, 97.

Israelow, B., Song, E., Mao, T., Lu, P., Meir, A., Liu, F., Alfajaro, M.M., Wei, J., Dong, H., Homer, R.J., Ring, A., Wilen, C.B., Iwasaki, A., 2020. Mouse model of SARS-CoV-2 reveals inflammatory role of type I interferon signaling. J. Exp. Med. 217.

Ji, W., Wang, W., Zhao, X., Zai, J., Li, X., 2020. Cross-species transmission of the newly identified coronavirus 2019-nCoV. J. Med. Virol. 92, 433.

Jiang, R.D., Liu, M.Q., Chen, Y., Shan, C., Zhou, Y.W., Shen, X.R., Li, Q., Zhang, L., Zhu, Y., Si, H.R., Wang, Q., Min, J., Wang, X., Zhang, W., Li, B., Zhang, H.J., Baric, R.S., Zhou, P., Yang, X.L., Shi, Z.L., 2020. Pathogenesis of SARS-CoV-2 in transgenic mice expressing human angiotensin-converting enzyme 2. Cell 182, 50.

Kan, B., Wang, M., Jing, H., Xu, H., Jiang, X., Yan, M., Liang, W., Zheng, H., Wan, K., Liu, Q., Cui, B., Xu, Y., Zhang, E., Wang, H., Ye, J., Li, G., Li, M., Cui, Z., Qi, X., Chen, K., Du, L., Gao, K., Zhao, Y.T., Zou, X.Z., Feng, Y.J., Gao, Y.F., Hai, R., Yu, D., Guan, Y., Xu, J., 2005. Molecular evolution analysis and geographic investigation of severe acute respiratory syndrome coronavirus-like virus in palm civets at an animal market and on farms. J. Virol. 79, 11892.

Kim, J., Yang, Y.L., Jeong, Y., Jang, Y.S., 2020a. Middle East respiratory syndrome-coronavirus infection into established hDPP4-transgenic mice accelerates lung damage via activation of the pro-inflammatory response and pulmonary fibrosis. J. Microbiol. Biotechnol. 30, 427.

Kim, Y.I., Kim, S.G., Kim, S.M., Kim, E.H., Park, S.J., Yu, K.M., Chang, J.H., Kim, E.J., Lee, S., Casel, M.A.B., Um, J., Song, M.S., Jeong, H.W., Lai, V.D., Kim, Y., Chin, B.S., Park, J.S., Chung, K.H., Foo, S.S., Poo, H., Mo, I.P., Lee, O.J., Webby, R.J., Jung, J.U., Choi, Y.K., 2020b. Infection and rapid transmission of SARS-CoV-2 in ferrets. Cell Host Microbe 27, 704.

Kim, C., Ryu, D.K., Lee, J., Kim, Y.I., Seo, J.M., Kim, Y.G., Jeong, J.H., Kim, M., Kim, J.I., Kim, P., Bae, J.S., Shim, E.Y., Lee, M.S., Kim, M.S., Noh, H., Park, G.S., Park, J.S., Son, D., An, Y., Lee, J.N., Kwon, K.S., Lee, J.Y., Lee, H., Yang, J.S., Kim, K.C., Kim, S.S., Woo, H.M., Kim, J.W., Park, M.S., Yu, K.M., Kim, S.M., Kim, E.H., Park, S.J., Jeong, S.T., Yu, C.H., Song, Y., Gu, S.H., Oh, H., Koo, B.S., Hong, J.J., Ryu, C.M., Park, W.B., Oh, M.D., Choi, Y.K., Lee, S.Y., 2021. A therapeutic neutralizing antibody targeting receptor binding domain of SARS-CoV-2 spike protein. Nat. Commun. 12, 288.

Kiros, M., Andualem, H., Kiros, T., Hailemichael, W., Getu, S., Geteneh, A., Alemu, D., Abegaz, W.E., 2020. COVID-19 pandemic: current knowledge about the role of pets and other animals in disease transmission. Virol. J. 17, 143.

Klous, G., Huss, A., Heederik, D.J.J., Coutinho, R.A., 2016. Human-livestock contacts and their relationship to transmission of zoonotic pathogens, a systematic review of literature. One Health 2, 65.

Koo, B.S., Oh, H., Kim, G., Hwang, E.H., Jung, H., Lee, Y., Kang, P., Park, J.H., Ryu, C.M., Hong, J.J., 2020. Transient lymphopenia and interstitial pneumonia with endotheliitis in SARS-CoV-2-infected macaques. J. Infect. Dis. 222, 1596.

Koopmans, M., 2020. SARS-CoV-2 and the human-animal interface: outbreaks on mink farms. Lancet Infect. Dis.

Anna Michelitsch et al.

Ku, M.W., Bourgine, M., Authié, P., Lopez, J., Nemirov, K., Moncoq, F., Noirat, A., Vesin, B., Nevo, F., Blanc, C., Souque, P., Tabbal, H., Simon, E., Hardy, D., Le Dudal, M., Guinet, F., Fiette, L., Mouquet, H., Anna, F., Martin, A., Escriou, N., Majlessi, L., Charneau, P., 2020. Intranasal vaccination with a lentiviral vector protects against SARS-CoV-2 in preclinical animal models. Cell Host Microbe.

Lacroix, A., Vidal, N., Keita, A.K., Thaurignac, G., Esteban, A., De Nys, H., Diallo, R., Toure, A., Goumou, S., Soumah, A.K., Povogui, M., Koivogui, J., Monemou, J.L., Raulino, R., Nkuba, A., Foulongne, V., Delaporte, E., Ayouba, A., Peeters, M., 2020. Wide diversity of coronaviruses in frugivorous and insectivorous bat species: a pilot study in Guinea, West Africa. Viruses 12.

Lam, S.D., Bordin, N., Waman, V.P., Scholes, H.M., Ashford, P., Sen, N., van Dorp, L., Rauer, C., Dawson, N.L., Pang, C.S.M., Abbasian, M., Sillitoe, I., Edwards, S.J.L., Fraternali, F., Lees, J.G., Santini, J.M., Orengo, C.A., 2020a. SARS-CoV-2 spike protein predicted to form complexes with host receptor protein orthologues from a broad range of mammals. Sci. Rep. 10, 16471.

Lam, T.T., Jia, N., Zhang, Y.W., Shum, M.H., Jiang, J.F., Zhu, H.C., Tong, Y.G., Shi, Y.X., Ni, X.B., Liao, Y.S., Li, W.J., Jiang, B.G., Wei, W., Yuan, T.T., Zheng, K., Cui, X.M., Li, J., Pei, G.Q., Qiang, X., Cheung, W.Y., Li, L.F., Sun, F.F., Qin, S., Huang, J.C., Leung, G.M., Holmes, E.C., Hu, Y.L., Guan, Y., Cao, W.C., 2020b. Identifying SARS-CoV-2-related coronaviruses in Malayan pangolins. Nature 583, 282.

Lassaunière, R., Fonager, J., Rasmussen, M., Frische, A., Strandh, C., Rasmussen, T., Bøtner, A., Fomsgaard, A., 2020. SARS-CoV-2 Spike Mutations Arising in Danish Mink and Their Spread to Humans. Online available: https://files.ssi.dk/Mink-cluster-5-short-report_AFO2. last accessed: 26. January 2021.

Latinne, A., Hu, B., Olival, K.J., Zhu, G., Zhang, L., Li, H., Chmura, A.A., Field, H.E., Zambrana-Torrelio, C., Epstein, J.H., Li, B., Zhang, W., Wang, L.F., Shi, Z.L., Daszak, P., 2020. Origin and cross-species transmission of bat coronaviruses in China. Nat. Commun. 11, 4235.

Lau, S.K.P., Woo, P.C.Y., Li, K.S.M., Huang, Y., Tsoi, H.-W., Wong, B.H.L., Wong, S.S.Y., Leung, S.-Y., Chan, K.-H., Yuen, K.-Y., 2005. Severe acute respiratory syndrome coronavirus-like virus in Chinese horseshoe bats. Proc. Natl. Acad. Sci. U. S. A. 102, 14040.

Li, K., McCray, P.B., Jr., 2020. Development of a mouse-adapted MERS coronavirus. Methods Mol. Biol. 2099, 161.

Li, W., Shi, Z., Yu, M., Ren, W., Smith, C., Epstein, J.H., Wang, H., Crameri, G., Hu, Z., Zhang, H., Zhang, J., McEachern, J., Field, H., Daszak, P., Eaton, B.T., Zhang, S., Wang, L.-F., 2005. Bats are natural reservoirs of SARS-like coronaviruses. Science 310, 676.

Li, R., Zanin, M., Xia, X., Yang, Z., 2018. The tree shrew as a model for infectious diseases research. J. Thorac. Dis. 10, S2272.

Li, W., Drelich, A., Martinez, D.R., Gralinski, L., Chen, C., Sun, Z., Liu, X., Zhelev, D., Zhang, L., Peterson, E.C., Conard, A., Mellors, J.W., Tseng, C.T., Baric, R.S., Dimitrov, D.S., 2020a. Potent neutralization of SARS-CoV-2 in vitro and in an animal model by a human monoclonal antibody. bioRxiv.

Li, W., Chen, C., Drelich, A., Martinez, D.R., Gralinski, L.E., Sun, Z., Schäfer, A., Kulkarni, S.S., Liu, X., Leist, S.R., Zhelev, D.V., Zhang, L., Kim, Y.J., Peterson, E.C., Conard, A., Mellors, J.W., Tseng, C.K., Falzarano, D., Baric, R.S., Dimitrov, D.S., 2020b. Rapid identification of a human antibody with high prophylactic and therapeutic efficacy in three animal models of SARS-CoV-2 infection. Proc. Natl. Acad. Sci. U. S. A. 117, 29832.

Liu, P., Jiang, J.Z., Wan, X.F., Hua, Y., Li, L., Zhou, J., Wang, X., Hou, F., Chen, J., Zou, J., Chen, J., 2020. Are pangolins the intermediate host of the 2019 novel coronavirus (SARS-CoV-2)? PLoS Pathog. 16, e1008421.

Lu, R., Zhao, X., Li, J., Niu, P., Yang, B., Wu, H., Wang, W., Song, H., Huang, B., Zhu, N., Bi, Y., Ma, X., Zhan, F., Wang, L., Hu, T., Zhou, H., Hu, Z., Zhou, W., Zhao, L., Chen, J., Meng, Y., Wang, J., Lin, Y., Yuan, J., Xie, Z., Ma, J., Liu, W.J., Wang, D., Xu, W., Holmes, E.C., Gao, G.F., Wu, G., Chen, W., Shi, W., Tan, W., 2020a. Genomic characterisation and epidemiology of 2019 novel coronavirus: implications for virus origins and receptor binding. Lancet 395, 565.

Lu, S., Zhao, Y., Yu, W., Yang, Y., Gao, J., Wang, J., Kuang, D., Yang, M., Yang, J., Ma, C., Xu, J., Qian, X., Li, H., Zhao, S., Li, J., Wang, H., Long, H., Zhou, J., Luo, F., Ding, K., Wu, D., Zhang, Y., Dong, Y., Liu, Y., Zheng, Y., Lin, X., Jiao, L., Zheng, H., Dai, Q., Sun, Q., Hu, Y., Ke, C., Liu, H., Peng, X., 2020b. Comparison of nonhuman primates identified the suitable model for COVID-19. Signal Transduct. Target. Ther. 5, 157.

Luan, J., Jin, X., Lu, Y., Zhang, L., 2020. SARS-CoV-2 spike protein favors ACE2 from Bovidae and Cricetidae. J. Med. Virol. 92, 1649.

Maisonnasse, P., Guedj, J., Contreras, V., Behillil, S., Solas, C., Marlin, R., Naninck, T., Pizzorno, A., Lemaitre, J., Gonçalves, A., Kahlaoui, N., Terrier, O., Fang, R.H.T., Enouf, V., Dereuddre-Bosquet, N., Brisebarre, A., Touret, F., Chapon, C., Hoen, B., Lina, B., Calatrava, M.R., van der Werf, S., de Lamballerie, X., Le Grand, R., 2020. Hydroxychloroquine use against SARS-CoV-2 infection in non–human primates. Nature 585, 584.

Malaiyan, J., Arumugam, S., Mohan, K., Gomathi Radhakrishnan, G., 2020. An update on the origin of SARS-CoV-2: despite closest identity, bat (RaTG13) and pangolin derived coronaviruses varied in the critical binding site and O–linked glycan residues. J. Med. Virol.

Mallapaty, S., 2020. COVID mink analysis shows mutations are not dangerous—yet. Nature 587, 340.

Mapara, M., Thomas, B.S., Bhat, K.M., 2012. Rabbit as an animal model for experimental research. Dent. Res. J. (Isfahan) 9, 111.

Marsh, G.A., McAuley, A.J., Brown, S., Pharo, E.A., Crameri, S., Au, G.G., Baker, M.L., Barr, J., Bergfeld, J., Bruce, M., Burkett, K., Durr, P.A., Holmes, C., Izzard, L., Layton, R., Lowther, S., Neave, M.J., Poole, T., Riddell, S., Rowe, B., Soldani, E., Stevens, V., Suen, W., Sundaramoorthy, V., Tachedjian, M., Todd, S., Trinidad, L., Williams, S.M., Druce, J.D., Drew, T.W., Vasan, S.S., 2021. In vitro characterisation of SARS-CoV-2 and susceptibility of domestic ferrets (Mustela putorius furo). Transbound. Emerg. Dis.

Martina, B.E., Haagmans, B.L., Kuiken, T., Fouchier, R.A., Rimmelzwaan, G.F., Van Amerongen, G., Peiris, J.S., Lim, W., Osterhaus, A.D., 2003. Virology: SARS virus infection of cats and ferrets. Nature 425, 915.

McAloose, D., Laverack, M., Wang, L., Killian, M.L., Caserta, L.C., Yuan, F., Mitchell, P.K., Queen, K., Mauldin, M.R., Cronk, B.D., Bartlett, S.L., Sykes, J.M., Zec, S., Stokol, T., Ingerman, K., Delaney, M.A., Fredrickson, R., Ivančić, M., Jenkins–Moore, M., Mozingo, K., Franzen, K., Bergeson, N.H., Goodman, L., Wang, H., Fang, Y., Olmstead, C., McCann, C., Thomas, P., Goodrich, E., Elvinger, F., Smith, D.C., Tong, S., Slavinski, S., Calle, P.P., Terio, K., Torchetti, M.K., Diel, D.G., 2020. From people to panthera: natural SARS-CoV-2 infection in tigers and lions at the Bronx Zoo. mBio 11.

McMahan, K., Yu, J., Mercado, N.B., Loos, C., Tostanoski, L.H., Chandrashekar, A., Liu, J., Peter, L., Atyeo, C., Zhu, A., Bondzie, E.A., Dagotto, G., Gebre, M.S.,

Jacob-Dolan, C., Li, Z., Nampanya, F., Patel, S., Pessaint, L., Van Ry, A., Blade, K., Yalley-Ogunro, J., Cabus, M., Brown, R., Cook, A., Teow, E., Andersen, H., Lewis, M.G., Lauffenburger, D.A., Alter, G., Barouch, D.H., 2020. Correlates of protection against SARS-CoV-2 in rhesus macaques. Nature.

Meekins, D.A., Morozov, I., Trujillo, J.D., Gaudreault, N.N., Bold, D., Carossino, M., Artiaga, B.L., Indran, S.V., Kwon, T., Balaraman, V., Madden, D.W., Feldmann, H., Henningson, J., Ma, W., Balasuriya, U.B.R., Richt, J.A., 2020. Susceptibility of swine cells and domestic pigs to SARS-CoV-2. Emerg. Microbes Infect. 9, 2278.

Michelitsch, A., Hoffmann, D., Wernike, K., Beer, M., 2020. Occurrence of antibodies against SARS-CoV-2 in the domestic cat population of Germany. Vaccine 8.

Molenaar, R.J., Vreman, S., Hakze-van der Honing, R.W., Zwart, R., de Rond, J., Weesendorp, E., Smit, L.A.M., Koopmans, M., Bouwstra, R., Stegeman, A., van der Poel, W.H.M., 2020. Clinical and pathological findings in SARS-CoV-2 disease out-breaks in farmed mink (Neovison vison). Vet. Pathol. 300985820943535.

Muñoz-Fontela, C., Dowling, W.E., Funnell, S.G.P., Gsell, P.S., Riveros-Balta, A.X., Albrecht, R.A., Andersen, H., Baric, R.S., Carroll, M.W., Cavaleri, M., Qin, C., Crozier, I., Dallmeier, K., de Waal, L., de Wit, E., Delang, L., Dohm, E., Duprex, W.P., Falzarano, D., Finch, C.L., Frieman, M.B., Graham, B.S., Gralinski, L.E., Guilfoyle, K., Haagmans, B.L., Hamilton, G.A., Hartman, A.L., Herfst, S., Kaptein, S.J.F., Klimstra, W.B., Knezevic, I., Krause, P.R., Kuhn, J.H., Le Grand, R., Lewis, M.G., Liu, W.C., Maisonnasse, P., McElroy, A.K., Munster, V., Oreshkova, N., Rasmussen, A.L., Rocha-Pereira, J., Rockx, B., Rodríguez, E., Rogers, T.F., Salguero, F.J., Schotsaert, M., Stittelaar, K.J., Thibaut, H.J., Tseng, C.T., Vergara-Alert, J., Beer, M., Brasel, T., Chan, J.F.W., García-Sastre, A., Neyts, J., Perlman, S., Reed, D.S., Richt, J.A., Roy, C.J., Segalés, J., Vasan, S.S., Henao-Restrepo, A.M., Barouch, D.H., 2020. Animal models for COVID-19. Nature 586, 509.

Munster, V.J., Feldmann, F., Williamson, B.N., van Doremalen, N., Pérez-Pérez, L., Schulz, J., Meade-White, K., Okumura, A., Callison, J., Brumbaugh, B., Avanzato, V.A., Rosenke, R., Hanley, P.W., Saturday, G., Scott, D., Fischer, E.R., de Wit, E., 2020. Respiratory disease in rhesus macaques inoculated with SARS-CoV-2. Nature 585, 268.

Mykytyn, A.Z., Lamers, M.M., Okba, N.M.A., Breugem, T.I., Schipper, D., van den Doel, P.B., van Run, P., van Amerongen, G., de Waal, L., Koopmans, M.P.G., Stittelaar, K.J., van den Brand, J.M.A., Haagmans, B.L., 2021. Susceptibility of rabbits to SARS-CoV-2. Emerg. Microbes Infect. 10, 1.

Neira, V., Brito, B., Agüero, B., Berrios, F., Valdés, V., Gutierrez, A., Ariyama, N., Espinoza, P., Retamal, P., Holmes, E.C., Gonzalez-Reiche, A.S., Khan, Z., Guchte, A.V., Dutta, J., Miorin, L., Kehrer, T., Galarce, N., Almonacid, L.I., Levican, J., Bakel, H.V., García-Sastre, A., Medina, R.A., 2020. A household case evi-dences shorter shedding of SARS-CoV-2 in naturally infected cats compared to their human owners. Emerg. Microbes Infect. 1.

Newman, A., Smith, D., Ghai, R.R., Wallace, R.M., Torchetti, M.K., Loiacono, C., Murrell, L.S., Carpenter, A., Moroff, S., Rooney, J.A., 2020. First reported cases of SARS-CoV-2 infection in companion animals—New York, March–April 2020. Morb. Mortal. Wkly. Rep. 69, 710.

OIE, 2021a. One Health. Online available: https://www.oie.int/en/for-the-media/onehealth/;. last accessed: 25 January 2021.

OIE, 2021b. Events in Animals. Online available: https://www.oie.int/en/scientific-expertise/specific-information-and-recommendations/questions-and-answers-on-2019 novel-coronavirus/events-in-animals/. last accessed: 25 January 2021.

Oladunni, F.S., Park, J.G., Pino, P.A., Gonzalez, O., Akhter, A., Allué-Guardia, A., Olmo-Fontánez, A., Gautam, S., Garcia-Vilanova, A., Ye, C., Chiem, K., Headley, C., Dwivedi, V., Parodi, L.M., Alfson, K.J., Staples, H.M., Schami, A., Garcia, J.I., Whigham, A., Platt 2nd, R.N., Gazi, M., Martinez, J., Chuba, C., Earley, S., Rodriguez, O.H., Mdaki, S.D., Kavelish, K.N., Escalona, R., Hallam, C.R.A., Christie, C., Patterson, J.L., Anderson, T.J.C., Carrion, R., Jr., Dick, E.J., Jr., Hall-Ursone, S., Schlesinger, L.S., Alvarez, X., Kaushal, D., Giavedoni, L.D., Turner, J., Martinez-Sobrido, L., Torrelles, J.B., 2020. Lethality of SARS-CoV-2 infection in K18 human angiotensin-converting enzyme 2 transgenic mice. Nat. Commun. 11, 6122.

Opriessnig, T., Huang, Y.W., 2020. Coronavirus disease 2019 (COVID-19) outbreak: could pigs be vectors for human infections? Xenotransplantation 27, e12591.

Oreshkova, N., Molenaar, R.J., Vreman, S., Harders, F., Oude Munnink, B.B., Hakze-van der Honing, R.W., Gerhards, N., Tolsma, P., Bouwstra, R., Sikkema, R.S., Tacken, M.G., de Rooij, M.M., Weesendorp, E., Engelsma, M.Y., Bruschke, C.J., Smit, L.A., Koopmans, M., van der Poel, W.H., Stegeman, A., 2020. SARS-CoV-2 infection in farmed minks, the Netherlands, April and May 2020. Euro. Surveill. 25.

Osterrieder, N., Bertzbach, L.D., Dietert, K., Abdelgawad, A., Vladimirova, D., Kunec, D., Hoffmann, D., Beer, M., Gruber, A.D., Trimpert, J., 2020. Age-dependent progression of SARS-CoV-2 infection in Syrian hamsters. Viruses 12.

Oude Munnink, B.B., Sikkema, R.S., Nieuwenhuijse, D.F., Molenaar, R.J., Munger, E., Molenkamp, R., van der Spek, A., Tolsma, P., Rietveld, A., Brouwer, M., Bouwmeester-Vincken, N., Harders, F., Hakze-van der Honing, R., Wegdam-Blans, M.C.A., Bouwstra, R.J., GeurtsvanKessel, C., van der Eijk, A.A., Velkers, F.C., Smit, L.A.M., Stegeman, A., van der Poel, W.H.M., Koopmans, M.P.G., 2020. Transmission of SARS-CoV-2 on mink farms between humans and mink and back to humans. Science.

Overgaauw, P.A.M., Vinke, C.M., Hagen, M., Lipman, L.J.A., 2020. A one health perspective on the human–companion animal relationship with emphasis on zoonotic aspects. Int. J. Environ. Res. Public Health 17.

Palmer, M.V., Martins, M., Falkenberg, S., Buckley, A.C., Caserta, L.C., Mitchell, P.K., Cassmann, E., Rollins, A., Zylich, N.C., Renshaw, R.W., Guarino, C., Wagner, B., Lager, K., Diel, D.G., 2021. Susceptibility of white-tailed deer (Odocoileus virginianus) to SARS-CoV-2. bioRxiv.

Pan, Y., Tian, X., Qin, P., Wang, B., Zhao, P., Yang, Y.L., Wang, L., Wang, D., Song, Y., Zhang, X., Huang, Y.W., 2017. Discovery of a novel swine enteric alphacoronavirus (SeACoV) in southern China. Vet. Microbiol. 211, 15.

Patterson, E.I., Elia, G., Grassi, A., Giordano, A., Desario, C., Medardo, M., Smith, S.L., Anderson, E.R., Prince, T., Patterson, G.T., Lorusso, E., Lucente, M.S., Lanave, G., Lauzi, S., Bonfanti, U., Stranieri, A., Martella, V., Solari Basano, F., Barrs, V.R., Radford, A.D., Agrimi, U., Hughes, G.L., Paltrinieri, S., Decaro, N., 2020. Evidence of exposure to SARS-CoV-2 in cats and dogs from households in Italy. Nat. Commun. 11, 6231.

Perera, R.A., Wang, P., Gomaa, M.R., El-Shesheny, R., Kandeil, A., Bagato, O., Siu, L.Y., Shehata, M.M., Kayed, A.S., Moatasim, Y., Li, M., Poon, L.L., Guan, Y., Webby, R.J., Ali, M.A., Peiris, J.S., Kayali, G., 2013. Seroepidemiology for MERS coronavirus using microneutralisation and pseudoparticle virus neutralisation assays reveal a high prevalence of antibody in dromedary camels in Egypt, June 2013. Eurosurveillance 18, 20574.

Pickering, B.S., Smith, G., Pinette, M.M., Embury-Hyatt, C., Moffat, E., Marszal, P., Lewis, C.E., 2021. Susceptibility of domestic swine to experimental infection with Severe Acute Respiratory Syndrome Coronavirus 2. Emerg. Infect. Dis. 27, 104.

ProMED-mail, 2020a. COVID-19 update (33): Sweden, Zoo, Tiger, Lion. Archive Number: 20210125.8134087. http://www.promedmail.org. (posted 25 January 2021).

ProMED-mail, 2020b. COVID-19 update (135): Netherlands (NB) Animal, Farmed Mink. Archive Number: 20200427.7272289. http://www.promedmail.org. (posted 27 April 2020).

ProMED-mail, 2020c. COVID-19 update (525): Spain, Animal, Zoo, Lion, Human. Archive Number: 20201208.8002466. http://www.promedmail.org. (posted 08 December 2020).

ProMED-mail, 2020d. COVID-19 update (536): Animal, USA (UT) Wild Mink, 1st Case. Archive Number: 20201213.8015608. http://www.promedmail.org. (posted 13 December 2020).

Proud, P.C., Tsitoura, D., Watson, R.J., Chua, B.Y., Aram, M.J., Bewley, K.R., Cavell, B.E., Cobb, R., Dowall, S., Fotheringham, S.A., Ho, C.M.K., Lucas, V., Ngabo, D., Rayner, E., Ryan, K.A., Slack, G.S., Thomas, S., Wand, N.I., Yeates, P., Demaison, C., Zeng, W., Holmes, I., Jackson, D.C., Bartlett, N.W., Mercuri, F., Carroll, M.W., 2020. Prophylactic intranasal administration of a TLR2/6 agonist reduces upper respiratory tract viral shedding in a SARS-CoV-2 challenge ferret model. EBioMedicine 63, 103153.

Rabalski, L., Kosinski, M., Smura, T., Aaltonen, K., Kant, R., Sironen, T., Szewczyk, B., Grzybek, M., 2020. Detection and molecular characterisation of SARS-CoV-2 in farmed mink (Neovision vision) in Poland. bioRxiv. 2020.12. 24.422670.

Rathnasinghe, R., Strohmeier, S., Amanat, F., Gillespie, V.L., Krammer, F., García-Sastre, A., Coughlan, L., Schotsaert, M., Uccellini, M.B., 2020. Comparison of transgenic and adenovirus hACE2 mouse models for SARS-CoV-2 infection. Emerg. Microbes Infect. 9, 2433.

Reusken, C.B.E.M., Haagmans, B.L., Müller, M.A., Gutierrez, C., Godeke, G.-J., Meyer, B., Muth, D., Raj, V.S., Vries, L.S.-D., Corman, V.M., Drexler, J.-F., Smits, S.L., El Tahir, Y.E., De Sousa, R., van Beek, J., Nowotny, N., van Maanen, K., Hidalgo-Hermoso, E., Bosch, B.-J., Rottier, P., Osterhaus, A., Gortázar-Schmidt, C., Drosten, C., Koopmans, M.P.G., 2013. Middle East respiratory syndrome coronavirus neutralising serum antibodies in dromedary camels: a comparative serological study. Lancet Infect. Dis. 13, 859.

Richard, M., Kok, A., de Meulder, D., Bestebroer, T.M., Lamers, M.M., Okba, N.M.A., Fentener van Vlissingen, M., Rockx, B., Haagmans, B.L., Koopmans, M.P.G., Fouchier, R.A.M., Herfst, S., 2020. SARS-CoV-2 is transmitted via contact and via the air between ferrets. Nat. Commun. 11, 3496.

Rockx, B., Kuiken, T., Herfst, S., Bestebroer, T., Lamers, M.M., Oude Munnink, B.B., de Meulder, D., van Amerongen, G., van den Brand, J., Okba, N.M.A., Schipper, D., van Run, P., Leijten, L., Sikkema, R., Verschoor, E., Verstrepen, B., Bogers, W., Langermans, J., Drosten, C., Fentener van Vlissingen, M., Fouchier, R., de Swart, R., Koopmans, M., Haagmans, B.L., 2020. Comparative pathogenesis of COVID-19, MERS, and SARS in a nonhuman primate model. Science 368, 1012.

Rosenke, K., Meade-White, K., Letko, M., Clancy, C., Hansen, F., Liu, Y., Okumura, A., Tang-Huau, T.L., Li, R., Saturday, G., Feldmann, F., Scott, D., Wang, Z., Munster, V., Jarvis, M.A., Feldmann, H., 2020. Defining the Syrian hamster as a highly susceptible preclinical model for SARS-CoV-2 infection. Emerg. Microbes Infect. 1.

Ryan, K.A., Bewley, K.R., Fotheringham, S.A., Slack, G.S., Brown, P., Hall, Y., Wand, N.I., Marriott, A.C., Cavell, B.E., Tree, J.A., Allen, L., Aram, M.J., Bean, T.J., Brunt, E., Buttigieg, K.R., Carter, D.P., Cobb, R., Coombes, N.S., Findlay-Wilson, S.J., Godwin, K.J., Gooch, K.E., Gouriet, J., Halkerston, R., Harris, D.J., Hender, T.H., Humphries, H.E., Hunter, L., Ho, C.M.K.,

Kennard, C.L., Leung, S., Longet, S., Ngabo, D., Osman, K.L., Paterson, J., Penn, E.J., Pullan, S.T., Rayner, E., Skinner, O., Steeds, K., Taylor, I., Tipton, T., Thomas, S., Turner, C., Watson, R.J., Wiblin, N.R., Charlton, S., Hallis, B., Hiscox, J.A., Funnell, S., Dennis, M.J., Whittaker, C.J., Catton, M.G., Druce, J., Salguero, F.J., Carroll, M.W., 2021. Dose-dependent response to infection with SARS-CoV-2 in the ferret model and evidence of protective immunity. Nat. Commun. 12, 81.

Sailleau, C., Dumarest, M., Vanhomwegen, J., Delaplace, M., Caro, V., Kwasiborski, A., Hourdel, V., Chevaillier, P., Barbarino, A., Comtet, L., Pourquier, P., Klonjkowski, B., Manuguerra, J.C., Zientara, S., Le Poder, S., 2020. First detection and genome sequencing of SARS-CoV-2 in an infected cat in France. Transbound. Emerg. Dis.

Schalk, A., Hawn, M.C., 1931. An apparently new respiratory disease of baby chicks. J. Am. Vet. Med. Assoc. 78, 413.

Schlottau, K., Rissmann, M., Graaf, A., Schön, J., Sehl, J., Wylezich, C., Höper, D., Mettenleiter, T.C., Balkema-Buschmann, A., Harder, T., Grund, C., Hoffmann, D., Breithaupt, A., Beer, M., 2020. SARS-CoV-2 in fruit bats, ferrets, pigs, and chickens: an experimental transmission study. Lancet Microbe 1, e218.

Segalés, J., Puig, M., Rodon, J., Avila-Nieto, C., Carrillo, J., Cantero, G., Terrón, M.T., Cruz, S., Parera, M., Noguera-Julián, M., Izquierdo-Useros, N., Guallar, V., Vidal, E., Valencia, A., Blanco, I., Blanco, J., Clotet, B., Vergara-Alert, J., 2020. Detection of SARS-CoV-2 in a cat owned by a COVID-19–affected patient in Spain. Proc. Natl. Acad. Sci. U. S. A. 117, 24790.

Seo, S.H., Jang, Y., 2020. Cold-adapted live attenuated SARS-CoV-2 vaccine completely protects human ACE2 transgenic mice from SARS-CoV-2 infection. Vaccines (Basel) 8.

Shan, C., Yao, Y.F., Yang, X.L., Zhou, Y.W., Gao, G., Peng, Y., Yang, L., Hu, X., Xiong, J., Jiang, R.D., Zhang, H.J., Gao, X.X., Peng, C., Min, J., Chen, Y., Si, H.R., Wu, J., Zhou, P., Wang, Y.Y., Wei, H.P., Pang, W., Hu, Z.F., Lv, L.B., Zheng, Y.T., Shi, Z.L., Yuan, Z.M., 2020. Infection with novel coronavirus (SARS-CoV-2) causes pneumonia in Rhesus macaques. Cell Res. 30, 670.

Shi, J., Wen, Z., Zhong, G., Yang, H., Wang, C., Huang, B., Liu, R., He, X., Shuai, L., Sun, Z., Zhao, Y., Liu, P., Liang, L., Cui, P., Wang, J., Zhang, X., Guan, Y., Tan, W., Wu, G., Chen, H., Bu, Z., 2020. Susceptibility of ferrets, cats, dogs, and other domesticated animals to SARS–coronavirus 2. Science 368, 1016.

Sia, S.F., Yan, L.M., Chin, A.W.H., Fung, K., Choy, K.T., Wong, A.Y.L., Kaewpreedee, P., Perera, R., Poon, L.L.M., Nicholls, J.M., Peiris, M., Yen, H.L., 2020. Pathogenesis and transmission of SARS-CoV-2 in golden hamsters. Nature 583, 834.

Singh, D.K., Singh, B., Ganatra, S.R., Gazi, M., Cole, J., Thippeshappa, R., Alfson, K.J., Clemmons, E., Gonzalez, O., Escobedo, R., Lee, T.H., Chatterjee, A., Goez-Gazi, Y., Sharan, R., Gough, M., Alvarez, C., Blakley, A., Ferdin, J., Bartley, C., Staples, H., Parodi, L., Callery, J., Mannino, A., Klaffke, B., Escareno, P., Platt 2nd, R.N., Hodara, V., Scordo, J., Gautam, S., Vilanova, A.G., Olmo-Fontanez, A., Schami, A., Oyejide, A., Ajithdoss, D.K., Copin, R., Baum, A., Kyratsous, C., Alvarez, X., Ahmed, M., Rosa, B., Goodroe, A., Dutton, J., Hall-Ursone, S., Frost, P.A., Voges, A.K., Ross, C.N., Sayers, K., Chen, C., Hallam, C., Khader, S.A., Mitreva, M., Anderson, T.J.C., Martinez-Sobrido, L., Patterson, J.L., Turner, J., Torrelles, J.B., Dick, E.J., Jr., Brasky, K., Schlesinger, L.S., Giavedoni, L.D., Carrion, R., Jr., Kaushal, D., 2021. Responses to acute infection with SARS-CoV-2 in the lungs of rhesus macaques, baboons and marmosets. Nat. Microbiol. 6, 73.

Sit, T.H.C., Brackman, C.J., Ip, S.M., Tam, K.W.S., Law, P.Y.T., To, E.M.W., Yu, V.Y.T., Sims, L.D., Tsang, D.N.C., Chu, D.K.W., Perera, R., Poon, L.L.M., Peiris, M., 2020. Infection of dogs with SARS-CoV-2. Nature 586, 776.

Song, T.Z., Zheng, H.Y., Han, J.B., Jin, L., Yang, X., Liu, F.L., Luo, R.H., Tian, R.R., Cai, H.R., Feng, X.L., Liu, C., Li, M.H., Zheng, Y.T., 2020. Delayed severe cytokine storm and immune cell infiltration in SARS-CoV-2-infected aged Chinese rhesus macaques. Zool. Res. 41, 503.

Suarez, D.L., Pantin-Jackwood, M.J., Swayne, D.E., Lee, S.A., DeBlois, S.M., Spackman, E., 2020. Lack of susceptibility to SARS-CoV-2 and MERS-CoV in poultry. Emerg. Infect. Dis. 26, 3074.

Sun, J., Zhuang, Z., Zheng, J., Li, K., Wong, R.L., Liu, D., Huang, J., He, J., Zhu, A., Zhao, J., Li, X., Xi, Y., Chen, R., Alshukairi, A.N., Chen, Z., Zhang, Z., Chen, C., Huang, X., Li, F., Lai, X., Chen, D., Wen, L., Zhuo, J., Zhang, Y., Wang, Y., Huang, S., Dai, J., Shi, Y., Zheng, K., Leidinger, M.R., Chen, J., Li, Y., Zhong, N., Meyerholz, D.K., McCray, P.B., Jr., Perlman, S., Zhao, J., 2020a. Generation of a broadly useful model for COVID-19 pathogenesis, vaccination, and treatment. Cell 182, 734.

Sun, S.H., Chen, Q., Gu, H.J., Yang, G., Wang, Y.X., Huang, X.Y., Liu, S.S., Zhang, N.N., Li, X.F., Xiong, R., Guo, Y., Deng, Y.Q., Huang, W.J., Liu, Q., Liu, Q.M., Shen, Y.L., Zhou, Y., Yang, X., Zhao, T.Y., Fan, C.F., Zhou, Y.S., Qin, C.F., Wang, Y.C., 2020b. A mouse model of SARS-CoV-2 infection and pathogenesis. Cell Host Microbe 28, 124.

Temmam, S., Barbarino, A., Maso, D., Behillil, S., Enouf, V., Huon, C., Jaraud, A., Chevallier, L., Backovic, M., Pérot, P., Verwaerde, P., Tiret, L., van der Werf, S., Eloit, M., 2020. Absence of SARS-CoV-2 infection in cats and dogs in close contact with a cluster of COVID-19 patients in a veterinary campus. One Health 10, 100164.

Tomley, F.M., Shirley, M.W., 2009. Livestock infectious diseases and zoonoses. Philos. Trans. R. Soc. Lond. B Biol. Sci. 364, 2637.

Tostanoski, L.H., Wegmann, F., Martinot, A.J., Loos, C., McMahan, K., Mercado, N.B., Yu, J., Chan, C.N., Bondoc, S., Starke, C.E., Nekorchuk, M., Busman-Sahay, K., Piedra-Mora, C., Wrijil, L.M., Ducat, S., Custers, J., Atyeo, C., Fischinger, S., Burke, J.S., Feldman, J., Hauser, B.M., Caradonna, T.M., Bondzie, E.A., Dagotto, G., Gebre, M.S., Jacob-Dolan, C., Lin, Z., Mahrokhian, S.H., Nampanya, F., Nityanandam, R., Pessaint, L., Porto, M., Ali, V., Benetiene, D., Tevi, K., Andersen, H., Lewis, M.G., Schmidt, A.G., Lauffenburger, D.A., Alter, G., Estes, J.D., Schuitemaker, H., Zahn, R., Barouch, D.H., 2020. Ad26 vaccine protects against SARS-CoV-2 severe clinical disease in hamsters. Nat. Med. 26, 1694.

Trimpert, J., Vladimirova, D., Dietert, K., Abdelgawad, A., Kunec, D., Dökel, S., Voss, A., Gruber, A.D., Bertzbach, L.D., Osterrieder, N., 2020. The Roborovski dwarf hamster is a highly susceptible model for a rapid and fatal course of SARS-CoV-2 infection. Cell Rep. 33, 108488.

Tseng, C.T., Huang, C., Newman, P., Wang, N., Narayanan, K., Watts, D.M., Makino, S., Packard, M.M., Zaki, S.R., Chan, T.S., Peters, C.J., 2007. Severe acute respiratory syndrome coronavirus infection of mice transgenic for the human Angiotensin-converting enzyme 2 virus receptor. J. Virol. 81, 1162.

Tu, C., Crameri, G., Kong, X., Chen, J., Sun, Y., Yu, M., Xiang, H., Xia, X., Liu, S., Ren, T., Yu, Y., Eaton, B.T., Xuan, H., Wang, L.F., 2004. Antibodies to SARS coronavirus in civets. Emerg. Infect. Dis. 10, 2244.

Ulrich, L., Michelitsch, A., Halwe, N.J., Wernike, K., Hoffmann, D., Beer, M., 2020a. Experimental SARS-CoV-2 infection of bank voles. Emerg. Infect. Dis.

Ulrich, L., Wernike, K., Hoffmann, D., Mettenleiter, T.C., Beer, M., 2020b. Experimental infection of cattle with SARS-CoV-2. Emerg. Infect. Dis. 26, 2979.

van Doremalen, N., Lambe, T., Spencer, A., Belij-Rammerstorfer, S., Purushotham, J.N., Port, J.R., Avanzato, V.A., Bushmaker, T., Flaxman, A., Ulaszewska, M., Feldmann, F., Allen, E.R., Sharpe, H., Schulz, J., Holbrook, M., Okumura, A., Meade-White, K., Pérez-Pérez, L., Edwards, N.J., Wright, D., Bissett, C., Gilbride, C., Williamson, B.N., Rosenke, R., Long, D., Ishwarbhai, A., Kailath, R., Rose, L., Morris, S., Powers, C., Lovaglio, J., Hanley, P.W., Scott, D., Saturday, G., de Wit, E., Gilbert, S.C., Munster, V.J., 2020. ChAdOx1 nCoV-19 vaccine prevents SARS-CoV-2 pneumonia in rhesus macaques. Nature 586, 578.

Vergara-Alert, J., van den Brand, J.M., Widagdo, W., Munoz, M.t., Raj, S., Schipper, D., Solanes, D., Cordon, I., Bensaid, A., Haagmans, B.L., Segales, J., 2017a. Livestock susceptibility to infection with Middle East respiratory syndrome coronavirus. Emerg. Infect. Dis. 23, 232.

Vergara-Alert, J., Raj, V.S., Munoz, M., Abad, F.X., Cordon, I., Haagmans, B.L., Bensaid, A., Segales, J., 2017b. Middle East respiratory syndrome coronavirus experimental transmission using a pig model. Transbound. Emerg. Dis. 64, 1342.

Vergara-Alert, J., Rodon, J., Carrillo, J., Te, N., Izquierdo-Useros, N., Rodriguez de la Concepcion, M.L., Avila-Nieto, C., Guallar, V., Valencia, A., Cantero, G., Blanco, J., Clotet, B., Bensaid, A., Segales, J., 2020. Pigs are not susceptible to SARS-CoV-2 infection but are a model for viral immunogenicity studies. Transbound. Emerg. Dis.

Vijgen, L., Keyaerts, E., Moes, E., Thoelen, I., Wollants, E., Lemey, P., Vandamme, A.M., Van Ranst, M., 2005. Complete genomic sequence of human coronavirus OC43: molecular clock analysis suggests a relatively recent zoonotic coronavirus transmission event. J. Virol. 79, 1595.

Vijgen, L., Keyaerts, E., Lemey, P., Maes, P., Van Reeth, K., Nauwynck, H., Pensaert, M., Van Ranst, M., 2006. Evolutionary history of the closely related group 2 coronaviruses: porcine hemagglutinating encephalomyelitis virus, bovine coronavirus, and human coronavirus OC43. J. Virol. 80, 7270.

Wacharapluesadee, S., Tan, C.W., Maneeorn, P., Duengkae, P., Zhu, F., Joyjinda, Y., Kaewpom, T., Chia, W.N., Ampoot, W., Lim, B.L., Worachotsueptrakun, K., Chen, V.C., Sirichan, N., Ruchisrisarod, C., Rodpan, A., Noradechanon, K., Phaichana, T., Jantarat, N., Thongnumchaima, B., Tu, C., Crameri, G., Stokes, M.M., Hemachudha, T., Wang, L.F., 2021. Evidence for SARS-CoV-2 related coronaviruses circulating in bats and pangolins in Southeast Asia. Nat. Commun. 12, 972.

Wahba, L., Jain, N., Fire, A.Z., Shoura, M.J., Artiles, K.L., McCoy, M.J., Jeong, D.E., 2020. An extensive meta-metagenomic search identifies SARS-CoV-2-homologous sequences in pangolin lung viromes. mSphere 5.

Wan, Y., Shang, J., Graham, R., Baric, R.S., Li, F., 2020. Receptor recognition by the novel coronavirus from Wuhan: an analysis based on decade-long structural studies of SARS coronavirus. J. Virol. 94.

Wang, Q., Vlasova, A.N., Kenney, S.P., Saif, L.J., 2019. Emerging and re-emerging coronaviruses in pigs. Curr. Opin. Virol. 34, 39.

Wang, J., Shuai, L., Wang, C., Liu, R., He, X., Zhang, X., Sun, Z., Shan, D., Ge, J., Wang, X., Hua, R., Zhong, G., Wen, Z., Bu, Z., 2020. Mouse-adapted SARS-CoV-2 replicates efficiently in the upper and lower respiratory tract of BALB/c and C57BL/6J mice. Protein Cell 11, 776.

WHO, 2003. Consensus document on the epidemiology of severe acute respiratory syndrome (SARS). Online available: https://apps.who.int/iris/handle/10665/70863. last accessed: 26 January 2021.

WHO, 2010. What Is a Pandemic? Online available: https://www.who.int/csr/disease/swineflu/frequently_asked_questions/pandemic/en/. last accessed: 21 January 2021.

WHO, 2013. State of knowledge and data gaps of Middle East Respiratory Syndrome Coronavirus (MERS-CoV) in humans. PLoS Curr. 5.

WHO, 2019. MERS Situation Update September 2019. Online available: https://applications.emro.who.int/docs/EMROPub-MERS-SEP-2019-EN.pdf?ua=1&ua=1. last accessed: 22 January 2021.

WHO, 2020a. COVID-19 Strategy Update—14 April 2020. Online available: https://www.who.int/publications-detail/covid-19-strategy-update- – -14-april-2020. last accessed: 16 January 2021.

WHO, 2020b. SARS-CoV-2 Mink-Associated Variant Strain—Denmark. Online available: https://www.who.int/csr/don/03-december-2020-mink-associated-sars-cov2-denmark/en/;. last accessed: 26 January 2021 Disease Outbreak News: Update.

WHO, 2020c. SARS-CoV-2 Variants. Disease Outbreak News 31 December 2020. Online available: https://www.who.int/csr/don/31-december-2020-sars-cov2-variants/en/. last accessed: 26 January 2021.

WHO, 2021. One Health. Online available: https://www.euro.who.int/en/health-topics/health-policy/one-health;. last accessed: 25 January 2021.

Widagdo, W., Sooksawasdi Na Ayudhya, S., Hundie, G.B., Haagmans, B.L., 2019a. Host determinants of MERS-CoV transmission and pathogenesis. Viruses 11.

Widagdo, W., Okba, N.M.A., Richard, M., de Meulder, D., Bestebroer, T.M., Lexmond, P., Farag, E., Al-Hajri, M., Stittelaar, K.J., de Waal, L., van Amerongen, G., van den Brand, J.M.A., Haagmans, B.L., Herfst, S., 2019b. Lack of Middle East respiratory syndrome coronavirus transmission in rabbits. Viruses 11.

Wiethoelter, A.K., Beltran-Alcrudo, D., Kock, R., Mor, S.M., 2015. Global trends in infectious diseases at the wildlife–livestock interface. Proc. Natl. Acad. Sci. U. S. A. 112, 9662.

Wille, M., Holmes, E.C., 2020. Wild birds as reservoirs for diverse and abundant gamma- and deltacoronaviruses. FEMS Microbiol. Rev. 44, 631.

Williamson, B.N., Feldmann, F., Schwarz, B., Meade-White, K., Porter, D.P., Schulz, J., van Doremalen, N., Leighton, I., Yinda, C.K., Pérez-Pérez, L., Okumura, A., Lovaglio, J., Hanley, P.W., Saturday, G., Bosio, C.M., Anzick, S., Barbian, K., Cihlar, T., Martens, C., Scott, D.P., Munster, V.J., de Wit, E., 2020. Clinical benefit of remdesivir in rhesus macaques infected with SARS-CoV-2. Nature 585, 273.

Winkler, E.S., Bailey, A.L., Kafai, N.M., Nair, S., McCune, B.T., Yu, J., Fox, J.M., Chen, R.E., Earnest, J.T., Keeler, S.P., Ritter, J.H., Kang, L.I., Dort, S., Robichaud, A., Head, R., Holtzman, M.J., Diamond, M.S., 2020. SARS-CoV-2 infection of human ACE2-transgenic mice causes severe lung inflammation and impaired function. Nat. Immunol. 21, 1327.

Wong, G., Bi, Y.H., Wang, Q.H., Chen, X.W., Zhang, Z.G., Yao, Y.G., 2020. Zoonotic origins of human coronavirus 2019 (HCoV-19/SARS-CoV-2): why is this work important? Zool. Res. 41, 213.

Woolsey, C., Borisevich, V., Prasad, A.N., Agans, K.N., Deer, D.J., Dobias, N.S., Heymann, J.C., Foster, S.L., Levine, C.B., Medina, L., Melody, K., Geisbert, J.B., Fenton, K.A., Geisbert, T.W., Cross, R.W., 2020. Establishment of an African green monkey model for COVID-19. bioRxiv.

WSAVA, 2020. WSAVA Advice for Pet Owners During the COVID-19 Pandemic.

Wu, Z., McGoogan, J.M., 2020. Characteristics of and important lessons from the coronavirus disease 2019 (COVID-19) outbreak in China: summary of a report of 72314 cases from the Chinese Center for Disease Control and Prevention. JAMA 323, 1239.

Xiao, K., Zhai, J., Feng, Y., Zhou, N., Zhang, X., Zou, J.J., Li, N., Guo, Y., Li, X., Shen, X., Zhang, Z., Shu, F., Huang, W., Li, Y., Zhang, Z., Chen, R.A., Wu, Y.J., Peng, S.M., Huang, M., Xie, W.J., Cai, Q.H., Hou, F.H., Chen, W., Xiao, L., Shen, Y., 2020. Isolation of SARS-CoV-2-related coronavirus from Malayan pangolins. Nature 583, 286.

Xu, L., Yu, D.D., Ma, Y.H., Yao, Y.L., Luo, R.H., Feng, X.L., Cai, H.R., Han, J.B., Wang, X.H., Li, M.H., Ke, C.W., Zheng, Y.T., Yao, Y.G., 2020. COVID-19-like symptoms observed in Chinese tree shrews infected with SARS-CoV-2. Zool. Res. 41, 517.

Yadav, P.D., Shete-Aich, A., Nyayanit, D.A., Pardeshi, P., Majumdar, T., Balasubramanian, R., Ullas, P.T., Mohandas, S., Dighe, H., Sawant, P., Patil, S., Patil, D., Gokhale, M.D., Mathapati, B., Sudeep, A.B., Baradkar, S., Kumar, A., Kharde, R., Salve, M., Joshi, Y., Gupta, N., Mourya, D.T., 2020. Detection of coronaviruses in Pteropus & Rousettus species of bats from different States of India. Indian J. Med. Res. 151, 226.

Yasuhara, J., Watanabe, K., Takagi, H., Sumitomo, N., Kuno, T., 2021. COVID-19 and multisystem inflammatory syndrome in children: a systematic review and meta-analysis. Pediatr. Pulmonol.

Yinda, C.K., Port, J.R., Bushmaker, T., Offei Owusu, I., Purushotham, J.N., Avanzato, V.A., Fischer, R.J., Schulz, J.E., Holbrook, M.G., Hebner, M.J., Rosenke, R., Thomas, T., Marzi, A., Best, S.M., de Wit, E., Shaia, C., van Doremalen, N., Munster, V.J., 2021. K18-hACE2 mice develop respiratory disease resembling severe COVID-19. PLoS Pathog. 17, e1009195.

Yu, J., Tostanoski, L.H., Peter, L., Mercado, N.B., McMahan, K., Mahrokhian, S.H., Nkolola, J.P., Liu, J., Li, Z., Chandrashekar, A., Martinez, D.R., Loos, C., Atyeo, C., Fischinger, S., Burke, J.S., Slein, M.D., Chen, Y., Zuiani, A., Lelis, F.J.N., Travers, M., Habibi, S., Pessaint, L., Van Ry, A., Blade, K., Brown, R., Cook, A., Finneyfrock, B., Dodson, A., Teow, E., Velasco, J., Zahn, R., Wegmann, F., Bondzie, E.A., Dagotto, G., Gebre, M.S., He, X., Jacob-Dolan, C., Kirilova, M., Kordana, N., Lin, Z., Maxfield, L.F., Nampanya, F., Nityanandam, R., Ventura, J.D., Wan, H., Cai, Y., Chen, B., Schmidt, A.G., Wesemann, D.R., Baric, R.S., Alter, G., Andersen, H., Lewis, M.G., Barouch, D.H., 2020a. DNA vaccine protection against SARS-CoV-2 in rhesus macaques. Science 369, 806.

Yu, P., Qi, F., Xu, Y., Li, F., Liu, P., Liu, J., Bao, L., Deng, W., Gao, H., Xiang, Z., Xiao, C., Lv, Q., Gong, S., Liu, J., Song, Z., Qu, Y., Xue, J., Wei, Q., Liu, M., Wang, G., Wang, S., Yu, H., Liu, X., Huang, B., Wang, W., Zhao, L., Wang, H., Ye, F., Zhou, W., Zhen, W., Han, J., Wu, G., Jin, Q., Wang, J., Tan, W., Qin, C., 2020b. Age-related rhesus macaque models of COVID-19. Anim. Model Exp. Med. 3, 93.

Zhang, Q., Zhang, H., Gao, J., Huang, K., Yang, Y., Hui, X., He, X., Li, C., Gong, W., Zhang, Y., Zhao, Y., Peng, C., Gao, X., Chen, H., Zou, Z., Shi, Z.L., Jin, M., 2020a. A serological survey of SARS-CoV-2 in cat in Wuhan. Emerg. Microbes Infect. 9, 2013.

Zhang, C., Zheng, W., Huang, X., Bell, E.W., Zhou, X., Zhang, Y., 2020b. Protein structure and sequence reanalysis of 2019-nCoV genome refutes snakes as its intermediate host and the unique similarity between its spike Pprotein insertions and HIV-1. J. Proteome Res. 19, 1351.

Zhang, A.J., Lee, A.C., Chan, J.F., Liu, F., Li, C., Chen, Y., Chu, H., Lau, S.Y., Wang, P., Chan, C.C., Poon, V.K., Yuan, S., To, K.K., Chen, H., Yuen, K.Y., 2020c. Co-infection by severe acute respiratory syndrome coronavirus 2 and influenza A(H1N1)pdm09 virus enhances the severity of pneumonia in golden Syrian hamsters. Clin. Infect. Dis.

Zhang, T., Wu, Q., Zhang, Z., 2020d. Probable pangolin origin of SARS-CoV-2 associated with the COVID-19 outbreak. Curr. Biol. 30, 1346.

Zhao, Y., Wang, J., Kuang, D., Xu, J., Yang, M., Ma, C., Zhao, S., Li, J., Long, H., Ding, K., Gao, J., Liu, J., Wang, H., Li, H., Yang, Y., Yu, W., Yang, J., Zheng, Y., Wu, D., Lu, S., Liu, H., Peng, X., 2020a. Susceptibility of tree shrew to SARS-CoV-2 infection. Sci. Rep. 10, 16007.

Anna Michelitsch et al.

Zhao, J., Cui, W., Tian, B.P., 2020b. The potential intermediate hosts for SARS-CoV-2. Front. Microbiol. 11, 580137.

Zheng, J., Wong, L.R., Li, K., Verma, A.K., Ortiz, M.E., Wohlford-Lenane, C., Leidinger, M.R., Knudson, C.M., Meyerholz, D.K., McCray, P.B., Jr., Perlman, S., 2020a. COVID-19 treatments and pathogenesis including anosmia in K18-hACE2 mice. Nature.

Zheng, H., Li, H., Guo, L., Liang, Y., Li, J., Wang, X., Hu, Y., Wang, L., Liao, Y., Yang, F., Li, Y., Fan, S., Li, D., Cui, P., Wang, Q., Shi, H., Chen, Y., Yang, Z., Yang, J., Shen, D., Cun, W., Zhou, X., Dong, X., Wang, Y., Chen, Y., Dai, Q., Jin, W., He, Z., Li, Q., Liu, L., 2020b. Virulence and pathogenesis of SARS-CoV-2 infection in rhesus macaques: a nonhuman primate model of COVID-19 progression. PLoS Pathog. 16, e1008949.

Zhong, N.S., Zheng, B.J., Li, Y.M., Poon, L.L., Xie, Z.H., Chan, K.H., Li, P.H., Tan, S.Y., Chang, Q., Xie, J.P., Liu, X.Q., Xu, J., Li, D.X., Yuen, K.Y., Peiris, J.S., Guan, Y., 2003. Epidemiology and cause of severe acute respiratory syndrome (SARS) in Guangdong, People's Republic of China, in February, 2003. Lancet 362, 1353.

Zhou, P., Yang, X.L., Wang, X.G., Hu, B., Zhang, L., Zhang, W., Si, H.R., Zhu, Y., Li, B., Huang, C.L., Chen, H.D., Chen, J., Luo, Y., Guo, H., Jiang, R.D., Liu, M.Q., Chen, Y., Shen, X.R., Wang, X., Zheng, X.S., Zhao, K., Chen, Q.J., Deng, F., Liu, L.L., Yan, B., Zhan, F.X., Wang, Y.Y., Xiao, G.F., Shi, Z.L., 2020. A pneumonia outbreak associated with a new coronavirus of probable bat origin. Nature 579, 270.

CHAPTER III: STUDY OBJECTIVES

III. STUDY OBJECTIVES

Living with SARS-CoV-2 and COVID-19 for almost two years has led to increased evidence on the virus epidemiology, pathogenesis, and strategies to combat it. But as the still high numbers of infections and re-infections show, this battle has not yet come to an end and needs further effort. In this present work three objectives have been codified to enhance understanding of the virus and pandemic.

Objective I: Testing different animal species for their susceptibility towards infection with SARS-CoV-2.

Publication I & II

Right from the beginning of the pandemic it was speculated that (wildlife-) animals harbor SARS-CoV-2, but no naturally SARS-CoV-2 infected animals were found in this early phase. The risk of an animal species with reservoir properties that could account for continuous (re-) introduction of this agent into human population, however, was not eliminated. Furthermore, susceptible species could act as `recombination-vessels´ for the emergence of novel recombinant isolates with altered biological traits. Third, research and control of pandemics, relies on robust animal models. Hence, evaluating the role of different animal species for susceptibility, and for their eligibility to host, transmit, and spread SARS-CoV-2 to conspecifics, was aimed.

Objective II: Characterization of SARS-CoV-2 variants in a multi-step, competitive transmission trial in different animal species.

Publication III & IV

Public health actions and precautions, preparedness of stakeholders in health care service, and vaccine adjustment relies on early detection and warning of virulent strains. SARS-CoV-2 pandemic, though, has been fueled by the rise of new viral variants, which displace endemic variants. Moreover, emerging variants bear the risk of not only increased transmissibility, but also disease severity and immune-evasion. The chosen approach to test variants one vs. one in a competitive transmission trial accelerates knowledge on their traits and helps to gain valuable time.

Objective III: Developing a challenge-trial in highly SARS-CoV-2 susceptible animals for safety and efficacy testing of promising vaccine-precursors.

Publication V

Defeating COVID-19, or at least catching up a little with its rapid evolution is critically depending on the availability of efficacious vaccines. Particularly COVID-19 has brought back to memory, that vaccine development is a rugged and long way to go. Vaccines have to be safe, with little risk of adverse effects and have to significantly improve outcomes of vaccinated people. In turn, public acceptance of vaccines depends on these factors. For ethical and moral reasons, a challenge study in humans vaccinated with non-characterized vaccines are strictly excluded. So, to test vaccine-induced immunity and protection, as well as safety, a highly standardized and highly susceptible challenge model needs to be found.

CHAPTER IV: RESULTS

IV. RESULTS

Publications appear in a grouped order, according to the related "study objectives"-section. Figure and table numbering are according to the original paper and references are presented in the respective journal style and do not appear in the reference section of this document. The original work can be found under the denoted digital object identifier (doi). Where supplemental material is not added in this thesis, it can also be found there.

1. Publication I: Experimental Infection of Cattle with SARS-CoV-2

Publication I

Experimental Infection of Cattle with SARS-CoV-2

Lorenz Ulrich, Kerstin Wernike, Donata Hoffmann, Thomas C. Mettenleiter, Martin Beer

Experimental Infection of Cattle with SARS-CoV-2

Lorenz Ulrich, Kerstin Wernike, Donata Hoffmann, Thomas C. Mettenleiter, Martin Beer

We inoculated 6 cattle with severe acute respiratory syndrome coronavirus 2 and kept them together with 3 in-contact, virus-naive cattle. We observed viral replication and specific seroreactivity in 2 inoculated animals, despite high levels of preexisting antibody titers against a bovine betacoronavirus. The in-contact animals did not become infected.

After spilling over from an unknown animal host to humans, a novel betacoronavirus called severe acute respiratory syndrome coronavirus 2 (SARS-CoV-2) emerged in December 2019 (1,2) and induced a global pandemic. This virus, which causes coronavirus disease, was first identified in humans in Wuhan, China (3). The role of livestock and wildlife species at the human-animal interface in disease emergence and dynamics was extensively discussed, focusing on the identification of susceptible species, potential reservoirs, and intermediate hosts. Natural or experimental infections have demonstrated the susceptibility of fruit bats (*Rousettus aegyptiacus*), ferrets, felids, dogs, and minks to the virus; however, pigs, chicken, and ducks are not susceptible (4–6). Besides ducks, chicken, and pigs, other major livestock species, including >1.5 billion cattle (*Bos taurus*), live with close contact with humans. Non-SARS-CoV-2 betacoronaviruses are widespread in bovines (7); seroprevalences reach up to 90% (8), but these infections are usually subclinical (7). However, whether any ruminant species are susceptible to SARS-CoV-2 infection or whether there is any cross-reactivity of antibodies against bovine coronaviruses (BCoVs) and SARS-CoV-2 is unknown. We examined the susceptibility of cattle to SARS-CoV-2 infection and characterized the course of infection.

The Study

From a group of 9 dairy calves, we intranasally inoculated 6 with 1 x 10⁵ 50% tissue culture infectious dose of SARS-CoV-2 (strain 2019_nCoV Muc-IMB-1). We

reintroduced the other 3 SARS-CoV-2–naive (hereafter in-contact) cattle to the 6 infected animals 24 hours after inoculation. We monitored body temperature and clinical signs daily. We also obtained and processed blood samples and nasal, oral, and rectal swab samples (Appendix, https://wwwnc.cdc.gov/EID/article/26/12/20-3799-App1.pdf). The experimental protocol was assessed and approved by the ethics committee of the State Office of Agriculture, Food Safety, and Fisheries in Mecklenburg–Western Pomerania, Germany (permission no. MV/TSD/7221.3–2-010/18).

Before infection, all animals tested negative for SARS-CoV-2 RNA in nasal, oral, and rectal swab samples and antibodies against SARS-CoV-2 in serum samples. Veterinarians conducted daily physical examinations and noted that none of the animals (inoculated or not) showed signs of clinical SARS-CoV-2 infection (Appendix). Throughout the study, the animals' body temperatures, feed intake, and general condition remained within normal limits (Appendix).

We demonstrated viral replication in 2 of the inoculated animals. One animal (no. 776) tested positive for viral RNA in the nCoV IP4 real-time reverse transcription PCR (RT-PCR) on days 2 (quantification cycle [Cq] value 29.97) and 3 (Cq 33.79) after infection. Another calf (no. 768) tested positive on day 3 (Cq 38.13) (Figure, panel A). We confirmed the results with a second real-time RT-PCR selective for the *E* gene; we measured Cq values of 29.26 (no. 776, day 2 after infection), 32.12 (no. 776, day 3), and 36.18 (no. 768, day 3). We verified the results with real-time RT-PCR using the ID GENE SARS-COV-2 DUPLEX kit (IDvet, https://www.id-vet.com) (Cq values 29.17 [no. 776, day 2 after infection], 30.55 [no. 776, day 3], and 36.07 [no. 768, day 3]). These animals tested positive only in the nasal swab samples.

We tested serum samples with an indirect ELISA specific to the SARS-CoV-2 receptor binding domain (RBD-ELISA). An increase in seroreactivity was observed for animal 776 from day 12 onward, indicating seroconversion (Figure, panel B). On day 20, we took serum samples that confirmed the positive ELISA findings and used an indirect immunofluorescence assay

Figure. Characterization of SARS-CoV-2 infection in cattle. Animals directly inoculated shown in black. In-contact animals shown in blue. Individual animals are indicated by the same symbol in every figure panel. A) Viral load in nasal swab samples measured by real-time RT-PCR. Animals 776 and 768 had detectable viral loads on days 2 and 3 (no. 776) or day 3 only (no. 768). B) Results of indirect ELISA specific to the SARS-CoV-2 receptor binding domain. Serum samples taken on days -1 before infection and 6, 12, and 20 days after infection. Values below the dashed line are considered negative for antibodies against SARS-CoV-2. C) Results of indirect immunofluorescence assay for BCoV. D) Results of virus neutralization test for BCoV. Indirect immunofluorescence and virus neutralization test showed that animal 842, which tested positive for BCoV in the nasal swab sample by real-time RT-PCR, had an increase in antibody titer against BCoV. Preinfection antibody titers against BCoV did not affect infection with SARS-CoV-2, as animals 776 and 768, which tested positive for SARS-CoV-2, showed no infection-related reaction of BCoV antibody titers. BCoV, bovine coronavirus; ND_{50}, 50% neutralizing dose, RT-PCR, reverse transcription PCR; SARS-CoV-2, severe acute respiratory syndrome coronavirus 2.
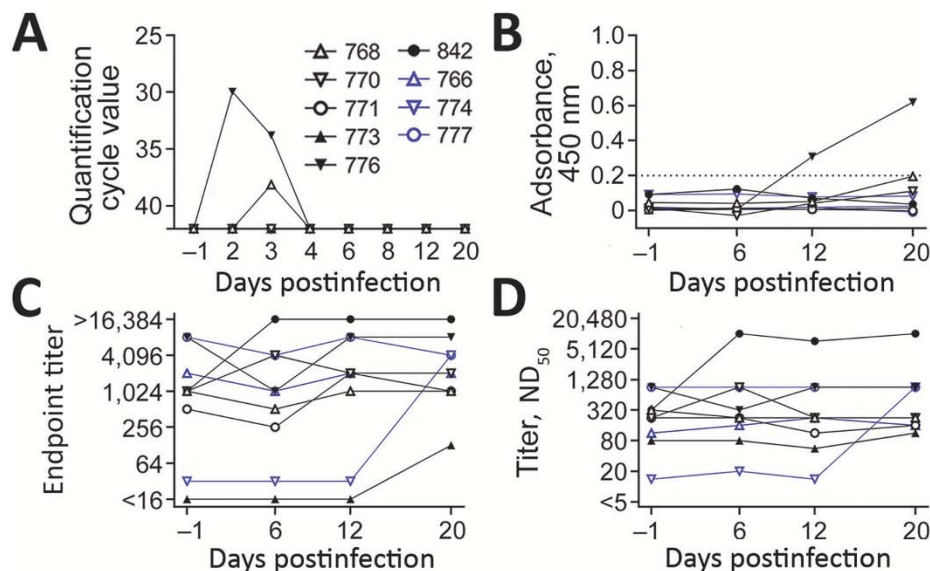
(iIFA) to measure a low antibody titer of 1:4. In addition, a virus neutralization test (VNT) (serum dilution 1:2) showed a visible, although incomplete, inhibition of viral replication. Samples taken on day 20 from animal 768 showed only slightly increased seroreactivity in ELISA, whereas iIFA and VNT results remained negative. These differences might be attributable to varying test sensitivities or a possible restriction of viral replication to the upper respiratory tract. Throughout the study, the other animals tested negative for antibodies against SARS-CoV-2 by ELISA, iIFA, and VNT.

We also tested the BCoV status of each calf. Before SARS-CoV-2 infection, all animals had neutralizing antibodies against BCoV, although the titers differed substantially among individual animals (Figure, panel D). Three animals showed an increase in antibody titers against BCoV by iIFA (no. 842 and 773, which were directly infected with SARS-CoV-2, and no. 774, an in-contact animal) and 2 also by VNT (no. 842 and 774) within the study period (Figure). To show that this increase was caused by a natural BCoV infection and not SARS-CoV-2, we tested nasal swab samples for BCoV using RT-PCR selective for the *RdRp* region (9). Animal 842 tested positive by PCR for BCoV RNA 1 day before our experimental SARS-CoV-2 infection and 2 days after infection. We used Sanger sequencing to confirm the BCoV infection, which had increased the titer of anti-

bodies against BCoV in this animal (Figure). Animal 842 presumably infected animal 774 with BCoV. However, we did not observe any cross-reactivity of the bovine coronavirus with the applied SARS-CoV-2 tests, because all animals tested negative by the nCoV IP4 PCR for SARS-CoV-2, the iIFA and VNT specific to SARS-CoV-2, and the RBD-ELISA (Figure) before infection. Moreover, 2 animals (nos. 776 and 768) with high BCoV seroreactivity tested positive for SARS-CoV-2 RNA after inoculation, whereas those with lower BCoV-specific titers could not be infected, further confirming a lack of any cross-reactivity or cross-protection.

Conclusions

Our findings demonstrate that under experimental conditions cattle show low susceptibility to SARS-CoV-2 infection. This finding corresponds with a predicted medium susceptibility of cattle species on the basis of a computational modelling of their angiotensin-I-converting enzyme 2, the cellular receptor for SARS-CoV-2 (10).

We inoculated 6 cattle with SARS-CoV-2; of these animals, 2 later tested positive for the virus in PCR of nasal swab samples and show specific seroconversion by RBD-ELISA. Even though the genome loads detected in animal 768 at day 3 were low, there is evidence that this animal was confronted with real viral

replication. RNA residues from inoculation are only detectable shortly after inoculation; here, the day 2 nasal swab tested repeatedly PCR negative. Furthermore, other studies using the same infection dose and vaporization device also found no residual RNA on day 2 (5). In addition, the low-level viral replication led to a slight, but detectable, serologic reaction in the applied ELISA (Figure, panel B).

In our study, we did not observe intraspecies transmission to in-contact cattle. Thus, we have no indication that cattle play any role in the human pandemic, and no reports of naturally infected bovines exist. Nevertheless, in regions with large cattle populations and high prevalence of SARS-CoV-2 infection in humans, such as the United States or countries in South America, close contact between livestock and infected animal owners or caretakers could cause anthropo-zoonotic infections of cattle, as has been already described for highly susceptible animal species such as minks, felids, and dogs (6,11). When assessing the risk for virus circulation within bovine populations, one should consider the age, husbandry practices, and underlying health conditions of the animals. Outbreak investigations might include cattle, particularly if direct contact has occurred between animals and persons infected with SARS-CoV-2. In addition to direct detection by PCR, serologic screenings with sensitive and specific ELISAs should also be taken into consideration. In this context, the wide distribution of BCoV is of special interest, especially because the presence of a preexisting coronavirus did not protect from infection with another betacoronavirus in this study. Double infections of individual animals might lead to recombination events between SARS-CoV-2 and BCoV, a phenomenon already described for other pandemic coronaviruses (12). A resulting chimeric virus, comprising characteristics of both viruses, could threaten human and livestock populations and should therefore be monitored.

This article was preprinted at https://www.biorxiv.org/content/10.1101/2020.08.25.254474v1.

About the Author

Mr. Ulrich is a veterinarian and doctoral candidate at the Friedrich-Loeffler-Institut, Greifswald-Insel Riems, Germany. His research interests include pathogenesis and prevention of zoonotic viruses.

References
1. World Health Organization. COVID-19 strategy update—14 April 2020. 2020 [cited 2020 May 16]. https://www.who.int/publications/i/item/covid-19-strategy-update---14-april-2020
2. Andersen KG, Rambaut A, Lipkin WI, Holmes EC, Garry RF. The proximal origin of SARS-CoV-2. Nat Med. 2020;26:450–2. https://doi.org/10.1038/s41591-020-0820-9
3. Zhu N, Zhang D, Wang W, Li X, Yang B, Song J, et al.; China Novel Coronavirus Investigating and Research Team. A novel coronavirus from patients with pneumonia in China, 2019. N Engl J Med. 2020;382:727–33. https://doi.org/10.1056/NEJMoa2001017
4. Shi J, Wen Z, Zhong G, Yang H, Wang C, Huang B, et al. Susceptibility of ferrets, cats, dogs, and other domesticated animals to SARS-coronavirus 2. Science. 2020;368:1016–20. https://doi.org/10.1126/science.abb7015
5. Schlottau K, Rissmann M, Graaf A, Schön J, Sehl J, Wylezich C, et al. SARS-CoV-2 in fruit bats, ferrets, pigs, and chickens: an experimental transmission study. Lancet Microbe. 2020 Jul 7 [Epub ahead of print]. https://doi.org/10.2807/1560-7917.ES.2020.25.23.2001005
6. Oreshkova N, Molenaar RJ, Vreman S, Harders F, Oude Munnink BB, Hakze-van der Honing RW, et al. SARS-CoV-2 infection in farmed minks, the Netherlands, April and May 2020. Euro Surveill. 2020;25:25. https://doi.org/10.2807/1560-7917.ES.2020.25.23.2001005
7. Hodnik JJ, Ježek J, Starič J. Coronaviruses in cattle. Trop Anim Health Prod. 2020 Jul 17 [Epub ahead of print]. https://doi.org/10.1007/s11250-020-02354-y
8. Boileau MJ, Kapil S. Bovine coronavirus associated syndromes. Vet Clin North Am Food Anim Pract. 2010;26:123–46. https://doi.org/10.1016/j.cvfa.2009.10.003
9. Dominguez SR, O'Shea TJ, Oko LM, Holmes KV. Detection of group 1 coronaviruses in bats in North America. Emerg Infect Dis. 2007;13:1295–300. https://doi.org/10.3201/eid1309.070491
10. Damas J, Hughes GM, Keough KC, Painter CA, Persky NS, Corbo M, et al. Broad host range of SARS-CoV-2 predicted by comparative and structural analysis of ACE2 in vertebrates. Proc Natl Acad Sci U S A. 2020;117:22311–22. https://doi.org/10.1073/pnas.2010146117
11. Sailleau C, Dumarest M, Vanhomwegen J, Delaplace M, Caro V, Kwasiborski A, et al. First detection and genome sequencing of SARS-CoV-2 in an infected cat in France. Transbound Emerg Dis. 2020 Jun 5 [Epub ahead of print]. https://doi.org/10.1111/tbed.13659
12. Forni D, Cagliani R, Clerici M, Sironi M. Molecular evolution of human coronavirus genomes. Trends Microbiol. 2017;25:35–48. https://doi.org/10.1016/j.tim.2016.09.001

Address for correspondence: Martin Beer, Institute of Diagnostic Virology, Friedrich-Loeffler-Institut, Südufer 10, 17493 Greifswald-Insel Riems, Germany; email: martin.beer@fli.de

Experimental Infection of Cattle with SARS-CoV-2

Appendix

Experimental Design and Clinical Examination

Six 4–5 month-old, male Holstein-Friesian dairy calves were intranasally inoculated under BSL-3 conditions with 1×10^5 tissue culture infectious dose 50% ($TCID_{50}$) of SARS-CoV-2 strain "2019_nCoV Muc-IMB-1" (GISAID ID_EPI_ISL_406862, designation "hCoV-19/Germany/BavPat1/2020") at 1 mL per nostril, using a vaporization device (Teleflex Medical, Germany). Twenty-four hours after inoculation three contact cattle, that were separated before infection, were re-introduced. Body temperature was monitored daily and nasal, oral and rectal swabs were taken on days −1, 2, 3, 4, 6, 8, 12 and 20, and blood samples on days −1, 6, 12 and 20 after infection. Extensive physical examination was carried out once per day by veterinarians considering parameters as general and feeding behavior, liveliness, body temperature, and posture with a special focus on respiratory disease related signs, such as nasal and ocular discharge, labored breathing, and respiratory sounds. Additionally, for each cattle a daily clinical score has been determined. A value of 0 to 3 points each representing physiologic conditions to severe disease signs was awarded for liveliness, posture, motion and feed intake. Body temperature was also scored: a value of 0 was used for temperatures <39.5°C, 1 for a slightly increased temperature of 39.5° to 40.0°C, 2 for fever between 40.1° and 40.5°C, and a value of 3 for temperatures exceeding 40.5°C. The individual values for each category were summarized, and any animal with a clinical score larger than 3 out of 15 was monitored by a veterinarian at least 3 times a day. Additionally, the cattle were taken care of in the daily morning and evening routine by staff animal caretakers. During the entire study, a clinical score of 0 was calculated for all animals and every day with the exception of animal 771 (scores of 1 two days before infection, 1 one day before infection, and 3 on the day of SARS-CoV-2 inoculation, due to increased body temperature) and the in-contact cattle 774 1 day post co-housing (score of 2 due to an increase in body temperature) (Appendix Figure). Since no other clinical signs were obvious for animal 774, and body temperature dropped below 39.5°C within 8 hours, no further measures were taken. The slight increases in body temperature were not considered to be related to the

Page 1 of 3

82

SARS-CoV-2 inoculation, as they occurred either before infection or immediately after co-housing.

Sample Processing

Swabs (Medical Wire & Equipment, UK) were immediately resuspended in 1.25 mL serum-free cell culture medium supplemented with penicillin, streptomycin, gentamycin, and amphotericin B. Nucleic acid was extracted from 100μl of swab fluid using the NucleoMag Vet kit (Macherey-Nagel, Germany), and subsequently tested by the real-time RT-PCR "nCoV_IP4" targeting the RNA-dependent RNA polymerase (RdRp) gene (*1*). Positive results were confirmed by a second real-time RT-PCR based on an E gene target (*2*) and a commercial real-time RT-PCR kit (ID GENE SARS-COV-2 DUPLEX, ID.vet, France). Serum samples were tested by indirect immunofluorescence (iIFA) and virus neutralization assays (VNT) against SARS-CoV-2 as described before (*3*), and by an ELISA based on the receptor-binding domain (RBD) of SARS-CoV-2 (K. Wernike, unpub. data, https://www.biorxiv.org/content/10.1101/2020.08.26.266825v1). In addition, the sera were investigated by iIFA using CRFK cells (L0115, collection of cell lines in veterinary medicine (CCLV), Insel Riems) infected with BCoV strain Nebraska as antigen matrix and by VNT against this BCoV strain on MDBK cells (L0261, CCLV).

References

1. World Health Organization. Coronavirus disease (COVID-19) technical guidance: laboratory testing for 2019-nCoV in humans. 2020 [cited 2020 May 16]. https://www.who.int/emergencies/diseases/novel-coronavirus-2019/technical-guidance/laboratory-guidance</eref>

2. Corman VM, Landt O, Kaiser M, Molenkamp R, Meijer A, Chu DKW, et al. Detection of 2019 novel coronavirus (2019-nCoV) by real-time RT-PCR. Euro Surveill. 2020;25:2000045. PubMed https://doi.org/10.2807/1560-7917.ES.2020.25.3.2000045

3. Schlottau K, Rissmann M, Graaf A, Schön J, Sehl J, Wylezich C, et al. SARS-CoV-2 in fruit bats, ferrets, pigs, and chickens: an experimental transmission study. Lancet Microbe. 2020 Jul 7 [Epub ahead of print].

Page 2 of 3
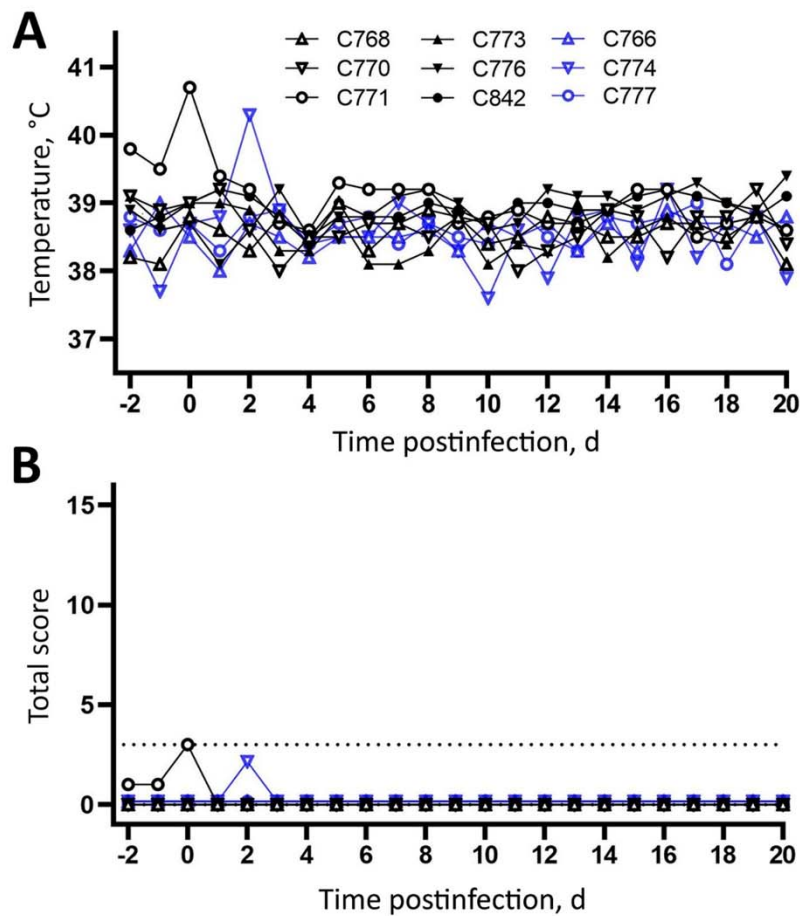
Appendix Figure. Rectal body temperature curves and clinical scores for cattle infected with SARS-CoV-2 and in-contact cattle. Animals directly inoculated are shown in black, while in-contact animals are depicted in blue. A) The daily body temperatures plotted starting 2 days before infection. B) The clinical scores were determined for every animal on each study day and the total score (from 0 to 15) was obtained by summarizing the values awarded for liveliness, posture, motion, feed intake, and body temperature. Any animal with a clinical score >3 (dashed line) was monitored by a veterinarian ≥3 times a day.

2. Publication II: EXPERIMENTAL SARS-COV-2 INFECTION OF BANK VOLES

<u>Publication II</u>

Experimental SARS-CoV-2 Infection of Bank Voles

Lorenz Ulrich, Anna Michelitsch, Nico Halwe, Kerstin Wernike, Donata Hoffmann,

Martin Beer

Experimental SARS-CoV-2 Infection of Bank Voles

Lorenz Ulrich,[1] Anna Michelitsch,[1] Nico Halwe,[1] Kerstin Wernike, Donata Hoffmann, Martin Beer

After experimental inoculation, severe acute respiratory syndrome coronavirus 2 infection was confirmed in bank voles by seroconversion within 8 days and detection of viral RNA in nasal tissue for up to 21 days. However, transmission to contact animals was not detected. Thus, bank voles are unlikely to establish effective transmission cycles in nature.

Severe acute respiratory syndrome coronavirus 2 (SARS-CoV-2) led to a global pandemic in the human population within months after its first reporting (1). Potential wildlife reservoirs of SARS-CoV-2 remain unknown; susceptibility of various animal species has been described (2,3). Among rodent species, the Syrian hamster (*Mesocricetus auratus*) (4) and the North American deer mouse (*Peromyscus maniculatus*) (A. Fagre et al., unpub. data, https://doi.org/10.1101/2020.08.07.241810; B.D. Griffin et al., unpub. data, https://doi.org/10.1101/2020.07.25.221291), both *Cricetidae* species, have proved to be highly susceptible. These rodents transmit SARS-CoV-2 to co-housed contact animals and therefore are likely to develop effective infection chains, which could result in independent SARS-CoV-2 transmission cycles in nature and sequential reintroduction to the human population (4; B.D. Griffin et al., unpub. data, https://doi.org/10.1101/2020.07.25.221291). In Europe, bank voles (*Myodes glareolus*) are a widespread *Cricetidae* species (5). We aimed to characterize SARS-CoV-2 infection in bank voles and their ability to maintain sustainable infection chains.

We intranasally inoculated 9 bank voles with SARS-CoV-2 strain Muc-IMB-1 and, 24 hours later, co-housed 1 contact animal with each of 3 groups of 3 inoculated animals (donor–recipient ratio [d:r] 3:1). We took swab samples regularly from all animals (Appendix, https://wwwnc.cdc.gov/EID/article/27/4/20-4945-App1.pdf); we euthanized 1 or 2 animals at predefined times (Appendix). One bank vole did not survive initial anesthesia for inoculation.

Neither inoculated nor contact animals showed clinical signs during the study. We detected seroconversion for all directly inoculated animals euthanized 8, 12, and 21 days postinfection (dpi), whereas the animals euthanized 4 dpi and the contact animals were all clearly seronegative for SARS-CoV-2 antibodies in an already validated indirect multispecies ELISA based on the receptor-binding domain (6).

All directly inoculated bank voles tested positive for SARS-CoV-2 by quantitative reverse transcription PCR (qRT-PCR) by oral and rhinarium swab specimens at 2 dpi. At 4 dpi, 5 of these 8 animals were positive by oral swab specimen; 2 were also positive by rhinarium swab specimen. On both sampling days, rectal swab specimens of 2 animals tested positive for SARS-CoV-2 by qRT-PCR. Groupwise collected fecal samples also tested positive by qRT-PCR at 2 and 4 dpi. All swabs collected 8, 12, and 16 dpi from directly inoculated animals and every swab from the co-housed contact animals tested negative by qRT-PCR (Table; Figure).

Two animals were euthanized at 4 dpi; nasal conchae, trachea, lung, and olfactory bulb samples tested positive for SARS-CoV-2 RNA by qRT-PCR (quantification cycle [Cq] 25.45–37.15). One animal showed viral genome in cerebrum and cerebellum samples, whereas the spleen sample from the other animal was positive for the viral genome. At 8 dpi another 2 animals were euthanized; both exhibited viral RNA only within the nasal conchae. The animal euthanized at 12 dpi was negative in all collected tissue samples. Nasal conchae of 3 inoculated animals euthanized at 21 dpi tested positive by qRT-PCR (Cq values 34.78, 34.97, 36.25), whereas all 3 contact animals euthanized at the same time tested negative in the nasal conchae.

Reisolation of viable virus from tissue materials in cell culture (Vero E6) was successful for 1 nasal conchae sample taken at 4 dpi. However, isolation

---

[1]These authors contributed equally to this article.

Table. Quantitative reverse transcription PCR results of swab sampling for all inoculated and contact bank voles in experimental study of SARS-CoV-2 transmission*

Box	Status	Swab	−1 dpi	2 dpi	4 dpi	8 dpi	12 dpi	16 dpi
Box 1	Inoculated	Oral	Neg	32.45	Neg	Neg	Neg	Neg
		Nasal	Neg	32.29	Neg	Neg	Neg	Neg
		Rectal	Neg	Neg	Neg	Neg	Neg	Neg
	Inoculated	Oral	Neg	NA	NA	NA	NA	NA
		Nasal	Neg	NA	NA	NA	NA	NA
		Rectal	Neg	NA	NA	NA	NA	NA
	Inoculated	Oral	Neg	32.09	28.16	Neg	Neg	Neg
		Nasal	Neg	31.72	34.03	Neg	Neg	Neg
		Rectal	Neg	36.54	36.39	Neg	Neg	Neg
	Contact	Oral	Neg	Neg	Neg	Neg	Neg	Neg
		Nasal	Neg	Neg	Neg	Neg	Neg	Neg
		Rectal	Neg	Neg	Neg	Neg	Neg	Neg
	Collected feces		Neg	36.58	37.66	Neg	Neg	Neg
Box 2	Inoculated	Oral	Neg	29.40	32.41	NA	NA	NA
		Nasal	Neg	32.68	34.72	NA	NA	NA
		Rectal	Neg	Neg	Neg	NA	NA	NA
	Inoculated	Oral	Neg	30.46	32.54	Neg	NA	NA
		Nasal	Neg	32.30	Neg	Neg	NA	NA
		Rectal	Neg	36.67	Neg	Neg	NA	NA
	Inoculated	Oral	Neg	32.72	37.07	Neg	Neg	Neg
		Nasal	Neg	34.74	Neg	Neg	Neg	Neg
		Rectal	Neg	Neg	Neg	Neg	Neg	Neg
	Contact	Oral	Neg	Neg	Neg	Neg	Neg	Neg
		Nasal	Neg	Neg	Neg	Neg	Neg	Neg
		Rectal	Neg	Neg	Neg	Neg	Neg	Neg
	Collected feces		Neg	36.06	36.65	Neg	Neg	Neg
Box 3	Inoculated	Oral	Neg	30.98	Neg	Neg	NA	NA
		Nasal	Neg	31.63	Neg	Neg	NA	NA
		Rectal	Neg	Neg	Neg	Neg	NA	NA
	Inoculated	Oral	Neg	30.66	34.32	NA	NA	NA
		Nasal	Neg	34.52	Neg	NA	NA	NA
		Rectal	Neg	Neg	34.89	NA	NA	NA
	Inoculated	Oral	Neg	32.64	Neg	Neg	Neg	NA
		Nasal	Neg	35.46	Neg	Neg	Neg	NA
		Rectal	Neg	Neg	Neg	Neg	Neg	NA
	Contact	Oral	Neg	Neg	Neg	Neg	Neg	Neg
		Nasal	Neg	Neg	Neg	Neg	Neg	Neg
		Rectal	Neg	Neg	Neg	Neg	Neg	Neg
	Collected feces		Neg	36.62	37.02	Neg	Neg	Neg

*Positive results are given as quantification cycle values. dpi, days postinoculation; NA, not applicable; Neg, negative; SARS-CoV-2, severe acute respiratory syndrome coronavirus 2.

from samples with Cq >28 failed, in line with findings of other groups (*3,7*).

Overall, bank voles proved to be susceptible to infection with SARS-CoV-2 but did not transmit the virus to co-housed direct contact animals (initial d:r 3:1), in contrast to highly susceptible hamsters or deer mice, which transmit SARS-CoV-2 to each contact animal (d:r 1:1) within 5 days (*4*; B.D. Griffin et al., unpub. data, https://doi.org/10.1101/2020.07.25.221291). Our results suggest a tissue tropism for SARS-CoV-2 replication in bank voles to the upper respiratory tract, as seen for other species, such as ferrets, fruit bats, and raccoon dogs (*3,7*). The persistence of viral genome for at least 3 weeks in nasal tissue of directly inoculated animals was unexpected, especially because the last positive sample was retrieved 4 dpi from the respective bank voles (Table). This finding is most likely the result of the suspected clustering of SARS-CoV-2 infection foci in narrow areas of the upper respiratory tract (L.M. Zaeck et al., unpub. data, https://doi.org/10.1101/2020.10.17.339051). Considering that virus isolation from these 21 dpi samples was not successful, the persistence of SARS-CoV-2 is unlikely to lead to the same shedding of infectious virus as it was shown previously for deer mice (A. Fagre et al., unpub. data, https://doi.org/10.1101/2020.08.07.241810; B.D. Griffin et al., unpub. data, https://doi.org/10.1101/2020.07.25.221291). Deer mice also seem to shed virus through the rectum. However, in bank voles, the SARS-CoV-2 genome could not be detected in the intestines. Although rectal swabs and fecal samples were qRT-PCR positive, the detected Cq values were high, indicating low viral RNA levels. Therefore, the detected viral RNA likely represents residues, which might have resulted from extensive grooming behavior and therefore do not correspond with actual virus shedding from the rectum or feces.
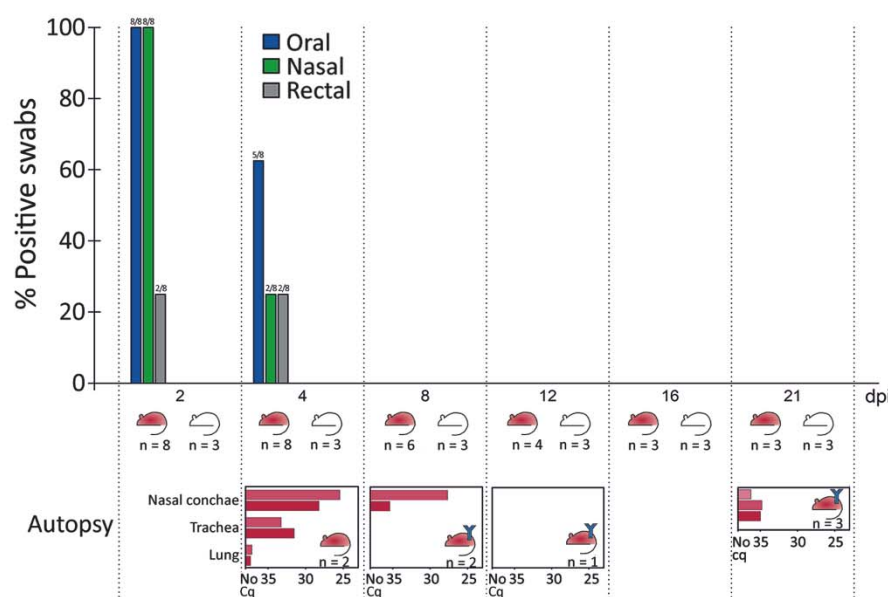
Figure. Percentage of swab specimens positive by quantitative reverse transcription PCR for SARS-CoV-2 on all sampling time points in study of experimental infection of bank voles. The red mouse symbols symbolize inoculated bank voles; the white mouse symbols represent co-housed contact bank voles. Blue Y symbols stand for detected antibodies against SARS-CoV-2 in the respective bank vole group. Quantitative reverse transcription PCR results for the sampled organs of the euthanized, inoculated bank voles are given below the main chart for each time point. Cq, quantification cycle; dpi, days postinoculation; n, number of bank voles; SARS-CoV-2, severe acute respiratory syndrome coronavirus 2.

This study proves a general susceptibility of bank voles toward SARS-CoV-2 infection. However, bank voles did not transmit SARS-CoV-2 to contact animals, making them unlikely to maintain sustainable infection chains in nature. Therefore, the risk of bank voles becoming a reservoir for SARS-CoV-2 in nature (for example, after contact with infected cats) is low.

About the Author

Mr. Ulrich and Dr. Michelitsch are veterinarians and Mr. Halwe is a biologist at the Friedrich-Loeffler-Institut, Greifswald–Insel Riems, Germany. Their research interests include pathogenesis and prevention of zoonotic viruses.

References

1. Zhu N, Zhang D, Wang W, Li X, Yang B, Song J, et al.; China Novel Coronavirus Investigating and Research Team. A novel coronavirus from patients with pneumonia in China, 2019. N Engl J Med. 2020;382:727–33. https://doi.org/10.1056/NEJMoa2001017
2. Muñoz-Fontela C, Dowling WE, Funnell SGP, Gsell PS, Riveros-Balta AX, Albrecht RA, et al. Animal models for COVID-19. Nature. 2020;586:509–15. https://doi.org/10.1038/s41586-020-2787-6
3. Freuling CM, Breithaupt A, Müller T, Sehl J, Balkema-Buschmann A, Rissmann M, et al. Susceptibility of raccoon dogs for experimental SARS-CoV-2 Infection. Emerg Infect Dis. 2020;26:2982–5. https://doi.org/10.3201/eid2612.203733
4. Sia SF, Yan LM, Chin AWH, Fung K, Choy KT, Wong AYL, et al. Pathogenesis and transmission of SARS-CoV-2 in golden hamsters. Nature. 2020;583:834–8. https://doi.org/10.1038/s41586-020-2342-5
5. Michelitsch A, Wernike K, Klaus C, Dobler G, Beer M. Exploring the reservoir hosts of tick-borne encephalitis virus. Viruses. 2019;11:669. https://doi.org/10.3390/v11070669
6. Wernike K, Aebischer A, Michelitsch A, Hoffmann D, Freuling C, Balkema-Buschmann A, et al. Multi-species ELISA for the detection of antibodies against SARS-CoV-2 in animals. Transbound Emerg Dis. 2020;tbed.13926. https://doi.org/10.1111/tbed.13926
7. Schlottau K, Rissmann M, Graaf A, Schön J, Sehl J, Wylezich C, et al. SARS-CoV-2 in fruit bats, ferrets, pigs, and chickens: an experimental transmission study. Lancet Microbe. 2020;1:e218–25. https://doi.org/10.1016/S2666-5247(20)30089-6

Address for correspondence: Martin Beer, Institute of Diagnostic Virology, Friedrich-Loeffler-Institut, Südufer 10, 17493 Greifswald–Insel Riems, Germany; email: martin.beer@fli.de

Experimental SARS-CoV-2 Infection of Bank Voles

Appendix

Animals and Housing Conditions

We obtained 8 female and 4 male bank voles, 7–9 weeks of age, from an in-house breeding colony at the Friedrich-Loeffler-Institut, Insel Riems, Germany. Prior to infection, we determined negative serologic status toward SARS-CoV-2 of the breeding colony by an indirect receptor-binding domain (RBD)-ELISA (*1*). All animals used in the trial tested RT-qPCR negative for SARS-CoV-2 on the day before infection by rhinarium, oral, and rectal swabs. For the duration of the study the animals were kept in individually ventilated cages (IVCs) with a light regime of 12 hours illumination and 12 hours darkness. Drinking water and a rodent diet were provided ad libitum. All handling procedures were performed under biosafety level 3 (BSL-3) conditions.

Study Design

We inoculated 9 bank voles with 1×10^5 tissue culture infection dose 50 ($TCID_{50}$) of the SARS-CoV-2 strain 2019_nCoV Muc-IMB-1 (GISAID ID_EPI_ISL_406862, designation hCoV-19/Germany/BavPat1/2020) by administering 70 μL virus suspension to the nostrils and rhinarium. Inoculation took place under a short-term isoflurane-based inhalation anesthesia. Three inoculated bank voles were housed together in 1 IVC. Twenty-four hours after inoculation another 3 naïve in-contact bank voles, 1 per IVC, were co-housed with the directly inoculated animals. Physical examinations following a defined clinical score regarding general behavior, respiration, eyes, and neurologic symptoms were performed daily and bodyweight changes were monitored regularly (0, 2, 3, 4, 6, 7, 8, 9, 10, 12, 14, 16, and 21 days postinfection [dpi]). Oral, rhinarium, and cloacal swabs were taken from each animal at 2, 4, 8, 12, and 16 dpi. A fecal sample was taken from each IVC at these sampling points.

Two bank voles each were euthanized at 4 and 8 dpi and another at 12 dpi. At autopsy, a serum sample was collected and the nasal conchae, trachea, lung, heart, olfactory bulb, forebrain, cerebellum, liver, spleen, kidney, and small and large intestines were sampled. The remaining animals were euthanized at 21 dpi and serum samples were collected, as well as a sample of the nasal conchae.

Antibody Detection

Serum samples taken during euthanasia were tested by RBD-ELISA (*1*). Absorbance values >0.3 were considered antibody positive, those <0.2 antibody negative, and those in between as questionable (Appendix Table).

RNA Extraction and RT-qPCR

Before sampling, swabs (nerbe plus GmbH, https://www.nerbe-plus.de; Copan Italia S.p.A., https://www.copangroup.com) were dampened with Hank's 692 balanced salts (HBS) and Earle's balanced salts (EBS) in minimum essential medium (MEM). After sampling, the swabs were resuspended in 1 mL HBS and EBS MEM with the addition of penicillin and streptomycin. Fecal samples were directly collected in 1 mL of HBS and EBS MEM with the addition of penicillin and streptomycin. Organ samples were transferred in 1 mL of HBS and EBS MEM with an added steel bead and homogenized at 30,000 Hz for 2 minutes with the TissueLyserII (QIAGEN, https://www.qiagen.com). Nucleic acid was extracted from 100 µL of the supernatant of all samples with the NucleoMag Vet kit (Macherey-Nagel, https://www.mn-net.com). Extracted viral RNA levels were determined by the already validated RT-qPCR nCoV_IP4, targeting the viral RNA-dependent RNA polymerase (*2*). We used a quantification cycle (Cq) value of 38 as a cutoff value (Appendix Table).

Virus Isolation

We attempted virus reisolation in cell culture on a Vero E6 cell line (L0929, collection of cell lines in veterinary medicine, Insel Riems, Germany) using HBS and EBS MEM with the addition of penicillin and streptomycin. Viral replication was determined by cytopathic effect within 72 hours after inoculation. Cultures with no visible cytopathic effect in the first passage were passaged once more.

Page 2 of 3

References

1. Wernike K, Aebischer A, Michelitsch A, Hoffmann D, Freuling C, Balkema-Buschmann A, et al. Multi-species ELISA for the detection of antibodies against SARS-CoV-2 in animals. Transbound Emerg Dis. 2020;tbed.13926. PubMed https://doi.org/10.1111/tbed.13926

2. World Health Organization. Coronavirus disease (COVID-19) technical guidance: laboratory testing for 2019-nCoV in humans [cited 2020 May 16]. https://wwwwhoint/emergencies/diseases/novel-coronavirus-2019/technical-guidance/laboratory-guidance

Appendix Table. RT-qPCR results from organ samples of all inoculated and contact bank voles as well as results from the indirect, multispecies ELISA*

dpi	Status	RBD ELISA absorbance/result	RT-qPCR quantification cycle (Cq)						
			Nasal conchae	Trachea	Lung	Bulbus olfactorius	Cerebrum	Cerebellum	Spleen
4	Inoculated	0.01/negative	25.45	33.26	37.15	32.77	34.17	32.67	Neg
	Inoculated	0.01/negative	28.23	31.53	37.32	37.05	Neg	Neg	35.21
8	Inoculated	0.86/positive	27.66	Neg	Neg	Neg	Neg	Neg	Neg
	Inoculated	0.98/positive	35.38	Neg	Neg	Neg	Neg	Neg	Neg
12	Inoculated	1.02/positive	Neg	Neg	Neg	Neg	Neg	Neg	Neg
21	Inoculated	0.93/positive	36.25	ND	ND	ND	ND	ND	ND
	Inoculated	0.39/positive	34.78	ND	ND	ND	ND	ND	ND
	Inoculated	0.60/positive	34.97	ND	ND	ND	ND	ND	ND
	Contact	0.01/negative	Neg	ND	ND	ND	ND	ND	ND
	Contact	−0.00/negative	Neg	ND	ND	ND	ND	ND	ND
	Contact	−0.00/negative	Neg	ND	ND	ND	ND	ND	ND

*RT-qPCR results are given in quantification cycle values (Cq). dpi: days postinoculation; ND, not done; Neg, negative; RBD, receptor-binding domain.

Page 3 of 3

3. PUBLICATION III: SARS-COV-2 SPIKE D614G CHANGE ENHANCES REPLICATION AND TRANSMISSION

<u>Publication III</u>

SARS-CoV-2 spike D614G change enhances replication and transmission

Bin Zhou, Tran Thi Nhu Thao, Donata Hoffmann, Adriano Taddeo, Nadine Ebert, Fabien Labroussaa, Anne Pohlmann, Jacqueline King, Silvio Steiner, Jenna N. Kelly, Jasmine Portmann, Nico Joel Halwe, Lorenz Ulrich, Bettina Salome Trüeb, Xiaoyu Fan, Bernd Hoffmann, Li Wang, Lisa Thomann, Xudong Lin, Hanspeter Stalder, Berta Pozzi, Simone de Brot, Nannan Jiang, Dan Cui, Jaber Hossain, Malania M. Wilson, Matthew W. Keller, Thomas J. Stark, John R. Barnes, Ronald Dijkman, Joerg Jores, Charaf Benarafa, David E. Wentworth, Volker Thiel & Martin Beer

Article

SARS-CoV-2 spike D614G change enhances replication and transmission

Bin Zhou[1,12], Tran Thi Nhu Thao[2,3,4,12], Donata Hoffmann[5,12], Adriano Taddeo[2,3,12], Nadine Ebert[2,3], Fabien Labroussaa[3,6], Anne Pohlmann[5], Jacqueline King[5], Silvio Steiner[2,3,4], Jenna N. Kelly[2,3], Jasmine Portmann[2,3], Nico Joel Halwe[5], Lorenz Ulrich[5], Bettina Salome Trüeb[3,6], Xiaoyu Fan[1], Bernd Hoffmann[5], Li Wang[1], Lisa Thomann[2,3], Xudong Lin[7], Hanspeter Stalder[2,3], Berta Pozzi[8], Simone de Brot[9], Nannan Jiang[10], Dan Cui[7], Jaber Hossain[1], Malania M. Wilson[1], Matthew W. Keller[1], Thomas J. Stark[1], John R. Barnes[1], Ronald Dijkman[2,3,11], Joerg Jores[3,6], Charaf Benarafa[2,3,13 ✉], David E. Wentworth[1,13 ✉], Volker Thiel[2,3,13 ✉] & Martin Beer[5,13 ✉]

During the evolution of SARS-CoV-2 in humans, a D614G substitution in the spike glycoprotein (S) has emerged; virus containing this substitution has become the predominant circulating variant in the COVID-19 pandemic[1]. However, whether the increasing prevalence of this variant reflects a fitness advantage that improves replication and/or transmission in humans or is merely due to founder effects remains unknown. Here we use isogenic SARS-CoV-2 variants to demonstrate that the variant that contains S(D614G) has enhanced binding to the human cell-surface receptor angiotensin-converting enzyme 2 (ACE2), increased replication in primary human bronchial and nasal airway epithelial cultures as well as in a human ACE2 knock-in mouse model, and markedly increased replication and transmissibility in hamster and ferret models of SARS-CoV-2 infection. Our data show that the D614G substitution in S results in subtle increases in binding and replication in vitro, and provides a real competitive advantage in vivo—particularly during the transmission bottleneck. Our data therefore provide an explanation for the global predominance of the variant that contains S(D614G) among the SARS-CoV-2 viruses that are currently circulating.

In late 2019, SARS-CoV-2 was detected in Wuhan (Hubei province, China)[2,3] and rapidly led to the COVID-19 pandemic; by December 2020, 70 million cases and 1.5 million deaths attributable to this disease had been confirmed[4]. SARS-CoV-2 causes a life-threatening pneumonia in vulnerable groups of people[5]. The entry of SARS-CoV-2 into cells is dependent on the interaction of S and ACE2[3,6]. S is a homotrimeric class-I fusion protein that comprises two subunits (S1 and S2) that are separated by a protease cleavage site. S1 forms a globular head and is essential for receptor binding, and S2 mediates fusion of the viral envelope with host cell membranes. During entry, the receptor-binding domain within the S1 subunit binds ACE2, which generates conformational changes in the S2 subunit and facilitates internalization of the virus[7,8]. S(D614G) is a variant of S that contains a substitution outside of the receptor-binding domain that is thought to cause a conformational change in the protein, which improves ACE2 binding and increases the probability of infection[1,9].

As the pandemic has progressed, the SARS-CoV-2 variant that contains S(D614G) (hereafter, SARS-CoV-2[G614])) has rapidly superseded the parental variant (with D in amino acid position 614 of S; hereafter, SARS-CoV-2[D614]) in frequency to become globally dominant. Such a shift in genotype frequency might be caused by a founder effect following introduction into a highly interconnected population; alternatively, SARS-CoV-2[G614] may have a fitness advantage over SARS-CoV-2[D614]. Some studies have suggested the D614G substitution in S may confer a fitness advantage on the virus by improving cell entry[8,9]. To address the role of D614G substitution in S in the dissemination and predominance of SARS-CoV-2[G614] during the COVID-19 pandemic, we characterized S binding to human ACE2 (hACE2) and replication kinetics in vitro, and evaluated infection and transmission dynamics in vivo using three animal models. Our data show that the D614G substitution in S confers increased binding to the hACE2 receptor and increased replication in primary human airway epithelial cultures. Moreover, comparison of recombinant isogenic SARS-CoV-2 variants demonstrates that the D614G substitution in S provides competitive advantage in a hACE2 knock-in mouse model, and markedly increases replication and transmission in Syrian hamster and ferret models of SARS-CoV-2 infection.

D614G substitution in S enhances hACE2 binding

To measure the effects of the D614G substitution in S, we first quantified the binding of S1 domain monomers to hACE2 using biolayer

[1]CDC COVID-19 Response, Centers for Disease Control and Prevention, Atlanta, GA, USA. [2]Institute of Virology and Immunology (IVI), Mittelhäusern, Switzerland. [3]Department of Infectious Diseases and Pathobiology, Vetsuisse Faculty, University of Bern, Bern, Switzerland. [4]Graduate School for Biomedical Science, University of Bern, Bern, Switzerland. [5]Institute of Diagnostic Virology, Friedrich-Loeffler-Institut, Greifswald-Insel Riems, Germany. [6]Institute of Veterinary Bacteriology, Vetsuisse Faculty, University of Bern, Bern, Switzerland. [7]Battelle Memorial Institute, Atlanta, GA, USA. [8]Institute of Cell Biology, University of Bern, Bern, Switzerland. [9]COMPATH, Institute of Animal Pathology, University of Bern, Bern, Switzerland. [10]Oak Ridge Institute for Science and Education, Oak Ridge, TN, USA. [11]Institute for Infectious Diseases, University of Bern, Bern, Switzerland. [12]These authors contributed equally: Bin Zhou, Tran Thi Nhu Thao, Donata Hoffmann, Adriano Taddeo. [13]These authors jointly supervised this work: Charaf Benarafa, David E. Wentworth, Volker Thiel, Martin Beer. ✉e-mail: charaf.benarafa@vetsuisse.unibe.ch; dwentworth@cdc.gov; volker.thiel@vetsuisse.unibe.ch; martin.beer@fli.de
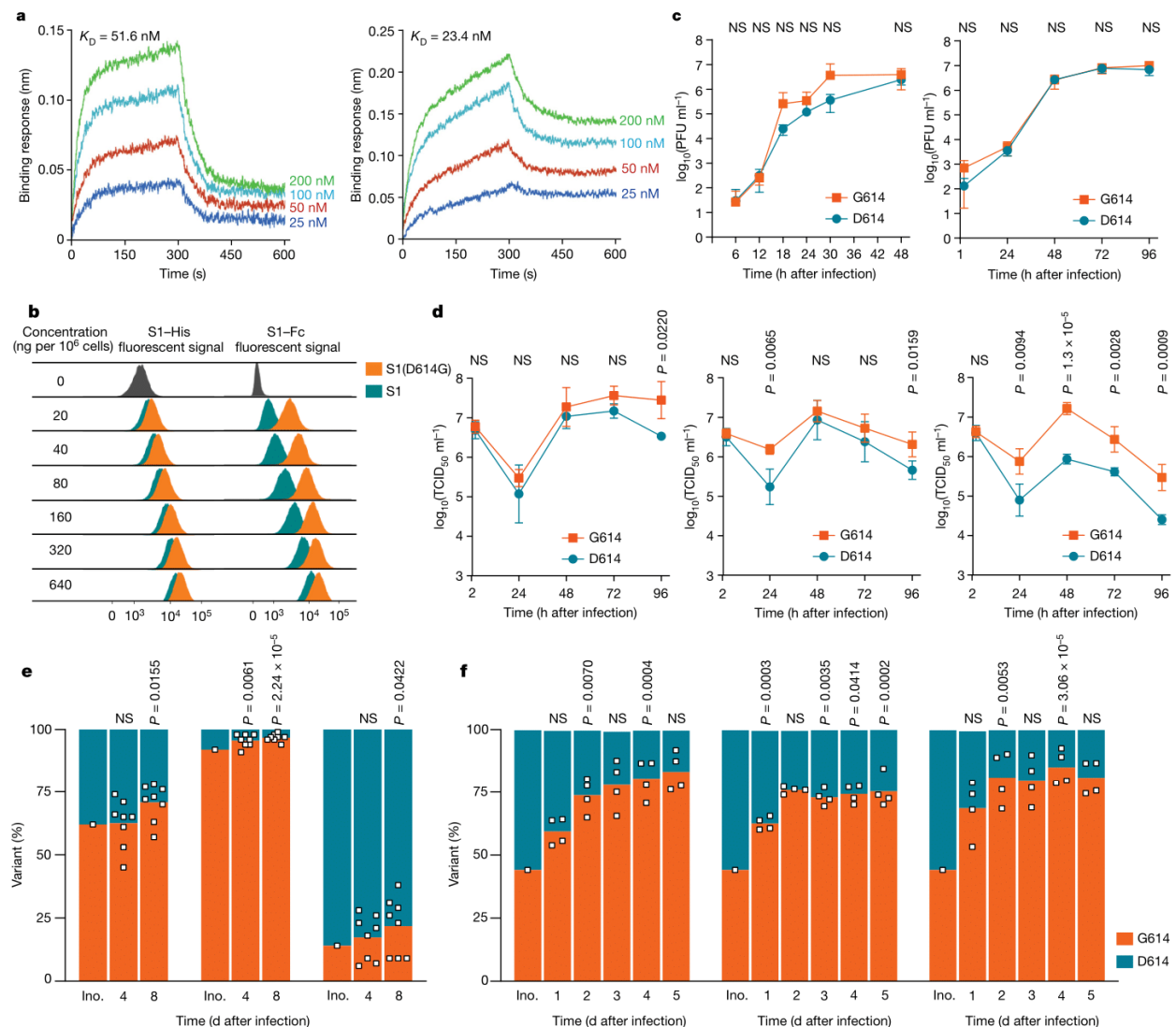
Fig. 1 | In vitro characterization of S1 and of recombinant SARS-CoV-2^{D614} and SARS-CoV-2^{G614}. a, Affinity between S1 and hACE2 determined by biolayer interferometry. Fc-tagged ACE2 protein was loaded onto surface of anti-human Fc capture biosensors. Association was conducted using S1 (left) or S1(D614G) (right), followed by dissociation. Data represent three biological replicates. **b**, Binding of polyhistidine-tagged or Fc-tagged S1 to BHK–hACE2 cells is shown as peaks of fluorescence, detected by flow cytometry. **c**, Replication kinetics of recombinant viruses in Vero E6 cells at 37 °C (left) and human nasal epithelial cells at 33 °C (right). Supernatant was collected at the indicated time points and titrated by plaque assay. D614, SARS-CoV-2^{D614}; G614, SARS-CoV-2^{G614}. **d**, Replication kinetics of recombinant viruses in human NBE cells at 33 °C (left), 37 °C (middle) and 39 °C (right). Supernatant was collected daily and titrated by TCID$_{50}$ assay. In **c**, **d**, data are mean ± s.d. of three biological replicates (Vero E6 cells) or four technical replicates (human nasal epithelial and human NBE cells).

Statistical significance was determined by two-sided, unpaired Student's *t*-test without adjustments for multiple comparisons. **e**, **f**, Competition assay of recombinant viruses in human nasal epithelial cells at 33 °C (**e**) and human NBE cells at 33 °C (**f**, left), 37 °C (**f**, middle) and 39 °C (**f**, right). The inoculum (ino.) was prepared by mixing two viruses and used for infection of human nasal epithelial (1:1 (**e**, left), 1:10 (**e**, middle) and 10:1 (**e**, right) PFU ratios, 8 technical replicates each) and human NBE (1:1 PFU ratio, 4 technical replicates each) cells. Apical wash and supernatant were collected daily, and extracted RNA was used for NGS. Bar graphs show percentage of sequence reads encoding S or S(D614G). In competition experiments in human nasal epithelial and human NBE cells, each square represents an individual data point. For each time point, a linear regression model was generated on the basis of the sequencing read counts for S and S(D614G), and *P* values were calculated for the group (variant) coefficient. NS, not significant (*P* > 0.05).

interferometry. Both S1 and S1(D614G) bind efficiently to hACE2; however, S1(D614G) showed an affinity about twofold higher than that of S1 (Fig. 1a, Supplementary Table 2). Similarly, S(D614G) had a higher affinity to hACE2 than that of S when full-length monomeric forms were used (Extended Data Fig. 1a, Supplementary Table 2). The D614G substitution in S also resulted in enhanced S1 binding to hACE2 exogenously expressed in baby hamster kidney cells (hereafter, BHK–hACE2 cells)

(Fig. 1b, Extended Data Fig. 1b). The binding of polyhistidine-tagged S1 or S1(D614G) to BHK–hACE2 cells showed that more S1(D614G) bound to BHK–hACE2 cells than did S1, by flow cytometry (Fig. 1b, Extended Data Fig. 1b). When using homodimeric recombinant constructs comprising S1 attached to an IgG C terminus, we observed a more notable effect in the increased binding of the S1(D614G) protein to the BHK–hACE2 cell (Fig. 1b, Extended Data Fig. 1b).
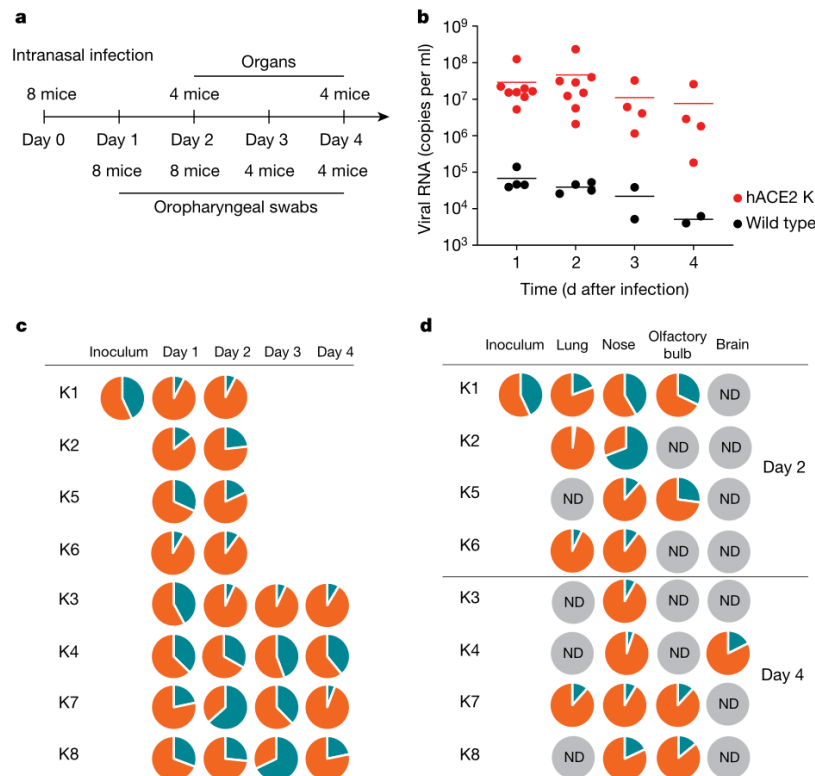
Article

Fig. 2 | Replication of SARS-CoV-2^D614 and SARS-CoV-2^G614 in hACE2 knock-in mice. a, Experimental scheme for intranasal infection of hACE2 knock-in mice with recombinant SARS-CoV-2^D614 and SARS-CoV-2^G614. Oropharyngeal swabs were sampled daily and tissue samples were analysed in subgroups of 4 mice at 2 and 4 days after infection in 2 independent experiments. **b**, Quantitative PCR with reverse transcription (RT–qPCR) analysis of oropharyngeal swabs of inoculated hACE2 knock-in (KI) and wild-type mice. **c, d**, Pie chart of the mean frequencies of the A or G nucleotide at position 23,403 (corresponding to D (in blue) or G (in orange) at amino acid position 614, respectively). K1 to K8 denote individual mice. Each pie chart illustrates the ratio of A/G detected from individual oropharyngeal swab samples (**c**) and tissues (**d**) at the indicated time after infection. ND, not detected.

SARS-CoV-2^G614 replication in epithelial cells

To assess the effect of S(D614G) in the context of virus infection, we generated an isogenic SARS-CoV-2^D614 and SARS-CoV-2^G614 pair using a SARS-CoV-2 reverse genetics system[10]. The molecular clone based on the Wuhan-Hu-1 isolate is representative of SARS-CoV-2^D614 (refs. [10,11]). The sequence of the isogenic SARS-CoV-2^G614 was engineered with an A-to-G transition at position 23,403 to encode a glycine at position 614 of S. The identity of the resulting recombinant SARS-CoV-2^G614 was confirmed by genomic next-generation sequencing (NGS) of virus stock (passage 1) used in subsequent experiments. The replication kinetics of SARS-CoV-2^D614 and SARS-CoV-2^G614 in Vero E6 cells differed only marginally (Fig. 1c). We assessed replication kinetics in primary human nasal epithelial and primary normal human bronchial epithelial (human NBE) cell cultures grown under air–liquid interface conditions that resemble the pseudostratified epithelial lining of the human respiratory epithelium. We observed no significant difference in the primary human nasal epithelial cells after infection of SARS-CoV-2^D614 or SARS-CoV-2^G614 at 33 °C (the temperature of the nasal epithelium) (Fig. 1c). By contrast, SARS-CoV-2^G614 displayed elevated titres in human NBE cells at 33 °C, 37 °C and 39 °C, which mimic the temperatures of the upper respiratory tract, lower respiratory tract and fever, respectively (Fig. 1d). Infection kinetics of human NBE cells with the natural isolates SARS-CoV-2/USA-WA1/2020 (SARS-CoV-2^D614) or SARS-CoV-2/Massachusetts/VPT1/2020 (SARS-CoV-2^G614) showed a more subtle advantage for SARS-CoV-2^G614 at 37 °C and 39 °C (Extended Data Fig. 1c). To refine

this analysis, we performed competition experiments by infecting human nasal epithelial and human NBE cell cultures with a mixture of isogenic SARS-CoV-2^D614 and SARS-CoV-2^G614 at defined ratios. In both of the primary human respiratory cell culture systems, the ratio of SARS-CoV-2^G614 to SARS-CoV-2^D614 shifted in favour of SARS-CoV-2^G614 across five or eight days of infection (Fig. 1e, f, Extended Data Figs. 1d, e, 2a, b). Collectively, these results show that the D614G substitution in S is associated with enhanced hACE2 binding and increased replication in primary human airway epithelial cell models of SARS-CoV-2 infection.

SARS-CoV-2^G614 replication in humanized *ACE2* mice

Mice do not support the efficient replication of SARS-CoV-2 unless they are genetically engineered to express hACE2[12,13]. To evaluate the relative fitness of SARS-CoV-2^G614 in vivo, we generated knock-in mice that express human *ACE2* under the endogenous regulatory elements of mouse *Ace2* (Extended Data Fig. 3a). We intranasally inoculated eight heterozygous female mice with an equal mixture of both viruses (SARS-CoV-2^D614 and SARS-CoV-2^G614) in a competition experiment, by pooling 1×10^5 plaque-forming units (PFU) of each variant (Fig. 2a). We monitored viral RNA loads in oropharyngeal swabs daily, and in various tissues (at days 2 and 4 after inoculation) by real-time PCR. We did not observe any significant loss of body weight in hACE2 knock-in mice up to day 4 after inoculation (Extended Data Fig. 3b). Our longitudinal analysis of oropharyngeal swabs revealed efficient virus replication in
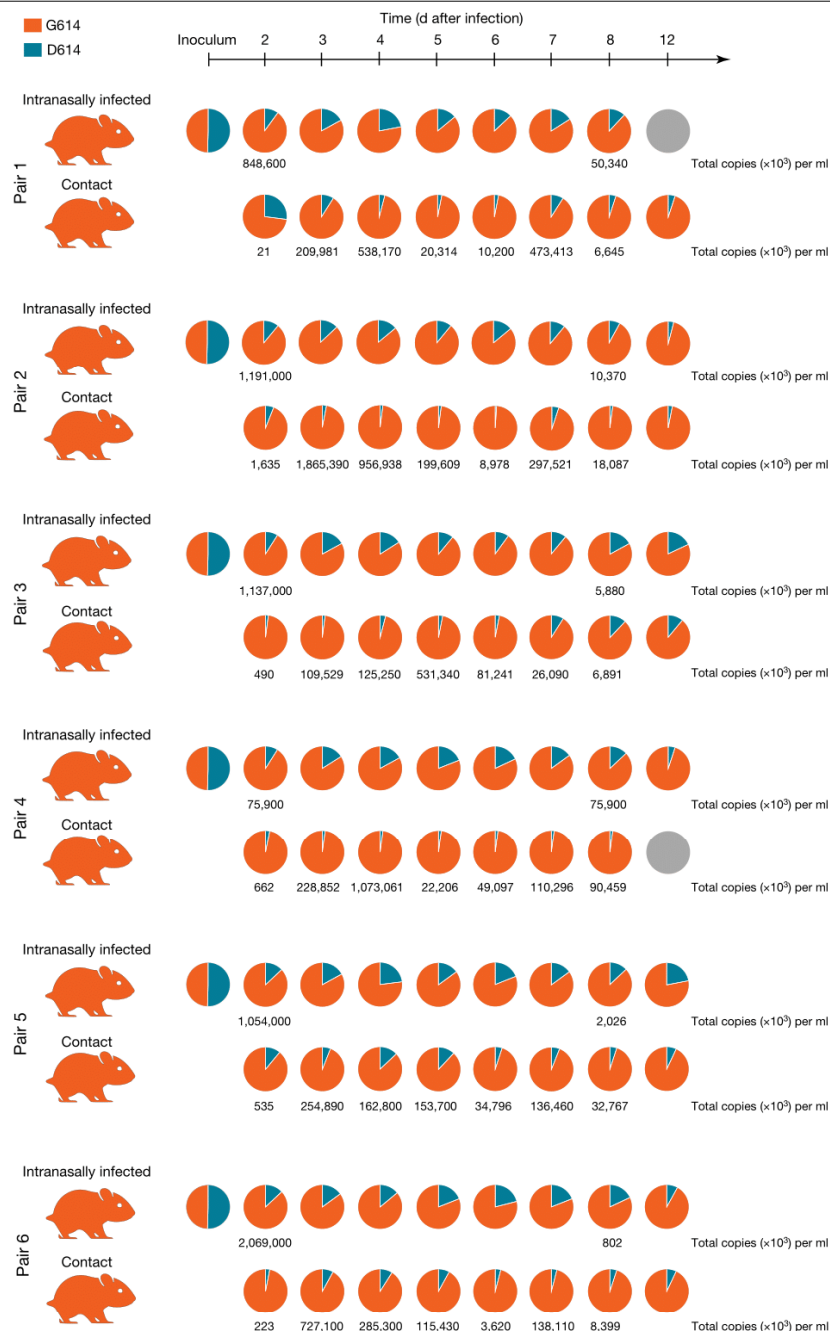
Fig. 3 | Replication and transmission of SARS-CoV-2[D614] and SARS-CoV-2[G614] in Syrian hamsters. The transmission of SARS-CoV-2[D614] and SARS-CoV-2[G614] by hamsters in a pairwise one-by-one setup with direct contact of donor and cohoused contact hamsters is illustrated. Samples of nasal washings were taken daily between day 2 and day 8 after infection (dpi), and finally at 12 days after infection, and were then analysed. Pie chart of the fraction of A or G nucleotide at position 23,403 (corresponding to D or G at amino acid position 614, respectively), measured by NGS of amplicons. Genome copies were calculated from RT–qPCR using an RNA standard. Orange colouring of the hamster silhouette refers to the detection of G (that is, SARS-CoV-2[G614]) and blue to the detection of A (that is, SARS-CoV-2[D614]) at most time points. Grey colouring, no infection detected.

the upper respiratory tract of hACE2 knock-in mice relative to wild-type mice (Fig. 2b). Accordingly, tissue samples collected at days 2 and 4 after inoculation revealed high viral loads in the nasal conchae, lungs and olfactory bulbs, and lower levels in the brain (Extended Data Fig. 3c, d). Levels of viral RNA were low to undetectable in spleen, small intestine, kidneys and faeces (data not shown). We did not find any overt pathological lesions in the lungs at days 2 and 4 after inoculation (Supplementary Table 3, 4). NGS of the oropharyngeal swabs revealed a net advantage for SARS-CoV-2[G614] over SARS-CoV-2[D614] in most mice and at most time points (Fig. 2c, Extended Data Fig. 3e, f). We found a similar replication advantage for SARS-CoV-2[G614] in the organs (Fig. 2d). Collectively, these

results demonstrate increased replication of SARS-CoV-2[G614] in a mouse model that expresses authentic human *ACE2*.

SARS-CoV-2[G614] infection in hamsters and ferrets

Hamsters are highly susceptible to SARS-CoV-2 infection and develop disease that closely resembles pan-respiratory, moderate-to-severe COVID-19 in humans[14–16]. To examine the replication kinetics of the SARS-CoV-2 variants using a hamster model, we intranasally inoculated seven hamsters with SARS-CoV-2[D614] or SARS-CoV-2[G614] ($1 \times 10^{5.1}$ tissue culture infectious dose ($TCID_{50}$) per hamster, and $10^{4.5}$ $TCID_{50}$ per hamster, respectively,
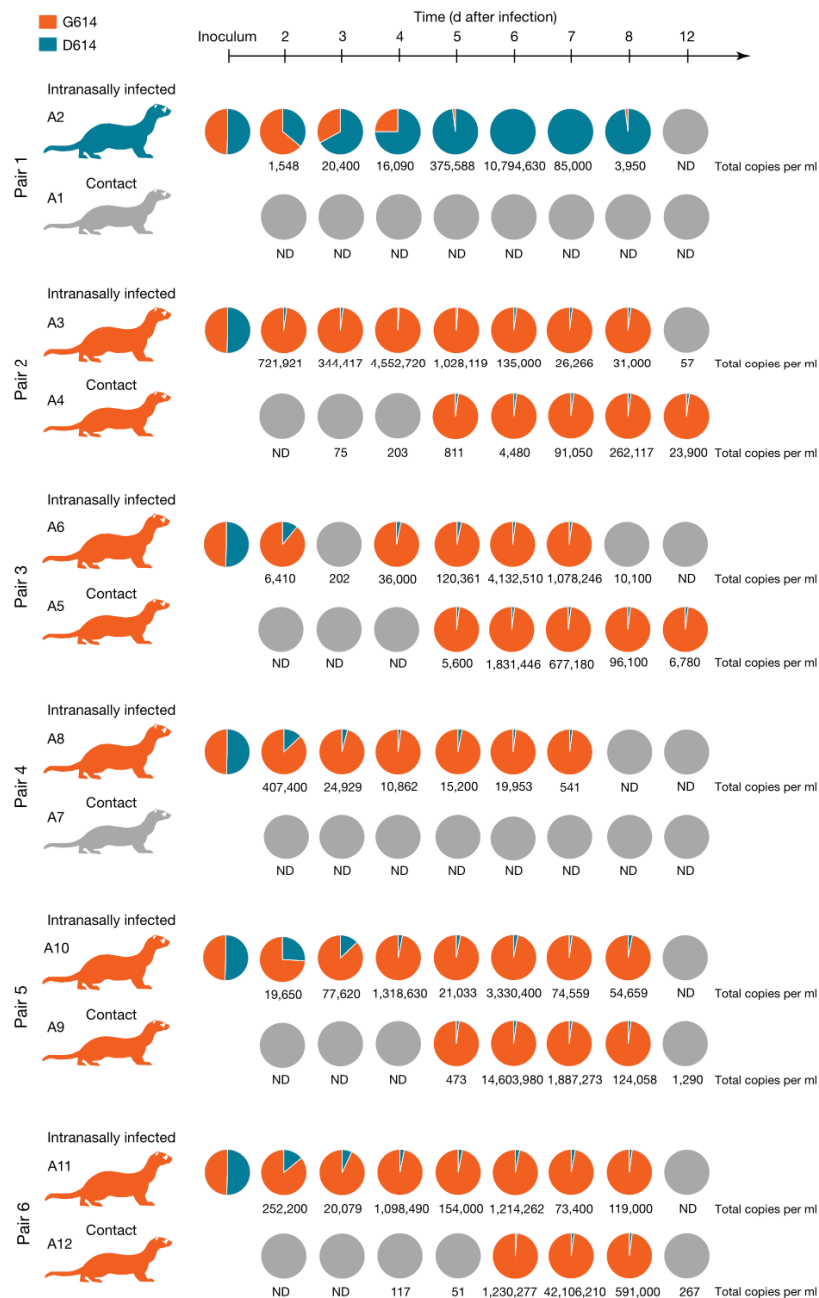
Article

Fig. 4 | Replication and transmission of SARS-CoV-2^D614 and SARS-CoV-2^G614 in ferrets. Schematic of the experimental setup, in which six pairs of one donor ferret cohoused with one naive contact ferret were used. Samples of nasal washings were taken daily between day 2 and day 8 after infection, and finally at 12 days after infection, and were then analysed. Pie chart of fraction of A or G nucleotide at position 23,403 (corresponding to D or G at amino acid position 614, respectively). Each pie chart illustrates the ratio of A/G detected from individual nasal washing samples over time. Orange colouring of the ferret silhouette refers to the detection of G (that is, SARS-CoV-2^G614) at most time points, and blue indicates detection of A (that is, SARS-CoV-2^D614). Numbers represent total genome copies per ml. Grey, no infection or viral genome number too low to determine the A/G ratio by NGS.

calculated from back titration of the inoculum) and monitored them for four consecutive days. We did not observe any marked differences in body weight, titres of shed virus or viral loads in respiratory tract tissue between the two groups in the acute phase (Extended Data Fig. 4c–e). For both variants, the highest genome loads were found in the nasal conchae followed by the pulmonary tissue (Extended Data Fig. 4e). These observations suggest that the D614G substitution in S does not have strong effect on clinical outcomes or a detectable replication advantage in infections with SARS-CoV-2^D614 versus SARS-CoV-2^G614 in the hamster model.

We therefore set up an in vivo competition experiment to better elucidate the potential replication and/or transmission differences between the variants. We intranasally inoculated six donor Syrian hamsters with

a 1:1 mixture (on the basis of infectious PFU titre) of SARS-CoV-2^D614 and SARS-CoV-2^G614 in direct 'one-to-one' transmission experiments. We later confirmed the RNA ratio of the two variants within the inoculum using NGS, and absolute quantification using digital-droplet PCR with allele-specific locked nucleic acid probes (Fig. 3). At 24 h after inoculation, each inoculated hamster was cohoused with a naive hamster. Viral RNA load in daily nasal washings, changes in body weight and clinical signs all agreed with previously published data[14–16] (Extended Data Fig. 4a, b). NGS of the viral RNA sequence composition of nasal washings revealed a prominent shift towards SARS-CoV-2^G614 within 48 h of inoculation (Fig. 3, Extended Data Fig. 4f, g). The transmission efficiency was 100%, and analysis of the RNA sequence composition showed that SARS-CoV-2^G614

represented over 90% of the viral RNA in the contact hamsters (Fig. 3). In summary, at 24 h after inoculation hamsters inoculated with an equal ratio of SARS-CoV-2[D614] and SARS-CoV-2[G614] transmit primarily SARS-CoV-2[G614].

We further investigated the competitive advantage of S(D614G) in ferrets, which represent a good model of SARS-CoV-2 transmission[17] in which the virus replicates primarily within the upper respiratory tract (resembling mild infections in humans). We intranasally inoculated six ferrets with a 1:1 mixture (on the basis of infectious PFU titre) of SARS-CoV-2[D614] and SARS-CoV-2[G614] in direct one-to-one transmission experiments. For all six inoculated ferrets, SARS-CoV-2-infection was confirmed: body weight changes and viral RNA loads in nasal washings (Fig. 4, Extended Data Fig. 5a, b) were consistent with previously published data[17,18]. In five of the six inoculated ferrets, SARS-CoV-2[G614] became the dominant variant (Fig. 4, Extended Data Fig. 5c, d). In addition, SARS-CoV-2 transmission occurred in four of the six ferret pairs. In each pair with successful transmission, SARS-CoV-2[G614] prevailed over SARS-CoV-2[D614] (Fig. 4). All NGS data from the ferret samples were retested by absolute quantification using allele-specific locked nucleic acid probes and digital droplet PCR analysis. Notably, the inoculated ferret from pair 1 (in which SARS-CoV-2[D614] predominated the viral population) did not transmit virus to the contact, despite a high peak viral genome load of more than 10 million copies per ml. By contrast, the lack of transmission in pair 4 (in which SARS-CoV-2[G614] became the dominant variant) was connected to peak viral loads of below 500,000 genome copies per ml (Fig. 4). In summary, the competition experiment in ferrets revealed that SARS-CoV-2[G614] preferentially infected and replicated in five out of six inoculated ferrets, and the successful transmission events occurred only with SARS-CoV-2[G614].

Discussion

The evolution of SARS-CoV-2 in humans has been proposed to be a nondeterministic process in which virus diversification results mainly from random genetic drift, suggesting no strong selective pressure is acting on its adaptation in humans[19]. However, since the emergence of the D614G substitution in S in early 2020, the SARS-CoV-2[G614] variant has become globally prevalent[1]. Both a founder effect and structural changes to S have previously been proposed as driving forces in establishing the prevalence of SARS-CoV-2[G614]. Previous structural studies and the use of pseudotyped viruses have suggested that SARS-CoV-2[G614] may confer increased infectivity as a result of an increased 'open' conformation of the receptor-binding domain for receptor binding or increased S stability[1,9]. In contrast to these studies (which used recombinant trimeric S), we used a reductionist approach to eliminate complications due to 'open' or 'closed' conformations of the receptor-binding domain in trimeric S. We found that S1(D614G) or monomeric S(D614G) both had increased affinity to hACE2, which may be another mechanism that underlies the increased replication and transmission of SARS-CoV-2[G614].

Studies using isogenic SARS-CoV-2[D614] and SARS-CoV-2[G614] to assess the phenotype in the context of SARS-CoV-2 infection have recently been reported[20,21]. Both of these studies have demonstrated that SARS-CoV-2[G614] increased replication in vitro, and one[21] observed earlier transmission in a hamster model. We extended these studies by exploiting a range of in vitro and in vivo models of SARS-CoV-2 infection: primary human nasal epithelial and human NBE cell cultures, a hACE2 knock-in mouse model, a hamster model and a ferret model. Throughout these experimental systems, we consistently observed an increased replicative fitness of SARS-CoV-2[G614] over SARS-CoV-2[D614], by applying NGS techniques and allele-specific absolute quantification for confirmation. The advantage provided by the D614G substitution in S was most prominent in competition and transmission experiments in hamsters and ferrets, and must therefore be considered as a driving force that has led to the global dominance of SARS-CoV-2[G614].

Our data also agree with previously reported functional changes conferred by the D614G substitution in S[1], and with previously reported increased infectivity of pseudotyped viruses containing

this substitution[9,22]. Although our studies establish a phenotype of increased replication and transmission of SARS-CoV-2[G614], there is no evidence for a change in pathogenicity in any of the animal models we used. This is important because infection with SARS-CoV-2[G614] is not associated with the development of severe COVID-19 in humans[1].

The ongoing pandemic will probably give rise to additional variants of SARS-CoV-2 that may display phenotypic changes and further adaptations to human or animal (such as mink) reservoirs. The ability to rapidly identify emerging variants using genomics, reconstructing emerging virus variants and assessing their phenotypes in vitro and in vivo will allow a rapid response to their emergence with appropriate countermeasures. The mouse model described in this Article, which is based on hACE2 expression under the endogenous regulatory elements of mouse *Ace2*, is a valuable tool and will complement existing animal models of SARS-CoV-2 infection. Similar to our demonstration here of the increased replication and transmissibility of SARS-CoV-2[G614], the phenotypic assessment of future variants will probably require several complementary animal models that together reflect aspects of SARS-CoV-2 replication, transmission and pathogenicity in humans.

Online content

Any methods, additional references, Nature Research reporting summaries, source data, extended data, supplementary information, acknowledgements, peer review information; details of author contributions and competing interests; and statements of data and code availability are available at https://doi.org/10.1038/s41586-021-03361-1.

1. Korber, B. et al. Tracking changes in SARS-CoV-2 spike: evidence that D614G increases infectivity of the COVID-19 virus. *Cell* **182**, 812–827.e19 (2020).
2. Zhu, N. et al. A novel coronavirus from patients with pneumonia in china, 2019. *N. Engl. J. Med.* **382**, 727–733 (2020).
3. Zhou, P. et al. A pneumonia outbreak associated with a new coronavirus of probable bat origin. *Nature* **579**, 270–273 (2020).
4. ECDC. *Communicable disease threats report, week 51, 13–19 December 2020*. https://www.ecdc.europa.eu/sites/default/files/documents/Communicable-disease-threats-report-19-dec-2020.pdf (2020).
5. Huang, C. et al. Clinical features of patients infected with 2019 novel coronavirus in Wuhan, China. *Lancet* **395**, 497–506 (2020).
6. Letko, M., Marzi, A. & Munster, V. Functional assessment of cell entry and receptor usage for SARS-CoV-2 and other lineage B betacoronaviruses. *Nat. Microbiol.* **5**, 562–569 (2020).
7. Wrapp, D. et al. Cryo-EM structure of the 2019-nCoV spike in the prefusion conformation. *Science* **367**, 1260–1263 (2020).
8. Hoffmann, M. et al. SARS-CoV-2 cell entry depends on ACE2 and TMPRSS2 and is blocked by a clinically proven protease inhibitor. *Cell* **181**, 271–280.e8 (2020).
9. Yurkovetskiy, L. et al. Structural and functional analysis of the D614G SARS-CoV-2 spike protein variant. *Cell* **183**, 739–751.e8 (2020).
10. Thi Nhu Thao, T. et al. Rapid reconstruction of SARS-CoV-2 using a synthetic genomics platform. *Nature* **582**, 561–565 (2020).
11. Wu, F. et al. A new coronavirus associated with human respiratory disease in China. *Nature* **579**, 265–269 (2020).
12. Bao, L. et al. The pathogenicity of SARS-CoV-2 in hACE2 transgenic mice. *Nature* **583**, 830–833 (2020).
13. Jiang, R.D. et al. Pathogenesis of SARS-CoV-2 in transgenic mice expressing human angiotensin-converting enzyme 2. *Cell* **182**, 50–58.e8 (2020).
14. Sia, S. F. et al. Pathogenesis and transmission of SARS-CoV-2 in golden hamsters. *Nature* **583**, 834–838 (2020).
15. Osterrieder, N. et al. Age-dependent progression of SARS-CoV-2 infection in Syrian hamsters. *Viruses* **12**, 779 (2020).
16. Imai, M. et al. Syrian hamsters as a small animal model for SARS-CoV-2 infection and countermeasure development. *Proc. Natl Acad. Sci. USA* **117**, 16587–16595 (2020).
17. Richard, M. et al. SARS-CoV-2 is transmitted via contact and via the air between ferrets. *Nat. Commun.* **11**, 3496 (2020).
18. Kim, Y. I. et al. Infection and rapid transmission of SARS-CoV-2 in ferrets. *Cell Host Microbe* **27**, 704–709.e2 (2020).
19. Alouane, T. et al. Genomic diversity and hotspot mutations in 30,983 SARS-CoV-2 genomes: moving toward a universal vaccine for the "confined virus"? *Pathogens* **9**, 829 (2020).
20. Plante, J. A. et al. Spike mutation D614G alters SARS-CoV-2 fitness. *Nature* https://doi.org/10.1038/s41586-020-2895-3 (2020).
21. Hou, Y. J. et al. SARS-CoV-2 D614G variant exhibits efficient replication ex vivo and transmission in vivo. *Science* **370**, 1464–1468 (2020).
22. Li, Q. et al. The impact of mutations in SARS-CoV-2 spike on viral infectivity and antigenicity. *Cell* **182**, 1284–1294.e9 (2020).

Article

Methods

No statistical methods were used to predetermine sample size. The experiments were not randomized, and investigators were not blinded to allocation during experiments and outcome assessment except where indicated.

Cell and culture conditions

Vero E6 cells (a gift from M, Müller) were cultured in Dulbecco's modified Eagle's medium (DMEM) supplemented with 10% fetal bovine serum, 1× non-essential amino acids, 100 units ml^{-1} penicillin and 100 μg ml^{-1} streptomycin. Baby hamster kidney (BHK) cells expressing SARS-CoV nucleoprotein (N)[23,24] were maintained in minimal essential medium (MEM) supplemented with 5% fetal bovine serum (FBS), 1× non-essential amino acids, 100 units ml^{-1} penicillin and 100 μg ml^{-1} streptomycin, 500 μg ml^{-1} G418 and 10 μg ml^{-1} puromycin. Twenty-four hours before electroporation, the BHK cells expressing SARS-CoV N were treated with 1 μg ml^{-1} doxycyclin to express SARS-CoV N protein. All cell lines were maintained at 37 °C and in a 5% CO_2 atmosphere.

Recombinant proteins

The Expi293 Expression system (ThermoFisher Scientific) was used to produce hACE2 and S. Mammalian expression plasmids were constructed to encode codon-optimized Fc(human IgG1)-tagged hACE2 (hACE2–Fc) or polyhistidine-tagged S (S and S(D614G)), which contain the full-length ectodomain of S (residues 1–1208, with a mutated furin cleavage site and K986P/V987P substitutions). Expi293F cells were transfected with the plasmids and cultured at 37 °C with 8% CO_2 at a shaking speed of 125 rpm. The supernatant was collected on day 5 by centrifugation at 3,000g for 20 min at 4 °C. The hACE2–Fc protein was purified using HiTrap Protein A column (GE Life Sciences) in elution buffer containing 0.1 M citric acid, pH 3.0. S was purified using HisTrap FF column (GE Life Sciences) in elution buffer containing 20 mM sodium phosphate, 0.5 M NaCl and 500 mM imidazole, pH 7.4. The eluents were desalted using Zeba spin desalting column 7K MWCO (Thermo Fisher Scientific). The purified proteins were further concentrated on Amicon Ultra Centrifugal Filters 50K NMWL (Sigma-Aldrich) and quantified using Qubit protein assay (ThermoFisher Scientific).

Biolayer interferometry assay

Affinity between hACE2–Fc and S1 (ABclonal, RP01262), S1(D614G) (ABclonal, RP01287), S or S(D614G) was evaluated using Octet RED96 instrument (ForteBio) at 30 °C with a shaking speed of 1,000 rpm. Following 20 min of prehydration of anti-human Fc capture biosensors and 1 min of sensor check, 7.5 nM hACE2–Fc in 10× kinetic buffer (ForteBio) was loaded onto the surface of biosensors for 5 min. After 1.5 min of baseline equilibration, 5 min of association was conducted with 25 to 200 nM of S1 or S1(D614G), or with 10–100 nM of S or S(D614G), followed by 5 min of dissociation in the same buffer used for baseline equilibration. The data were corrected by subtracting the reference sample; a 1:1 binding model with global fit was used for the determination of affinity constants.

Flow cytometry

A stable clone of BHK–hACE2 cells was pelleted and resuspended in reaction buffer (PBS pH 7.4 with 0.02% Tween-20 and 4% BSA) at a concentration of 5 × 10^6 cells per ml. One hundred microlitres per well of the cells were aliquoted into a round-bottom 96-well plate and incubated on ice for at least 5 min. Polyhistidine-tagged S1 (40591-V08H) and S1(D614G) (40591-V08H3) and Fc-tagged S1 (40591-v02H) and S1(D614G) (40591-v02H3) proteins were purchased from Sino Biological, and diluted in reaction buffer on ice. Fifty microlitres of S1 diluents were added into corresponding wells of cells and incubated on ice for 20 min with shaking. After incubation, cells were washed in 200 μl PBST washing solution (PBS pH 7.4 with 0.02% Tween-20) once, and

then 100 μl of 1:300 diluted secondary antibody (ThermoFisher cat. no. A-21091 for the Fc tag and ThermoFisher cat. no. MA1-21315-647 for the polyhistidine tag) was added into each well of cells, mixed and incubated on ice with shaking for 15 min. After washing twice, cells were resuspended in 200 μl PBST and analysed using a BD FACSCanto II Flow Cytometer. Data were processed using Flowjo v.10.6.1. Results for BHK control cells (which do not express hACE2) and the gating strategy are provided in Supplementary Figs. 1, 2.

Generation of infectious cDNA clones using transformation-associated recombination cloning and rescue of recombinant viruses

To introduce the mutation for the D614G substitution into the *S* gene, PCR mutagenesis (Supplementary Table 1) was performed on the pUC57 plasmid containing SARS-CoV-2 fragment 10[10] using a Q5 Site-Directed Mutagenesis Kit (New England BioLab). Both *S* and *S^{D614G}* infectious cDNA clones were generated using in-yeast transformation-associated recombination cloning method as previously described[10]. In vitro transcription was performed for EagI-cleaved YAC and PCR-amplified SARS-CoV-2 *N* gene using the T7 RiboMAX Large Scale RNA production system (Promega) as previously described[4]. Transcribed capped mRNA was electroporated into baby hamster kidney cells (BHK-21 cells) expressing SARS-CoV N protein. Electroporated cells were cocultured with susceptible Vero E6 cells to produce passage 0 of recombinant SARS-CoV-2^{D614} and SARS-CoV-2^{G614}. Subsequently, progeny viruses were used to infect fresh Vero E6 cells to generate passage 1 stocks for downstream experiments.

Virus growth kinetics and plaque assay

The characterization of virus growth kinetics in Vero E6 was performed as previously described[10]. Twenty-four hours before infection, cells were seeded in a 24-well plate at a density of 2.0 × 10^5 cells per ml. After washing once with PBS, cells were inoculated with viruses at multiplicity of infection of 0.01. After 1 h, the inoculum was removed and cells were washed three times with PBS followed by supply with appropriate culture medium.

PFUs per ml of recombinant SARS-CoV-2^{D614} and SARS-CoV-2^{G614} were determined by plaque assay in a 24-well format. One day before infection, Vero E6 cells were seeded at a density of 2.0 × 10^5 cells per ml. After washing once with PBS, cells were inoculated with viruses serially diluted in cell culture medium at 1:10 dilution. After 1 h of incubation, inoculum was removed, and cells were washed with PBS and subsequently overlaid with 1:1 mix of 2.4% Avicel and 2× DMEM supplemented with 20% fetal bovine serum, 200 units ml^{-1} penicillin and 200 μg ml^{-1} streptomycin. After 2 days of incubation at 37 °C, cells were fixed in 4% (v/v) neutral-buffered formalin before stained with crystal violet.

Statistical significance was determined by two-sided unpaired Student's *t*-test without adjustment for multiple comparisons.

Infection of human nasal and bronchial epithelial cells

Primary human nasal epithelial cell cultures (MucilAir EP02, Epithelix Sàrl) were purchased and handled according to the manufacturer's instructions. Human NBE cells were purchased (from Emory University) and cultured according to recommended protocols. The human nasal epithelial cultures were inoculated with 0.5 × 10^5 PFU per well, or mixtures of 1:1, 10:1 and 1:10 of SARS-CoV-2^{D614} and SARS-CoV-2^{G614}. Human NBE cell cultures were inoculated with 1.0 × 10^5 PFU per well, or with the wild-type isolates SARS-CoV-2/USA-WA1/2020 (SARS-CoV-2^{D614}) or SARS-CoV-2/Massachusetts/VPT1/2020 (SARS-CoV-2^{G614}), at 2 × 10^5 TCID$_{50}$ per well. For competition experiments, human NBE cells were inoculated with 1:1 or 9:1 mixed SARS-CoV-2^{D614} and SARS-CoV-2^{G614} at 1 × 10^5 PFU per well. After incubation at 33 °C for 1 or 2 h, for human nasal epithelial or human NBE cell cultures, respectively, inoculum was removed (or collected for human NBE as 2-h samples), cells were washed, and subsequently incubated (as indicated) at 33 °C, 37 °C or

101

39 °C. To monitor viral replication, apical washes were collected every 24 h. All titre were determined by standard plaque assay or $TCID_{50}$ on Vero E6 cells.

For competition experiments, viral RNA was extracted from apical washes using the QIAamp 96 Virus QIAcube HT Kit (QIAGEN). The SARS-CoV-2 genome was amplified using a highly multiplexed tiling PCR reaction based on the Artic Network protocol (https://www.protocols.io/view/ncov-2019-sequencing-protocol-bbmuik6w) with some modification. In brief, primers were designed to produce overlapping 1-kb amplicons (Supplementary Table 1). Reverse transcriptase was performed as described in the Artic Network protocol. The single cDNA reaction was carried forward by preparing two PCR reactions (one each for the odd and even pool of primers). Two primer pools (odd and even) were prepared to contain 0.1 µM of each individual primer. Tiling PCR of the resultant cDNA was performed by combining 12.5 µl 2× Q5 polymerase, 5.5 µl water, 2 µl of the primer pool and 5 µl of cDNA followed by incubating the reaction at 98 °C for 30 s, 38 cycles of 98 °C for 15 s and 63 °C for 5 min, and holding at 4 °C. Corresponding odd and even amplicons were normalized and pooled for library preparation. Fragmented libraries were prepared using the Nextera XT DNA library preparation kit and sequenced using Illumina MiSeq. Analyses were performed using IRMA[25] with a SARS-CoV-2 module.

RNA extraction and RT–PCR

Preparation of viral RNA for NGS was performed as previously described[10]. In brief, Vero E6 cells were infected with passage-1 viruses. Extraction of total cellular RNA was done using Nucleospin RNA Plus kit (Macherey-Nagel) according to the manufacturers' instructions.

RNA from apical washes of human nasal epithelial cells and mouse oropharyngeal swabs were prepared using QIAamp Viral RNA Mini Kit (QIAGEN) and Nucleospin RNA kit (Macherey-Nagel) according to the manufacturers' protocols.

To determine the ratios of SARS-CoV-2[D614] to SARS-CoV-2[G614] in competition assays in human nasal epithelial cell cultures and hACE2 knock-in mice, reverse-transcription PCR was performed on extracted RNA using SuperScript IV One-step RT–PCR System (Invitrogen). The sequence-specific primers were used to generate an amplicon of 905 bp covering the D614 region: 5′-AATCTATCAGGCCGGTAGCAC-3′ and 5′-CAACAGCTATTCCAGTTAAAGCAC-3′. RT–PCR reaction was performed in a 50-µl reaction using 0.01 pg to 1 µg total RNA. The cycling parameters were set as follows: 50 °C for 10 min, 98 °C for 2 min; 35 cycles at 98 °C for 10 s, 55 °C for 15 s, and 72 °C for 30 s; and a 5-min incubation at 72 °C. DNA concentration was determined using Qubit dsDNA HS (High Sensitivity) Assay (Thermo Fisher), and subsequently diluted to 200 ng in 50 µl of nuclease-free water for sequencing by Nanopore sequencing MinION.

RNA extraction and preparation of RT–PCR reactions were performed in low- and no-copy laboratory environment to avoid contamination.

Sequencing and computational analysis

Recombinant SARS-CoV-2[D614] or SARS-CoV-2[G614] RNAs of passage-1 stock were sequenced by NGS as previously described[10]. In brief, RNA was extracted from Vero E6 cells infected with either recombinant SARS-CoV-2[D614] or SARS-CoV-2[G614] using the NucleoSpin RNA Plus kit (Macherey-Nagel) according to the manufacturer's guidelines. Sequencing libraries were subsequently prepared using the Illumina TruSeq Stranded mRNA Library Prep Kit (Illumina, 20020595) and pooled cDNA libraries were sequenced across two lanes on a NovaSeq 6000 S1 flow cell (2 × 50 bp, 100 cycles) using the Illumina NovaSeq 6000 platform (Next Generation Sequencing Platform of the University of Bern). For data analysis, TrimGalore v.0.6.5 was used to remove low-quality reads and adaptors from the raw sequencing files. The resulting trimmed paired-end reads were then aligned to the SARS-CoV-2 genome (GenBank accession MT108784) using Bowtie2 v.2.3.5. Finally, a consensus sequence was generated for each virus stock using Samtools v.1.10 with

the -d option set to 10,000. Data analysis was performed on UBELIX, the high-performance computing cluster at the University of Bern (http://www.id.unibe.ch/hpc).

For virus competition experiments in human nasal epithelial cells, hACE2 knock-in mice, hamsters and ferrets, amplicons were sequenced on the MinION system from Oxford Nanopore. Real-time high-accuracy base calling, demultiplexing and barcode and adaptor trimming was performed with MinKnow v.20.06.17, running Guppy v.s4.0.11. Downstream analysis was done in Geneious 2019 v.s2.3. Read length was filtered to eliminate reads <800 and >1,100 nt and the remaining reads were mapped in subsets of 10,000 reads to the amplicon reference undergoing 2 iterations, with custom sensitivity allowing a maximum of 5% gaps and maximum mismatch of 30%. Variants were analysed at specific positions calculating P values for each variant. The ratio fraction A/G was calculated from the numbers of reads, as fraction = A reads/(A reads + G reads).

Statistical analyses for virus competition experiments and relative replicative fitness calculations were performed using the catseyes package in R. Relative replicative fitness values for SARS-CoV-2[G614] over SARS-CoV-2[D614] were determined by dividing the initial SARS-CoV-2[G614]/SARS-CoV-2[D614] ratio (i_0) by the final (after infection) SARS-CoV-2[G614]/SARS-CoV-2[D614] ratio (f_0) according to the formula $w = (f_0/i_0)$. Specifically, to model f_0/i_0 in each experiment, the t_1/t_0 ratio was calculated on the basis of the sequencing counts attained for each virus in individual samples (after infection, time point t_1) and in the inoculum (initial time point t_0). For each time point, a linear regression model was generated in R and fitness ratios between the two groups (variants) were assessed by means of the coefficient of the model's group term. When multiple experiments were performed, the experiment variable was included in the model. All statistical tests were performed in R (v.4.0.2) with two-sided $\alpha = 0.05$. Cat's eye plots showing the relative replicative fitness of SARS-CoV-2[G614] over SARS-CoV-2[D614] for each time point in each experiment were created using the catseyes package in R[26], as previously described[20].

Animal studies

Ethics declarations. The hACE2 knock-in mice were originally generated at the Wadsworth Center, New York State Department of Health (IACUC protocol no. 09-405) (principal investigator D.E.W.). Mouse experiments were conducted in compliance with the Swiss Animal Welfare legislation, and animal studies were reviewed and approved by the commission for animal experiments of the canton of Bern under licence BE-43/20. All of the ferret and hamster experiments were evaluated by the responsible ethics committee of the State Office of Agriculture, Food Safety, and Fishery in Mecklenburg–Western Pomerania (LALLF M-V), and gained governmental approval under registration number LVL MV TSD/7221.3-1-041/20. This project also obtained clearance from the Animal Care and Use Program Office of the CDC.

hACE2 knock-in mouse study. For the generation of hACE2 knock-in mice, the hACE2 knock-in (B6) (*B6.Cg-Ace2*[tm1(ACE2)Dwnt]*/J*) line was generated by targeted mutagenesis to express human *ACE2* cDNA in place of the mouse *Ace2* gene. Thus, in this mouse model, hACE2 expression is regulated by the endogenous mouse *Ace2* promoter and enhancer elements. The targeting vector (WEN1-HR) had human *ACE2* cDNA inserted in frame with the endogenous initiation codon of the mouse *Ace2* (Extended Data Fig. 3a). The human cDNA was flanked by an FRT-neomycin-FRT-loxP cassette and a distal loxP site. WEN1-HR was used to transfect 129Sv/Pas embryonic stem cells and 837 embryonic stem cell clones were isolated and screened for homologous recombination by PCR and Southern blot. Eleven properly recombined embryonic stem cell clones were identified, and some of them were used for blastocyst injection and implantation into female mice to generate 22 male founder mice with chimerism (129Sv/Pas:C57BL/6) ranging from 50 to 100%. To complete the hACE2 knock-in, we crossed

Article

the chimeric male mice with C57BL/6J Flp-expressing female mice to excise the FRT-flanked neomycin selection cassette and generate the floxed humanized *ACE2* allele (Extended Data Fig. 3a). These hACE2 knock-in mice were identified by PCR and confirmed by Southern blot and were backcrossed to C57BL/6J mice for seven generations before this study. This line has been donated to The Jackson Laboratory for use by the scientific community (stock 035000).

Heterozygous hACE2 knock-in female mice were obtained from The Jackson Laboratory and C57BL/6J wild-type female mice were from Janvier Lab. All mice were acclimatized for at least 2 weeks in individually ventilated cages (blue line, Tecniplast), with 12-h/12-h light/dark cycle, 22 ± 1 °C ambient temperature and $50 \pm 5\%$ humidity, autoclaved acidified water, autoclaved cages including food, bedding, and environmental enrichment at the specific-pathogen-free facility of the Institute of Virology and Immunology, (Mittelhäusern). One week before infection, mice were placed in individually HEPA-filtered isolators (IsoCage N, Tecniplast). Mice (10 to 12 weeks old) were anaesthetized with isoflurane and infected intranasally with 20 µl (that is, 10 µl per nostril) with a 1:1 ratio of the SARS-CoV-2 variants (wild-type and hACE2 knock-in mice) or mock culture medium (wild-type mice only). After intranasal infection, mice were monitored daily for body weight loss and clinical signs. Throat swabs were collected daily under brief isoflurane anaesthesia using ultrafine sterile flock swabs (Hydraflock, Puritan, 25-3318-H). The tips of the swabs were placed in 0.5 ml of RA1 lysis buffer (Macherey-Nagel, ref. 740961) supplemented with 1% β-mercaptoethanol and vortexed. Groups of mice from two independent experiments were euthanized on days 2 and 4 after infection and organs were aseptically dissected, avoiding cross-contamination. Systematic tissue sampling was performed: (1) lung right superior lobe, right nasal concha, right olfactory bulb, part of the right brain hemisphere, apical part of the right kidney and parts of the distal small intestine (ileum) were collected for RNA isolation in RA1 lysis buffer; (2) lung middle, inferior and post-caval lobes, left nasal concha, left olfactory bulb, part of the right brain hemisphere and part of the right kidney were collected in MEM; and (3) lung left lobe, liver left lobe, left kidney, left brain hemisphere and part of the jejunum and ileum were fixed in buffered formalin. Data were generated from two identically designed independent experiments.

Mouse tissue samples collected in RA1 lysis buffer supplemented with 1% β-mercaptoethanol were homogenized using a Bullet Blender Tissue Homogenizer (Next-Advance). Homogenates were centrifuged for 3 min at 18,000*g* and stored at −70 °C until processing. Total RNA was extracted from homogenates using the NucleoMag VET kit for viral and bacterial RNA and DNA from veterinary samples (Macherey Nagel, ref. 744200) and the KingFisher Flex automated extraction instrument (ThermoFisher Scientific) following the manufacturers' instructions. RNA purity was analysed with a NanoDrop 2000 (ThermoFisher Scientific). A 25-µl RT–PCR for the viral *E* gene was carried out using 5 µl of extracted RNA template using the AgPath-ID One-Step RT–PCR (Applied Biosystems). Samples were processed in duplicate. Amplification and detection were performed in an Applied Biosystem 7500 Real-Time PCR System under the following conditions: an initial reverse transcription at 45 °C for 10 min, followed by PCR activation at 95 °C for 10 min and 45 cycles of amplification (15 s at 95 °C, 30 s at 56 °C and 30 s at 72 °C).

Fixed mouse tissue samples were processed, sectioned and stained with haematoxylin and eosin at the COMPATH core facility (University of Bern). Histopathological lung slides of hACE2 knock-in mice and wild-type mice (infected and mock) were examined and scored by a board-certified veterinary pathologist (S.d.B.), who was blinded to the identity of the samples. Scoring criteria are detailed in Supplementary Table 4.

Hamster study. Six Syrian hamsters (*Mesocricetus auratus*) (Janvier Labs) were infected intranasally under a short-term inhalation anaesthesia with 70 µl of SARS-CoV-2^{D614} and SARS-CoV-2^{G614} at equal

ratios using $10^{4.77}$ TCID$_{50}$ per hamster (calculated from back titration of the original material). After 24 h of isolated housing in individually ventilated cages, six pairs (each with one directly inoculated donor hamster and one sham-inoculated contact hamster) were cohoused. The housing of each hamster pair was strictly separated in individual cage systems to prevent spillover between different pairs. For the following seven days (day 2 until day 8 after infection) and on day 12 after infection, viral shedding was monitored in addition to a daily physical examination and body weighing routine.

To evaluate viral shedding, nasal washes were individually collected from each hamster under a short-term isoflurane anaesthesia. Starting with the contact hamster of each pair, each nostril was rinsed with 100 µl PBS (1.0× phosphate-buffered saline) and reflux was immediately gathered. A new pipette tip for every nostril and hamster was used to prevent indirect spillover transmission from one hamster to another. Furthermore, in between the respective pairs, a new anaesthesia system was used for each pair of hamsters. At day 8 after infection, one contact hamster was found dead. Although they lost up to almost 20% of their body weight, every other hamster recovered from disease. Under euthanasia, serum samples were collected from each hamster.

For the single-virus infection experimental setup, seven hamsters each were infected via the intranasal route with $10^{5.1}$ TCID$_{50}$ per hamster of SARS-CoV-2^{D614}, or $10^{4.5}$ TCID$_{50}$ per hamster of SARS-CoV-2^{G614} (calculated from back titration of the original material). From day 1 to day 4, nasal washes were obtained from these hamsters and body weight changes recorded. A tissue panel from respiratory organs—including nasal conchae, tracheal tissue, cranial, medial and caudal portions of the right lung, and the pulmonary lymph node—were collected after euthanasia from these hamsters.

Ferret study. In accordance with the hamster study, twelve ferrets (*Mustela putorius furo*) from in-house breeding were divided into six groups of two individuals. Ferret pairs were of equal age (between 4 and 18 months). In total, four ferrets were female (two pairs) and eight ferrets were male or neutered male (four pairs). The housing of each ferret pair was strictly separated in individual cage systems, to prevent spillover between different pairs. Per separate cage, one individual ferret was inoculated intranasally by instillation of 125 µl of the aforementioned inoculum ($10^{5.4}$ TCID$_{50}$ per ferret, calculated from back titration of the equally mixed original material) into each nostril under a short-term isoflurane-based inhalation anaesthesia. Time points and sampling technique corresponded to the methods used for the hamsters, although ferret nasal washing was performed using 2× 700 µl PBS per ferret. The contact ferret was not inoculated.

Specimen work up, viral RNA detection, and sequencing and quantification analyses. Organ samples were homogenized in a 1 ml mixture of equal volumes composed of Hank's balanced salts MEM and Earle's balanced salts MEM containing 2 mM L-glutamine, 850 mg l^{-1} NaHCO$_3$, 120 mg l^{-1} sodium pyruvate supplemented with 10% fetal calf serum and 1% penicillin–streptomycin at 300 Hz for 2 min using a Tissuelyser II (Qiagen) and centrifuged to clarify the supernatant. Nucleic acid was extracted from 100 µl of the nasal washes after a short centrifugation step or organ sample supernatant using the Nucleo-Mag Vet kit (Macherey Nagel). Viral loads in these samples were determined using the nCoV_IP4 RT–PCR[27] including standard RNA that were absolute-quantified by digital droplet PCR with a sensitivity of 10 copies per reaction. The extracted RNA was afterwards subjected to MinION sequencing and digital droplet PCR. For MinION sequencing, amplicons were produced with primers (WU-21-F: AATCTATCAGGCCG GTAGCAC; WU-86-R: CAACAGCTATTCCAGTTAAAGCAC) using Super-Script IV One-step RT–PCR (Thermo Fisher Scientific). Amplicons were sequenced on a MinION system from Oxford Nanopore using Native Barcoding 1–12 (EXP-NBD104) and 13–24 (EXP-NBD114), respectively, with Ligation Kit SQK-LSK109 (Oxford Nanopore). Libraries were loaded

on R9.4.1 Flow Cells (FLO-MIN106D) on a MinION coupled to a MinIT. MinION data analysis was performed as described in 'Sequencing and computational analysis'.

For rare mutation and sequence analysis based on digital droplet PCR, the QX200 Droplet Digital PCR System from Bio-Rad was used. The One-Step RT-ddPCR Advanced Kit for Probes (Bio-Rad) was applied according to the supplier's instructions. For the amplification of an 86-bp fragment of both variants of S, the forward primer SARS2-S-1804-F (5′-ACA AAT ACT TCT AAC CAG GTT GC-3′) and the reverse primer SARS2-S-1889-R (5′-GTA AGT TGA TCT GCA TGA ATA GC-3′) were used. For the detection of the D and G variants in one sample, two allele-specific locked nucleic acid probes were applied: SARS2-S-v1D-1834FAM (5′-FAM-TaT cAG gat GTt AAC-BHQ1-3′) and SARS2-S-v3G-1834HEX (5′-HEX-T cAG ggt GTt AAC-BHQ1-3′) (the locked nucleic acid positions are in lowercase). The concentration of the primers and probes was 20 μM and 5 μM, respectively. For data analysis, the QuantaSoft Analysis Pro software (v.1.0.596) was used.

Reporting summary

Further information on research design is available in the Nature Research Reporting Summary linked to this paper.

Data availability

Sequence data are available on the NCBI Sequence Read Archive (SRA) under the BioProject accession number PRJNA669553. Source data are provided with this paper.

23. van den Worm, S. H. et al. Reverse genetics of SARS-related coronavirus using vaccinia virus-based recombination. *PLoS ONE* **7**, e32857 (2012).
24. Thiel, V., Herold, J., Schelle, B. & Siddell, S. G. Infectious RNA transcribed in vitro from a cDNA copy of the human coronavirus genome cloned in vaccinia virus. *J. Gen. Virol.* **82**, 1273–1281 (2001).
25. Shepard, S. S. et al. Viral deep sequencing needs an adaptive approach: IRMA, the iterative refinement meta-assembler. *BMC Genomics* **17**, 708 (2016).
26. Anderson, C. Catseyes: create catseye plots illustrating the normal distribution of the means. R package version 0.2.3. https://CRAN.R-project.org/package=catseyes (2019).
27. WHO. Protocol: real-time RT–PCR assays for the detection of SARS-CoV-2, https://www.who.int/docs/default-source/coronaviruse/real-time-rt-pcr-assays-for-the-detection-of-sars-cov-2-institut-pasteur-paris.pdf?sfvrsn=3662fcb6_2 (accessed 3 December 2020).

Article

Extended Data Fig. 1 | See next page for caption.

Extended Data Fig. 1 | Additional in vitro characterization of S and of SARS-CoV-2^{D614} and SARS-CoV-2^{G614} isolates. a, Affinity between S and hACE2 determined by biolayer interferometry. Fc-tagged hACE2 was loaded onto surface of anti-human Fc capture biosensors and association was conducted using S (S-614D) or S(D614G) (S-614G) followed by dissociation. Data represent three biological replicates, and all repeats with statistical analysis are provided in Supplementary Table 2. **b**, Binding of polyhistidine-tagged or Fc-tagged S1 to BHK–hACE2 cells, determined by flow cytometry. Mean fluorescence intensity is shown for the corresponding S1 protein concentration. Data are mean ± s.d. of three biological replicates. **c**, Replication of the isolates SARS-CoV-2/USA-WA1/2020 (isolate 614D) and SARS-CoV-2/Massachusetts/VPT1/2020 (isolate 614G) in human NBE cells at 33 °C (left), 37 °C (middle) and 39 °C (right). Human NBE cells were infected with 200,000 TCID$_{50}$ of each virus. Supernatants were collected every 24 h and titrated by TCID$_{50}$ assay. Data are mean ± s.d. of four replicates. Statistical significance was determined by two-sided unpaired Student's t-test without adjustments S1 protein for multiple comparisons. P values (from left to right): left, NS (not significant), $P = 0.8098$; NS, $P = 0.7874$; *$P = 0.0328$; NS, $P = 0.1887$; and NS, $P = 0.5296$; middle, NS, $P = 0.1689$; NS, $P = 0.1475$; NS,

$P = 0.1415$; **$P = 0.0033$; and NS, $P = 0.3184$; right, *$P = 0.0197$; NS, $P = 0.6018$; NS, $P = 0.3903$; NS, $P = 0.0898$; and *$P = 0.0445$. **d**, Competition assay of recombinant SARS-CoV-2^{D614} (614D) and SARS-CoV-2^{G614} (614G) in human NBE cells at 33 °C, 37 °C and 39 °C. The inoculum was prepared by mixing two viruses at 9:1 ratio based on PFU per ml. Human NBE cells were infected with 100,000 PFU of the 9:1 virus mix ($n = 4$). Viral RNA was extracted from daily supernatant and sequenced by NGS. Percentage of sequencing reads encoding S or S(D614G). Each square represents one individual data point in competition experiment. For each time point, a linear regression model was generated based on the sequence read counts for S and S(D614G), and P values were calculated for the group (variant) coefficient. P values (left to right): left, NS, $P = 0.1796$; NS, $P = 0.087$; NS, $P = 0.1147$; NS, $P = 0.1244$; and *$P = 0.0401$; middle, NS, $P = 0.9114$; NS, $P = 0.0715$; NS, $P = 0.1696$; NS, $P = 0.1696$; and NS, $P = 0.1657$; right, NS, $P = 0.1041$; *$P = 0.013$; NS, $P = 0.0645$; *$P = 0.0102$; and *$P = 0.0308$. **e**, Cat's eye plot illustrating the relative replicative fitness values of SARS-CoV-2^{G614} over SARS-CoV-2^{D614} in human NBE cells for the competition experiments performed in **d**. Each dot represents an individual data point, the centre line represents the mean and the shaded area represents the s.d.

Article
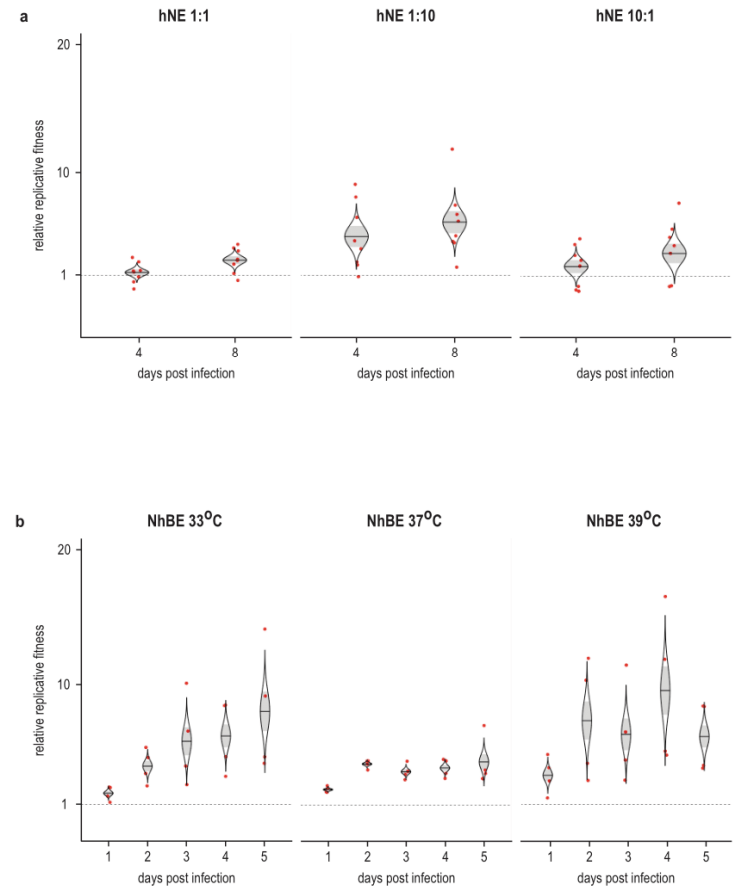
Extended Data Fig. 2 | Relative replicative fitness of SARS-CoV-2 variants. **a**, **b**, Cat's eye plots illustrating the relative replicative fitness values of SARS-CoV-2^{D614} over SARS-CoV-2^{G614} in human nasal epithelial (**a**) and human NBE (**b**) cells for the competition experiments shown in Fig. 1e, f. Each dot represents an individual data point, the centre line represents the mean and the shaded area represents the s.d.
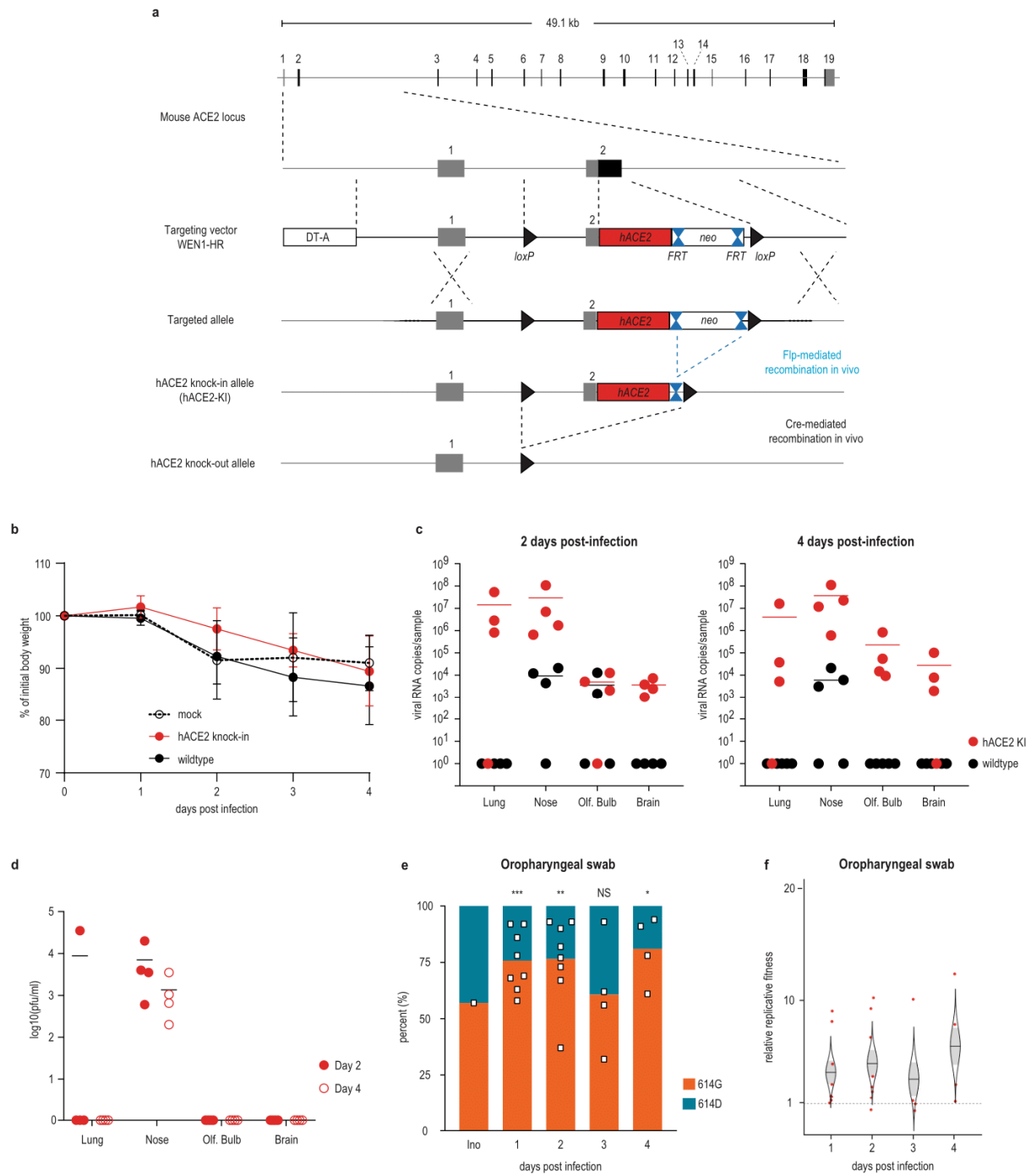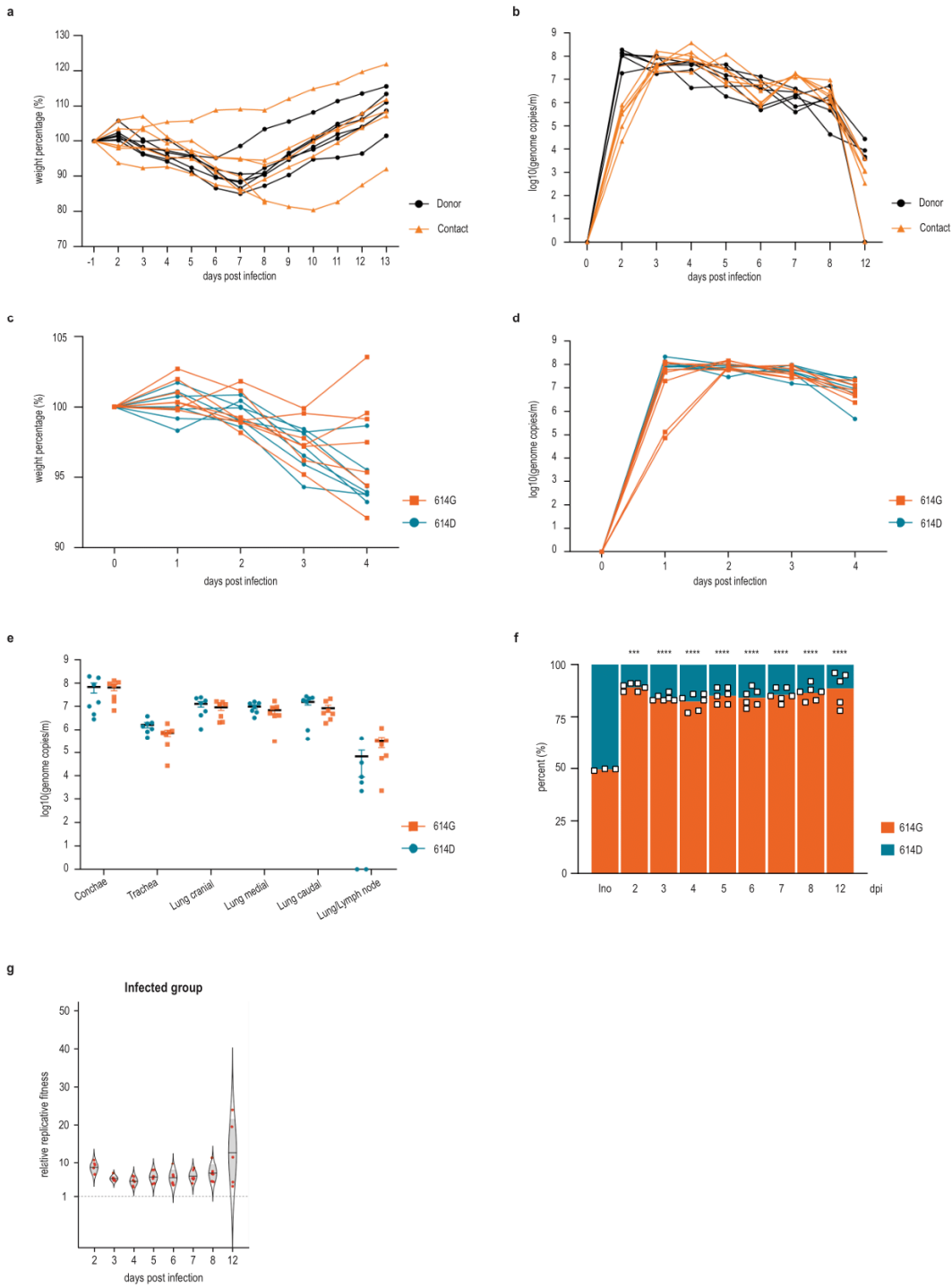
Extended Data Fig. 3 | See next page for caption.

Article

Extended Data Fig. 3 | hACE2 knock-in mouse generation, and infection with SARS-CoV-2^{D614} and SARS-CoV-2^{G614}. a, Design and generation of hACE2 knock-in mice. The human *ACE2* cDNA was inserted in-frame with the endogenous initiation codon of mouse *Ace2* in exon 2, which was deleted. The human *ACE2* cDNA was flanked 5′ with a loxP site (black triangle) and 3′ with a FRT–neomycin–FR–-loxP cassette. The targeting construct included a negative selection cassette (PGK-DTA) to improve selection of clones with homologous recombination. Chimeric male mice transmitting the targeted locus were crossed with Flp deleter female mice to generate the floxed human *ACE2* knock-in allele. This allele can be used: (1) without further Cre-mediated recombination (as shown here) to study hACE2 knock-in mice, in which the human *ACE2* cDNA is expressed in place of mouse *Ace2*; (2) after crossing with a Cre-deleter mouse line to generate constitutive *Ace2*-knockout mice; and (3) after crossing with a tissue-specific Cre line. Ubiquitous and tissue-specific knockout mice can be crossed with conventional hACE2 transgenic mice to remove the endogenous mouse ACE2, which could confound pathogenesis studies (owing to heterodimerization of ACE2). **b**, Loss of body weight at indicated time points after infection of hACE2 knock-in mice ($n = 8$) and wild-type mice ($n = 10$), and for mock-infected wild-type mice sampled identically ($n = 10$). **c, d**, RT–qPCR analysis (**c**) and viral titres (**d**) of tissue homogenates of inoculated hACE2 knock-in and wild-type mice at indicated time points. Olf., olfactory. **e**, Percentage of sequencing reads encoding S or S(D614G). Each square represents data for one individual mouse in a competition experiment. For each time point, a linear regression model was generated on the basis of the sequence read counts for S and S(D614G). *P* values were calculated for the group (variant) coefficient. *P* values (left to right): ***$P = 0.0009$; **$P = 0.0020$; NS, $P = 0.7875$; and *$P = 0.0180$. **f**, Cat's eye plot illustrating the relative replicative fitness values of SARS-CoV-2^{D614} over SARS-CoV-2^{G614} from oropharyngeal swabs of hACE2 knock-in mice in the competition experiment shown in Fig. 2. Ratios of SARS-CoV-2^{G614} to SARS-CoV-2^{D614} were measured after competition using the MinION sequencing platform at the time point indicated on the plot. Each dot represents one infected hACE2 knock-in mouse, the centre line represents the mean and the shaded area represents the s.d.

Extended Data Fig. 4 | See next page for caption.

Article

Extended Data Fig. 4 | Virus replication in infected Syrian hamsters. a, Loss of body weight at indicated time points after infection of Syrian hamsters. Donor hamsters ($n = 6$) (black dots) were intranasally inoculated with SARS-CoV-2^{D614} and SARS-CoV-2^{G614} at equal ratio ($1 \times 10^{4.77}$ TCID$_{50}$ per hamster, as determined by back-titration of the original inoculum). Twenty-four h after infection, naive hamsters ($n = 6$) (orange triangles) were housed in direct contact in a one-to-one experimental setup. **b**, RT–qPCR analysis of individual nasal washing samples obtained from donor and contact hamsters. **c**, Loss of body weight at the indicated time points after infection of the hamsters. Syrian hamsters were inoculated with $10^{5.1}$ TCID$_{50}$ per hamster of SARS-CoV-2^{D614} ($n = 7$) (blue dots) or $10^{4.5}$ TCID$_{50}$ per hamster of SARS-CoV-2^{G614} ($n = 7$) (red triangles) via the intranasal route. Titres were determined by back titration of the original inoculation material. **d**, Viral genome copy numbers are shown as determined by RT–qPCR from individual nasal washing samples of the hamsters inoculated with single variant virus. **e**, RT–qPCR analysis of tissue homogenates of inoculated hamsters of the SARS-CoV-2^{D614} group ($n = 7$) (blue dots) versus the SARS-CoV-2^{G614} group ($n = 7$) (red triangles). **f**, Percentage of sequencing reads encoding S or S(D614G). Each square represents data for one individual hamster in the competition experiment. For each time point, a linear regression model was generated on the basis of the sequencing read counts for S and S(D614G). P values were calculated for the group (variant) coefficient. ***$P = 0.0007$; ****$P < 0.0001$. **g**, Cat's eye plot showing the relative replicative fitness values of SARS-CoV-2^{G614} over SARS-CoV-2^{D614} for infected hamsters from the competition experiment shown in Fig. 3. Ratios of SARS-CoV-2^{G614} to SARS-CoV-2^{D614} were measured after competition using the MinION sequencing platform at the time points indicated on the plot. Each dot represents one infected hamster ($n = 6$), the centre line represents the mean and the shaded area represents the s.d.
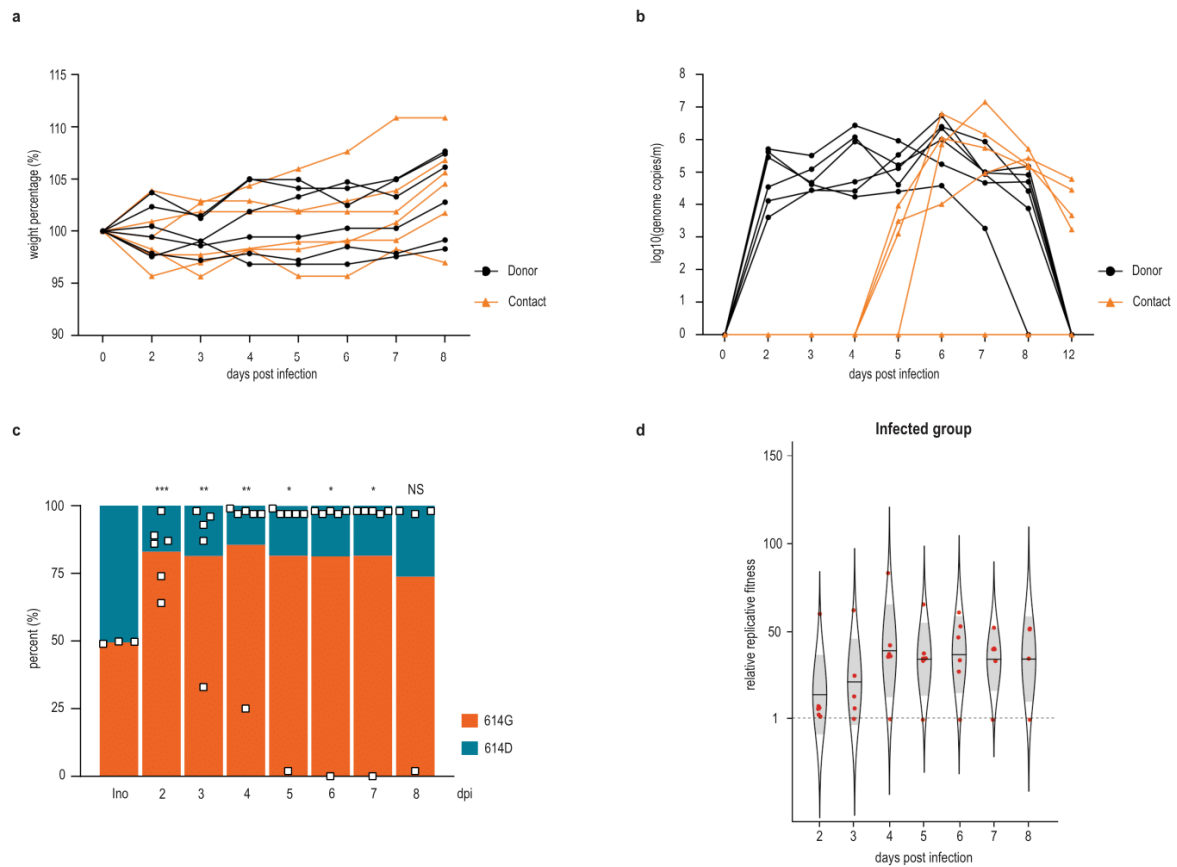
Extended Data Fig. 5 | Twin inoculation of donor ferrets with equal ratios of SARS-CoV-2^{D614} and SARS-CoV-2^{G614}. Donor ferrets (black dots) ($n=6$) were intranasally inoculated with $10^{5.4}$ TCID$_{50}$ per ferret, as determined by back titration of an inoculum comprising equal ratios of SARS-CoV-2^{D614} and SARS-CoV-2^{G614}. Twenty-four hours after inoculation, one contact ferret (orange triangle) ($n=6$) was commingled with one donor ferret, creating six donor–contact ferret pairs. **a**, Individual body weight of ferrets at the indicated days relative to the day of inoculation is plotted. **b**, Genome copy numbers for inoculated donor and contact ferrets. Individual nasal washing samples of the indicated days were analysed by RT–qPCR nCoV_IP4, and absolute numbers were calculated using a set of standard RNA. All donor ferrets (black dots) tested positive for viral RNA, starting from day 2 after inoculation ($n=6$). Four out of six contact ferrets (orange triangles) tested positive for viral RNA, starting from day 4 (corresponding to day 3 after contact). Two of the six contact ferrets never tested positive for viral RNA throughout the study. **c**, Percentage of sequencing reads encoding S or S(D614G). Each square represents data for one individual ferret in the competition experiment. For each time point, a linear regression model was generated on the basis of the sequence read counts for S and S(D614G). P values were calculated for the group (variant) coefficient. P values (left to right): ***$P=0.0001$; **$P=0.0090$; **$P=0.0030$; *$P=0.0352$; *$P=0.0393$; *$P=0.0411$; and NS, $P=0.2883$. **d**, Cat's eye plot illustrating the relative replicative fitness values of SARS-CoV-2^{G614} over SARS-CoV-2^{D614} in infected ferrets from the competition experiment shown in Fig. 4. Ratios of SARS-CoV-2^{G614} to SARS-CoV-2^{D614} were measured after competition using the MinION sequencing platform at the time points indicated on the plot. Each dot represents one infected ferret ($n=6$), the centre line represents the mean and the shaded area represents the s.d.

4. PUBLICATION IV: ENHANCED FITNESS OF SARS-COV-2 VARIANT OF CONCERN ALPHA BUT NOT BETA

Publication IV

Enhanced fitness of SARS-CoV-2 variant of concern Alpha but not Beta

Lorenz Ulrich, Nico Joel Halwe, Adriano Taddeo, Nadine Ebert, Jacob Schön, Christelle Devisme, Bettina Salome Trüeb, Bernd Hoffmann, Manon Wider, Xiaoyu Fan, Meriem Bekliz, Manel Essaidi-Laziosi, Marie Luisa Schmidt, Daniela Niemeyer, Victor Max Corman, Anna Kraft, Aurélie Godel, Laura Laloli, Jenna N. Kelly, Brenda M. Calderon, Angele Breithaupt, Claudia Wylezich, Inês Berenguer Veiga, Mitra Gultom, Sarah Osman, Bin Zhou, Kenneth Adea, Benjamin Meyer, Christiane S. Eberhardt, Lisa Thomann, Monika Gsell, Fabien Labroussaa, Jörg Jores, Artur Summerfield, Christian Drosten, Isabella Anne Eckerle, David E. Wentworth, Ronald Dijkman, Donata Hoffmann, Volker Thiel, Martin Beer, Charaf Benarafa

Article

Enhanced fitness of SARS-CoV-2 variant of concern Alpha but not Beta

Lorenz Ulrich[1,17], Nico Joel Halwe[1,17], Adriano Taddeo[2,3,17], Nadine Ebert[2,3,17], Jacob Schön[1], Christelle Devisme[2,3], Bettina Salome Trüeb[2,3,4], Bernd Hoffmann[1], Manon Wider[5], Xiaoyu Fan[6], Meriem Bekliz[7], Manel Essaidi-Laziosi[7], Marie Luisa Schmidt[8], Daniela Niemeyer[8,9], Victor Max Corman[8,9], Anna Kraft[1], Aurélie Godel[2,3], Laura Laloli[5,10], Jenna N. Kelly[2,3], Brenda M. Calderon[6], Angele Breithaupt[11], Claudia Wylezich[1], Inês Berenguer Veiga[2,3], Mitra Gultom[5,10], Sarah Osman[6], Bin Zhou[6], Kenneth Adea[7], Benjamin Meyer[12], Christiane S. Eberhardt[12,13,14], Lisa Thomann[2,3], Monika Gsell[5], Fabien Labroussaa[4], Jörg Jores[4,15,16], Artur Summerfield[2,3], Christian Drosten[8,9], Isabella Anne Eckerle[7,15,16], David E. Wentworth[6], Ronald Dijkman[5,18], Donata Hoffmann[1,18], Volker Thiel[2,3,18 ✉], Martin Beer[1,18 ✉] & Charaf Benarafa[2,3,18 ✉]

Emerging variants of concern (VOCs) are driving the COVID-19 pandemic[1,2]. Experimental assessments of replication and transmission of major VOCs and progenitors are needed to understand the mechanisms of replication and transmission of VOCs[3]. Here we show that the spike protein (S) from Alpha (also known as B.1.1.7) and Beta (B.1.351) VOCs had a greater affinity towards the human angiotensin-converting enzyme 2 (ACE2) receptor than that of the progenitor variant S(D614G) in vitro. Progenitor variant virus expressing S(D614G) (wt-S[614G]) and the Alpha variant showed similar replication kinetics in human nasal airway epithelial cultures, whereas the Beta variant was outcompeted by both. In vivo, competition experiments showed a clear fitness advantage of Alpha over wt-S[614G] in ferrets and two mouse models—the substitutions in S were major drivers of the fitness advantage. In hamsters, which support high viral replication levels, Alpha and wt-S[614G] showed similar fitness. By contrast, Beta was outcompeted by Alpha and wt-S[614G] in hamsters and in mice expressing human ACE2. Our study highlights the importance of using multiple models to characterize fitness of VOCs and demonstrates that Alpha is adapted for replication in the upper respiratory tract and shows enhanced transmission in vivo in restrictive models, whereas Beta does not overcome Alpha or wt-S[614G] in naive animals.

Uncontrolled transmission of SARS-CoV-2 in the human population has contributed to the persistence of the COVID-19 pandemic. The emergence of new variants in largely immunologically naive populations suggests that adaptive mutations in the viral genome continue to improve the fitness of this zoonotic virus. In March 2020, a single amino acid change in the S protein at position 614 (S(D614G)) was identified in a small fraction of sequenced samples—this became the predominant variant worldwide within a few weeks[4]. The fitness advantage conferred by this single amino acid change was supported by major increases in infectivity, viral load and transmissibility in vitro and in animal models[3,5,6].

In the second half of 2020, SARS-CoV-2 VOCs with a combination of several mutations emerged, including Alpha, first described in southeast England[7], and Beta, first identified in South Africa[8]. In February–March 2021, Alpha rapidly became the prevailing variant in many regions of the world and a higher reproduction number was inferred from early epidemiological data[9–11]. Beyond S(D614G), Alpha has 18 further mutations in its genome compared with the progenitor, with two deletions and six substitutions within the *S* gene[12]. Some of the S mutations, such as N501Y and the H69/V70 deletion, have been hypothesized to enhance replication and transmission, but there is a lack of clear experimental evidence for this[13,14]. Beta has nine mutations in S, including N501Y,

[1]Institute of Diagnostic Virology, Friedrich-Loeffler-Institut, Greifswald-Insel Riems, Germany. [2]Institute of Virology and Immunology, Mittelhäusern, Switzerland. [3]Department of Infectious Diseases and Pathobiology, Vetsuisse Faculty, University of Bern, Bern, Switzerland. [4]Institute of Veterinary Bacteriology, Vetsuisse Faculty, University of Bern, Bern, Switzerland. [5]Institute for Infectious Diseases, University of Bern, Bern, Switzerland. [6]CDC COVID-19 Emergency Response, Centers for Disease Control and Prevention, Atlanta, GA, USA. [7]Department of Microbiology and Molecular Medicine, Faculty of Medicine, University of Geneva, Geneva, Switzerland. [8]Charité–Universitätsmedizin Berlin, Institute of Virology, Berlin, Germany. [9]German Centre for Infection Research (DZIF), Berlin, Germany. [10]Graduate School for Biomedical Science, University of Bern, Bern, Switzerland. [11]Department of Experimental Animal Facilities and Biorisk Management, Friedrich-Loeffler-Institut, Greifswald-Insel Riems, Germany. [12]Centre for Vaccinology, Department of Pathology and Immunology, University of Geneva, Geneva, Switzerland. [13]Division of General Paediatrics, Department of Woman, Child and Adolescent Medicine, Faculty of Medicine, University of Geneva, Geneva, Switzerland. [14]Center for Vaccinology, Geneva University Hospitals, Geneva, Switzerland. [15]Division of Infectious Disease, Geneva University Hospitals, Geneva, Switzerland. [16]Division of Laboratory Medicine, Laboratory of Virology, Geneva University Hospitals, Geneva, Switzerland. [17]These authors contributed equally: Lorenz Ulrich, Nico Joel Halwe, Adriano Taddeo, Nadine Ebert. [18]These authors jointly supervised this work: Ronald Dijkman, Donata Hoffmann, Volker Thiel, Martin Beer, Charaf Benarafa. ✉e-mail: volker.thiel@vetsuisse.unibe.ch; martin.beer@fli.de; charaf.benarafa@vetsuisse.unibe.ch
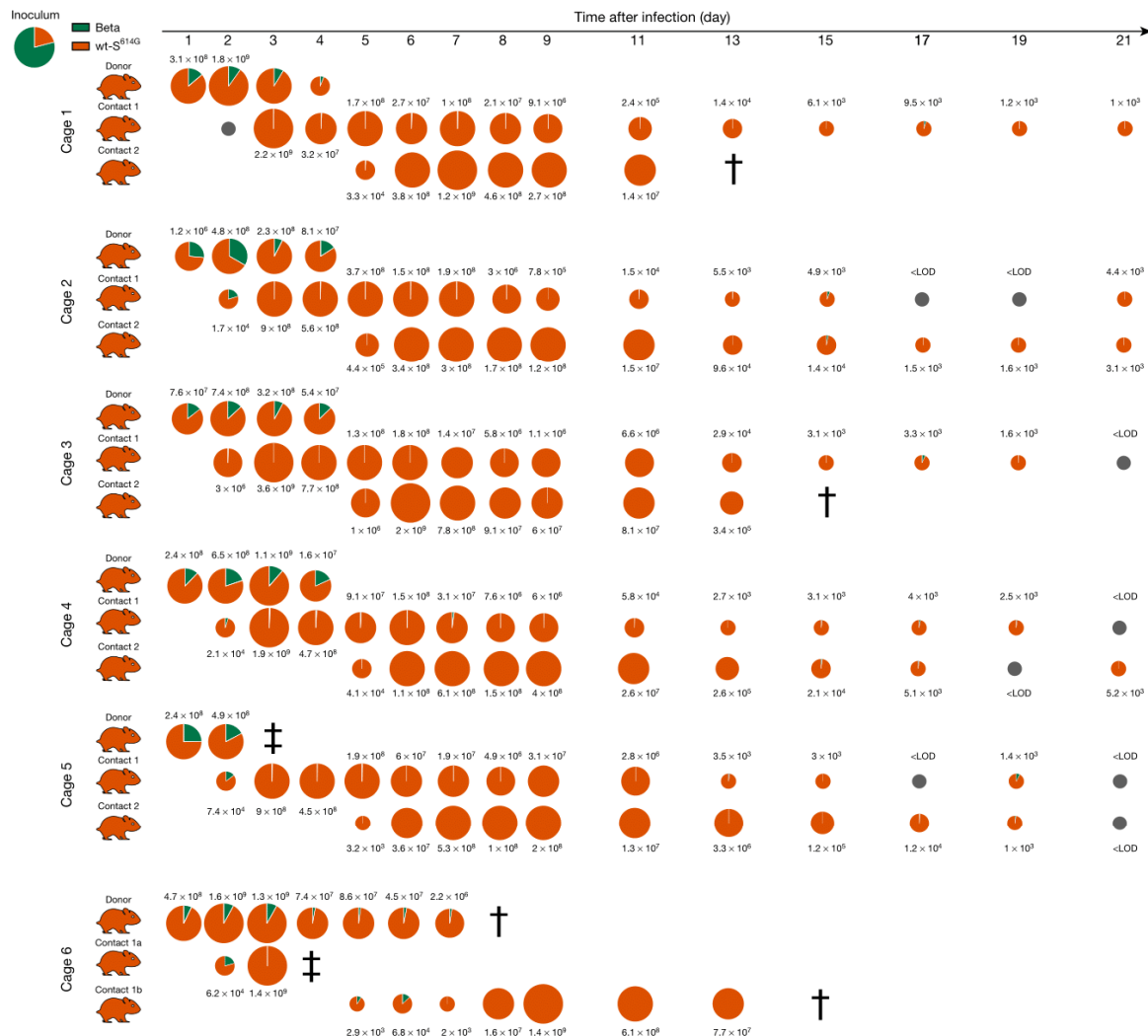
Article

Fig. 1 | Competitive replication and transmission of Beta and wt-S^{614G} in Syrian hamsters. Six donor hamsters were each inoculated with a median tissue culture infectious dose (TCID$_{50}$) of $10^{4.25}$, determined by back titration and comprising a mixture of wt-S^{614G} (orange) and Beta (green) at a 1:3.8 ratio, determined by quantitative PCR with reverse transcription (RT–qPCR). Donor, contact 1 and contact 2 hamsters were co-housed sequentially as shown in Extended Data Fig. 2a. Nasal washes were performed daily from 1–9 dpi and then every 2 days until 21 dpi. Pie charts show the ratio of variants detected in nasal washes at the indicated dpi. Pie chart sizes are proportional to the total number of viral genome copies per ml, as shown above or below each chart. Grey pies indicate values below the limit of detection (LOD; <10^3 viral genome copies per ml). Hamster silhouettes are coloured according to the dominant variant (>66%) detected in the last positive sample from each animal. Daggers indicate that the animal reached the humane endpoint; double daggers indicate a hamster that died during inhalation anaesthesia at 3 and 4 dpi. This required changes in the group composition in cage 6—the donor hamster was kept until 7 dpi and was co-housed in two different pairs: donor–contact 1a and donor–contact 1b.

and two in the S receptor-binding domain (RBD), K417N and E484K. E484K is thought to be responsible for the ability of Beta to escape neutralization by plasma from convalescent individuals[15–17]. Whether S mutations are solely responsible for the putative fitness advantage and if so, which ones, remains unknown.

Here we investigate the fitness of Alpha and Beta VOCs relative to wt-S^{614G}, the predominant parental strain containing the S(D614G) substitution—in relevant primary airway culture systems in vitro, and in ferrets, Syrian hamsters and two mouse models expressing human ACE2—to assess specific advantages in replication and transmission and to evaluate the effects of Alpha S mutations alone in vivo. Neither Alpha nor Beta showed enhanced replication in human airway epithelial cell (AEC) cultures compared with wt-S^{614G}. Competitive transmission

experiments in Syrian hamsters showed similar replication and transmission of wt-S^{614G} and Alpha, which both outcompeted Beta. However, competitive experiments in ferrets and transgenic mice expressing human ACE2 controlled by the *KRT18* promoter (hACE2-K18Tg), which overexpress human ACE2 in epithelial cells, showed increased fitness of Alpha compared with wt-S^{614G}. Finally, Alpha and a recombinant clone of progenitor virus expressing the Alpha S protein (wt-S^{Alpha}) both outcompeted the parental wt-S^{614G} strain, resulting in higher virus load in the upper respiratory tract (URT) of mice expressing human ACE2 instead of mouse ACE2 under the endogenous mouse *Ace2* promoter (hACE2-KI mice). Similar to results from AEC cultures, Beta showed lower fitness than wt-S^{614G} in hACE2-KI mice. Infections with Alpha and wt-S^{614G} virus resulted in similar pathologies in all the in vivo models.
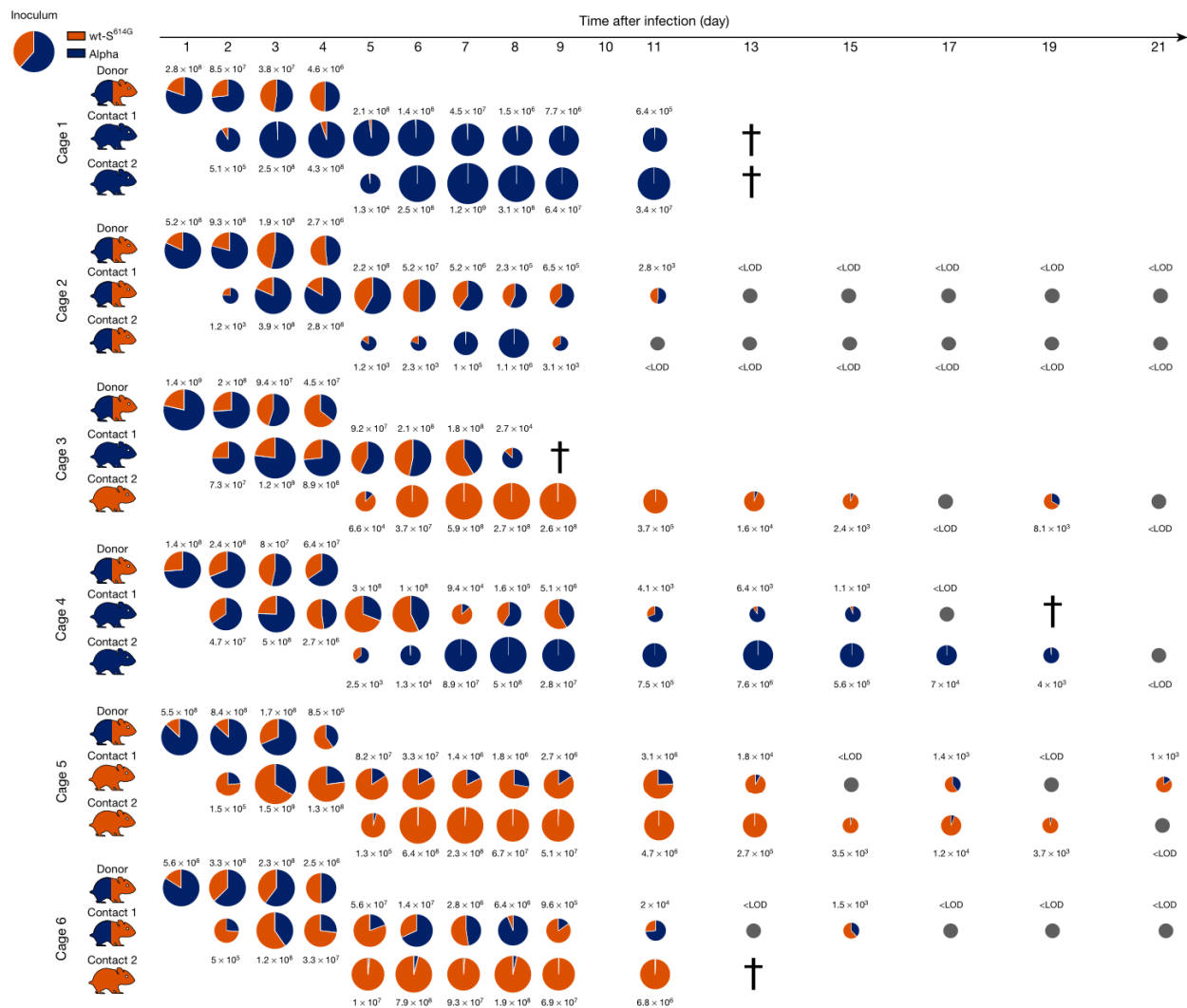
116

Fig. 2 | Competitive replication and transmission of Alpha and wt-S⁶¹⁴ᴳ in Syrian hamsters. Six donor hamsters were each inoculated with a $TCID_{50}$ of $10^{4.3}$, determined by back titration and comprising a mixture of wt-S^{614G} and Alpha at a 1:1.6 ratio, determined by RT–qPCR. Donor, contact 1 and contact 2 hamsters were co-housed sequentially as shown in Extended Data Fig. 2a. Nasal washes were performed daily from 1–9 dpi and then every 2 days until 21 dpi. Pie charts show the ratio of variants detected in nasal washes at the indicated dpi.

Pie chart sizes are proportional to the total number of viral genome copies per ml, as shown above or below each chart. Grey pies indicate values below the LOD. Hamster silhouettes are coloured to indicate the dominant variant (>66%) detected in the last positive sample from each hamster; a silhouette with two colours indicates that there is no dominant variant. Daggers indicate that the hamster reached the humane endpoint.

Binding and replication of VOCs in vitro

The evolution of SARS-CoV-2 variants is associated with accumulation of mutations in the S protein. We determined dissociation constant (K_D) values for recombinant trimeric S with immobilized dimeric human ACE2 using bio-layer interferometry. S protein from Alpha (S^{Alpha}) or Beta (S^{Beta}) exhibited a fourfold higher affinity for human ACE2 than that of S(D614G) protein (Extended Data Fig. 1a). Replication kinetics of Alpha, Beta and a wild-type clinical isolate with the S(D614G) mutation were similar in relation to viral copies and titres in AEC cultures incubated at 33 and 37 °C (Extended Data Fig. 1b). However, in direct competition experiments in AEC cultures, Alpha had no advantage over wt-S^{614G}, whereas Beta was outcompeted by both Alpha and wt-S^{614G} (Extended Data Fig. 1c), indicating that competition experiments can expose differences in replication that are not detected in individual growth kinetic assays.

Alpha and wt-S⁶¹⁴ᴳ outcompete Beta in hamsters

We inoculated groups of six Syrian hamsters intranasally with a mixture of two SARS-CoV-2 strains comprising equivalent numbers of genome copies in three one-to-one competition experiments: Alpha versus Beta, Beta versus wt-S^{614G}, and Alpha versus wt-S^{614G}. All experimentally infected 'donor' hamsters were kept strictly in isolation cages to prevent intergroup spill-over infections. Each donor hamster was co-housed with a naive 'contact 1' hamster 1 day post infection (dpi), creating six donor–contact 1 pairs to evaluate shedding and transmission. At 4 dpi, donor hamsters were euthanized and six subsequent transmission pairs were set up by co-housing each contact 1 hamster with a naive contact 2 hamster (Extended Data Fig. 2a).

In two competition experiments, wt-S^{614G} and Alpha outcompeted Beta, as indicated by nasal washes of the donor hamsters from 1 dpi until
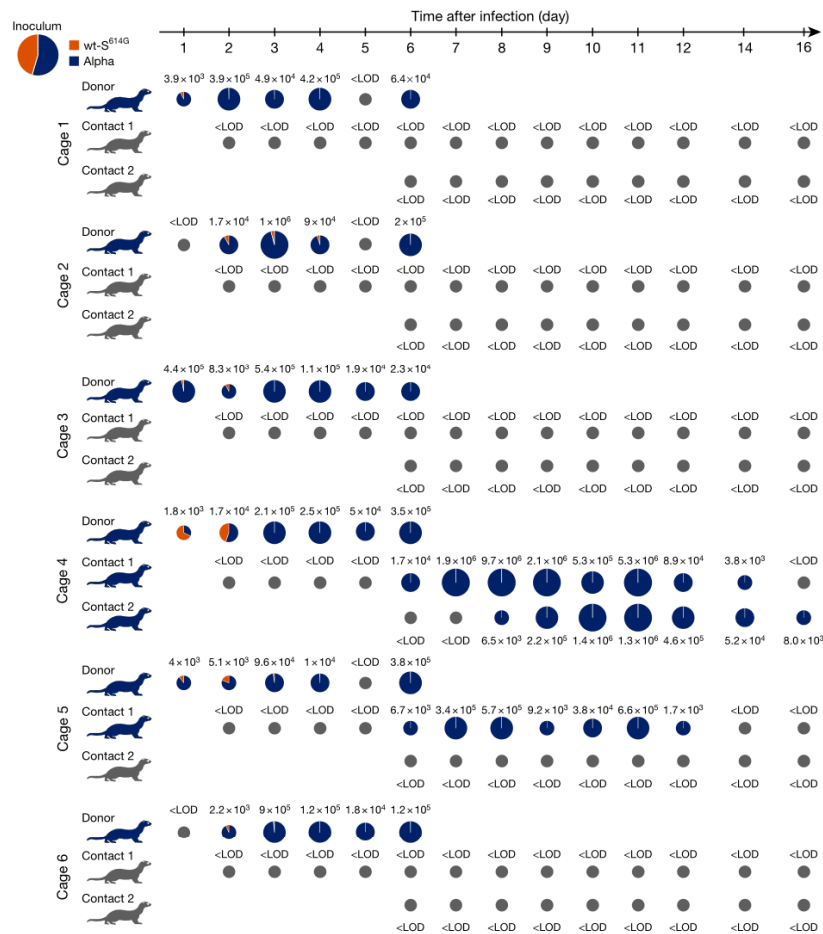
Article

Fig. 3 | Replication and transmission of SARS-CoV-2 Alpha and wt-S^{614G} in ferrets. Six donor ferrets were each inoculated with a TCID$_{50}$ of $10^{5.9}$, determined by back titration and comprising a mixture of wt-S^{614G} and Alpha at a 1:1.2 ratio, determined by RT–qPCR. Donor, contact 1 and contact 2 ferrets were co-housed sequentially as shown in Extended Data Fig. 2b. Pie charts show the ratio of variants detected in nasal washes at the indicated dpi. Pie chart sizes are proportional to the total number of viral genome copies per ml, as shown above or below each chart. Grey pies indicate values below the LOD. Viral genome copies were below the LOD at 18 and 20 dpi (not shown). Ferret silhouettes are coloured to indicate the dominant SARS-CoV-2 variant (>66%) detected in the last positive sample from each ferret.

euthanasia at 4 dpi. The viral load reached 10^9 genome copies (gc) per ml for wt-S^{614G} and Alpha, whereas Beta viral loads were tenfold lower at corresponding time points. Consequently, transmission of Beta was limited or undetectable in contact 1 and contact 2 hamsters compared with the competing variants wt-S^{614G} (Fig. 1) and Alpha (Extended Data Fig. 3). Transmission to contact hamsters was associated with clinical signs and weight loss (Extended Data Fig. 4a, b). In donor and contact hamsters, viral genome loads in the URT (comprising nasal conchae and trachea) revealed increased replication of Alpha and wt-S^{614G} compared with Beta (Extended Data Fig. 5a, b), which may explain the lower transmission rate of Beta in a competition context. Of note, Beta replicated to high titres in the lower respiratory tract (LRT; comprising cranial, medial and caudal lung lobes) of donor hamsters, similar levels as observed for the competing Alpha and wt-S^{614G} virus (Extended Data Fig. 5a, b).

Competition between Alpha and wt-S^{614G} showed no clear difference in virus titres in nasal washes of donor hamsters, and both variants were detected at all time points in each donor with numbers of individual variants ranging from 10^5 to 10^9 gc ml^{-1} (Fig. 2). Of note, Alpha was dominant over wt-S^{614G} in the donor hamsters at 1 dpi, but these strains were balanced by the endpoint at 4 dpi. In organ samples from the donor hamsters, the highest viral loads were found in the LRT, where Alpha was predominant

(more than 66% of genome copies) overall with more than tenfold more viral genome copies than wt-S^{614G} in 14 out of 18 lung samples from the 6 donor hamsters (Extended Data Fig. 5c). Sequential transmission to contact animals was associated with body weight loss (Extended Data Fig. 4c) and was highly efficient for Alpha and wt-S^{614G} variants, which were both detected in nasal washes of almost all contact 1 hamsters (Fig. 2). Whereas all donor and contact 1 hamsters transmitted both viruses to their respective contacts, contact 2 hamsters mainly shed one variant at high levels in nasal washes, demonstrating similar transmission ability for wt-S^{614G} and Alpha. At the individual endpoints for contact 1 hamsters, Alpha appeared to dominate in the LRT when both variants were found at similar levels in the nasal washes and URT. In contact 2 hamsters, the variant that was dominant in the URT was also dominant in the LRT (Extended Data Fig. 5c). High levels of SARS-CoV-2 replication in hamsters induced a rapid humoral immune response, as shown by serum reactivity in RBD-based ELISA in all but one of the contact hamsters (Extended Data Fig. 6a–c). We observed a twofold increase in in vitro binding affinity of recombinant trimeric S^{Alpha} to hamster ACE2 compared with S(D614G) (Extended Data Fig. 1d). These findings suggest that although S^{Alpha} has an increased binding affinity for ACE2, this factor was not predictive of the outcome of experimental infections in hamsters.

Alpha dominates wt-S^{614G} in ferrets

In a similar approach, we inoculated six donor ferrets with a mixture of wt-S^{614G} and Alpha at equivalent numbers of genome copies and monitored sequential transmission in naive contact 1 and contact 2 ferrets (Extended Data Fig. 2b). Alpha rapidly became the dominant variant in nasal washes from 2 dpi with up to 10^5 gc ml^{-1} (Fig. 3). Correspondingly, the nasal concha of donor ferrets revealed high levels of replication in the nasal epithelium and up to 100-fold higher load of Alpha (up to $10^{8.2}$ gc ml^{-1}) than wt-S^{614G} (up to $10^{6.5}$ gc ml^{-1}) (Extended Data Fig. 7a). Although histopathological analysis clearly indicated viral replication in the nasal epithelium of the donor ferrets (Extended Data Fig. 7b−e), we did not observe severe clinical signs of infection (Extended Data Fig. 4d, e). Transmission to contact 1 ferrets was detected in only two pairs of ferrets, and only one contact 1 ferret transmitted the virus to the contact 2 ferret. However, in each of these three transmission events, the Alpha variant was highly dominant and replicated to similarly high titres as in donor ferrets (Fig. 3). The 3 contact ferrets with virus shedding seroconverted by 15−20 days post contact (dpc), confirming active infection (Extended Data Fig. 6d).

Alpha dominates wt-S^{614G} in K18Tg mice

To assess further adaptation of Alpha to human ACE2, four hACE2-K18Tg mice, which overexpress hACE2 in respiratory epithelium[18], were inoculated with a mixture of SARS-CoV-2 wt-S^{614G} and Alpha with equivalent numbers of genomic copies (Fig. 4a). Each inoculated mouse was co-housed with a contact hACE2-K18Tg mouse at 1 dpi. Alpha was dominant in the oropharyngeal samples of all four inoculated mice from 1 to 4 dpi with up to 10^6 gc ml^{-1}. The increased replicative fitness of Alpha over wt-S^{614G} was further reflected throughout the respiratory tract, with higher numbers of genome copies in nose, lungs, olfactory bulb and most brain samples at 4 dpi (Fig. 4a), and inoculated mice showed loss of body weight at 4 dpi (Extended Data Fig. 8a). A relatively high infectious dose was used to promote transmission in these experiments, and was associated with high viral load (up to 10^8 viral genome copies per sample) in the lung and brain, leading to encephalitis—as previously reported in hACE2-K18Tg mice[19,20]. Viral loads were lower in nasal and oropharyngeal swabs from these mice, and only limited transmission was observed from these samples (two out of four contacts). None of the contact mice lost weight, but only Alpha was detectable in the lungs of contact mice at 7 dpc (Extended Data Fig. 8b).

We performed a similar competition experiment between wt-S^{614G} and an isogenic recombinant virus expressing S^{Alpha} (wt-S^{Alpha}). We inoculated hACE2-K18Tg mice with an equal mixture of wt-S^{Alpha} and wt-S^{614G} and housed them with a contact hACE2-K18Tg mouse at 1 dpi. The replicative advantage of wt-S^{Alpha} was less clear in this experiment, and both wt-S^{Alpha} and wt-S^{614G} were present with similarly high numbers of viral genome copies in lung and brain samples (Fig. 4b). Transmission to contact mice was inefficient, and wt-S^{Alpha} was the only virus detected in lungs of contact mice at 7 dpc (Extended Data Fig. 8b). These results indicate that the S^{Alpha} spike mutations contribute to the replication advantage of Alpha over wt-S^{614G} in the URT of mice that express high levels of human ACE2.

Competition in hACE2-KI mice

To further address this question, we next used hACE2-KI homozygous mice[3]. In contrast to hACE2-K18Tg mice, hACE2-KI mice show physiological expression of human ACE2, with no ectopic expression of human ACE2 in the brain, and no expression of mouse ACE2, which has been shown to be permissive to the spike mutation N501Y contained in S^{Alpha}. We inoculated 4 groups of hACE2-KI mice intranasally with 10^4 plaque-forming units (PFU) per mouse of either wt-S^{614G}, Alpha, wt-S^{Alpha} or Beta ($n = 8$ mice per group) as individual virus infections.
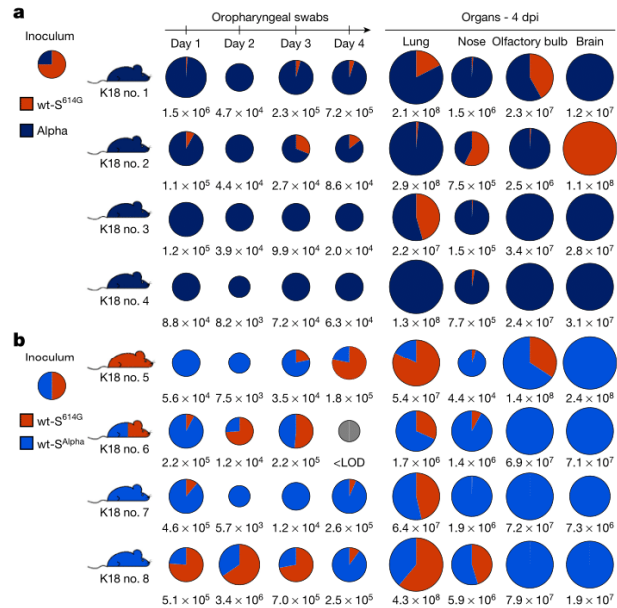

Fig. 4 | Replication of Alpha, wt-S^{Alpha}, and wt-S^{614G} in hACE2-K18Tg mice. **a**, **b**, Two groups of four donor hACE2-K18Tg mice were inoculated with 1×10^4 PFU, determined by back titration and comprising a mixture of wt-S^{614G} (orange) and Alpha (dark blue) at a 3:1 ratio (**a**), or a mixture of wt-S^{614G} and wt-S^{Alpha} (light blue) at a 1:1 ratio (**b**). Pie charts show the ratio of variants detected in each sample at the indicated dpi. Pie chart sizes are proportional to the total number of viral genome copies per ml (swabs) or per sample (tissues), as shown below each chart. Grey pies indicate values below the LOD. Mouse silhouettes are coloured to indicate the dominant SARS-CoV-2 variant (>66%) in the last positive swab sample from the corresponding mouse; a silhouette with two colours indicates that there is no dominant variant. K18 nos. 1 to 8 denote individual hACE-K18Tg donor mice.

We observed significantly higher viral genome copy numbers in mice infected with Alpha, wt-S^{Alpha} or Beta compared with wt-S^{614G} in oropharyngeal swabs at 1 dpi (Extended Data Fig. 9a). Moreover, there were significantly higher numbers of viral genome copies of Alpha and wt-S^{Alpha} in the nose at 2 dpi and in the olfactory bulb at 4 dpi compared with wt-S^{614G} and Beta (Extended Data Fig. 9b). Of note, viral titres in the nasal airways and lungs showed SARS-CoV-2 persistence at 4 dpi in 3 out of 4 mice infected with either Alpha or with wt-S^{Alpha}, but not in mice inoculated with wt-S^{614G}, whereas Beta persisted in the lungs of 2 out of 4 mice (Extended Data Fig. 9c). The apparent discrepancy between genome copy number and PFU reflects the non-homogeneous distribution of the virus in the different samples processed for each assay. We observed no difference in weight loss (Extended Data Fig. 9d) or lung histopathology score (Supplementary Table 1) between groups.

Finally, we performed competition experiments to compare the replication of the VOCs in groups of hACE2-KI mice. We observed a complete predominance of Alpha and wt-S^{Alpha} over wt-S^{614G} (Fig. 5a−c). By contrast, Beta showed reduced fitness compared with wt-S^{614G} (Fig. 5d). Together, the two mouse models support enhanced fitness of SARS-CoV-2 Alpha VOC over its progenitor wt-S^{614G} with increased replication and persistence in the URT and more systemic spread, mediated in part by changes in the Alpha S sequence.

Discussion

Epidemiological data indicate that new SARS-CoV-2 variant lineages with specific amino acid changes have a fitness advantage over
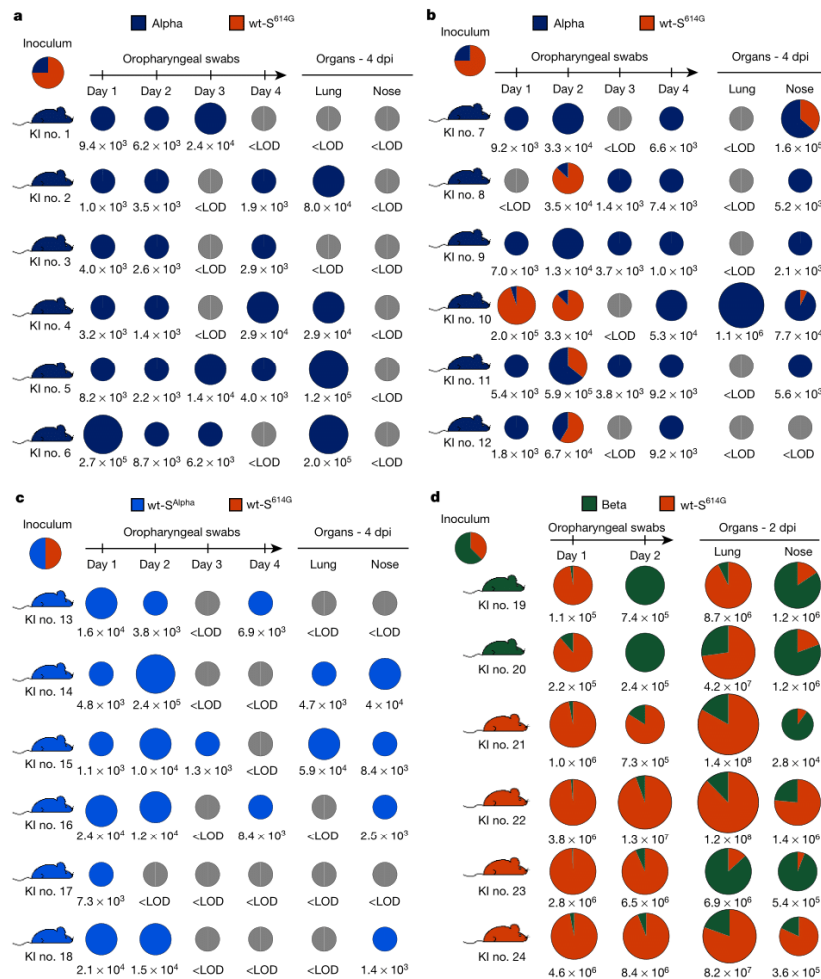
Article

Fig. 5 | Replication of Alpha, wt-S^Alpha, and Beta in competition with wt-S^614G in hACE2-KI mice. a–d, Groups of hACE2-KI male (**a**, **c**, **d**) and female (**b**) mice were inoculated with 1×10^4 PFU, determined by back titration and comprising a mixture of wt-S^614G and Alpha at a 3:1 ratio (**a**, **b**), a mixture of wt-S^614G and wt-S^Alpha at a 1:1 ratio (**c**), and a mixture of wt-S^614G and Beta at a 1:1.6 ratio (**d**). Pie charts show the ratio of variants detected in each sample at the indicated dpi.

Pie chart sizes are proportional to the total number of viral genome copies per ml (swabs) or per sample (tissues), as shown below each chart. Grey pies indicate values below the LOD. Mouse silhouettes are coloured to indicate the dominant SARS-CoV-2 variant (>66%) in the last positive swab sample from the corresponding mouse. KI nos. 1 to 24 denote individual hACE2-KI mice.

contemporary strains. VOCs such as Alpha and Beta are particularly concerning for their hypothesized ability to supersede progenitor strains and establish immune escape properties, respectively. Here we provide experimental evidence that SARS-CoV-2 Alpha has a clear replication advantage over wt-S614G in ferrets and in two humanized mouse models. Moreover, Alpha was exclusively transmitted to contact animals in competition experiments, in which ferrets and hACE2-K18Tg mice were inoculated with mixtures of Alpha and wt-S^614G. Because SARS-CoV-2 replicates to lower levels in ferrets and hACE2-KI mice, the inability to detect wt-S^614G in some samples from inoculated animals also reflects the limit of detection of the assays using PCR with reverse transcription (RT–PCR) (approximately 10^3 gc ml^{-1}).

We have shown that the molecular mechanism underlying the fitness advantage of Alpha in vivo is largely dependent on a few changes in S, including three amino acid deletions (H69, V70 and Y144) and six substitutions (N501Y, A570D, P681H, T716I, S982A and D1118H). In hACE2-KI mice, higher genome copies and/or titres of Alpha and wt-S^Alpha compared with wt-S^614G were found in the URT (oropharynx and nose) and olfactory bulb. Increased replication and transmission of wt-S^Alpha over

wt-S^614G were also evident in hACE2-K18Tg mice. Transmission events are rare in mice; however, we observed transmission of Alpha and wt-S^Alpha in 50% of the contact hACE2-K18Tg mice and no detection of wt-S^614G in any contact mouse. In vitro, Alpha S mutations increased its affinity for hamster and human ACE2 by twofold and fourfold, respectively, indicating an overall improvement in binding abilities rather than a specialization towards human ACE2.

Beta showed a higher binding affinity for human ACE2 than its progenitor wt-S^614G and an equal level of replication to Alpha and wt-S^614G in single infections of AEC cultures and in hACE2-KI mice. However, Beta replication was outcompeted in direct competition with wt-S^614G in vitro and in hACE2-KI mice. In hamsters, wt-S^614G and Alpha also outcompeted Beta in relation to replication and transmission to contact animals, in which Beta was outnumbered by one or two orders of magnitude. This reduced fitness was also evident in previous experiments in K18-hACE2 mice[21]. The relative reduced intrinsic fitness of Beta in immunologically naive hosts supports the hypothesis that the epidemiological advantage of Beta may be principally owing to immune escape, as indicated by reduced efficiency in serum neutralization tests[16]. In convalescent

or vaccinated populations, the immune escape advantage of Beta may prove to be sufficient to compensate its reduced intrinsic fitness and explains, for example, the low prevalence of this variant in regions with a mainly naive population.

Alpha and wt-S[614G] exhibited similar replication and transmission in hamsters, a model with very high susceptibility and replication efficacy, in which the impact of a marginally fitter SARS-CoV-2 variant may not become apparent. Indeed, efficient simultaneous transmission of both variants to contact hamsters was observed in association with high viral loads in infected animals. In models supporting high replication, such as human AEC cultures and hamsters, only major improvements in replication and transmission can be detected when the variants compared already have a high fitness. By contrast, in ferrets and mouse models—in which SARS-CoV-2 replication is overall less efficient—VOCs with modestly enhanced replication and transmission can be identified. The similar replication and transmission efficacies in hamsters are in line with recent publications using VOCs in the hamster model[22].

The basal rate of replication is an important factor in the assertion of a variant over a contemporary variant in a naive population. Some individuals with higher bioaerosol exhalation levels can initiate disproportionate numbers of transmission events, possibly because of higher viral load in the URT, and are therefore called 'superspreaders'[23]. The hamster model might thus resemble the human superspreader scenario, since there is no clear indication of a specific predominance in transmission between two SARS-CoV-2 variants with high fitness levels, such as wt-S[614G] and Alpha. However, we did not perform strict aerosol transmission studies, so this remains only a proposition. The ferret and hACE2-KI models are more restricted in that infection is predominantly in the URT. Therefore, these models more closely mimic the situation in humans, in which infections are predominantly mild. Although the rate of transmission was not high overall (3 out of 8 pairs in ferrets, and 4 out of 8 pairs in hACE2-K18Tg mice), the almost exclusive transmission of Alpha relative to wt-S[614G] mirrored increased transmission of Alpha in the human population; Alpha has been responsible for more than 90% of infections in most countries in Europe[24].

Overall, our study demonstrates that multiple complementary models are necessary to comprehensively evaluate different aspects of human SARS-CoV-2 infection and the impact of emerging VOCs on the course of the ongoing pandemic. The hamster and ferret provide complementary models for transmission efficiency. The mouse models used here may become critical for VOCs demonstrating higher specificity for binding to human ACE2 relative to those from other species. Together, our results show the clear fitness advantage of Alpha and a concomitant disadvantage of Beta, in line with the observed epidemiological predominance of Alpha in the context of a relatively naive population. Notably and reassuringly, despite the apparent fitness differences of these VOCs, there is no indication of different pathologies.

Online content

Any methods, additional references, Nature Research reporting summaries, source data, extended data, supplementary information, acknowledgements, peer review information; details of author contributions and competing interests; and statements of data and code availability are available at https://doi.org/10.1038/s41586-021-04342-0.

1. Harvey, W. T. et al. SARS-CoV-2 variants, spike mutations and immune escape. *Nat. Rev. Microbiol.* **19**, 409–424 (2021).
2. Tao, K. et al. The biological and clinical significance of emerging SARS-CoV-2 variants. *Nat. Rev. Genet.* **22**, 757–773 (2021).
3. Zhou, B. et al. SARS-CoV-2 spike D614G change enhances replication and transmission. *Nature* **592**, 122–127 (2021).
4. Korber, B. et al. Tracking changes in SARS-CoV-2 spike: evidence that D614G increases infectivity of the COVID-19 virus. *Cell* **182**, 812–827.e819 (2020).
5. Plante, J. A. et al. Spike mutation D614G alters SARS-CoV-2 fitness. *Nature* **592**, 116–121 (2021).
6. Hou, Y. J. et al. SARS-CoV-2 D614G variant exhibits efficient replication ex vivo and transmission in vivo. *Science* **370**, 1464–1468 (2020).
7. Volz, E. et al. Assessing transmissibility of SARS-CoV-2 lineage B.1.1.7 in England. *Nature* **593**, 266–269 (2021).
8. Tegally, H. et al. Detection of a SARS-CoV-2 variant of concern in South Africa. *Nature* **592**, 438–443 (2021).
9. Davies, N. G. et al. Estimated transmissibility and impact of SARS-CoV-2 lineage B.1.1.7 in England. *Science* **372**, eabg3055 (2021).
10. Washington, N. L. et al. Emergence and rapid transmission of SARS-CoV-2 B.1.1.7 in the United States. *Cell* **184**, 2587–2594.e2587 (2021).
11. Weber, S., Ramirez, C. M., Weiser, B., Burger, H. & Doerfler, W. SARS-CoV-2 worldwide replication drives rapid rise and selection of mutations across the viral genome: a time-course study—potential challenge for vaccines and therapies. *EMBO Mol. Med.* **13**, e14062 (2021).
12. Galloway, S. E. et al. Emergence of SARS-CoV-2 B.1.1.7 lineage—United States, December 29, 2020–January 12, 2021. *Morb. Mortal. Wkly Rep.* **70**, 95–99 (2021).
13. Liu, Y. et al. The N501Y spike substitution enhances SARS-CoV-2 infection and transmission. *Nature* https://doi.org/10.1038/s41586-021-04245-0 (2021).
14. Kemp, S. et al. Recurrent emergence and transmission of SARS-CoV-2 spike deletion H69/V70 and its role in the Alpha variant B.1.1.7. *Cell Rep.* **35**, 109292 (2021).
15. Cele, S. et al. Escape of SARS-CoV-2 501Y.V2 from neutralization by convalescent plasma. *Nature* **593**, 142–146 (2021).
16. Hoffmann, M. et al. SARS-CoV-2 variants B.1.351 and P.1 escape from neutralizing antibodies. *Cell* **184**, 2384–2393.e2312 (2021).
17. Wibmer, C. K. et al. SARS-CoV-2 501Y.V2 escapes neutralization by South African COVID-19 donor plasma. *Nat. Med.* **27**, 622–625 (2021).
18. McCray, P. B., Jr et al. Lethal infection of K18-hACE2 mice infected with severe acute respiratory syndrome coronavirus. *J. Virol.* **81**, 813–821 (2007).
19. Yinda, C. K. et al. K18-hACE2 mice develop respiratory disease resembling severe COVID-19. *PLoS Pathog.* **17**, e1009195 (2021).
20. Zheng, J. et al. COVID-19 treatments and pathogenesis including anosmia in K18-hACE2 mice. *Nature* **589**, 603–607 (2021).
21. Hoffmann, D. et al. CVnCoV and CV2CoV protect human ACE2 transgenic mice from ancestral B BavPat1 and emerging B.1.351 SARS-CoV-2. *Nat. Commun.* **12**, 4048 (2021).
22. Abdelnabi, R. et al. Comparing infectivity and virulence of emerging SARS-CoV-2 variants in Syrian hamsters. *EBioMedicine* **68**, 103403 (2021).
23. Edwards, D. A. et al. Exhaled aerosol increases with COVID-19 infection, age, and obesity. *Proc. Natl Acad. Sci. USA* **118**, e2021830118 (2021).
24. Variants of concern. *European Centre for Disease Prevention and Control* https://www.ecdc.europa.eu/en/covid-19/variants-concern (accessed 3 June 2021).

121

Article

Methods

Cell lines

Vero E6 cells (ATCC CRL-1586) (provided by D. Muth, M. Müller and C. Drosten) or Vero-TMPRSS2[25] (provided by S. Pöhlmann) were propagated in Dulbecco's Modified Eagle Medium-GlutaMAX supplemented with 1 mM sodium pyruvate, 10% (v/v) heat-inactivated fetal bovine serum (FBS), 100 µg ml^{-1} streptomycin, 100 IU ml^{-1} penicillin, 1% (w/v) nonessential amino acids and 15 mM HEPES (Gibco). Cells were maintained at 37 °C in a humidified incubator with 5% CO_2.

Viruses

Viruses are listed in Extended Data Table 1 together with the corresponding in vitro and in vivo experiments in which they were used. Specific amino acid changes are shown schematically in Extended Data Fig. 10. Contemporary clinical isolates from the B.1.160 (S^{D614G}) (EPI_ISL_414019), Alpha (EPI_ISL_2131446, EPI_ISL_751799 (L4549)) and Beta (EPI_ISL_803957 (L4550)) were isolated and minimally passaged on Vero E6 cells. Beta (EPI_ISL_981782) was initially isolated on A549 cells expressing human ACE2 before passaging on Vero E6 cells. SARS-CoV-2 Alpha (L4549) and Beta (L4550)[21] were received from the Robert-Koch-Institut Berlin, Germany. Isogenic variants with the Alpha spike (wt-S^{Alpha}) or individual Alpha spike mutations were introduced into a wild-type SARS-COV-2 'Wuhan' backbone strain comprising the D614G amino acid change (wt-S^{614G}), as described[3,26]. Isogenic viruses were grown on Vero-TMPRSS2 cells after one passage on human bronchial airway epithelial cells. All viruses were verified by performing whole-genome next generation sequencing (NGS). For SARS-CoV-2 Alpha (L4549, SARS-CoV-2 B.1.1.7 NW-RKI-I-0026/2020 passage 3), one silent mutation in the ORF1a (sequence position 11741) was determined (C to T with 27% T, 57% strand bias). For SARS-CoV-2 Beta (L4550, available under ENA study accession number MZ433432), one nucleotide exchange was detected (A12022C) resulting in the amino acid exchange D3923A in ORF1a and one SNP at sequence position 11730 (C to T with 41%, stand bias 52%).

For all in vivo virus competition experiments, we generated inoculum mixtures aiming for a 1:1 ratio of each variant based on virus stock titres. The reported mixture inoculum titres are based on back-titration of the inoculum mixtures and the indicated ratio of each variant was determined by standard RT–qPCR. SARS-CoV-2 wt-S^{614G} (PRJEB45736; wt-S614G ID#49 vial 2) and SARS-CoV-2 Beta (L4550) were used to inoculate hamsters in the wt-S^{614G} versus Beta study; SARS-CoV-2 Alpha (L4549), and SARS-CoV-2 Beta (L4550) were used for inoculation in the Alpha versus Beta hamster study. SARS-CoV-2 wt-S^{614G}, wt-S^{Alpha}, Alpha (L4549) and Beta (L4550) were used to inoculate hACE2 humanized mice in all single virus or mixed virus competition experiments.

Next-generation sequencing

NGS was used to verify the sequence of isolates and isogenic clones prior to experimentation. RNA was extracted using the RNAdvance Tissue kit (Beckman Coulter) and the KingFisher Flex System (Thermo Fisher Scientific). Subsequently, RNA was transcribed into cDNA and sequencing libraries were generated as described[27] and were sequenced using the Ion Torrent S5XL Instrument (ThermoFisher). Samples with C_t values >20 for SARS-CoV-2 were additionally treated with RNA baits (myBaits, Arbor Biosciences) for SARS-CoV-2 enrichment before sequencing[28]. Sequence datasets were analysed by reference mapping with the Genome Sequencer Software Suite (version 2.6, Roche), default software settings for quality filtering and mapping using EPI_ISL_414019 (Alpha), EPI_ISL_2131446 (Alpha) and EPI_ISL_981782 (Beta) as references. To identify potential single nucleotide polymorphisms in the read data, the variant analysis tool integrated in Geneious Prime (2019.2.3) was applied (default settings).

AEC cultures

Human nasal AEC cultures were purchased from Epithelix (EP02MP Nasal MucilAir, pool of 14 donors). Maintenance of primary nasal AEC cultures were performed according to manufacturer's guidelines. Individual SARS-CoV-2 infections with contemporary virus isolates were conducted at either 33 °C or 37 °C as described elsewhere[29] using a multiplicity of infection (MOI) of 0.02, whereas all competition experiments and replication kinetics were performed with an MOI of 0.005 as described[30]. Quantification of viral load of individual SARS-CoV-2 infections with contemporary virus isolates was performed using the NucliSens easyMAG (BioMérieux) and RT–qPCR targeting the E gene of SARS-CoV-2 as described[31,32]. In competition experiments, nucleic acids were extracted using the Quick-RNA Viral 96 kit (Zymo research) and RT–qPCR primers and probe sequences are shown in Extended Data Table 2. The viral replication of individual isogenic variants was monitored by plaque assay.

Plaque titration assay

Viruses released into the apical compartments were titrated by plaque assay on Vero E6 cells as described[30,33]. In brief, 2×10^5 cells per ml were seeded in 24-well plates 1 day prior to titration and inoculated with tenfold serial dilutions of virus solutions. Inocula were removed 1 h post-infection and replaced with overlay medium consisting of DMEM supplemented with 1.2% Avicel (RC-581, FMC biopolymer), 15 mM HEPES, 5 or 10% heat-inactivated FBS, 100 µg ml^{-1} streptomycin and 100 IU ml^{-1} penicillin. Cells were incubated at 37 °C, 5% CO_2 for 48 h, fixed with 4% (v/v) neutral buffered formalin, and stained with crystal violet.

Protein expression, purification and bio-layer interferometry assay

SARS-CoV-2 S protein expression plasmids were constructed to encode the ectodomain of S protein S(D614G) or S^{Alpha} (residues 1–1208, with a mutated furin cleavage site and K986P/V987P substitutions) followed by a T4 fold on the trimerization domain and a polyhistidine purification tag. ACE2 protein (human, hamster or ferret) expression plasmids were constructed to encode the ectodomain of ACE2 followed by a human IgG1 Fc purification tag. The recombinant proteins were expressed using the Expi293 Expression system (ThermoFisher Scientific) and purified with HisTrap FF columns (for polyhistidine-tagged spike proteins) or with HiTrap Protein A column (for Fc-tagged ACE2 proteins) in FPLC (Cytiva) system. Recombinant proteins were further purified with Superose 6 Increase 10/300 GL column (Cytiva) as needed.

Binding affinity between the trimeric spike and dimeric ACE2 was evaluated using an Octet RED96e instrument at 30 °C with a shaking speed of 1,000 rpm (ForteBio). Anti-human IgG Fc biosensors (ForteBio) were used. Following 20 min of pre-hydration of anti-human IgG Fc biosensors and 1 min of sensor check, 7.5 nM of human ACE2–Fc, 7.5 nM of hamster ACE2–Fc in 10× kinetic buffer (ForteBio) were loaded onto the surface of anti-human IgG Fc biosensors for 5 min. After 1.5 min of baseline equilibration, 5 min of association was conducted at 10–100 nM S(D614G), S^{Alpha} or S^{Beta}, followed by 5 min of dissociation in the same buffer, which was used for baseline equilibration. The data were collected using ForteBio Data Acquisition Software 12.0.1 and corrected by subtracting signal from the reference sample and a 1:1 binding model with global fit was used for determination of affinity constants.

Animal experiment ethics declarations

All ferret and hamster experiments were evaluated by the responsible ethics committee of the State Office of Agriculture, Food Safety, and Fishery in Mecklenburg–Western Pomerania (LALLF M-V) and gained governmental approval under registration number LVL MV TSD/7221.3-1-004/21. Mouse studies were approved by the Commission for Animal Experimentation of the Cantonal Veterinary Office of Bern and

conducted in compliance with the Swiss Animal Welfare legislation and under license BE-43/20.

Hamster studies

Six Syrian hamsters (*Mesocricetus auratus*) (Janvier Labs) were inoculated intranasally under a brief inhalation anaesthesia with a 70 μl mixture of two SARS-CoV-2 VOCs (wt-S^{614G} and Alpha mixture, wt-S^{614G} and Beta mixture, or Alpha and Beta mixture). Each inoculum was back-titrated and ratios of each variant were determined by RT–qPCR. The wt-S^{614G} and Alpha mixture held a 1:1.6 ratio with $TCID_{50}$ of $10^{4.3}$ per hamster, the wt-S^{614G} versus Beta mixture held a 1:3.8 ratio with $TCID_{50}$ of $10^{4.25}$ per hamster, and the Alpha versus Beta mixture held a 1.8:1 ratio with $TCID_{50}$ of $10^{5.06}$ per hamster.

Inoculated donor hamsters were isolated in individually ventilated cages for 24 h. Thereafter, contact hamster 1 was co-housed with each donor, creating six donor–contact 1 pairs (Extended Data Fig. 2a). The housing of each hamster pair was strictly separated in individual cage systems to prevent spillover between different pairs. At 4 dpi, the individual donor hamsters (inoculated animal) were euthanized. To simulate a second transmission cycle, the original contact hamsters (referred to as contact 1) were commingled with a further six naive hamsters (referred to as contact 2), which equates to another six contact 1 and contact 2 pairs (Extended Data Fig. 2a). These pairs were co-housed until the end of the study at 21 dpi. Because the first contact hamster (cage 6) in the competition trial wt-S^{614G} versus Alpha, died at 2 dpc, the second contact hamster for this cage was also co-housed with the donor hamster; thus the first and second contact hamsters in this cage were labelled contact 1a and contact 1b, respectively. To enable sufficient contact between the donor hamster and contact 1b hamster, which was commingled routinely on 4 dpi, the donor hamster was euthanized at 7 dpi (instead of at 4 dpi), when it reached the humane end-point criterion for bodyweight (below 80% of 0 dpi body weight).

Viral shedding was monitored by nasal washes in addition to a daily physical examination and body weighing routine. Nasal wash samples were obtained under a short-term isoflurane anaesthesia from individual hamsters by administering 200 μl PBS to each nostril and collecting the reflux. Animals were sampled daily from 1 dpi to 9 dpi, and then every other day until 21 dpi. Under euthanasia, serum samples and an organ panel comprising representative URT and LRT tissues were collected from each hamster. All animals were observed daily for signs of clinical disease and weight loss. Hamsters reaching the humane endpoint, that is, falling below 80% of the initial body weight relative to 0 dpi, were humanely euthanized.

Ferret studies

Similar to the hamster study, 12 ferrets (six donor ferrets and six transmission 1 ferrets) from the FLI in-house breeding were housed pairwise in strictly separated cages to prevent spillover contamination. Of these, six ferrets were inoculated with an equal 250 μl mixture of SARS-CoV-2 wt-S^{614G} and Alpha. The inoculum was back-titrated and the ratio of each variant was determined by RT–qPCR. The wt-S^{614G} versus Alpha mixture held a 1:1.2 ratio with $10^{5.875}$ $TCID_{50}$ distributed equally into each nostril of donor ferrets. Ferrets were separated for the first 24 h following inoculation. Subsequently, the ferret pairs were co-housed again, allowing direct contact of donor to contact 1 ferrets. All ferrets were sampled via nasal washes with 750 μl PBS per nostril under a short-term inhalation anaesthesia. Donor ferrets were sampled until euthanasia at 6 dpi, which was followed by the introduction of one additional naive contact 2 ferret per cage (*n* = 6), resulting in a 1:1 pairwise setup with contact 1 and contact 2 ferrets (Extended Data Fig. 2b). All ferrets, which were in the study group on the respective days, were sampled on the indicated days. Bodyweight, temperature and physical condition of all ferrets were monitored daily throughout the experiment. URT and LRT organ samples, as well as blood samples of all ferrets were taken at respective euthanasia time points.

Full autopsy was performed on all animals under BSL3 conditions. The lung, trachea and nasal conchae were collected and fixed in 10% neutral-buffered formalin for 21 days. The nasal atrium, decalcified nasal turbinates (cross-sections every 3–5 mm), trachea and all lung lobes were trimmed for paraffin embedding. Based on PCR results, tissue sections (3 μm) of all donors (day 6) and one recipient (no. 8, day 20) were cut and stained with haematoxylin and eosin for light microscopical examination. Immunohistochemistry was performed using an anti-SARS nucleocapsid antibody (Novus Biologicals NB100-56576, dilution 1:200) according to standardized avidin–biotin–peroxidase complex-method producing a red labelling and haematoxylin counterstain. For each immunohistochemistry staining, positive control slides and a negative control for the primary antibodies were included. Histopathology was performed on at least five consecutive tissue samples per animal, yielding comparable results in all cases. Lung tissue pathology was evaluated according to a detailed score sheet developed by Angele Breithaupt (DipECVP) (Supplementary Table 2). Evaluation and interpretation was performed by board-certified veterinary pathologists (DiplECVP) (AB, IBV).

Mouse studies

hACE2-KI mice (B6.Cg-*Ace2^{tm1(ACE2)Dwnt}*) and hACE2-K18Tg mice (Tg(K18-hACE2)2Prlmn) were described previously[3,18]. All mice were produced at the specific-pathogen-free facility of the Institute of Virology and Immunology (Mittelhäusern), where they were maintained in individually ventilated cages (blue line, Tecniplast), with 12-h:12-h light:dark cycle, 22 ± 1 °C ambient temperature and 50 ± 5% humidity, autoclaved food and acidified water. At least 7 days before infection, mice were placed in individually HEPA-filtered cages (IsoCage N, Tecniplast). Mice (10 to 12 weeks old) were anaesthetized with isoflurane and infected intranasally with 20 μl per nostril with the virus inoculum described in the results section. One day after inoculation, infected hACE2-K18Tg mice were placed in the cage of another hACE2-K18Tg contact mouse. Mice were monitored daily for bodyweight loss and clinical signs. Oropharyngeal swabs were collected under brief isoflurane anaesthesia using ultrafine sterile flock swabs (Hydraflock, Puritan, 25-3318-H). The tips of the swabs were placed in 0.5 ml of RA1 lysis buffer (Macherey-Nagel, 740961) supplemented with 1% β-mercaptoethanol and vortexed. At 2 or 4 dpi, mice were euthanized, and organs were aseptically dissected. Systematic tissue sampling was performed as detailed previously[3].

Animal specimens work up, viral RNA detection and quantification

Organ samples from ferrets and hamsters were homogenized in a 1 ml mixture composed of equal volumes of Hank's balanced salts MEM and Earle's balanced salts MEM containing 2 mM L-glutamine, 850 mg l^{-1} NaHCO3, 120 mg l^{-1} sodium pyruvate and 1% penicillin–streptomycin) at 300 Hz for 2 min using a Tissuelyser II (Qiagen) and centrifuged to clarify the supernatant. Organ samples from mice were either homogenized in 0.5 ml of RA1 lysis buffer supplemented with 1% β-mercaptoethanol using a Bullet Blender Tissue Homogenizer (Next-Advance) or in Tube M (Miltenyi Biotech, 130-096-335) containing 1 ml of DMEM using a gentleMACS Tissue Dissociator (Miltenyi Biotech). Nucleic acid was extracted from 100 μl of the nasal washes or 200 μl mouse oropharyngeal swabs after a short centrifugation step or 100 μl of organ sample supernatant using the NucleoMag Vet kit (Macherey Nagel). Nasal washes, oropharyngeal swabs, and organ samples were tested by RT–qPCR analysis for the ratio of the two different viruses used for inoculation, by applying two different assays, each of them specific for one variant: either the wt-S^{614G}, Alpha or Beta variant (Extended Data Tables 2, 3). Viral RNA copies in swabs and organs in studies using a single variant inoculum in mice were determined using the E protein RT–qPCR exactly as described[3].

Four specific RT–qPCR assays for SARS-CoV-2 wt-S^{614G}, Alpha and Beta were designed based on the specific genome deletions within ORF1

Article

and the *S* gene (Extended Data Table 2). Here, virus-specific primers were used to achieve a high analytical sensitivity (less than 10 genome copies per µl template) of the PCR assays, and in samples with a high genome load of the non-matching virus.

The RT–qPCR reaction was prepared using the qScript XLT One-Step RT–qPCR ToughMix (QuantaBio) (hamsters and ferrets) or the AgPath-ID One-Step RT–PCR (ThermoFisher Scientific) (hACE2-K18Tg and hACE2-KI mice) in a volume of 12.5 µl including 1 µl of the respective FAM mix and 2.5 µl of extracted RNA. The reaction was performed for 10 min at 50 °C for reverse transcription, 1 min at 95 °C for activation, and 42 cycles of 10 s at 95 °C for denaturation, 10 s at 60 °C for annealing and 20 s at 68 °C for elongation. Fluorescence was measured during the annealing phase. RT–qPCRs were performed on a BioRad real-time CFX96 detection system (Bio-Rad) (hamsters and ferrets) or an Applied Biosystems 7500 Real-Time PCR System (ThermoFisher Scientific) (mice). Validation work was performed by comparison with established protocols (https://www.who.int/docs/default-source/coronaviruse/eal-time-rt-pcr-assays-for-the-detection-of-sars-cov-2-institut-pasteur-paris.pdf?sfvrsn=3662fcb6_2 and ref. [31]).

Serological tests of hamsters and ferrets

Serum samples from the wt-S^{614G} versus Alpha, wt-S^{614G} versus Beta, and Alpha versus Beta co-inoculated hamsters and ferrets were tested by ELISA for sero-reactivity against the RBD domain[34] using a Tecan i-control 2014 1.11 plate reader and data was analysed using Microsoft Excel 16.0. All samples were generated at the time point of euthanasia of the individual animal.

Statistical analysis

Statistical analysis was performed using GraphPad Prism 8 or R[35] (version 4.1), using the packages tidyverse[36] (v1.3.1), ggpubr (v0.4.0) and rstatix (v.0.7.0). Unless noted otherwise, the results are expressed as mean ± s.d. Two-way analysis of variance (ANOVA) with Tukey honest significance differences post hoc test was used to compare competition results at different time points after infection in vitro. One-way ANOVA with Tukey's multiple comparisons test was used to compare viral genome copies or titres at different time points post infection in individual virus mouse infection studies. Significance was defined as $P < 0.05$.

Reporting summary

Further information on research design is available in the Nature Research Reporting Summary linked to this paper.

Data availability

Sequence data are available on the NCBI Sequence Read Archive (SRA) under the accession numbers PRJEB45736 and PRJNA784099, or in GenBank under the accession numbers MT108784, MZ433432, OL675863, OL689430 and OL689583 as shown in Extended Data Table 1. Source data are provided with this paper.

25. Hoffmann, M. et al. SARS-CoV-2 cell entry depends on ACE2 and TMPRSS2 and is blocked by a clinically proven protease inhibitor. *Cell* **181**, 271–280.e278 (2020).
26. Thi Nhu Thao, T. et al. Rapid reconstruction of SARS-CoV-2 using a synthetic genomics platform. *Nature* **582**, 561–565 (2020).
27. Wylezich, C., Papa, A., Beer, M. & Hoper, D. A versatile sample processing workflow for metagenomic pathogen detection. *Sci. Rep.* **8**, 13108 (2018).
28. Wylezich, C. et al. Next-generation diagnostics: virus capture facilitates a sensitive viral diagnosis for epizootic and zoonotic pathogens including SARS-CoV-2. *Microbiome* **9**, 51 (2021).
29. Essaidi-Laziosi, M. et al. Propagation of respiratory viruses in human airway epithelia reveals persistent virus-specific signatures. *J. Allergy Clin. Immunol.* **141**, 2074–2084 (2018).
30. V'Kovski, P. et al. Disparate temperature-dependent virus-host dynamics for SARS-CoV-2 and SARS-CoV in the human respiratory epithelium. *PLoS Biol.* **19**, e3001158 (2021).
31. Corman, V. M. et al. Detection of 2019 novel coronavirus (2019-nCoV) by real-time RT–PCR. *Euro Surveill.* **25**, 2000045 (2020).
32. Baggio, S. et al. SARS-CoV-2 viral load in the upper respiratory tract of children and adults with early acute COVID-19. *Clin. Infect. Dis.* **73**, 148–150 (2020).
33. Jonsdottir, H. R. & Dijkman, R. Characterization of human coronaviruses on well-differentiated human airway epithelial cell cultures. *Methods Mol. Biol.* **1282**, 73–87 (2015).
34. Wernike, K. et al. Multi-species ELISA for the detection of antibodies against SARS-CoV-2 in animals. *Transbound. Emerg. Dis.* **68**, 1779-1785 (2020).
35. R: A language and environment for statistical computing (R Core Team, 2021).
36. Wickham, H. et al. Welcome to the Tidyverse. *J. Open Source Softw.* **4**, 1686 (2019).

Extended Data Fig. 1 | ACE2 receptor binding and replication kinetics of SARS-CoV-2 VOC in vitro. (**a**) Affinity between spike (S^{614G}, S^{Alpha}, and S^{Beta}) protein trimers and hACE2 dimers determined by Bio-layer interferometry. (**b**) Viral replication kinetics of SARS-CoV-2 Alpha, Beta, and wt-S^{614G} (MOI 0.02) at 33 °C and 37 °C in primary human nasal airway epithelial cell (AEC) cultures. (**c**) Viral replication kinetics of pairwise competition assays in primary nasal AEC cultures at 33 °C (MOI 0.005). (**b**, **c**) Data are presented as individual points with mean (line) and standard deviation; (**b**) n = 2 (Alpha and Beta), n = 4

(wt-S^{614G}), (**c**) n = 3 independent biological replicates. (**c**) P-values were determined by two-way ANOVA and Tukey Honest Significant Differences (HSD) post-hoc test. (**d**) Affinity between spike (S^{614G}, S^{Alpha}) protein trimers with hamster ACE2 determined by Bio-layer interferometry. (**a**, **d**) ACE2 with IgG1 Fc tag were loaded on anti-human IgG Fc biosensors and binding kinetics were conducted using indicated concentrations of spike trimers. Data is representative of 3 independent experiments.

Article
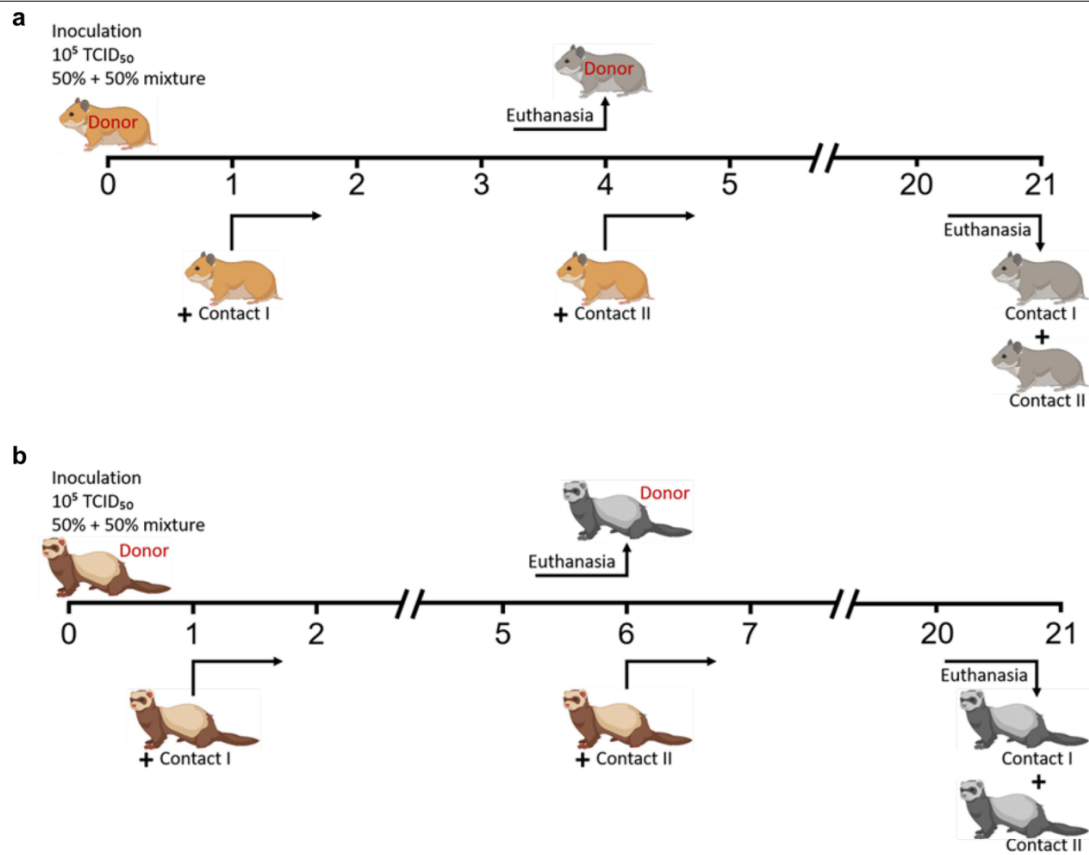
Extended Data Fig. 2 | Experimental workflow of competitive transmission experiments in Syrian hamsters and ferrets. (a) Timeline of the hamster experiments. Six intranasally inoculated donor hamsters each were co-housed with one naïve contact hamster (1 dpi), building six respective donor-contact I pairs. At 4 dpi, the donor hamsters were euthanized and the initial contact hamsters I were co-housed with one additional hamster (Contact II). **(b)** Timeline of the ferret experiment. The scheme was generated with BioRender (https://biorender.com/).

Extended Data Fig. 3 | Competitive transmission between Alpha and Beta in Syrian hamsters. Six donor hamsters were each inoculated with $10^{5.06}$ TCID$_{50}$ determined by back titration and composed of a mixture of Alpha (dark blue) and Beta (green) at 1.8:1 ratio determined by RT-qPCR. Donor hamsters, contact I and II hamsters were co-housed sequentially as shown in Extended Data Fig. 2a. Nasal washings were performed daily from 1–9 dpi and afterwards every two days until 21 dpi. Pie chart colors illustrate the ratio of variants detected in nasal washings at the indicated dpi. Pie chart sizes are proportional to the total viral genome copies reported above or below respective pies. Grey pies indicate values below the LOD (<103 viral genome copies per sample). Hamster silhouettes are colored according to the dominant variant (>66%) detected in the latest sample of each animal. † indicate that the corresponding animal reached the humane endpoint.

Article
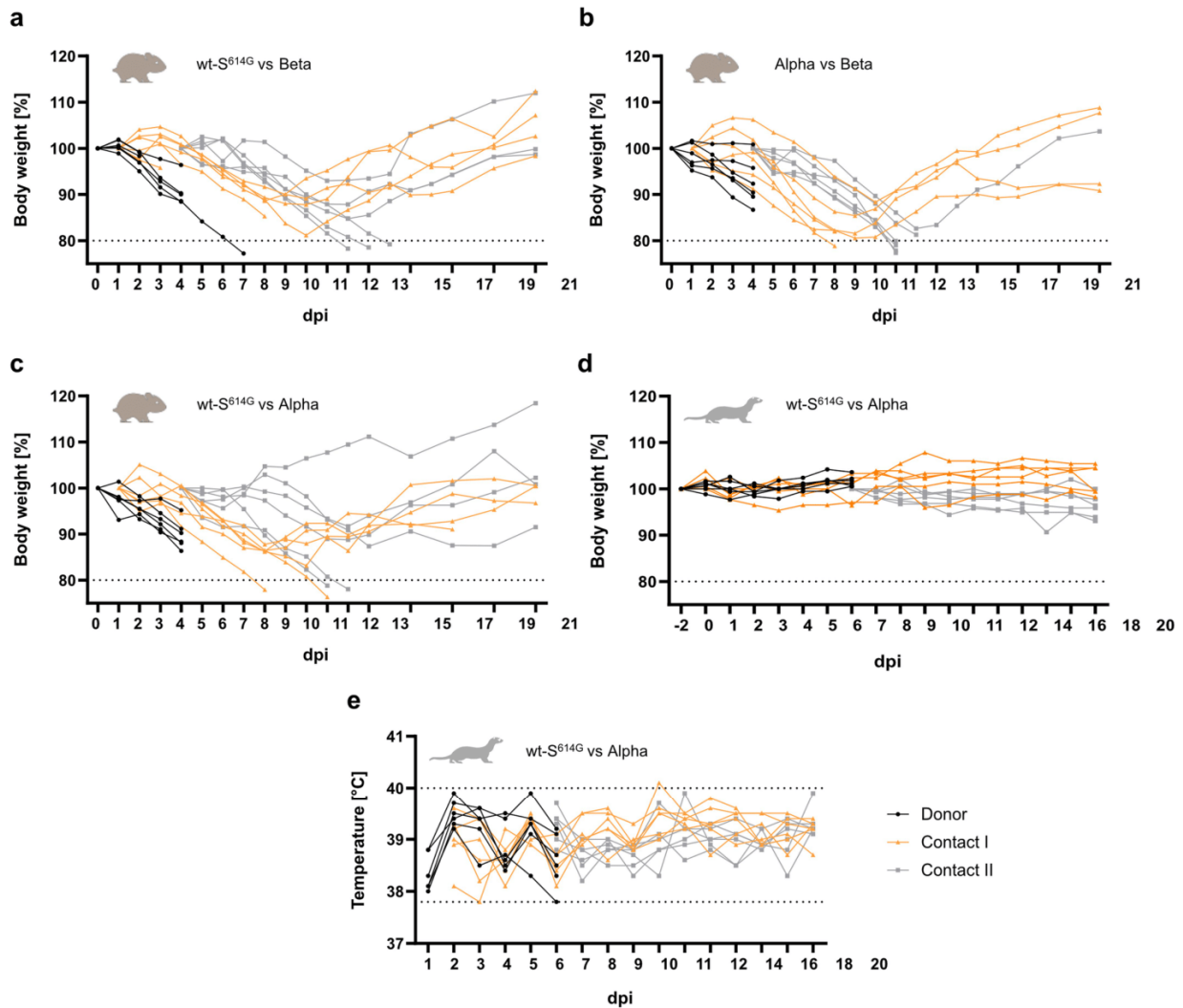
Extended Data Fig. 4 | Clinical features of hamsters and ferrets. (**a**–**c**) Syrian hamsters were inoculated with comparable genome equivalent mixture of either wt-S^{614G} and Beta (**a**), Alpha and Beta (**b**), or wt-S^{614G} and Alpha (**c**). In hamsters, body weight was monitored daily until 13 dpi, afterwards every two days until 21 dpi and plotted relative to bodyweight of day 0. The dotted line indicates the humane endpoint criterion of 20% body weight loss from initial bodyweight at which hamsters were promptly euthanized for animal welfare reasons. (**d**, **e**) Ferrets were inoculated intranasally with an equal mixture of wt-S^{614G} and Alpha. Body weight (**d**) and temperature (**e**) were monitored daily in ferrets until 12 dpi, and afterwards every 2 days. Grey dotted lines in e indicate the physiologic range for body temperature in ferrets.
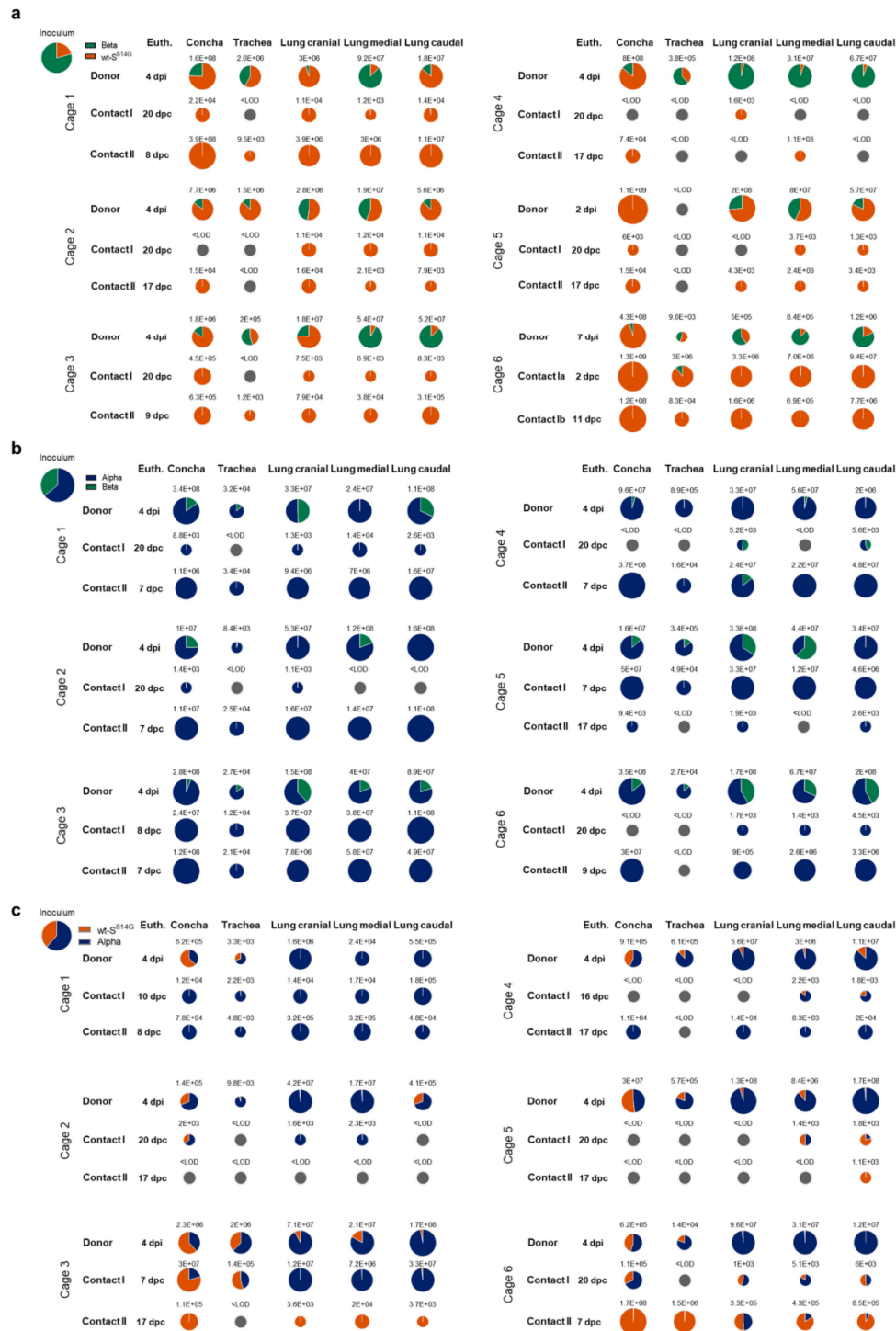
Extended Data Fig. 5 | Viral genome load in upper (URT) and lower (LRT) respiratory tract tissues of Syrian hamsters in the competitive transmission experiment between SARS-CoV-2 VOCs. (a–c) Syrian hamsters were inoculated with comparable genome equivalent mixture of either wt-S[614G] and Beta (**a**), Alpha and Beta (**b**), or wt-S[614G] and Alpha (**c**). Absolute quantification was performed by RT–qPCR analysis of tissue homogenates of donor, contact I and contact II hamsters in relation to a set of defined standards. Tissue samples were collected at euthanasia (Euth.). Pie chart colors illustrate the ratio of variants detected in each sample at the indicated dpi or days post contact (dpc). Pie chart sizes are proportional to the total viral genome copies reported below. Grey pies indicate values below the LOD (<10[3] viral genome copies per sample).

Article
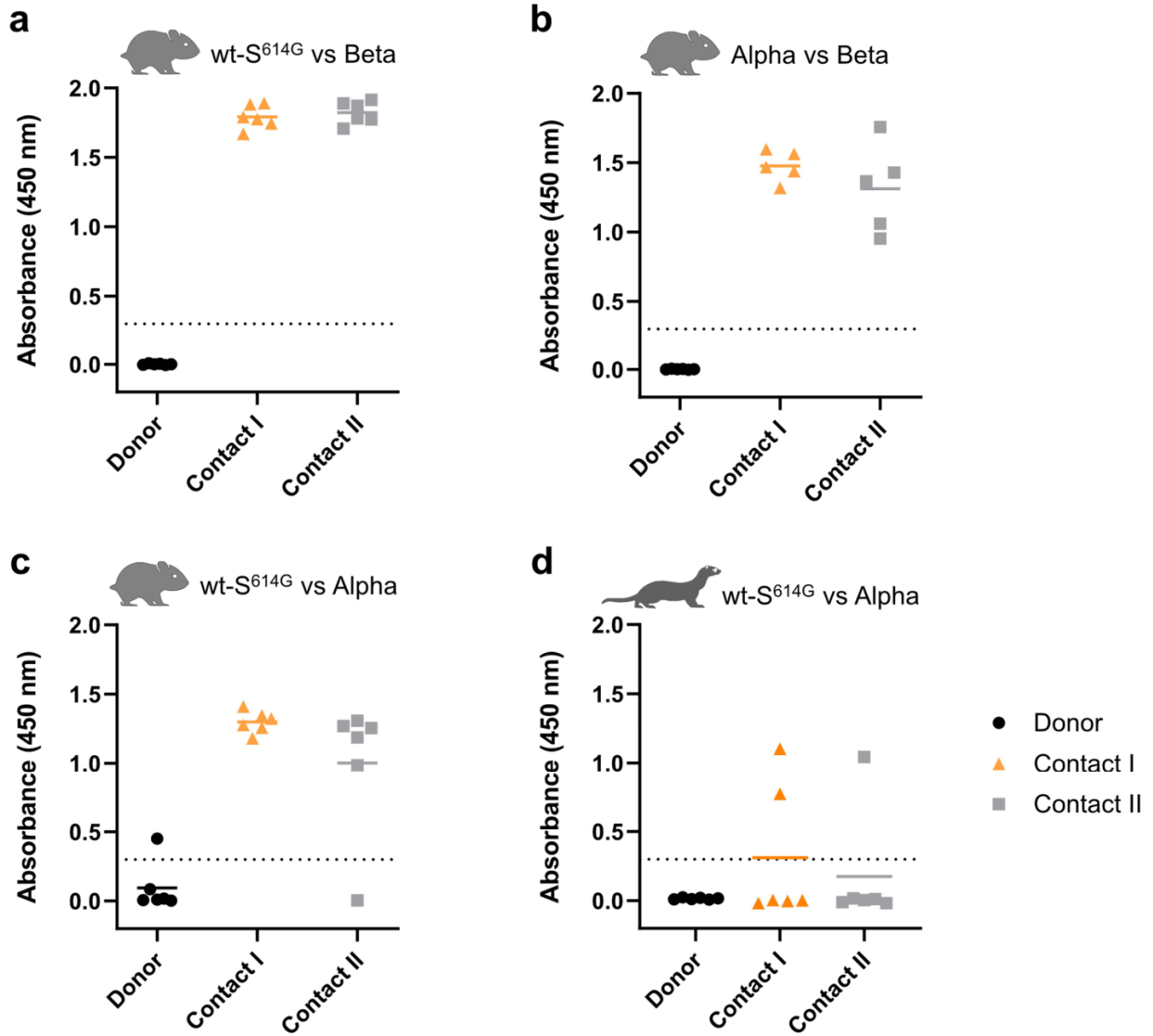
Extended Data Fig. 6 | Indirect ELISA against the RBD of SARS-CoV-2. Sera of donor hamsters (**a**, **b**, **c**) and ferrets (**d**) inoculated with the indicated SARS-CoV-2 VOC mixtures and sera of contact I and II animals were collected at their respective experimental endpoints. All sera were tested for specific reactivity against the SARS-CoV-2 RBD-SD1 domain (wt-S amino acids 319-519).
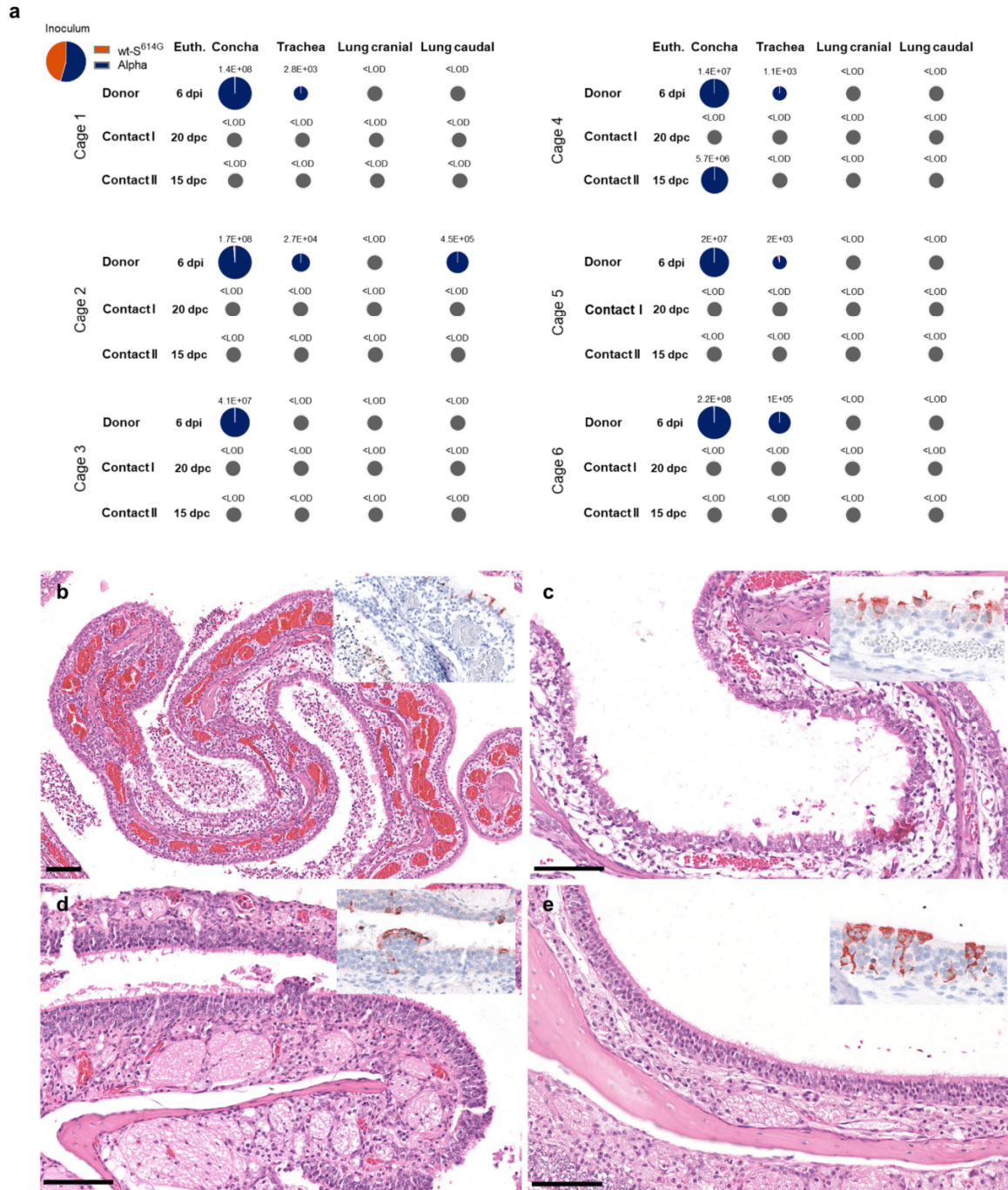
Extended Data Fig. 7 | Viral genome load in upper (URT) and lower (LRT) respiratory tract tissue of ferrets in the competitive transmission experiment between SARS-CoV-2 Alpha and wt-S^{614G}. (**a**) Absolute quantification was performed by RT–qPCR analysis of tissue homogenates of donor, contact I and contact II ferrets in relation to a set of defined standards. Tissue samples were collected at euthanasia (Euth.). Pie chart colors illustrate the ratio of variants detected in each sample at the indicated dpi or dpc. Pie chart sizes are proportional to the total viral genome copies reported below. Grey pies indicate values below the LOD (<10^3 viral genome copies per sample).

(**b–e**) Representative micrographs of hematoxylin and eosin staining of 3 μm sections of nasal conchae of donor ferrets (n = 6) 6 dpi with wt-S^{614G} and Alpha. Micrographs are representative of 5 consecutive tissue samples of each animal. Insets show immunohistochemistry staining of SARS-CoV-2 with anti-SARS nucleocapsid antibody with hematoxylin counterstain. The respiratory (**b**, **c**) and olfactory (**d**, **e**) nasal mucosa exhibited rhinitis with varying severity. Lesion-associated antigen was found in ciliated cells of the respiratory epithelium (**b**, **c**) and in sustentacular cells of the olfactory epithelium (**d**, **e**) in all donor animals (n = 6) at 6 dpi. Scale bars are 100 μm.

Article

a

b

Extended Data Fig. 8 | Body weight and transmission in hACE2-K18Tg mice. hACE2-K18Tg mice inoculated with a mixture of wt-S^{614G} and Alpha, or wt-S^{614G} and wt-S^{Alpha}. (**a**) Relative body weight of individual donor mice (n = 4 mice/group; left panel), and contact mice (n = 4 mice/group; right panel). (**b**) Pie chart colors illustrate the ratio of wt-S^{614G} (orange) with Alpha (dark blue), or with wt-S^{Alpha} (light blue) in corresponding experiments in lung homogenates of contact mice at 7 dpc (i.e., 8 dpi of donor mice). Pie chart sizes are proportional to the total viral genome copies reported below. Grey pies indicate values below the LOD (<10^3 viral genome copies per sample).

Extended Data Fig. 9 | Replication of VOC in hACE2-KI mice. (a–d) Groups hACE2-KI male mice were inoculated intranasally with 10^4 PFUs of SARS-CoV-2 wt-S^{614G}, Alpha, wt-S^{Alpha} and Beta (n = 8 mice/group). Genome copy numbers in daily oropharyngeal swabs (**a**) and in tissues (**b**), and virus titers (**c**) in tissues were determined at indicated dpi. Data were log10 transformed and presented as individual values and mean. *p<0.05, **p<0.01 by one-way ANOVA with Tukey's multiple comparisons test comparing the four groups. (**d**) Relative body weight of individual hACE2-KI mice overtime relative to weight at infection (n = 8 mice/group until 2 dpi, and n = 4 mice/group from 3 dpi).

Article
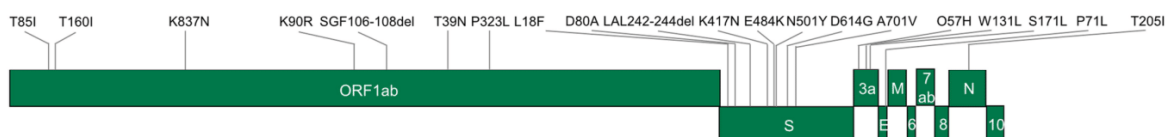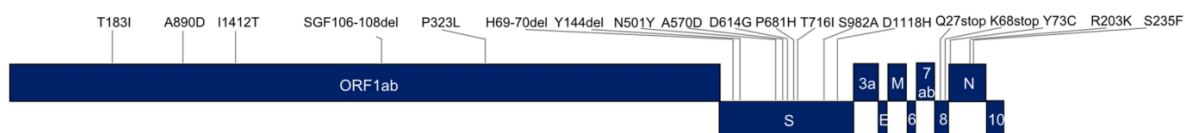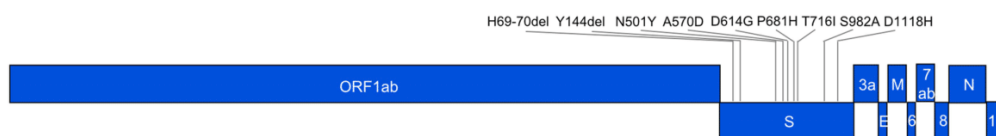
Extended Data Fig. 10 | Genome sequences of used SARS-CoV-2 variants. Colors of the variants represent respective viruses in the different experiments. Grey lines indicate positions of known mutations of each virus strain.

Extended Data Table 1 | Sequence mutations in S in SARS-CoV-2 recombinant strains

SARS-CoV-2 viruses	Mutations in S	Use	Accession ID (BioProject / GenBank / GISAID)
Isolates:			
wt-S^{614G} (B.1.610)	D614G	Kinetics in vitro	OL675863, EPI_ISL_414019
Alpha	H69/V70del, Y144del, N501Y, A570D, D614G, P681H, T716I, S982A, D1118H	Kinetics in vitro	OL689430, EPI_ISL_2131446
Beta	L18F, D80A, D215G, L242/A243/L244del, K417N, E484K, N501Y, D614G, A701V,	Kinetics in vitro	OL689583, EPI_ISL_981782
Alpha (L4549)	H69/V70del, Y144del, N501Y, A570D, D614G, P681H, T716I, S982A, D1118H	Competition wt-S^{614G} vs Alpha; in vitro, hamster, ferret, and mice Individual virus infection, mice	PRJEB45736, SARS-CoV-2 B.1.1.7 NW-RKI-I-0026/2020 passage 3 L4549, EPI_ISL_803957
Beta (L4550) (Ref. 21)	L18F, D80A, D215G, L242/L243/A244del K417N, E484K, N501Y, D614G, A701V	Competition wt-S^{614G} vs Beta; hamster, mice Competition Alpha vs Beta; hamster	MZ433432, L4550, EPI_ISL_751799
Recombinant clones:			
wt-S^{614G} (Ref. 3)	D614G	Competition wt-S^{614G} vs Beta; in vitro, hamster, mice Competition wt-S^{614G} vs Alpha; in vitro, mice Competition wt-S^{614G} vs wt-S^{Alpha}; mice Single virus infection, mice	MT108784
wt-S^{614G} (*) (L4595)	D614G, R685S	Competition wt-S^{614G} vs Alpha; hamster and ferret	PRJEB45736, wt-S614G ID#49 vial 2, L4595
wt-S^{Alpha}	H69/V70del, Y144del, N501Y, A570D, D614G, P681H, T716I, S982A, D1118H	Competition wt-S^{614G} vs wt-S^{Alpha}; mice Single virus infection, mice	PRJNA784099

(*) SARS-CoV-2 wt-S^{614G} used for the competitive experiments between wt-S^{614G} vs. Alpha in hamsters and ferrets had an exchange in 54% of the analyzed contigs from C to A in position 23615, located in the S gene.

Article

Extended Data Table 2 | Sequences of primer and probes for RT-qPCR assays

Oligo name	Sequence (5´- 3´)	Conc.	Position
SARS-CoV-2 wt-S^{614G} -ORF1 assay			
wt-S^{614G} -ORF1-1.2F	TGG TTG ATA CTA GTT TGT CTG GT	10 μM	11271-11293 *
wt-S^{614G} -ORF1-1.3R	GCA CCA TCA TCA TAC ACA GTT C	10 μM	11379-11358 *
wt-S^{614G} -ORF1-1FAM	FAM-TGC ATC AGC TGT AGT GTT ACT AAT CC-BHQ1	5 μM	11320-11345 *
SARS-CoV-2 wt-S^{614G} -S assay			
wt-S^{614G} -S-1.2F	TAC TTG GTT CCA TGC TAT ACA TGT	10 μM	21748-21771 *
wt-S^{614G} -S-1.5R	CCA ACT TTT GTT GTT TTT GTG GTA ATA	10 μM	22018-21992 *
wt-S^{614G} -S-1FAM	FAM-ACC CTG TCC TAC CAT TTA ATG ATG-BHQ1	5 μM	21804-21827 *
SARS-CoV-2 Alpha -ORF1 assay			
B117-ORF1-2.1F	GAT ATG GTT GAT ACT AGT TTG AAG	10 μM	11265-11288 **
wt-S^{614G} -ORF1-1.3R	See above		
wt-S^{614G} -ORF1-1FAM	See above		
SARS-CoV-2 Alpha -S assay			
B117-S-1.2F	TTA CTT GGT TCC ATG CTA TMT C	10 μM	21736-21757 **
B117-S-1.3R	AAC TTT TGT TGT TTT TGT GGT AAA C	10 μM	21996-21972 **
wt-S^{614G} -S-1FAM	See above		

* Position based on NC_045512; ** Position based on MW963651. Conc, concentration.

Extended Data Table 3 | Attribution of RT-qPCR assays used for the individual competitive transmission experiments

Assay	For detection of
wt-S^{614G} vs Alpha (hamsters, ferrets)	
SARS-CoV-2 wt-S^{614G} -ORF1 assay	SARS-CoV-2 wt-S^{614G}
SARS-CoV-2 Alpha -ORF1 assay	SARS-CoV-2 Alpha
wt-S^{614G} vs Alpha (human AEC cultures, mice)	
SARS-CoV-2 wt-S^{614G} -S assay	SARS-CoV-2 wt-S^{614G}
SARS-CoV-2 Alpha -S assay	SARS-CoV-2 Alpha
SARS-CoV-2 Alpha -S assay	SARS-CoV-2 wt-S^{Alpha}
wt-S^{614G} vs Beta (human AEC cultures, hamsters and mice)	
SARS-CoV-2 wt-S^{614G} -ORF1 assay	SARS-CoV-2 wt-S^{614G}
SARS-CoV-2 Alpha -ORF1 assay	SARS-CoV-2 Beta
Alpha vs Beta (human AEC cultures, hamsters)	
SARS-CoV-2 Alpha -S assay	SARS-CoV-2 Alpha
SARS-CoV-2 wt-S^{614G} -S assay	SARS-CoV-2 Beta

5. PUBLICATION V: CVnCoV AND CV2CoV PROTECT HUMAN ACE2 TRANSGENIC MICE FROM ANCESTRAL B BavPat1 AND EMERGING B.1.351 SARS-CoV-2

<u>Publication V</u>

CVnCoV and CV2CoV protect human ACE2 transgenic mice from ancestral B BavPat1 and emerging B.1.351 SARS-CoV-2

Donata Hoffmann, Björn Corleis, Susanne Rauch, Nicole Roth, Janine Mühe, Nico Joel Halwe, Lorenz Ulrich, Charlie Fricke, Jacob Schön, Anna Kraft, Angele Breithaupt, Kerstin Wernike, Anna Michelitsch, Franziska Sick, Claudia Wylezich, Bernd Hoffmann, Moritz Thran, Andreas Thess, Stefan O. Mueller, Thomas C. Mettenleiter, Benjamin Petsch, Anca Dorhoi & Martin Beer

ARTICLE

OPEN

CVnCoV and CV2CoV protect human ACE2 transgenic mice from ancestral B BavPat1 and emerging B.1.351 SARS-CoV-2

Donata Hoffmann [1,6], Björn Corleis[2,6], Susanne Rauch[3], Nicole Roth[3], Janine Mühe[3], Nico Joel Halwe [1], Lorenz Ulrich [1], Charlie Fricke [2], Jacob Schön[1], Anna Kraft [1], Angele Breithaupt [4], Kerstin Wernike [1], Anna Michelitsch [1], Franziska Sick[1], Claudia Wylezich [1], Bernd Hoffmann[1], Moritz Thran[3], Andreas Thess [3], Stefan O. Mueller[3], Thomas C. Mettenleiter[5], Benjamin Petsch[3], Anca Dorhoi [2✉] & Martin Beer [1✉]

The ongoing SARS-CoV-2 pandemic necessitates the fast development of vaccines. Recently, viral mutants termed variants of concern (VOC) which may escape host immunity have emerged. The efficacy of spike encoding mRNA vaccines (CVnCoV and CV2CoV) against the ancestral strain and the VOC B.1.351 was tested in a K18-hACE2 transgenic mouse model. Naive mice and mice immunized with a formalin-inactivated SARS-CoV-2 preparation were used as controls. mRNA-immunized mice develop elevated SARS-CoV-2 RBD-specific antibody and neutralization titers which are readily detectable, but significantly reduced against VOC B.1.351. The mRNA vaccines fully protect from disease and mortality caused by either viral strain. SARS-CoV-2 remains undetected in swabs, lung, or brain in these groups. Despite lower neutralizing antibody titers compared to the ancestral strain BavPat1, CVnCoV and CV2CoV show complete disease protection against the novel VOC B.1.351 in our studies.

[1] Institute of Diagnostic Virology, Friedrich-Loeffler-Institut, Greifswald-Insel Riems, Germany. [2] Institute of Immunology, Friedrich-Loeffler-Institut, Greifswald-Insel Riems, Germany. [3] CureVac AG, Tübingen, Germany. [4] Department of Experimental Animal Facilities and Biorisk Management, Friedrich-Loeffler-Institut, Greifswald-Insel Riems, Germany. [5] Friedrich-Loeffler-Institut, Federal Research Institute for Animal Health, Greifswald-Insel Riems, Germany. [6] These authors contributed equally: Donata Hoffmann, Björn Corleis. ✉email: anca.dorhoi@fli.de; martin.beer@fli.de

ARTICLE

oronavirus disease 2019 (COVID-19) severely affects human health and societies worldwide. It has accounted for >148 million morbidities and 3.1 million fatalities by end of April 2021 (World Health Organization (WHO), https://covid19.who.int). The responsible pathogen, severe acute respiratory syndrome coronavirus type 2 (SARS-CoV-2), has rapidly spread globally despite stringent intervention strategies[1]. To control pandemic spread and disease, vaccination is considered the most important and effective control measure[2]. Several vaccines based on mRNA technology or viral vectors are now authorized for emergency use and further products are in final licensing phases[3]. SARS-CoV-2 underwent adaptive mutations early during the pandemic, with the D614G variant becoming globally dominant at the beginning of 2020[4–6]. Viral evolution is a highly dynamic process that results in emergence of multiple, geographically distinct new variants, first identified in the UK (B1.1.7), South Africa (B.1.351), and Brazil (B.1.1.28; P1) (https://www.ecdc.europa.eu/en/publications-data/covid-19-risk-assessment-variants-vaccine-fourteenth-update-february-2021). These variants of concern (VOCs) acquired numerous mutations, particularly in the spike protein encoding gene (S), most frequently within the S1 and the receptor-binding domain (RBD)[7–9]. These mutations confer higher binding affinities and allow some VOCs to evade pre-existing immunity[10], resulting in increased transmissibility, including epidemiologic scenarios where herd immunity was expected[11]. Whereas variant B.1.1.7 might still be efficiently neutralized by vaccination-elicited antibodies despite the RBD mutations[12–14], variant B.1.351 showed a remarkable resistance to sera from vaccinated as well as from convalescent individuals[15–18]. VOCs that evade from efficient cross-neutralization may evolve into dominant strains and necessitate vaccine efficacy re-assessment. While indications for cross-neutralization exist, e.g., by sera from individuals vaccinated with SARS-CoV-2 mRNA vaccines[13,19], in vivo data from experimental immunization/challenge studies in standardized animal models are pending. In this work, we investigated the efficacy of mRNA vaccines CVnCoV and CV2CoV against SARS-CoV-2 using an early B lineage 614G strain and the novel VOC B1.351 in a human ACE2 (hACE2) transgenic mouse model of severe COVID-19[20]. The choice for the variant B.1.351 was related to the observed immune-escape features with a reduced neutralization efficacy[10] and decreased protective efficacy reported for a licensed vaccine[21].

Results

We used the K18-hACE2 transgenic mouse model[22] to determine the protective efficacy of two spike protein encoding mRNA vaccines, i.e., CVnCoV and CV2CoV, a clinical and preclinical stage vaccine, respectively. Both vaccines encode for the same protein, but differ in the non-coding regions of the mRNA. We chose a dose of 8 μg for CVnCoV, which conferred protection in hamsters[23] and non-human primates (NHPs)[24] in previous preclinical studies, and performed a dose titration ranging from 0.5 to 8 μg for the preclinical stage vaccine CV2CoV. Vaccine efficacy was tested against the ancestral SARS-CoV-2 B-lineage strain BavPat1 that closely matches the mRNA-encoded S protein and the heterologous VOC B.1.351 NW-RKI-I-0028. For immunization, CVnCoV vaccine, CV2CoV vaccine, or 20 μl of a formalin-inactivated and adjuvanted SARS-CoV-2-preparation (FI-Virus) were administered on days 0 and 28. Mice were challenged 4 weeks after boost vaccination with >10^5 tissue culture infectious dose 50 ($TCID_{50}$) of SARS-CoV-2 BavPat1 or B.1.351 NW-RKI-I-0028. A sham (NaCl) group served as non-vaccinated control (Fig. S1 and Table S1). Sera from all mRNA-vaccinated mice collected on days 28 and 55 showed a strong induction of anti-RBD total

immunoglobulin (Ig), irrespective of the mRNA amount. Anti-RBD total Ig levels were significantly higher in sera from all mRNA-vaccinated groups compared to levels induced by the FI-Virus preparation (Fig. 1a). The strong induction of anti-RBD antibodies in the mRNA vaccine groups was reflected by high virus neutralization titers (VNTs). Of note, even a low dose of 0.5 μg of CV2CoV elicited high levels of humoral responses in K18-hACE2 transgenic mice. Sera from day 55 after immunization with CVnCoV or CV2CoV showed a significantly higher neutralizing capacity compared to sera from animals that had received the FI-Virus preparation. Importantly, neutralization of VOC B.1.351 was less effective compared to BavPat1 for the CVnCoV and CV2CoV groups, but far exceeded the values recorded for the FI-Virus group (Fig. 1b). Similar results were obtained with a surrogate VNT assay with post prime immunization sera collected at day 28 (Table S2). Overall, the tested mRNA vaccines induced robust antibody responses in a prime–boost regime, capable of efficiently neutralizing both BavPat1 and VOC B.1.351 NW-RKI-I-0028 in vitro.

Subsequently, the potential of CVnCoV and CV2CoV to protect from SARS-CoV-2 challenge infection was analyzed. Stocks of both challenge viruses were characterized by deep-sequencing demonstrating the characteristic mutations of VOC B.1.351, but no other relevant alterations (Fig. S3 and Table S3). Immunized K18-hACE2 mice were studied using a high-dose challenge model, which induces severe clinical disease resembling COVID-19 in humans[25]. In addition, mice develop severe encephalitis specific to this animal model[20]. On day 4, animals in the sham group started succumbing to the BavPat1 infection (Fig. 1c). B.1.351 infection led to a delayed onset of severe disease compared to BavPat1, with 20% survival on day 10 after inoculation (Fig. 1d). Thus, K18-hACE2 mice were highly susceptible to both SARS-CoV-2 variants. Importantly, vaccination with 8 μg CVnCoV or 0.5–8 μg CV2CoV resulted in complete protection (100% survival) against BavPat1 and B.1.351, with no significant weight loss or disease symptoms throughout the course of the challenge infection (Fig. 1c, d and Fig. S4). In contrast, prior administration of the FI-Virus preparation provided sub-optimal protection against either BavPat1 or B.1.351, resulting in weight loss and signs of distress (Fig. 1 and Fig. S3). Some of the FI-Virus-immunized animals experienced very early weight loss and disease signs after VOC B.1.351 challenge infection, earlier than sham groups. In conclusion, survival rates, body weight changes, and disease scores revealed complete protection by the CVnCoV and CV2CoV vaccines in K18-hACE2 mice against lethal SARS-CoV-2 challenge, including against VOC B.1.351.

To investigate whether CVnCoV or CV2CoV vaccination prevented productive infection or dissemination of replicating SARS-CoV-2, we took oral swabs at 4 days post infection (dpi) to monitor viral RNA load in saliva. In the sham group, 4/4 and 4/5 samples were positive for viral genome after infection with BavPat1 or VOC B.1.351, respectively (Fig. 2a). FI-Virus administration prior to challenge did not significantly reduce viral genome load in saliva, with 40–60% of animals showing positive reverse transcription quantitative polymerase chain reaction (RT-qPCR) results on 4 dpi (Fig. 2a). In contrast, after CVnCoV or CV2CoV vaccination, no viral genomes were detected in oral swabs of either challenge groups irrespective of the vaccine and vaccine dose. Furthermore, the amount of sub-genomic RNA (sgRNA) was determined from swabs that scored positive for total viral RNA. Two different assays indicated sgRNA only in a few samples from sham-vaccinated and challenged individual mice (Table S4). To further explore the prevention of viral replication following challenge, we determined viral load in the upper respiratory tract (URT) (conchae) and the lower respiratory tract (LRT) (trachea, caudal lung, and cranial lung), as well as in the central nervous system (brain, cerebellum/
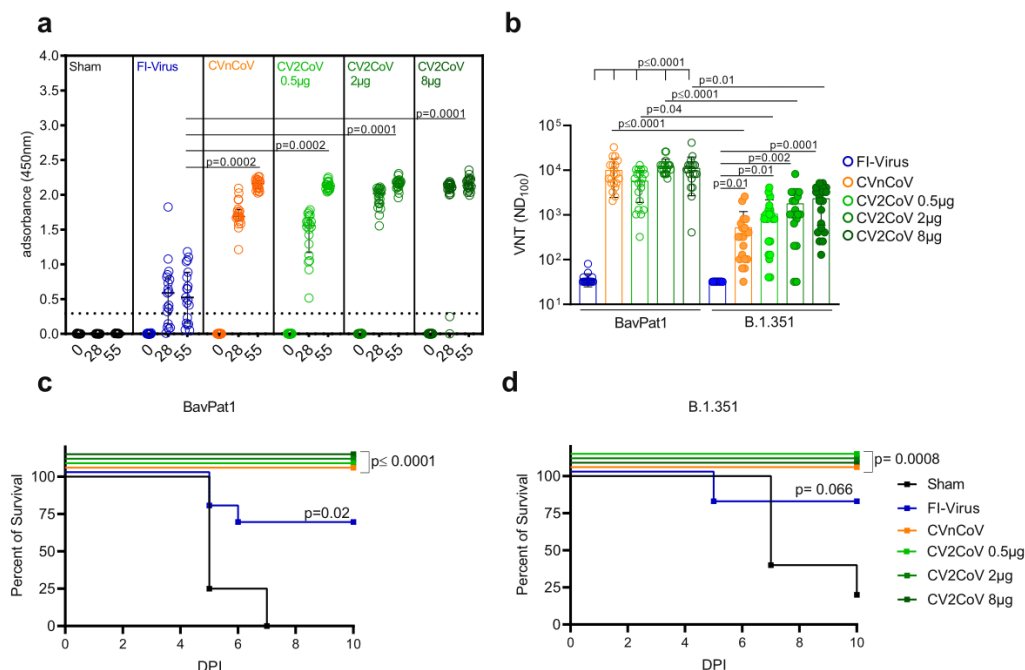
Fig. 1 CVnCoV and CV2CoV protect K18-hACE2 mice against SARS-CoV-2 variants BavPat1 and B1.351. K18-hACE2 mice that were vaccinated with 8 μg CVnCoV (orange) or different concentrations of CV2CoV (0.5 μg (light green), 2 μg (green), or 8 μg (dark green)), received 10^6 FI-Virus (blue) or NaCl (black) (sham) on days 0 and 28 followed by i.n. challenge with $10^{5.9}$ TCID$_{50}$ of SARS-CoV-2 variant BavPat1 or $10^{5.5}$ TCID$_{50}$ B1.351. **a** RBD ELISA with sera from K18-hACE2 mice on days 0, 28, and 55 of the respective groups: median and interquartile range are presented. Dashed line indicates threshold for positive anti-RBD antibody level. **b** Virus neutralization assay using day 55 sera from all the groups. Bars indicate mean with SD. **c**, **d** Survival curves (Kaplan–Meier) for K18-hACE2 mice from all the groups challenged either with BavPat1 (**c**) or B.1.351 (**d**) and followed up for 10 days post infection (DPI). **a**, **b** Each dot represents one individual mouse sample. Each sample was tested once (RBD ELISA) or in triplicates (VNT), and assays were repeated at least once. **c**, **d** Each line represents groups of mice as shown in **a**, **b** from a single experiment ($n = 5$ sham, $n = 10$ all other groups). p Values were determined by nonparametric one-way ANOVA and Dunn's multiple comparisons test (**a**, **b**) or two-sided log-rank (Mantel–Cox) test (**c**, **d**). Differences were considered significant at $p < 0.05$ with exact p values displayed in the figure. Source data are provided as a Source data file.

cerebrum) (Fig. 2b–f) in animals reaching the humane endpoint or at the day of termination (10 dpi). Similar to the quantitative RNA load results obtained from the oral swabs, the URT provided a niche for replication in both the sham and FI-Virus groups (Fig. 2b). In the CVnCoV and CV2CoV-vaccinated groups challenged with BavPat1, we observed a significant reduction of detectable viral replication in all groups with a maximum of 5/10 animals showing low genome copy numbers in the conchae. No animal in the LRT and only one sample from the brain was positive at a low level for SARS-CoV-2 genomic RNA, indicating complete protection from infection by BavPat1 in all the groups (Fig. 2c–f). The organ samples scoring positive for viral RNA were further evaluated using two distinct assays detecting sgRNAs. sgRNA was generally detected in samples that exhibited substantial total RNA loads (Table S5). More specifically, from CVnCoV- and CV2CoV-vaccinated mice that showed low levels of total RNA only a few single animals scored positive for sgRNA (Table S5). For VOC B.1.351, 5-7/10 CVnCoV or CV2CoV-vaccinated animals exhibited residual viral replication in the conchae. Here, viral levels were reduced without reaching statistical significance (Fig. 2b). Detection of sgRNA was limited to single individuals (Table S6). In contrast, both CVnCoV and CV2CoV almost completely prevented replication of this VOC in the LRT and the brain, with low viral copy numbers close to the limit of detection in the lung of 7/80 (40 cranial and 40 caudal) specimens and only 1/40 and 2/40 animals in the cerebellum and

cerebrum, respectively (Fig. 2c–f). No sgRNA could be amplified from these organs (Table S6). FI-Virus administration provided partial protection in the LRT in animals challenged with BavPat1, but not with VOC B.1.351, and did not significantly protect against viral replication in the cerebellum or cerebrum regardless of the SARS-CoV-2 variant (Fig. 2). These findings were verified by sgRNA detection (Tables S5 and S6). Of note, some of the animals receiving the FI-Virus preparation showed viral loads at the level of the sham group in the LRT (Fig. 2). In summary, aside conferring complete protection against lethal challenge with distinct SARS-CoV-2 lineages, CVnCoV and CV2CoV, at dosages ranging from 0.5 to 8 μg, prevented dissemination of SARS-CoV-2 from the inoculation site into other organs and provided solid protection against an ancestral SARS-CoV-2 and a VOC B.1.351 strain.

Discussion
The emergence of new strains with immune-escape potential, such as the VOC of the B.1.351 lineage that appeared first in South Africa, are of great concern, since all available COVID-19 vaccines are based on the ancestral SARS-CoV-2 strains. We therefore tested two mRNA vaccines in different concentrations against a standard ancestral SARS-CoV-2 B lineage strain (Bav-Pat1) in comparison to a VOC B.1.351 isolate in a transgenic mouse model.

ARTICLE
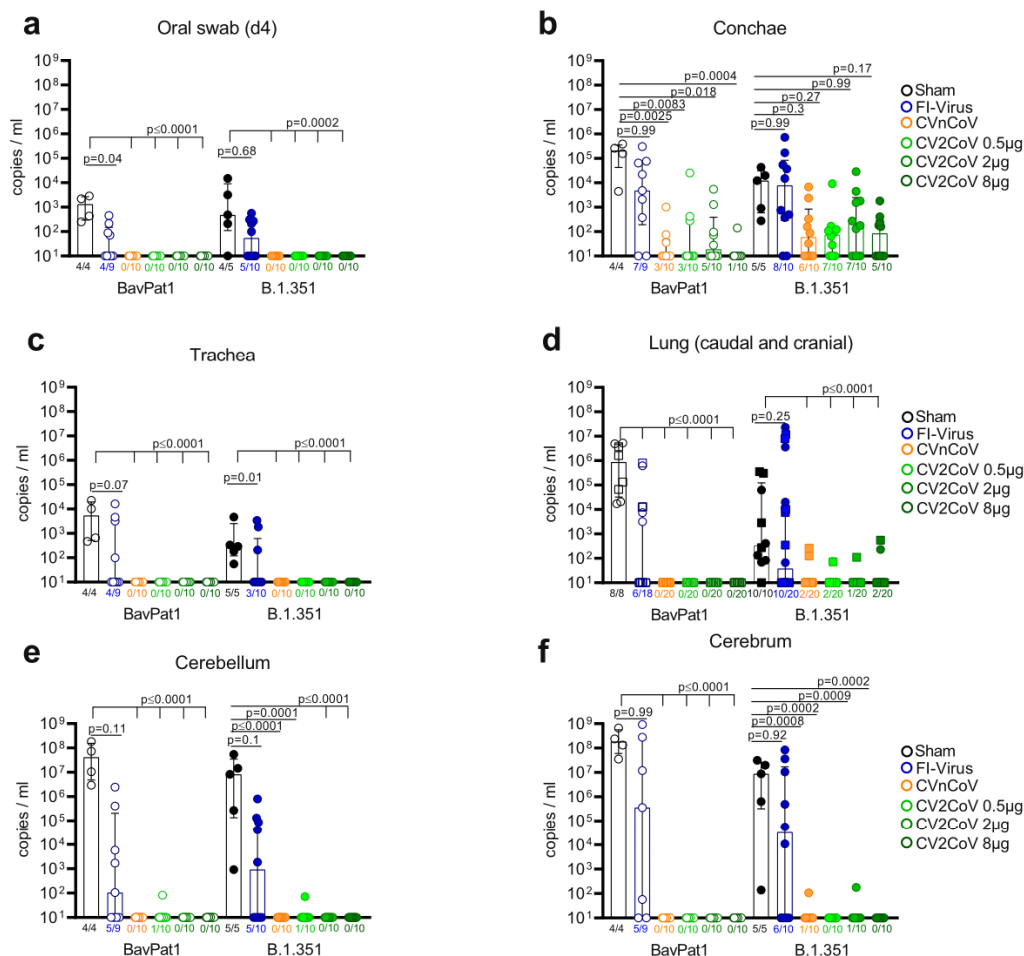
Fig. 2 CVnCoV and CV2CoV prevent replication of SARS-CoV-2 variants BavPat1 and B.1.351 in K18-hACE2 mice. RT-qPCR for genomic RNA of SARS-CoV-2 was performed with **a** oral swab samples at day 4 or from organ samples of **b** the upper respiratory tract, **c**, **d** the lower respiratory tract (caudal lung = circle; cranial lung = squares), and **e**, **f** the brain at day 10 or at the humane endpoint. Mice that were vaccinated with 8 µg CVnCoV (orange) or different concentrations of CV2CoV (0.5 µg (light green), 2 µg (green) or 8 µg (dark green)), received 10^6 FI-Virus (blue) or NaCl (black) (sham) on days 0 and 28 followed by i.n. challenge with $10^{5.9}$ TCID$_{50}$ of SARS-CoV-2 variant BavPat1 or $10^{5.5}$ TCID$_{50}$ B1.351. Each dot represents one individual mouse. Each sample was tested once, and assays were repeated at least once. *p* Values were determined by nonparametric one-way ANOVA and Dunn's multiple comparisons test. Scatter plots are labeled with median (height of the bar) and interquartile range. Differences were considered significant at *p* < 0.05, with exact *p* values displayed in the figure. Source data are provided as a Source data file.

Our data demonstrate that 8 µg CVnCoV and 0.5–8 µg CV2CoV fully protect mice against disease caused by two different SARS-CoV-2 variants. CVnCoV and CV2CoV vaccination, but not immunization with FI-Virus, rescued all transgenic mice from lethal infection caused by BavPat1 and VOC B.1.351 isolate NW-RKI-I-0028. The sub-optimal FI-Virus preparation reduced viral replication in the LRT solely after challenge with BavPat1, but showed no significant effect on viral dissemination as well as the viral genome loads in the URT. In contrast, both CVnCoV and CV2CoV immunization resulted in abundant RBD-specific and neutralizing antibodies and conferred complete and robust protection, including protection from viral replication in the lungs and brain. Only very limited viral replication was observed in the URT of mRNA-vaccinated animals challenged with VOC B.1.351. The relevance to disease transmission of this minimal viral replication in the conchae remains to be established. The reduced neutralizing capacity of sera from CVnCoV- and CV2CoV-vaccinated transgenic mice against VOC B.1.351, and

the insufficient prevention of replication in the conchae, might reflect the currently detected transmission rates of this VOC in human populations previously exposed to the ancestral strain. Nevertheless, our study provides the first evidence for the efficacy of a vaccine to prevent disease and viral dissemination from the site of infection against an emerging SARS-CoV-2 variant in a sensitive, well-established, and accepted in vivo model. Of note, this model might not fully recapitulate viral dissemination into respiratory compartments in humans. The very high neutralizing titers against BavPat1 elicited by the mRNA immunization as well as the fold reduction recorded for VOC B.1.351 may be unique to the mouse model employed in this study and require validation in other experimental models. In addition, the variable neutralizing capacity of individual sera against VOC B.1.351 is in line with serological responses detected in human vaccinees[26].

The pathophysiology of SARS-CoV-2 VOC infections remains largely unknown and detailed animal model data are missing. In our study, we observed a delayed course of disease in K18-hACE2

Results – Publication V: CVnCoV and CV2CoV protect human ACE2 transgenic mice from ancestral B BavPat1 and emerging B.1.351 SARS-CoV-2

ARTICLE

mice infected with a VOC B.1.351 strain and hypothesize that mutation accumulation might result in a changed in vivo phenotype. Short-term infections performed in hamsters have failed to detect diverging phenotypes in ancestral versus VOC lineages[27], but comparable data sets about the complete course and replication in the URT are still pending for all VOCs in other animal models. These apparently discordant findings call for further pathological and immunological assessments of pathogenicity of emerging lineages.

Here we report full protection against a VOC by CVnCoV and CV2CoV immunization, associated with high anti-RBD and neutralizing antibodies. Whether antibodies alone were sufficient for the beneficial outcome remains to be further validated. Broad immune responses elicited by vaccines, including cellular responses in addition to neutralizing antibodies, antibody-dependent cytotoxicity, or antibody-mediated innate immune effector functions, could help explain the protection. Potent T cell immunity could ensure the success of an immunization when antibodies decline. CVnCoV vaccination was previously shown to induce Th1 immunity and trigger S-specific CD8$^+$ T cell responses in mice[23]. Re-challenge studies in NHPs confirmed a role for CD8$^+$ T cells in protection[28]. Although point mutations in the major histocompatibility complex-I-restricted viral epitopes could subvert CD8$^+$ T cell surveillance[29], the majority of SARS-CoV-2 T cell epitopes recognized by convalescent individuals or vaccinees immunized with licensed mRNA vaccines appear unaffected by unique VOC mutations[30]. These findings indicate a role of cellular immunity in defense against SARS-CoV-2. Here we observed solid protection against disease upon challenge infection with VOC B.1.351 after CVnCoV or CV2CoV vaccination, despite reduced virus-neutralizing titers. These observations suggest that either complementary immune mechanisms are effective or that residual virus-neutralizing titers against B.1.351 are sufficient for in vivo neutralization in this model. In line with this, it has recently been demonstrated in a NHP infection model that relatively low neutralizing antibody titers can protect from SARS-CoV-2-related clinical signs[28]. The precise contribution of various immune compartments to CVnCoV and CV2CoV efficacy requires further evaluation.

Our proof-of-principle study demonstrates that mRNA vaccines can protect hACE2 mice against disease caused by SARS-CoV-2 independent from the lineages or virus variants.

Methods

Ethics. The animal experiments were evaluated and approved by the ethics committee of the State Office of Agriculture, Food safety, and Fishery in Mecklenburg – Western Pomerania (LALLF M-V: 7221.3-1-055/20). All procedures using SARS-CoV-2 were carried out in approved biosafety level 3 facilities.

Vaccination. Before challenge with SARS-CoV-2, mice were vaccinated prime day 0 and boost day 28 with either NaCl (sham), FI-Virus, or an mRNA vaccine (CVnCoV and CV2CoV) (Table S1).

The mRNA vaccines are based on the RNActive® platform (claimed and described in, e.g., WO2002098443 and WO2012019780) and are comprised of a 5′ cap1 structure, a GC-enriched open reading frame (ORF), 3′ untranslated region (UTR), and a vector-encoded polyA stretch and do not include chemically modified nucleosides. CVnCoV contains parts of the 3′ UTR of the *Homo sapiens* alpha hemoglobin gene as 3′ UTR followed by a polyA stretch, a C30 stretch, and a histone stem loop. CV2CoV further comprises a 5′ UTR from the human hydroxysteroid 17-beta dehydrogenase 4 gene and a 3′ UTR from human proteasome 20S subunit beta 3 gene followed by a histone stem loop and a polyA stretch. Lipid nanoparticle (LNP) encapsulation of mRNA was performed by Acuitas Therapeutics (Vancouver, Canada). The LNPs used in this study are particles of ionizable amino lipid, phospholipid, cholesterol, and a PEGylated lipid. The mRNA-encoded protein is based on the spike glycoprotein of SARS-CoV-2 NCBI Reference Sequence NC_045512.2, GenBank accession number YP_009724390.1, and encodes for full-length S featuring K986P and V987P mutations.

For comparison to CVnCoV and CV2CoV, we used FI-Virus combined with Alhydrogel® adjuvant. For this, 200 ml SARS-CoV-2 Germany/BavPat1/2020 (for

details, see section "Challenge infection") supernatant was concentrated using the PEG Virus Precipitation Kit (Biovision # BIV-K904) to a volume of 2 ml. Afterwards, this preparation was inactivated by formaldehyde (37%) at a dilution of 1:2000 at 37 °C for 24 h. Inactivation of the virus was confirmed by inoculation of VeroE6 cells. When no cytopathogenic effect (CPE) was detected, cell supernatants were passaged for three passages. For vaccination, freshly prepared stocks of 10^6 TCID$_{50}$ FI-Virus were mixed with 2% (final concentration) of Alhydrogel® in phosphate-buffered saline (PBS). Prior vaccination, 20 µl of NaCl (sham control), FI-Virus, CVnCoV, or CV2CoV were loaded into single-use insulin syringe with an integrated needle (30 G) no longer than 2 h before injection. First, the mice were anesthetized by inhalation of isoflurane and the hind leg was shorn with an electric clipper. For all the groups, 20 µl of the preparation was administered intramuscularly into the M. tibialis (day 0 right leg or left day 28). Before animals were placed back into their cages, 100–140 µl blood samples were obtained by puncture of the V. facialis on days 0, 28, and 55. For blood collection, the animals remained anesthetized under isoflurane anesthesia (5 vol.%). All groups were monitored for side effects of the injection and were scored at 24 h post injection. The injection sides were slightly swollen in all the groups 24 h post vaccination, which resolved after 48–72 h.

Serum collection. All blood samples were collected into Z-clot activator 200 µl microtube (Sarstedt). The samples were incubated at room temperature (RT) for 0.5–1 h and afterwards centrifuged for 5 min, 10,000 rcf, at RT. All serum samples were stored at <−70 °C.

Virus preparation. SARS-CoV-2 Germany/BavPat1/2020 (BavPat1) (GISAID accession EPI_ISL_406862) was kindly provided by Bundeswehr Institute of Microbiology, Munich, Germany. SARS-CoV-2 hCoV-19/Germany/NW-RKI-I-0029/2020 B.1.351-linage or VOC 202012/02 (B.1.351) (GISAID accession EPI_ISL_803957) was kindly provided by Robert-Koch-Institut, Berlin, Germany. Virus stocks were propagated (three passages and two passages, respectively) on Vero E6 cells (Collection of Cell Lines in Veterinary Medicine CCLV-RIE 0929) using a mixture of equal volumes of Eagle MEM (Hanks' balanced salts solution) and Eagle MEM (Earle's balanced salts solution) supplemented with 2 mM L-Glutamine, nonessential amino acids adjusted to 850 mg/l, NaHCO$_3$, 120 mg/l sodium pyruvate, and 10% fetal bovine serum, pH 7.2. The virus was harvested after 72 h, titrated on Vero E6 cells, and stored at −80 °C until further use.

Sequencing of the viral genome. Full genome sequencing of SARS-CoV-2 B1.351 hCoV-19/Germany/NW-RKI-I-0029/2020 P2+1 (passage of hCoV-19/Germany/NW-RKI-I-0029/2020) was performed using high-throughput sequencing (HTS). For this purpose, RNA was extracted from cell culture supernatant using a combined TRIzol LS Reagent (Invitrogen, Waltham, MA, USA) and QIAamp RNeasy Mini Kit (Qiagen, Hilden, Germany) protocol. The resulting RNA extracts were subjected to library preparation as described in detail [31]. The resulting library L4550 was quality-checked, quantified, and sequenced on the Ion Torrent S5XL platform on an Ion 530 sequencing chip using 400 bp chemistry.

The Genome Sequencer software suite (versions 2.6; Roche) was applied to execute reference mapping analyses. Since no complete whole-genome sequence was available of the original isolate (hCoV-19/Germany/NW-RKI-I-0029/2020| EPI_ISL_803957|2020-12-28), the genome sequence of SARS-CoV-2 B.1.351 isolate hCoV-19/Germany/BW-ChVir22275/2021|EPI_ISL_875344|2021-01-15 was used as initial reference. Subsequently, the mapping analysis was repeated with the obtained SARS-CoV-2 genome sequence as reference and the corresponding data set to compile the final SARS-CoV-2 genome sequence of the sample. This determined whole-genome sequence of sample L4550 was set as reference for variant calling. The Torrent Suite plugin Torrent variantCaller (version 5.12) was used to detect single-nucleotide polymorphism (SNP) variants (parameter settings: generic, S5/S5XL(530/540), somatic, low stringency, changed alignment arguments for the TMAP module from map 4 [default] to map1 map2). Identified SNP variants were visualized with Geneious Prime (10.2.3; Biomatters, Auckland, New Zealand) and compared with the SNP variants detected using the variant analysis tool implemented in Geneious Prime Molecular Biology and Sequence Analysis Software (version 10.2.3; (default settings, minimum variant frequency 0.02).

The SARS-CoV-2 genome sequence generated in this study is available under the accession number MZ433432.

Challenge infection. Mice in groups of up to five animals were kept in individually ventilated cages (IVCs) for the entire study (Table S1). The animals were infected under short-term isoflurane inhalation anesthesia with 25 µl of either $10^{5.875}$ TCID$_{50}$ SARS-CoV-2 BavPat1 (calculated from back-titration of the original material) or $10^{5.5}$ TCID$_{50}$ SARS-CoV-2 B1.351 (calculated from back-titration of the original material) per animal. To prevent spill-over between different pairs, the IVCs were strictly separated in individual cage systems. During the entire study, all animals were offered water ad libitum and were fed and checked for clinical scores and body weight daily by animal caretakers and study researchers. Animal housing was performed with 20–24 °C temperature, 45–65% humidity; and 12-h dark/light cycle with 30 min of dawn. A oral swab sample of each animal was taken at 4 dpi under short-term isoflurane inhalation anesthesia. Animals with signs of severe

ARTICLE

clinical symptoms and/or body weight loss over 20% were euthanized before the end of the study. All animals were euthanized at day 10 post infection.

RNA extraction and RT-qPCR. RNA from combined nasal/oral swabs and organ samples was extracted using the NucleoMag® VET Kit (Macherey-Nagel, Düren, Germany) in combination with a Biosprint 96 platform (Qiagen, Hilden, Germany). Each extracted sample was eluted in 100 µl. Viral RNA genome was detected and quantified by real-time RT-qPCR on a BioRad real-time CFX96 detection system (BioRad, Hercules, USA). Target sequence for amplification was the viral RNA-dependent RNA polymerase (WHO, https://www.who.int/docs/default-source/coronaviruse/real-time-rt-pcr-assays-for-the-detection-of-sars-cov-2-institut-pasteur-paris.pdf?sfvrsn=3662fcb6_2). Genome copies per µl RNA template were calculated based on a quantified standard RNA, where absolute quantification was done by the QX200 Droplet Digital PCR System in combination with the 1-Step RT-ddPCR Advanced Kit for Probes (BioRad, Hercules, USA). The limit of detection was calculated to be 10 copies per reaction.

sgRNA RT-qPCR assays. Samples (swabs/organs) that tested positive for viral genomic RNA were evaluated using assays specifically detecting sgRNA. The assay detecting sgRNA of the E-gene established by Speranza et al.[32] with the modification of omitting the ZEN™ quencher was used. In addition, a further assay was applied to detect sgRNA of the ORF7a, as Alexandersen and colleagues[33] demonstrated that this sgRNA is more abundantly quantifiable. Primer and probe sequences of this assay are summarized in Table S7. The RT-qPCR reaction of both assays was prepared using the qScript XLT One-Step RT-qPCR ToughMix (QuantaBio, Beverly, MA, USA) in a volume of 12.5 µl including 1 µl of the respective FAM mix and 2.5 µl of extracted RNA. The reaction was performed for 10 min at 50 °C for reverse transcription, 1 min at 95 °C for activation, and 42 cycles of 10 s at 95 °C for denaturation, 10 s at 60 °C for annealing, and 20 s at 68 °C for elongation. Fluorescence was measured during the annealing phase. All RT-qPCRs were performed on a BioRad real-time CFX96 detection system.

RBD antibody enzyme-linked immunosorbent assay (ELISA). Sera were analyzed using an indirect multi-species ELISA based on the RBD of SARS-CoV-2[34]. For this, ELISA plates (Greiner Bio-One GmbH) were coated with 100 ng/well RBD overnight at 4 °C in 0.1 M carbonate buffer ($1.59\,g\;Na_2CO_3$ and 2.93 g $NaHCO_3$, ad. 1 L aqua dest., pH 9.6) or were treated with the coating buffer only. Afterwards, the plates were blocked for 1 h at 37 °C using 5% skim milk in PBS. Sera were pre-diluted 1/100 in TBS-Tween (TBST) and incubated on the coated and uncoated wells for 1 h at RT. A multi-species conjugate (SBVMILK; obtained from ID Screen® Schmallenberg virus Milk Indirect ELISA; IDvet) was diluted 1/80 and then added for 1 h at RT. Following the addition of tetramethylbenzidine substrate (IDEXX), the ELISA readings were taken at a wavelength of 450 nm on a Tecan Spectra Mini instrument (Tecan Group Ltd.). Between each step, the plates were washed three times with TBST. The absorbance was calculated by subtracting the optical density measured on the uncoated wells from the values obtained from the protein-coated wells for the respective sample. Of note, the ELISA determines relative abundance of anti-RBD Ig levels and therefore does not allow a direct comparison between different studies.

Virus neutralization test (VNT). To evaluate specifically the presence of virus-neutralizing antibodies in serum samples (pre-challenge), we performed a VNT. Therefore, sera were pre-diluted 1/16 or 1/32 with Dulbecco's modified Eagle's medium (DMEM) in a 96-well deep well master plate. Three times 100 µl, representing three technical replicates, of this pre-dilution were transferred into a 96-well plate. A log2 dilution was conducted by passaging 50 µl of the serum dilution in 50 µl DMEM, leaving 50 µl of sera dilution in each well. Subsequently, 50 µl of the respective SARS-CoV-2 (BavPat1 or B.1.351) virus dilution (100 $TCID_{50}$/well) was added to each well and incubated for 1 h at 37 °C. Lastly, 100 µl of trypsinated VeroE6 cells (cells of one confluent TC175 flask per 100 ml) in DMEM with 1% penicillin/streptomycin supplementation was added to each well. After 72 h incubation at 37 °C, the cells were evaluated by light microscopy for a specific CPE. A serum dilution was counted as neutralizing in the case no specific CPE was visible. The virus titer was confirmed by virus titration; positive and negative serum samples were included.

SARS-CoV-2 surrogate VNT. Individual serum samples obtained after prime, but before boost vaccination, were evaluated by the use of a virus neutralization surrogate assay (GenScript Biotech, Leiden, The Netherlands). Number of samples matches the number of samples presented in Fig. 1. The assay was used according to the manufacturer's instructions.

Data availability
The authors declare that the data supporting the findings of this study are available within the paper and its supplementary information files and are available from the corresponding authors upon reasonable request. The SARS-CoV-2 genome sequence generated in this study is available under the accession number MZ433432. The following sequence data was used: SARS-CoV-2 NCBI Reference Sequence NC_045512.2, GenBank accession number YP_009724390.1; SARS-CoV-2 Germany/BavPat1/2020 (BavPat1) (GISAID accession EPI_ISL_406862); SARS-CoV-2 hCoV-19/Germany/NW-RKI-I-0029/2020 (GISAID accession EPI_ISL_803957). All non-commercial materials generated during the current study are available from the corresponding authors under an MTA with Friedrich-Loeffler-Institut. Source data are provided with this paper.

References
1. Hu, B., Guo, H., Zhou, P. & Shi, Z. L. Characteristics of SARS-CoV-2 and COVID-19. *Nat. Rev. Microbiol.* **19**, 141–154 (2021).
2. Krammer, F. SARS-CoV-2 vaccines in development. *Nature* **586**, 516–527 (2020).
3. Dong, Y. et al. A systematic review of SARS-CoV-2 vaccine candidates. *Signal Transduct. Target. Ther.* **5**, 237 (2020).
4. Hou, Y. J. et al. SARS-CoV-2 D614G variant exhibits efficient replication ex vivo and transmission in vivo. *Science* **370**, 1464–1468 (2020).
5. Korber, B. et al. Tracking changes in SARS-CoV-2 spike: evidence that D614G increases infectivity of the COVID-19 virus. *Cell* **182**, 812.e9–827.e9 (2020).
6. Zhou, B. et al. SARS-CoV-2 spike D614G change enhances replication and transmission. *Nature* **592**, 122–127 (2021).
7. Liu, Z. et al. Identification of SARS-CoV-2 spike mutations that attenuate monoclonal and serum antibody neutralization. *Cell host & microbe* **29**, 477–488.e4, https://doi.org/10.1016/j.chom.2021.01.014 (2021).
8. Santos, J. C. & Passos, G. A. The high infectivity of SARS-CoV-2 B.1.1.7 is associated with increased interaction force between Spike-ACE2 caused by the viral N501Y mutation. Preprint at *bioRxiv* https://doi.org/10.1101/2020.12.29.424708 (2021).
9. Tegally, H. et al. Sixteen novel lineages of SARS-CoV-2 in South Africa. *Nat. Med.* **27**, 440–446 (2021).
10. Zhou, D. et al. Evidence of escape of SARS-CoV-2 variant B.1.351 from natural and vaccine induced sera. *Cell* **184**, 2348.e6–2361.e6 (2021).
11. Sabino, E. C. et al. Resurgence of COVID-19 in Manaus, Brazil, despite high seroprevalence. *Lancet* **397**, 452–455 (2021).
12. Collier, D. et al. Sensitivity of SARS-CoV-2 B.1.1.7 to mRNA vaccine-elicited antibodies. *Nature* **593**, 136–141, https://doi.org/10.1038/s41586-021-03412-7 (2021).
13. Muik, A. et al. Neutralization of SARS-CoV-2 lineage B.1.1.7 pseudovirus by BNT162b2 vaccine-elicited human sera. *Science* **371**, 1152–1153 (2021).
14. Shen, S., Zhang, Z. & He, F. The phylogenetic relationship within SARS-CoV-2s: An expanding basal clade. *Mol. Phylogenet. Evol.* **157**, 107017 (2021).
15. Cele, S. et al. Escape of SARS-CoV-2 501Y.V2 variants from neutralization by convalescent plasma. *Nature* **593**, 142–146 (2021).
16. Garcia-Beltran, W. F. et al. COVID-19-neutralizing antibodies predict disease severity and survival. *Cell* **184**, 476.e1–488.e1 (2021).
17. Wibmer, C. K. et al. SARS-CoV-2 501Y.V2 escapes neutralization by South African COVID-19 donor plasma. *Nat. Med* **27**, 622–625 (2021).
18. Wu, K. et al. Serum Neutralizing Activity Elicited by mRNA-1273 Vaccine. *N. Eng. J. Med.* **384**, 1468–1470, https://doi.org/10.1056/NEJMc2102179 (2021).
19. Xie, X. et al. Neutralization of SARS-CoV-2 spike 69/70 deletion, E484K and N501Y variants by BNT162b2 vaccine-elicited sera. *Nat. Med.* **27**, 620–621 (2021).
20. Munoz-Fontela, C. et al. Animal models for COVID-19. *Nature* **586**, 509–515 (2020).
21. Madhi, S. A. et al. Efficacy of the ChAdOx1 nCoV-19 Covid-19 vaccine against the B.1.351 variant. *N. Engl. J. Med.* **384**, 1885–1898 (2021).
22. Winkler, E. S. et al. SARS-CoV-2 infection of human ACE2-transgenic mice causes severe lung inflammation and impaired function. *Nat. Immunol.* **21**, 1327–1335 (2020).
23. Rauch, S. et al. mRNA-based SARS-CoV-2 vaccine candidate CVnCoV induces high levels of virus-neutralising antibodies and mediates protection in rodents. *NPJ Vaccines* **6**, 57 (2021).

ARTICLE

24. Rauch, S. et al. mRNA vaccine CVnCoV protects non-human primates from SARS-CoV-2 challenge infection. Preprint at *bioRxiv* https://doi.org/10.1101/2020.12.23.424138 (2020).
25. Oladunni, F. S. et al. Lethality of SARS-CoV-2 infection in K18 human angiotensin-converting enzyme 2 transgenic mice. *Nat. Commun.* **11**, 6122 (2020).
26. Garcia-Beltran, W. F. et al. Multiple SARS-CoV-2 variants escape neutralization by vaccine-induced humoral immunity. *Cell* **184**, 2372.e9–2383.e9 (2021).
27. Abdelnabi, R. et al. Comparing infectivity and virulence of emerging SARS-CoV-2 variants in Syrian hamsters. *EBioMedicine.* **68**, 103403, https://doi.org/10.1016/j.ebiom.2021.103403 (2021).
28. McMahan, K. et al. Correlates of protection against SARS-CoV-2 in rhesus macaques. *Nature* **590**, 630–634 (2021).
29. Agerer, B. et al. SARS-CoV-2 mutations in MHC-I-restricted epitopes evade CD8(+) T cell responses. *Sci. Immunol.* **6**, eabg6461 (2021).
30. Tarke, A. et al. Comprehensive analysis of T cell immunodominance and immunoprevalence of SARS-CoV-2 epitopes in COVID-19 cases. *Cell Rep. Med.* **2**, 100204 (2021).
31. Wylezich, C., Papa, A., Beer, M. & Hoper, D. A versatile sample processing workflow for metagenomic pathogen detection. *Sci. Rep.* **8**, 13108 (2018).
32. Speranza, E. et al. Single-cell RNA sequencing reveals SARS-CoV-2 infection dynamics in lungs of African green monkeys. *Sci. Transl. Med.* **13**, eabe8146 (2021).
33. Alexandersen, S., Chamings, A. & Bhatta, T. R. SARS-CoV-2 genomic and subgenomic RNAs in diagnostic samples are not an indicator of active replication. *Nat. Commun.* **11**, 6059 (2020).
34. Wernike, K. et al. Multi-species ELISA for the detection of antibodies against SARS-CoV-2 in animals. *Transbound Emerg. Dis.* https://doi.org/10.1111/tbed.13926 (2020).

Acknowledgements

Author contributions

Conceptualization: D.H., B.C., S.R., J.M., S.O.M., T.C.M., B.P., A.D., M.B. Methodology: D.H., B.C., S.R., N.R., J.M., S.O.M., C.W., A.B., K.W., B.P., A.D., M.B. Formal analysis: D.H., B.C., N.J.H., L.U., J.S., A.K., A.B., C.W. Investigation: D.H., B.C., N.J.H., L.U., C.F., J.S., A.K., A.B., A.M., F.S., B.H., C.W. Resources: M.T., A.T., S.R., N.R., J.M., T.C.M., S.O.M., B.P., A.D., M.B. Data curation: D.H., B.C., N.J.H., L.U., J.S., C.W., A.D., M.B. Writing—original draft preparation: D.H., B.C., N.J.H., L.U., C.W., A.D., M.B. Writing—review and editing: D.H., B.C., S.R., N.R., A.B., K.W., C.W., S.O.M., T.C.M., B.P., A.D., M.B. Visualization: D.H., B.C., N.J.H., L.U., C.F., C.W. Supervision: D.H., B.C., A.B., K.W., S.O.M., T.C.M., B.P., A.D., M.B. Project administration: D.H., B.C., S.R., N.R., J.M., S.O.M., T.C.M., B.P., A.D., M.B. Funding acquisition: S.R., S.O.M., B.P., A.D., M.B., T.C.M.

Funding

Competing interests

S.R., B.P., N.R., J.M., A.T., M.T., and S.O.M. are employees of CureVac AG, Tübingen, Germany, a publically listed company developing mRNA-based vaccines and immunotherapeutics. Authors may hold shares in the company. S.R., B.P., N.R., A.T., and M.T. are inventors on several patents on mRNA vaccination and use thereof.

Additional information

Supplementary information The online version contains supplementary material available at https://doi.org/10.1038/s41467-021-24339-7.

Correspondence and requests for materials should be addressed to A.D. or M.B.

Peer review information *Nature Communications* thanks the anonymous reviewers for their contribution to the peer review of this work.

Reprints and permission information is available at http://www.nature.com/reprints

Publisher's note Springer Nature remains neutral with regard to jurisdictional claims in published maps and institutional affiliations.

1   **Supplemental Material**

2

3   **CVnCoV and CV2CoV protect human ACE2 transgenic mice from ancestral B BavPat1 and**

4   **emerging B.1.351 SARS-CoV-2**

5

6

7 Table S1: Experimental and control groups.

group	No. of animals	Vaccine	Dose, volume, route	Dosing	Serum collection	Challenge infection		End of the study
I	K18-hACE2 mice Female n=10	CVnCoV	8 µg, 20 µl, i.m.	d0, 28	d0, d28, d55	BavPat1		d69 (10dpc)
II			8 µg, 20 µl, i.m.				B1.351	
III		CV2CoV	0.5 µg, 20 µl, i.m.			BavPat1		
IV			0.5 µg, 20 µl, i.m.				B1.351	
V		CV2CoV	2 µg, 20 µl, i.m.			BavPat1		
VI			2 µg, 20 µl, i.m.				B1.351	
VII		CV2CoV	8 µg, 20 µl, i.m.			BavPat1		
VIII			8 µg, 20 µl, i.m.				B1.351	
IX		Formalin-inactivated virus +Alum	10^6 TCID$_{50}$, 20µl, i.m.			BavPat1		
X			10^6 TCID$_{50}$, 20µl, i.m				B1.351	
XI	n=5	Sham (NaCl)	-, 20 µl, i.m.			BavPat1		
XII			-, 20 µl, i.m.				B1.351	

8

9

10   Table S2. sVNT results of serum samples from day 28

Group	Median	IQR	p-value
Sham	6.83	3.69-7.94	N/A
FI -Virus	55.68	26.01-71.69	N/A
CVnCoV	94.83	93.89-95.27	0.0017
CV2CoV 0.5µg	93	88.69-95.34	0.03
CV2CoV 2µg	96.01	95.52-96.27	<0.0001
CV2CoV 8µg	96.46	96.09-96.68	<0.0001

11   IQR= interquartile range; P-values compare all RNA vaccine groups to the FI-Virus group and were

12   determined by nonparametric one-way ANOVA and Dunn's multiple comparisons test

13   Source data are provided as a Source Data file.

14

15

16   Table S3. Sequencing coverage of L4550 for mutations typically found in the spike protein gene of
17   B.1.351 variants and the spike protein polybasic cleavage site.

B.1.351 mutations Spike	Coverage	Variant
L18F	8,584 reads	None
D80A	6,361 reads	None
D215G	9,898 reads	None
Deletion 241-243	(9628 reads)	None
K417N	8,606 reads	None
E484K	9,094 reads	None
N501Y	9,868 reads	None
A701V	14,038 reads	None
Cleavage site	17,730 reads	None

18

19

20   Table S4: Viral RNA genome content detected in swab samples (4 dpi), expressed as Cq values for
21   total RNA and subgenomic RNA. This table includes samples that were positive for total RNA, all
22   further swab samples scored negative.

Vaccine	Challenge	ID	Genomic RNA	Subgenomic RNA	
				sgRNA E	sgRNA ORF7a
FI virus	BavPat1	FU5923	36.6	nd	nd
		QE7311	35.4	nd	nd
		VI9303	38.3	nd	nd
		KZ7407	37.9	nd	nd
	B.1.351.	QE7312	37.8	nd	nd
		QE7300	36.0	nd	nd
		VK1621	36.2	nd	nd
		KZ7411	36.6	nd	nd
		VI9302	35.0	nd	nd
sham	BavPat1	AO8979	32.9	nd	nd
		AO8971	35.4	nd	nd
		AO8960	32.5	nd	nd
		VK1079	36.3	nd	nd
	B.1.351.	KZ7412	35.3	nd	nd
		VI9315	32.3	nd	36.7
		VI9305	29.9	37.1	36.2
		KZ7416	36.6	nd	nd

23   nd: not detected

24

25 Table S5: Viral RNA genome content detected in organ samples (10 dpi or indicated dpi) from mice
26 challenged with the isolate BavPat1 (homologous spike), expressed as Cq value for total RNA and
27 subgenomic RNA. The table includes samples that were positive for total genomic RNA (Cq <40),
28 while all further organ samples scored negative.

Vaccine	Challenge	ID	Organ	Genomic RNA	Subgenomic RNA	
					sgRNA E	sgRNA ORF7a
FI virus	BavPat1	FU5923	Cerebellum	39.6	nd	nd
			Cerebrum	25.7	29.3	26.2
			Nasal conchae	26.4	32.7	31.4
			Nasal conchae	33.7	nd	nd
		QE7309	Cerebellum	34.1	nd	33.2
			Cerebrum	25.6	30.7	26.7
			Nasal conchae	36.5	nd	nd
		KZ7402	Nasal conchae	28.1	35.8	33.2
		VI9304	Cerebrum	39.5	nd	nd
			Trachea	32.5	39.1	38.4
		VI9303 (6dpc)	Cerebellum	31.4	38.7	32.9
			Cerebrum	19.4	24.7	21.4
			Nasal conchae	27.6	37.1	32.5
			Trachea	37.8	nd	nd
			Lung caudal	32.3	38.5	35.7
			Lung cranial	30.1	36.9	34.2
		QE7311 (5dpc)	Cerebellum	22.6	27.5	25.3
			Cerebrum	15	20.7	18.2
			Nasal conchae	32.6	nd	36.7
			Trachea	30.7	37.6	38.8
			Lung caudal	31.9	nd	37.3
			Lung cranial	31.1	nd	34.1
		VK1634 (5dpc)	Cerebellum	28.5	30.8	28.1
			Cerebrum	13.1	18.1	15.5
			Nasal conchae	30.2	nd	37.7
			Trachea	33.3	nd	36
			Lung caudal	24.8	30.3	27.4
			Lung cranial	24.4	29.8	27
sham	BavPat1	AO8971 (7dpc)	Cerebellum	20.3	24.3	21.4
			Cerebrum	18.3	22.7	19.5
			Nasal conchae	32.8	nd	nd
			Trachea	36.4	nd	nd
			Lung caudal	30.3	nd	nd
			Lung cranial	27.3	32.1	29.4
		VK1079 (5dpc)	Cerebellum	22.3	35.4	23.2
			Cerebrum	13.6	18.6	16.4
			Nasal conchae	26.2	34.7	30.4
			Trachea	31.4	36.9	34.7
			Lung caudal	21.9	27.1	23.5
			Lung cranial	30.6	nd	33.8
		AO8960 (5dpc)	Cerebellum	17.2	20.4	18.5
			Cerebrum	16.2	18.1	5.9
			Nasal conchae	27	30.3	29
			Trachea	35.8	nd	40.5
			Lung caudal	21.4	26.1	23.1
			Lung cranial	23.3	28	25.4
		AO8979 (5dpc)	Cerebellum	15.7	19.9	17
			Cerebrum	15.3	19.3	16.9
			Nasal Conchae	25.6	31.5	29.3
			Trachea	30.1	38.1	34.4

			Lung caudal	21.5	25.3	22.8
			Lung cranial	28.4	33.1	30
CVnCoV	BavPat1	QE7304	Nasal conchae	38.2	nd	nd
		FT9301	Nasal conchae	35.3	nd	nd
CV2CoV 8µg	BavPat1	KY5549	Nasal conchae	38.7	nd	nd
CV2CoV 2µg	BavPat1	VI9314	Nasal conchae	39.6	nd	nd
		VI9316	Trachea	37.7	nd	nd
		KZ7417	Nasal conchae	32.6	39.6	nd
		VK1078	Nasal conchae	35	nd	nd
		VK1072	Nasal conchae	39.1	nd	nd
CV2CoV 0.5µg	BavPat1	FT9319	Nasal conchae	36.1	nd	nd
		FT9307	Cerebellum	38.9	nd	nd
			Nasal conchae	36.3	nd	nd
		KY5552	Nasal conchae	30.5	37.1	36.2

29   nd: not detected

30

31 Table S6: Viral RNA genome content detected in organ samples (10 dpi or indicated) from mice
32 challenged with the B.1.351. isolate (heterologous spike), expressed as Cq value for total genomic
33 RNA and subgenomic RNA. This table includes samples that resulted positive for total RNA (Cq
34 <40), while all further organ samples scored negative.

Vaccine	Challenge	ID	Organ	Genomic RNA	Subgenomic RNA	
					sgRNA E	sgRNA ORF7a
FI virus	B.1.351.	QE7302	Cerebrum	29	35.8	31.1
			Nasal conchae	29.7	39.2	34.6
			Lung cranial	37.4	nd	nd
		VK1631	Nasal conchae	36.8	nd	nd
		QE7312	Cerebellum	29.6	39.7	31.9
			Cerebrum	31.7	nd	33.8
			Trachea	38.2	nd	nd
			Lung caudal	30.7	39.1	35.2
			Lung cranial	31.8	39.7	35.5
		KZ7403	Nasal conchae	29.1	nd	nd
		VI9309	Cerebellum	33.9	nd	34.8
			Cerebrum	25.1	31.2	28.3
			Nasal conchae	36.5	nd	nd
			Lung caudal	39.2	nd	nd
		KZ7413	Cerebellum	27.9	nd	31.4
			Cerebrum	18.3	26.3	23.8
			Nasal conchae	35.4	nd	nd
		KZ7411	Nasal conchae	30.7	38.2	nd
			Lung caudal	31.1	36.6	35.5
			Lung cranial	31.7	38.2	35.3
		QE7300 (5dpc)	Cerebellum	27.3	nd	30.4
			Cerebrum	20.3	25.7	22.4
			Nasal conchae	26.9	32.8	31.9
			Trachea	34.1	nd	37.6
			Lung caudal	22	25.5	24.1
			Lung cranial	20.7	25.8	24.5
		VI9302 (5dpc)	Cerebellum	24.4	29.1	26
			Cerebrum	16.9	22.7	20
			Nasal conchae	24.5	29.8	28.9
			Trachea	33.2	nd	nd
			Lung caudal	19	22.8	21.1
			Lung cranial	20.1	23.9	22.3
sham	B.1.351.	VI9305	Cerebellum	26.5	33.4	28.4
			Cerebrum	25.1	30	26.5
			Nasal conchae	31.5	36.4	36.6
			Trachea	38.3	nd	nd
			Lung caudal	39.6	-	-
		KZ7416	Cerebellum	35.8	nd	nd
			Cerebrum	38.9	nd	nd
			Nasal conchae	30.7	nd	34.8
			Trachea	37.7	nd	nd

			Lung caudal	28.9	33.9	31.6
			Lung cranial	26.3	32	29.4
		VI9306 (7dpc)	Cerebellum	19.7	23.9	20.1
			Cerebrum	19.3	24.2	20.6
			Nasal conchae	35.3	nd	nd
			Trachea	39.8	-	-
			Lung caudal	38.4	nd	nd
			Lung cranial	37.2	nd	39.8
		KZ7412 (7dpc)	Cerebellum	20.7	24.5	22.3
			Cerebrum	18.5	23.5	21.2
			Nasal conchae	29.1	36.3	34.1
			Trachea	32.7	nd	39.4
			Lung caudal	36.6	nd	nd
			Lung cranial	33.5	nd	38.4
		VI9315 (7dpc)	Cerebellum	17.6	21.2	18.2
			Cerebrum	20.6	25.9	23.1
			Nasal conchae	37.2	nd	nd
			Trachea	36.9	nd	nd
			Lung caudal	39.4	nd	nd
			Lung cranial	25.7	30	28.5
CVnCoV	B.1.351.	KY5553	Nasal conchae	39.1	nd	nd
		KY5554	Nasal conchae	37	nd	nd
		VK1636	Nasal conchae	34.5	nd	nd
		VK1633	Cerebrum	39.6	nd	nd
			Nasal conchae	32.7	nd	37.7
			Lung cranial	38.1	nd	nd
		QE7314	Nasal conchae	39	nd	nd
			Lung cranial	39.4	nd	nd
CV2CoV 8µg	B.1.351.	KZ6841	Nasal conchae	38	nd	nd
		FT9314	Nasal conchae	38.2	nd	nd
		KZ6850	Nasal conchae	34.3	nd	nd
		AO5179	Nasal conchae	37.5	nd	nd
		FT9309	Nasal conchae	36.7	nd	nd
			Lung caudal	37.6	nd	nd
			Lung cranial	36.2	nd	nd
CV2CoV 2µg	B.1.351.	AO8968	Nasal conchae	37.3	nd	nd
		VK1074	Nasal conchae	38	nd	nd
		VK1076	Nasal conchae	32.9	nd	nd
		VK1067	Nasal conchae	38.5	nd	nd
		AO8965	Nasal conchae	34.6	nd	nd
			Lung cranial	38.8	nd	nd

		AO8977	Nasal conchae	34.3	nd	nd
		VK1077	Cerebrum	38	nd	nd
			Nasal conchae	29.9	36.9	35.8
CV2CoV 0.5µg	B.1.351.	AO5160	Nasal conchae	38.5	nd	nd
		KY5557	Cerebellum	39.1	nd	nd
		QE6769	Nasal conchae	38.3	nd	nd
			Lung caudal	39.1	nd	nd
			Lung cranial	39.1	nd	nd
		AO5163	Nasal conchae	39.3	nd	nd
		FU7019	Nasal conchae	38.5	nd	nd
		AO5166	Nasal conchae	31.7	nd	38.6
		AO5177	Nasal conchae	39.2	nd	nd

35   nd: not detected; -: not tested

36

37

38   Table S7: Primer and probes used to detect genomic RNA and sgRNA from SARS-CoV-2 ORF7a

38   Table S7: Primer and probes used to detect genomic RNA and sgRNA from SARS-CoV-2 ORF7a

	sequence (5´-3´)	position*	amplicon
RdRp gene / nCoV_IP4 (https://www.who.int/docs/default-source/coronaviruse/real-time-rt-pcr-assays-for-the-detection-of-sars-cov-2-institut-pasteur-paris.pdf?sfvrsn=3662fcb6_2)			
nCoV_IP4-14059Fw	GGT AAC TGG TAT GAT TTC G	14080-14098	107 bp
nCoV_IP4-14146Rv	CTG GTC AAG GTT AAT ATA GG	14186-14167	
nCoV_IP4-14084Probe(+)	FAM-TCATACAAACCACGCCAGG-BHQ-1	14105-14123	
sgRNA ORF7a			
sgRNA-Lead-2F	CCA GGT AAC AAA CCA ACC AAC T	20-41	133bp
sgRNA-ORF7a-2R	ACC TCT AAC ACA CTC TTG GTA G	27471-27450	
sgRNA-ORF7a-2FAM	FAM-TCT TGG CAC TGA TAA CAC TCG CTA CT-BHQ1	27410-27435	

39   *position according to accession number NC_045512

40

41   Fig. S1
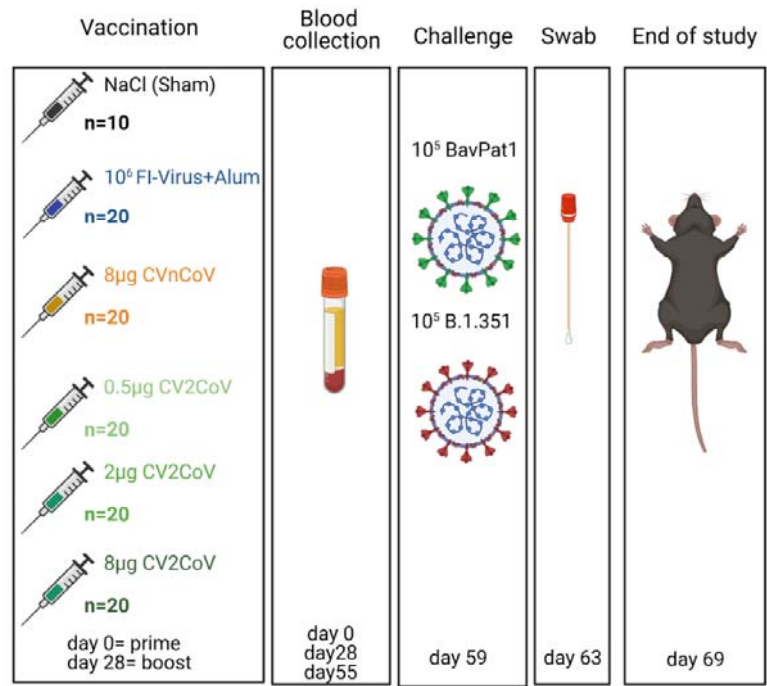
42

43   **Fig.S1. Experimental design.** K18-hACE2 mice were either vaccinated at day 0 (prime) and day 28

44   (boost) i.m. with 20µl of 8µg CVnCoV, 0.5µg CV2CoV, 2µg CV2CoV, 8µg CV2CoV or received 20µl

45   NaCl (Sham) or 20µl of 10^6 TCID$_{50}$ FI-Virus+2%Alhydrogel® in PBS which served as control groups.

46   Blood samples were collected at day 0, day 28 and day 55. Mice were either challenged with 10^5 SARS-

47   CoV-2 BavPat1 (Sham n=4, FI-Virus n=10, CVnCoV n=10) or 10^5 B.1.351 (Sham n=5, FI-Virus n=10,

48   CVnCoV n=10) at day 59 for a total of 10 days. An oral swab was taken at day 4. Viral load was

49   determined in selected organs at day 10 or when animals reached the humane endpoint of the study.

50   Image was generated using the illustration software Biorender (Biorender.com)

51

52

53   Fig. S2
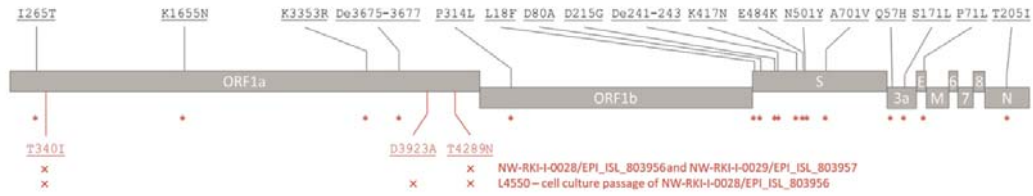
56   **Fig.S2 Cell culture passage of the VOC B.1.351 NW-RKI-I-0028 strain did not alter genome**

57   **sequence of the challenge virus stock L4550.** All characteristic mutations of VOC B.1.351 (upper

58   panel) were detected in the deeply sequenced stock of the challenge virus B.1.351 NW-RKI-I-0028

59   (L4550) as marked by red asterisks. Additional alterations for the B.1.351 NW-RKI-I-0028 and NW-

60   RKI-I-0029 strains and L4550 cell culture passage are shown (lower panel). Mean coverage of the virus

61   genome sequence of L4550 was 13,184 (± 7,958.4) reads. No single nucleotide polymorphism variants

62   were detected in the mutations (L18F, D80A, D215G, deletion De241-243, K417N, E484K, N501Y,

63   A701V) and in the cleavage site of the spike glycoprotein.

66   Fig. S3

67
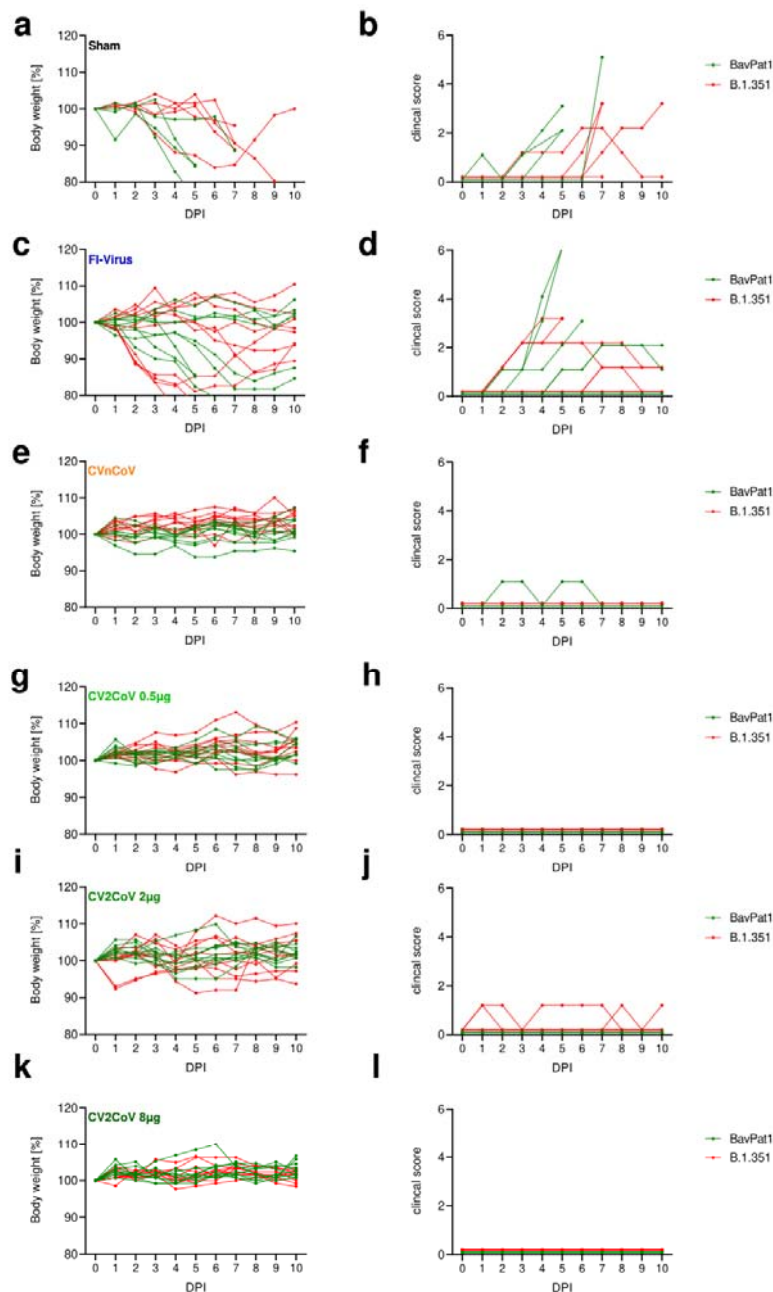
68

69   **Fig. S3 CVnCoV and CV2CoV protect K18-hACE2 mice against SARS-CoV-2 variants BavPat1**

70   **and B.1.351.** K18-hACE2 mice were vaccinated and challenged with SARS-CoV-2 variants BavPat1

71   or B.1.351 as indicated in Fig. 1. (**A, C, E, G, I, K**) Body weight and (**B, D, F, H, J, L**) clinical score

72   for K18-hACE2 mice in the (**A** and **B**) SHAM, (**C** and **D**) FI-Virus, (**E** and **F**) CVnCoV, (**G** and **H**)

73   CV2CoV 0.5µg, (**G** and **H**) CV2CoV 2µg, and (**G** and **H**) CV2CoV 8µg groups was monitored daily.

74   Lines represent individual animals over the course of the experiment (BavPat1 = green; B.1.351 =

75   red).

CHAPTER V: DISCUSSION

V.   DISCUSSION

Wild-life and livestock species are an unendingly reservoir for pathogens, of which a steadily growing fraction are associated with human infections. Such zoonoses are, according to OIE, responsible for approximately 60% of human infectious diseases per year and around 75% of newly emerging infectious diseases have a zoonotic origin (OIE, 2021). Also, for SARS-CoV-2 the origin is located in a wildlife population, and the virus found its way into human population via inter-species transmission (Holmes et al., 2021).

The past months of the COVID-19 pandemic have demonstrated primacy of scientific findings to combat the consequences of a global SARS-CoV-2 spread for individuals, societies, nations, and the environment including various animal species. A great variety of questions have become important, of which three aspects are further illuminated in this thesis. First, the susceptibility of elected animals for SARS-CoV-2 infection was analyzed in experimental inoculation-studies; second, emerging SARS-CoV-2 variants were analyzed and characterized in comparison to precursor variants in a competitive transmission experiment in different animal models; and third, an infection-challenge study for vaccinated, highly permissive, animals was established, in order to test vaccine candidates.

Objective I: Testing different animal species for their susceptibility towards infection with SARS-CoV-2.　　　→ Publication I & II

One critical aspect of the COVID-19 pandemic is the susceptibility of livestock-species towards SARS-CoV-2 infection (Mallapaty, 2021b). For various infectious diseases affecting humans, livestocks' role in disease dynamics is evidenced, e.g. poultry and swine in Influenza-A virus spread, ruminants for Q-fever, or dogs and bats for rabies (Yassine et al., 2013, Shi et al., 2018, Sun et al., 2020a, Mancera Gracia et al., 2020, Van den Brom et al., 2015, Vega et al., 2020). Apparently, these species do not play a role for SARS-CoV-2 spread, still, the risk for farm-animal or wildlife species to harbor and replicate SARS-CoV-2 is not banned (Schlottau et al., 2020, Shi et al., 2020). Indisputable, SARS-CoV-2 permissive animal species, which show high susceptibility and establish efficient transmission chains, would fuel human SARS-CoV-2 cases. Hence, it is of utmost importance to identify susceptible animals. Here, susceptibility and

potential to act as SARS-CoV-2 reservoirs or as an animal model was analyzed, for two relevant animal species: cattle and bank voles.

Prerequisites for infectivity would be a contagiosity of SARS-CoV-2 in these species, and efficient intra-species transmission among predisposed populations. To test for natural susceptibility, a study must modulate natural exposure to a pathogen along predisposed transmission routes. In the present work, this could be achieved, by intranasal application of virus-containing droplets, or suspension, which is the natural route for respiratory pathogens and droplet-, or aerosol-based shedding (CDC, 2021e, WHO, 2020d).

Cattle, with an estimated population of 1.5 billion, is an important livestock species in many culture areas (FAO, 2010). Close proximity between cattle and humans has e.g. facilitated species-jump of the human CoV OC43 from a rodent-reservoir, via the cattle intermediate host, to humans (Corman et al., 2018). Besides, cattle are affected in a large scale by *Bovine CoV* (BCoV), a *betacoronavirus* (Vlasova and Saif, 2021). Both raising concerns about cattle's susceptibility for SARS-CoV-2, but also about their potential to serve as an intermediate host-like recombination-vessel, or a new reservoir for human infections.

Although two out of six cattle in the presented study were infected with SARS-CoV-2, presence of viral genome in collected specimen was only short-termed, and at relatively low rates. Specific antibodies were detected in these respective animals. Genome and antibody detection in only these two animals are indicative for a real replication, and pure sero-reaction due to contact to a non-replicating agent is not very likely. However, transmission to non-inoculated contact animals was not observed (see Publication I).

Interestingly, at least one animal was actively infected with BCoV at the time of the trial, and all animals showed sero-reactivity against BCoV. However, obvious clinical signs could not be observed. Actually, the very two cattle, which were SARS-CoV-2 genome positive did not show a relevant increase in anti-BCoV titers and the animal, which was tested BCoV-positive had no detectable SARS-CoV-2 genome. Furthermore, the animal showing the most drastic increase in specific anti-BCoV response was a contact animal, which remained SARS-CoV-2-negative during the whole experiment. Conclusively, together with lack of clinical signs upon BCoV or SARS-CoV-2 infection, there is no hint at a recombination event in any of the animals. Ultimately, it could be shown, that neither a high anti-BCoV titer could prevent, nor a low anti-BCoV titer could favor SARS-CoV-2 infection. Taking these findings together, there was no

indication for an antigenic-recombination between these two closely related viruses, nor evidence for any substantial serological cross-reactivity.

Besides livestock, also wildlife species might act as a reservoir host for human SARS-CoV-2 cases. Knowing about the high susceptibility of deer mice in the U.S., a close relative, the European bank vole, was considered a highly permissive candidate for endemic infections (Griffin et al., 2021, Fagre et al., 2021). Bank voles are among the most populous mammals in Europe and an important reservoir species for infections with zoonotic cowpox virus, hanta viruses, and tick-borne encephalitis virus (Stoltz et al., 2011).

In the presented study, all eight directly inoculated bank voles were tested positive for SARS-CoV-2 genome. Frequency of positive swabs varied depending on time and the respective sampling site. Oral and nasal swabs exhibited the highest genome loads. Sporadically swabs from the circum-anal region also tested positive, however reflecting higher cq-values (quantification cycle) only. Irregular pattern and occurrence of SARS-CoV-2 genome in these swabs resulted most likely from carry-over from the genome-contaminated litter to the fur, or grooming behavior, which could also account for carry-over of viral genome from the oral cavity to the respective body regions. However, the virus load in nasal tissue of one bank vole was sufficient to re-isolate infectious virus (see Publication II). Scenarios of transmission from SARS-CoV-2 infected predators, such as a pet-cat, or naturally infected *Mustelidae*-species, also endemic in bank vole habitats, to an index-bank vole seem possible. But, due to the lack of intra-species transmission in this study, the risk for SARS-CoV-2 to become endemic among bank vole populations is very low.

Besides deer mice, high susceptibility of mink and white tailed deer towards SARS-CoV-2 infection has been described; efficient SARS-CoV-2 intra-species transmission was reported for these species and also zoo-anthroponotic mink to human spill-over infections (Chandler et al., 2021, Palmer et al., 2021, Oude Munnink et al., 2021, Chaintoutis et al., 2021). Opposing cattle and bank voles to these species draws a more diverse picture: although the bank vole shows a higher permissiveness for infection than cattle, because each inoculated individual became infected, genome was detected only at marginal levels, hence for bank voles the probability of SARS-CoV-2 spread does by far not reach that of deer mice or white-tailed deer. In bank vole turbinalia, however, low-level genome detection was prolonged. Still, what is most important: intra-species transmission was not observed for either cattle or bank voles.

Though just this must be considered the crucial linchpin to elevated susceptibility and enduring spread of SARS-CoV-2 in these putative reservoir populations. Also, the capability of both species as models for SARS-CoV-2 infections is limited.

Because of their low "overall susceptibility", it must be denied that cattle farming can play an analog role as mink holdings do for SARS-CoV-2 spread; the same is true for other relevant livestock animals like chicken, ducks and pigs (Schlottau et al., 2020, Shi et al., 2020). Nevertheless, targeted sero-surveillance studies using e.g. multispecies SARS-CoV-2 antibody tests (Wernike et al., 2021) are recommended especially for cattle populations in order to exclude any adaptation of the virus and its spread. Furthermore, since experimental infection data are missing, field studies about the seroprevalence of European deer species like roe deer, fellow deer and red deer are suggested.

Even though bank voles and cattle seem neglectable in COVID-19 outbreak dynamics, the latter appear to be eligible for post-outbreak investigation. In high-density cattle population areas, they might serve as an indicator for a high-level prevalence of SARS-CoV-2 among humans. Likewise, screening for SARS-CoV-2 antibodies in bank voles, which are caught within rodent surveillance programs should be taken into consideration, as an early indicator for SARS-CoV-2 circulation among wild predator species.

Objective II: Characterization of SARS-CoV-2 variants in a multi-step, competitive transmission trial in different animal species. → Publication III & IV

Emerging so-called SARS-CoV-2 variants (of concern / interest, VOI/VOC) made the human COVID-19 pandemic much more diverse. This is particularly concerning because some variants are associated with altered biological traits such as preferential transmission, immune escape, or a changed immunogenic profile, and because clinical disease severity and hospitalization rates are associated with the variants' spread (Planas et al., 2021, Dyson et al., 2021, Twohig et al., 2021). Yet, variant characterization is hardly keeping step with variant emergence and spread. Self-evident, early experimental characterization of variants would gain valuable time, improve preparedness plans, and ease the development of optimized vaccines. In the discussed work, variant characterization was attempted with a multi-species, competitive transmission animal study.

A hierarchically designed set with the transgenic mouse model, expressing human ACE2 (hACE2), the Syrian hamster, and the ferret, was used for *in-vivo* fitness characterization of SARS-CoV-2 variants. Using co-inoculated donor animals, and matching them with transmission animals 1:1, allows evaluation of clinical and virologic features. Furthermore, the highly important questions of transmission and replicative dominance ("viral fitness") can be addressed; this was even possible over a two-passage transmission chain.

On a global scale, the first variant to replace the precursor strain, was characterized by a point mutation in S at amino acid position 614 (S-614), with an exchange from aspartic acid (D) to glycine (G) (Korber et al., 2020). While rather slight advantages for S-614G were observed *in-vitro*, the *in-vivo* studies described in this thesis provide clear evidence for a marked fitness advantage of S-614G, as compared to S-D614. All applied animal models underlined the dominant replication and transmissibility of S-614G, and all data point to the great importance of this mutation, which should actually mark the first VOC (see Publication III). Yet, SARS-CoV-2 variants are not limited to the D614G exchange: The Alpha, Beta, Gamma, and Delta variant arose subsequently, all carrying, beside others, the initial S-614G mutation.

Two VOCs, the Alpha and the Beta variant, were also tested in this study *in-vitro* and *in-vivo* by a similar approach. However, contrary to S-614G, *in-vitro* approaches were not as efficient in portraying fitness differences of the Alpha or Beta VOC versus the S-614G variant. To overcome these issues, again the animal models were used. In the hACE2 mouse model, dominance of Alpha over S-614G could be demonstrated, likewise in ferrets. Findings of the hamster model, however, were less clear cut: either variant was transmitted to contact animals and no clear advantage of one variant could be observed in directly inoculated animals. Yet, animals where Alpha was dominant had a higher probability to die from infection. On the other hand, the hamster model has revealed its advantages for testing the Beta variant against S-614G and Alpha: as also observed during the human COVID-19 pandemic in the field, the Beta VOC did not manage to become dominant in direct competition with the other variants. Additional to nasal shedding data, viral loads in the respiratory tract organs were determined, which mainly underlined the shedding and transmission results. Although some animals had a diverging ratio of two variants between the upper and the lower respiratory tract tissue, it could be shown, that for transmission and "overall-dominance" the virus ratio in the upper respiratory tract is relevant. For the clinical outcome, however, the

viral loads and induced cellular reactions in lower respiratory tract tissue seem to be critical, as one hamster, although S-614G was dominant in the upper respiratory tract, and dominantly transmitted, died due to large loads of Alpha in the lungs (see publication IV).

With this approach, limitations of *in-vitro* – only testing and characterization of SARS-CoV-2 variants become apparent. As demonstrated here, reliable modeling of variant fitness, can be achieved with a broad range of competitive transmission studies in multiple animal models only. Here, also high permissiveness for SARS-CoV-2 of the used species comes into account but also their individually varying susceptibility. Syrian hamsters are e.g. suitable to carve out major fitness advantages of one SARS-CoV-2 variant over another only. They might somewhat act like human "super-spreaders", which replicate SARS-CoV-2 to very high titers, and spread it very efficiently. They also act as a model for severe human disease with a quite high rate of animals showing severe disease progression or even fatalities (Francis et al., 2021). Ferrets, and also hACE2 expressing mice, however, seem to be a little more delicate when choosing between two variants, as they can bring out fitness advantages of two variants that are less drastic and that cannot be differentiated with the Syrian hamster model. Coming back to these bottleneck-models seems necessary, if a more balanced fitness of two variants can be observed in the hamster model.

Single virus infections in animals, or approaches without contact animals, do not manage to underline the full range of variant's fitness, as only single aspects can be illuminated (Mohandas et al., 2021, Abdelnabi et al., 2021). However, there is a possibility that this set of animal models might not be final and best-fitting, since with ongoing evolution of SARS-CoV-2 in humans, an increasing adaptation to "human conditions" must be expected. A second aspect is that data on dual co-infections of SARS-CoV-2 variants in humans is still limited and their frequency might be overestimated (Zhou et al., 2021a, Liu et al., 2021b, Lythgoe et al., 2021, Valesano et al., 2021). Hence, the chosen approaches might be a little bit artificial in this respect – although modulation of SARS-CoV-2 variant's dominance was successful this far, and other international groups have adopted this approach (Port et al., 2021, Mok et al., 2021). Both, the growing adaptation to humans and the picayune artificial character of the experiments, might also explain some unanticipated results, as equal fitness of the initial S-614G strain and the Alpha VOC in hamsters (see publication IV).

Regardless, with a balanced combination of these complementary models up the sleeves of SARS-CoV-2 research, a valuable and reliable tool for variant characterization and fitness modeling has been established. This is surely boosting the understanding and risk-analyses of emerging variants, in parallel, or even ahead of their global spread, which ultimately supports disease-preparedness.

Objective III: Developing a challenge-trial in highly SARS-CoV-2 susceptible animals for safety and efficacy testing of promising vaccine-precursors. → Publication V

Despite unprecedented effort in COVID-19 control, SARS-CoV-2 has spread globally, scotching all international pushes (Dong et al., 2020a, WHO, 2021a). Only a potent COVID-19 vaccine is considered to noteworthy breach the pandemic and allow societies to catch up with the virus (Harris et al., 2021, Shah et al., 2021, Rossman et al., 2021, Victora et al., 2021, Gavin and Dabrera, 2021).

While advantages of a COVID-19 vaccine are indisputable, licensing of a vaccine is rightly associated to grand and strict requirements, which have to be met by a vaccine candidate (Wagner et al., 2021, Baylor and Marshall, 2013). This includes safety of the vaccine in the first place: vaccine-related, severe side-effects must be excluded. Secondly vaccine efficacy must be experimentally confirmed. Criteria for effectiveness of a vaccine reach from reducing the amount of shed pathogen, to shortening the shedding interval, to reducing disease severity in vaccinated individuals, or even preventing clinical disease, just to a sterile immunity, that prevents either infection itself, limits pathogen replication to its entry site, or inhibits transmission of the pathogen to another susceptible individual (Hodgson et al., 2021). Naturally these first safety and efficacy testings need to be performed in animal models (FDA, 2021). Animals accounting for such vaccine testing, need to show a high permissiveness for SARS-CoV-2 infection on one hand; on the other hand, infection in these animals should be well characterized.

Under these preconditions, transgenic K18-hACE2 mice were chosen to test different precursor mRNA vaccine candidates (Gan et al., 2021, Lee et al., 2021). Not only because these mice show a very high susceptibility towards SARS-CoV-2 infection with well characterized, lethal disease outcome, but also because they are an easy-to-handle animal model, which can

be analyzed in large numbers. Additionally, K18-hACE2 mice develop very severe clinical signs upon SARS-CoV-2 infection, facilitating clinical evaluation using a pre-defined scoring system, including e.g. documentation of body weight changes (Winkler et al., 2020, Yinda et al., 2021, Sun et al., 2020b). However, the clinical signs and the disease outcome are also driven by the artificial infection, and a strong cytokine response in the brain of these mice, which is a consequence of the over-expression of the hACE2-receptor (Carossino et al., 2021, Chen et al., 2020, Oladunni et al., 2020, Kumari et al., 2021).

Two vaccine preparations in different concentrations were tested for their safety and efficacy in transgenic immunized K18-hACE2 mice in comparison to non-vaccinated control animals and a vaccine consisting of inactivated virions. The animals were vaccinated in a prime-boost regime with 28 days between the vaccinations, followed by challenge on day 59 with either a reference SARS-CoV-2 isolate or VOC Beta. The deployed challenge dose was chosen quite high, to firstly guarantee for infection and secondly kill unprotected, naïve mice after such a challenge infection.

With this approach, clinical evaluation of the vaccinated, and challenged mice becomes possible and could be demonstrated in the presented study. Vaccine-related side effects were not evident, and clinical signs of SARS-CoV-2 infection were not observed in vaccinated mice post-challenge. All vaccinated mice had a 10-day survival of 100% following challenge infection. Furthermore, serologic responses of vaccinated and challenged mice were evaluated by collecting a small blood sample from the animals, which showed, that each vaccinated mouse developed detectable anti-SARS-CoV-2 serum antibody titers before challenge infection (see publication V).

To gain evidence on the efficacy of the tested vaccine, not only clinical features, but also viral shedding was evaluated by a regular swabbing routine. Additionally, viral loads in organs of sacrificed animals were determined. Comparing these findings between vaccinated and non-vaccinated animals allowed conclusions on how reliably a vaccine can prevent infection and transmission, but also systemic dissemination of a pathogen. Here, it was shown, that viral shedding could not be detected by oral swabbing, which hints at sterile immunity. However, in some organ samples residual viral RNA was found at very low levels. To test for the presence of replicating virus, these samples were retested, to detect subgenomic RNA. Since in most samples subgenomic RNA was not present, it can be assumed, that replication either did not

occur in these tissues, or only at a very basal level (Wong et al., 2021). Anyway, this falsifies the initial assumption, that vaccination led to a complete sterile immunity – anyhow virus shedding was suppressed.

Furthermore, vaccine efficacy was compared to sham-vaccinated animals, to guarantee for the virulence of the challenge virus, and animals, which had received a non-commercial, formaldehyde inactivated whole virus preparation to ensure that the observed effects can be led back to vaccination with the candidate mRNA vaccines. Interestingly, sham vaccinated and Beta-challenged mice developed a slower disease progression and challenge infection was less lethal on a group level, than for the respective mice, which were challenged with the reference SARS-CoV-2 isolate (see Publication V).

With the presented vaccination-challenge k18-ACE2 mouse model, safety and efficacy, also regarding development of a sterile immune response, of promising COVID-19 vaccine candidates can be reliably tested in a standardized, highly permissive, easy-to-handle animal model, before starting clinical studies in humans. The possibility to test vaccines against emerging SARS-CoV-2 variants adds further importance to this animal model (Abdool Karim and de Oliveira, 2021). However, it has to be mentioned that this highly valuable mouse model is very reactive and very high antibody titers can be observed following double immunization. Therefore, the dosages should be adapted as it was also done in other SARS-CoV-2-studies with transgenic mice (Liu et al., 2021a).

Concluding remarks

Animal models are of high importance and relevance in zoonoses research. The same holds true also for the COVID-19 pandemic, and animal models are crucial at different stages of the pandemic. Initially, the susceptibility of different species for SARS-CoV-2 is a topic of interest. Concomitant with these first steps, SARS-CoV-2 infection is characterized in animal models, and the field is extended to characterization of SARS-CoV-2 variants. Ultimately, animal models are needed to test specific immunoprophylactic and antiviral strategies, and therapies against SARS-CoV-2. The different animal models and approaches presented in this thesis support research progression with a comprehensive contribution employable at any stage of the pandemic.

CHAPTER V: SUMMARY

VI. SUMMARY

High consequence severe acute respiratory syndrome coronavirus 2 (SARS-CoV-2) is the youngest among known human coronaviruses. SARS-CoV-2 may cause severe disease in humans (COVID-19) and has affected every-day life in an unprecedented manner. Total number of cases and fatalities have reached an inconceivable level within only two years after the index case and are still increasing. The zoonotic SARS-CoV-2 has emerged in an animal reservoir and was transmitted to humans, triggering a pandemic wave. Besides humans, also some animal species have shown very high susceptibility towards infection with SARS-CoV-2, which can also lead to severe clinics in these species. Another major factor in COVID-19 pandemic is the continuing evolution of the virus and the ongoing emergence of new viral variants. The first year of the pandemic with its undamped SARS-CoV-2 spread has accentuated the importance for countermeasures to temper further dissemination and protect humans – most ideally with potent vaccines. Additionally, an improved understanding of SARS-CoV-2 biology, evolution, and emergence will be eminent to substantiate efficient control of COVID-19. Animal models are a substantial cornerstone on which research efforts are based. They are unexcelled to modulate pathogenesis and epidemiology of SARS-CoV-2 in a true-to-life approach. This cumulative thesis introduces, establishes, discusses, and synergizes three experimental settings in different animal models, to substantially add to knowledge in indexing animals' susceptibility for SARS-CoV-2, characterizing SARS-CoV-2 variants of concern, and testing vaccine-candidates.

Species susceptibility towards infection with SARS-CoV-2 was tested in an experimental transmission study, with directly inoculated donor animals. To test for transmission, virus-naïve contact animals were co-housed one day post inoculation. Subsequently, all animals were checked for clinical signs and relevant clinical specimen were collected. With this approach, SARS-CoV-2 infection in cattle and bank voles was tested. Both species revealed a very low susceptibility for this pathogen and transmission to in-contact conspecifics was not observed albeit bank voles' susceptibility is considered marginally higher than that of cattle.

In further studies, the fitness of virus variants, defined by replication efficiency and transmissibility, was characterized. In a competitive transmission experiment, one donor animal was experimentally co-inoculated with two variants simultaneously; thereupon each

donor was cohoused with a naïve transmission animal; for some variants, also second cycle transmission to another direct contact animal was investigated. Ferrets, transgenic hACE2 mice, and Syrian hamsters were used in the different experiments. With these models, dominance of the S-614G or the Alpha variant over precursor virus S-D614 and the Beta variant could be demonstrated.

Finally, the safety and efficacy of SARS-CoV-2 mRNA-vaccines were tested in an immunization-challenge trial. Groups of K18-hACE2 mice were challenged with two different SARS-CoV-2 variants after a prime-boost vaccination regime. With this model, a suitable approach to test vaccine safety and efficacy in a highly susceptible animal model was established; furthermore, the vaccine candidate itself was successfully tested, and the virulence of the different SARS-CoV-2 variants, which were used for challenge, could be evaluated.

Challenges in SARS-CoV-2 / COVID-19 pandemic are manifold. With the presented bundle of animal models for SARS-CoV-2 research, however, a profound base for the future, when we will need to cope with this pathogen, is set. Further questions will arise addressing reservoir species and the susceptibility of animals towards new SARS-CoV-2 variants, but also the risk-potential of further emerging variants. These experimental approaches can then easily be adapted to modified conditions and problems. When, hopefully, the quest for potent vaccines will even speed up and also new approaches and strategies for vaccination are pursued, reliable immunization-challenge models as presented in this study are of utmost importance. With these promising experimental approaches, mankind is forearmed to pit against the forces of SARS-CoV-2.

1. ZUSAMMENFASSUNG

Das *severe acute respiratory syndrome coronavirus 2,* SARS-CoV-2 (schweres, akutes, respiratorisches Syndrom Coronavirus 2) ist der jüngste Vertreter der bekannten Coronaviren des Menschen und Auslöser der *coronavirus disease-19*, COVID-19 (Coronavirus Krankheit 2019). SARS-CoV-2 kann bei Infizierten schwerwiegende Erkrankungen auslösen und hat das gesellschaftliche Leben in bis dato unbegreiflichem Ausmaß gewandelt. Die noch immer steigenden Erkrankungs- und Todeszahlen haben in den lediglich zwei Jahren nach Diagnose des ersten Indexfalles unvorstellbare Höhen erreicht. Als zoonotisches Virus entstand SARS-CoV-2 ursprünglich in einem Tierwirt, ist dann auf den Menschen übergesprungen, und hat

damit die Pandemie ins Rollen gebracht. Außer dem Menschen zeigen auch einige Tierarten eine sehr hohe Empfänglichkeit für dieses Virus – teilweise löst es auch bei ihnen sehr schwere klinische Verläufe aus. Ein sehr wesentlicher Treiber der Pandemie ist die ständige Evolution neuer Virusvarianten. Die ersten Monate der SARS-CoV-2 Pandemie haben bewiesen, dass sich das Virus fast ungehindert verbreiten kann und daher weitere Gegenmaßnahmen ergriffen werden müssen, um den Menschen zu schützen - im besten Falle durch Impfungen. Dennoch ist gerade eine verbesserte Kenntnis der SARS-CoV-2 Virusbiologie und seiner Entstehung grundlegend für eine erfolgreiche Bekämpfung. Dafür sind Tiermodelle eine unersetzliche Grundlage. Tierversuche dienen in besonderer Weise der Erforschung der Viruspathogenese und Epidemiologie in einem Organismus. Diese kumulative Doktorarbeit stellt drei unterschiedliche experimentelle Tierversuchsansätze für die SARS-CoV-2 Forschung vor, um einerseits die Empfänglichkeit unterschiedlicher Tierarten für SARS-CoV-2 zu bestimmen, neue Varianten zu charakterisieren und andererseits ein Tiermodell zur Testung von Impfstoffkandidaten zu etablieren.

Die Empfänglichkeit unterschiedlicher Tierarten für SARS-CoV-2 wurde in einer Transmissionsstudie mit experimentell inokulierten Donortieren und virus-negativen Kontakttieren, auf die das Virus möglicherweise übertragen wird und die einen Tag nach Inokulation zugestallt werden, ermittelt. Alle Tiere wurden regelmäßig klinisch untersucht und beprobt. Auf diese Weise wurde die Empfänglichkeit von Rindern und Rötelmäusen getestet. Obschon die Empfänglichkeit beider Arten sehr gering bzw. gering war und das Virus nicht auf Kontakttiere übertragen werden konnte, zeigten Rötelmäuse eine etwas höhere Empfänglichkeit als Rinder.

In einem weiteren experimentellen Ansatz wurde die Fitness von Virusvarianten, definiert durch replikative Dominanz und präferierte Übertragbarkeit, getestet. Hierfür wurde jeweils ein Donortier gleichzeitig mit einem Gemisch zweier Varianten ko-inokuliert. Kontakttiere wurden zugestallt und in einigen Teilversuchen auch ein zweites Kontakttier, um Infektionsketten simulieren zu können. Die Versuche an Frettchen, transgenen hACE2-Mäusen und Goldhamstern konnten eine Dominanz der S-614G und der Alpha Variante gegenüber der Ursprungsvariante S-D614 und auch der Beta Variante nachweisen.

Außerdem wurde ein Infektionsmodell an K18-hACE2 Mäusen etabliert, um die Sicherheit und Wirksamkeit von SARS-CoV-2 mRNA Impfstoffkandidaten zu untersuchen. Nach Erst- und

Zweitimpfung wurden die K18-ACE2 Mäuse experimentell mit jeweils einer von zwei Virusvarianten infiziert. In diesem Versuch konnte gezeigt werden, dass der Impfstoffkandidat sowohl sicher als auch wirksam war. Darüber hinaus konnte die Virulenz der verschiedenen verwendeten SARS-CoV-2-Varianten bestimmt werden.

Die durch SARS-CoV-2 / COVID-19 ausgelösten Herausforderungen sind vielfältig. Die unterschiedlichen in dieser Arbeit vorgestellten Tiermodelle für die SARS-CoV-2 Forschung tragen diesem Umstand Rechnung und bilden eine gute Grundlage, um sich in Zukunft erfolgreich mit dem Virus auseinandersetzen zu können. Die in dieser Arbeit etablierten Tiermodelle können ohne Weiteres an zukünftige Fragen nach der Empfänglichkeit und dem Gefahrenpotential weiterer Varianten angepasst werden. Zusätzlich ist ein zuverlässiges Modell zur Impfstofftestung nach dem Muster des hier vorgestellten besonders hilfreich, um die Impfstoffentwicklung weiter zu beschleunigen und bei der Suche nach optimierten Vakzinen zu unterstützen. Insbesondere mit diesem vielfältigen wissenschaftlichen Rüstzeug wird man den Herausforderungen von SARS-CoV-2 begegnen können.

CHAPTER VII: REFERENCES

VII. References

ABDELNABI, R., BOUDEWIJNS, R., FOO, C. S., SELDESLACHTS, L., SANCHEZ-FELIPE, L., ZHANG, X., DELANG, L., MAES, P., KAPTEIN, S. J. F., WEYNAND, B., VANDE VELDE, G., NEYTS, J. & DALLMEIER, K. 2021. Comparing infectivity and virulence of emerging SARS-CoV-2 variants in Syrian hamsters. *EBioMedicine,* 68**,** 103403.

ABDOOL KARIM, S. S. & DE OLIVEIRA, T. 2021. New SARS-CoV-2 Variants - Clinical, Public Health, and Vaccine Implications. *N Engl J Med,* 384**,** 1866-1868.

ADDIE, D. D., SCHAAP, I. A. T., NICOLSON, L. & JARRETT, O. 2003. Persistence and transmission of natural type I feline coronavirus infection. *J Gen Virol,* 84**,** 2735-2744.

AHRENFELDT, L. J., OTAVOVA, M., CHRISTENSEN, K. & LINDAHL-JACOBSEN, R. 2021. Sex and age differences in COVID-19 mortality in Europe. *Wien Klin Wochenschr,* 133**,** 393-398.

ALEXANDERSEN, S., CHAMINGS, A. & BHATTA, T. R. 2020. SARS-CoV-2 genomic and subgenomic RNAs in diagnostic samples are not an indicator of active replication. *Nat Commun,* 11**,** 6059.

ANDERSEN, K. G., RAMBAUT, A., LIPKIN, W. I., HOLMES, E. C. & GARRY, R. F. 2020. The proximal origin of SARS-CoV-2. *Nat Med,* 26**,** 450-452.

ANDRIKOPOULOU, M., MADDEN, N., WEN, T., AUBEY, J. J., AZIZ, A., BAPTISTE, C. D., BRESLIN, N., D'ALTON, M. E., FUCHS, K. M., GOFFMAN, D., GYAMFI-BANNERMAN, C., MATSEOANE-PETERSSEN, D. N., MILLER, R. S., SHEEN, J. J., SIMPSON, L. L., SUTTON, D., ZORK, N. & FRIEDMAN, A. M. 2020. Symptoms and Critical Illness Among Obstetric Patients With Coronavirus Disease 2019 (COVID-19) Infection. *Obstet Gynecol,* 136**,** 291-299.

ARYA, R., KUMARI, S., PANDEY, B., MISTRY, H., BIHANI, S. C., DAS, A., PRASHAR, V., GUPTA, G. D., PANICKER, L. & KUMAR, M. 2021. Structural insights into SARS-CoV-2 proteins. *J Mol Biol,* 433**,** 166725.

AZAD, G. K. & KHAN, P. K. 2021. Variations in Orf3a protein of SARS-CoV-2 alter its structure and function. *Biochem Biophys Rep,* 26**,** 100933.

AZIZ, M., PERISETTI, A., LEE-SMITH, W. M., GAJENDRAN, M., BANSAL, P. & GOYAL, H. 2020. Taste Changes (Dysgeusia) in COVID-19: A Systematic Review and Meta-analysis. *Gastroenterology,* 159**,** 1132-1133.

BAYLOR, N. W. & MARSHALL, V. B. 2013. Regulation and testing of vaccines. *Vaccines*.

BEAN, A. G., BAKER, M. L., STEWART, C. R., COWLED, C., DEFFRASNES, C., WANG, L. F. & LOWENTHAL, J. W. 2013. Studying immunity to zoonotic diseases in the natural host - keeping it real. *Nat Rev Immunol,* 13**,** 851-61.

BERGUIDO, F. J., BURBELO, P. D., BORTOLAMI, A., BONFANTE, F., WERNIKE, K., HOFFMANN, D., BALKEMA-BUSCHMANN, A., BEER, M., DUNDON, W. G., LAMIEN, C. E. & CATTOLI, G. 2021. Serological Detection of SARS-CoV-2 Antibodies in Naturally-Infected Mink and Other Experimentally-Infected Animals. *Viruses,* 13.

BESTLE, D., HEINDL, M. R., LIMBURG, H., VAN LAM VAN, T., PILGRAM, O., MOULTON, H., STEIN, D. A., HARDES, K., EICKMANN, M., DOLNIK, O., ROHDE, C., KLENK, H. D., GARTEN, W., STEINMETZER, T. & BOTTCHER-FRIEBERTSHAUSER, E. 2020. TMPRSS2 and furin are both essential for proteolytic activation of SARS-CoV-2 in human airway cells. *Life Sci Alliance,* 3.

BIANCHI, M., BENVENUTO, D., GIOVANETTI, M., ANGELETTI, S., CICCOZZI, M. & PASCARELLA, S. 2020. Sars-CoV-2 Envelope and Membrane Proteins: Structural Differences Linked to Virus Characteristics? *Biomed Res Int,* 2020**,** 4389089.

BLOOM, J. D. 2021. Recovery of deleted deep sequencing data sheds more light on the early Wuhan SARS-CoV-2 epidemic. *bioRxiv***,** 2021.06.18.449051.

BONTEMPI, E. & COCCIA, M. 2021. International trade as critical parameter of COVID-19 spread that outclasses demographic, economic, environmental, and pollution factors. *Environ Res,* 201**,** 111514.

References

BOSON, B., LEGROS, V., ZHOU, B., SIRET, E., MATHIEU, C., COSSET, F. L., LAVILLETTE, D. & DENOLLY, S. 2021. The SARS-CoV-2 envelope and membrane proteins modulate maturation and retention of the spike protein, allowing assembly of virus-like particles. *J Biol Chem,* 296**,** 100111.

BRIAN, D. A. & BARIC, R. S. 2005. Coronavirus genome structure and replication. *Curr Top Microbiol Immunol,* 287**,** 1-30.

BYAMBASUREN, O., CARDONA, M., BELL, K., CLARK, J., MCLAWS, M.-L. & GLASZIOU, P. 2020. Estimating the extent of asymptomatic COVID-19 and its potential for community transmission: Systematic review and meta-analysis. *Official Journal of the Association of Medical Microbiology and Infectious Disease Canada,* 5**,** 223-234.

CALDAS, L. A., CARNEIRO, F. A., HIGA, L. M., MONTEIRO, F. L., DA SILVA, G. P., DA COSTA, L. J., DURIGON, E. L., TANURI, A. & DE SOUZA, W. 2020. Ultrastructural analysis of SARS-CoV-2 interactions with the host cell via high resolution scanning electron microscopy. *Sci Rep,* 10**,** 16099.

CALLAWAY, E. 2021. 'A bloody mess': Confusion reigns over naming of new COVID variants. *Nature,* 589**,** 339.

CANTUTI-CASTELVETRI, L., OJHA, R., PEDRO, L. D., DJANNATIAN, M., FRANZ, J., KUIVANEN, S., VAN DER MEER, F., KALLIO, K., KAYA, T., ANASTASINA, M., SMURA, T., LEVANOV, L., SZIROVICZA, L., TOBI, A., KALLIO-KOKKO, H., OSTERLUND, P., JOENSUU, M., MEUNIER, F. A., BUTCHER, S. J., WINKLER, M. S., MOLLENHAUER, B., HELENIUS, A., GOKCE, O., TEESALU, T., HEPOJOKI, J., VAPALAHTI, O., STADELMANN, C., BALISTRERI, G. & SIMONS, M. 2020. Neuropilin-1 facilitates SARS-CoV-2 cell entry and infectivity. *Science,* 370**,** 856-860.

CAO, C., CAI, Z., XIAO, X., RAO, J., CHEN, J., HU, N., YANG, M., XING, X., WANG, Y., LI, M., ZHOU, B., WANG, X., WANG, J. & XUE, Y. 2021. The architecture of the SARS-CoV-2 RNA genome inside virion. *Nat Commun,* 12**,** 3917.

CARFI, A., BERNABEI, R., LANDI, F. & GEMELLI AGAINST, C.-P.-A. C. S. G. 2020. Persistent Symptoms in Patients After Acute COVID-19. *JAMA,* 324**,** 603-605.

CAROSSINO, M., MONTANARO, P., O'CONNELL, A., KENNEY, D., GERTJE, H., GROSZ, K. A., KURNICK, S. A., BOSMANN, M., SAEED, M., BALASURIYA, U. B. R., DOUAM, F. & CROSSLAND, N. A. 2021. Fatal neuroinvasion of SARS-CoV-2 in K18-hACE2 mice is partially dependent on hACE2 expression. *bioRxiv*.

CARROLL, E., NEUMANN, H., AGUERO-ROSENFELD, M. E., LIGHTER, J., CZEISLER, B. M., MELMED, K. & LEWIS, A. 2020. Post-COVID-19 inflammatory syndrome manifesting as refractory status epilepticus. *Epilepsia,* 61**,** e135-e139.

CASAS-ROJO, J. M., ANTÓN-SANTOS, J. M., MILLÁN-NÚÑEZ-CORTÉS, J., LUMBRERAS-BERMEJO, C., RAMOS-RINCÓN, J. M., ROY-VALLEJO, E., ARTERO-MORA, A., ARNALICH-FERNÁNDEZ, F., GARCÍA-BRUÑÉN, J. M., VARGAS-NÚÑEZ, J. A., FREIRE-CASTRO, S. J., MANZANO-ESPINOSA, L., PERALES-FRAILE, I., CRESTELO-VIÉITEZ, A., PUCHADES-GIMENO, F., RODILLA-SALA, E., SOLÍS-MARQUÍNEZ, M. N., BONET-TUR, D., FIDALGO-MORENO, M. P., FONSECA-AIZPURU, E. M., CARRASCO-SÁNCHEZ, F. J., RABADÁN-PEJENAUTE, E., RUBIO-RIVAS, M., TORRES-PEÑA, J. D. & GÓMEZ-HUELGAS, R. 2020. Clinical characteristics of patients hospitalized with COVID-19 in Spain: results from the SEMI-COVID-19 Registry. *Revista Clínica Española (English Edition),* 220**,** 480-494.

CAVANAGH, D. 2007. Coronavirus avian infectious bronchitis virus. *Vet Res,* 38, 281-97.

CDC, C. F. D. C. A. P. 2021a. *Interim Guidelines for COVID-19 Antibody Testing* [Online]. Available: https://www.cdc.gov/coronavirus/2019-ncov/lab/resources/antibody-tests-guidelines.html [Accessed 01.10.2021].

CDC, C. F. D. C. A. P. 2021b. *People with Certain Medical Conditions* [Online]. Available: https://www.cdc.gov/coronavirus/2019-ncov/need-extra-precautions/people-with-medical-conditions.html [Accessed 01.10.2021].

CDC, C. F. D. C. A. P. 2021c. *SARS-CoV-2 Variant Classifications and Definitions* [Online]. Available: https://www.cdc.gov/coronavirus/2019-ncov/variants/variant-info.html [Accessed 14.09.2021].

CDC, C. F. D. C. A. P. 2021d. *Symptoms of COVID-19* [Online]. Available: https://www.cdc.gov/coronavirus/2019-ncov/symptoms-testing/symptoms.html [Accessed 01.10.2021].

CDC, C. F. D. C. A. P. N. C. F. I. A. R. D. N. D. O. V. D. 2021e. *Scientific Brief: SARS-CoV-2 Transmission* [Online]. Available: https://www.cdc.gov/coronavirus/2019-ncov/science/science-briefs/sars-cov-2-transmission.html [Accessed 01.10.2021].

CHAINTOUTIS, S. C., THOMOU, Z., MOUCHTAROPOULOU, E., TSIOLAS, G., CHASSALEVRIS, T., STYLIANAKI, I., LAGOU, M., MICHAILIDOU, S., MOUTOU, E., KOENEN, J. J. H., DIJKSHOORN, J. W., PARASKEVIS, D., POUTAHIDIS, T., SIARKOU, V. I., SYPSA, V., ARGIRIOU, A., FORTOMARIS, P. & DOVAS, C. I. 2021. Outbreaks of SARS-CoV-2 in naturally infected mink farms: Impact, transmission dynamics, genetic patterns, and environmental contamination. *PLoS Pathog,* 17**,** e1009883.

CHAN, J. F., KOK, K. H., ZHU, Z., CHU, H., TO, K. K., YUAN, S. & YUEN, K. Y. 2020. Genomic characterization of the 2019 novel human-pathogenic coronavirus isolated from a patient with atypical pneumonia after visiting Wuhan. *Emerg Microbes Infect,* 9**,** 221-236.

CHANDLER, J. C., BEVINS, S. N., ELLIS, J. W., LINDER, T. J., TELL, R. M., JENKINS-MOORE, M., ROOT, J. J., LENOCH, J. B., ROBBE-AUSTERMAN, S., DELIBERTO, T. J., GIDLEWSKI, T., TORCHETTI, M. K. & SHRINER, S. A. 2021. SARS-CoV-2 exposure in wild white-tailed deer (Odocoileus virginianus). *bioRxiv,* 2021.07.29.454326.

CHEN, R., WANG, K., YU, J., HOWARD, D., FRENCH, L., CHEN, Z., WEN, C. & XU, Z. 2020. The Spatial and Cell-Type Distribution of SARS-CoV-2 Receptor ACE2 in the Human and Mouse Brains. *Front Neurol,* 11**,** 573095.

CLARK, L. K., GREEN, T. J. & PETIT, C. M. 2021. Structure of Nonstructural Protein 1 from SARS-CoV-2. *J Virol,* 95.

CLARK, M. A. 1993. Bovine coronavirus. *British Veterinary Journal,* 149**,** 51-70.

CORMAN, V. M., MUTH, D., NIEMEYER, D. & DROSTEN, C. 2018. Hosts and Sources of Endemic Human Coronaviruses. *Adv Virus Res,* 100**,** 163-188.

CORONAVIRIDAE STUDY GROUP OF THE INTERNATIONAL COMMITTEE ON TAXONOMY OF VIRUSES 2020. The species Severe acute respiratory syndrome-related coronavirus: classifying 2019-nCoV and naming it SARS-CoV-2. *Nat Microbiol,* 5**,** 536-544.

CORONAVIRUSES, V. 1968. Virology: Coronaviruses. *Nature,* 220**,** 650-650.

COTTAM, E. M., WHELBAND, M. C. & WILEMAN, T. 2014. Coronavirus NSP6 restricts autophagosome expansion. *Autophagy,* 10**,** 1426-41.

CUBUK, J., ALSTON, J. J., INCICCO, J. J., SINGH, S., STUCHELL-BRERETON, M. D., WARD, M. D., ZIMMERMAN, M. I., VITHANI, N., GRIFFITH, D., WAGONER, J. A., BOWMAN, G. R., HALL, K. B., SORANNO, A. & HOLEHOUSE, A. S. 2021. The SARS-CoV-2 nucleocapsid protein is dynamic, disordered, and phase separates with RNA. *Nat Commun,* 12**,** 1936.

CUI, J., LI, F. & SHI, Z. L. 2019. Origin and evolution of pathogenic coronaviruses. *Nat Rev Microbiol,* 17**,** 181-192.

DAVIS, J. T., CHINAZZI, M., PERRA, N., MU, K., PIONTTI, A. P. Y., AJELLI, M., DEAN, N. E., GIOANNINI, C., LITVINOVA, M., MERLER, S., ROSSI, L., SUN, K., XIONG, X., HALLORAN, M. E., LONGINI, I. M., VIBOUD, C. & VESPIGNANI, A. 2021. Cryptic transmission of SARS-CoV-2 and the first COVID-19 wave in Europe and the United States. *medRxiv*.

DE HAAN CA, R. P. 2005. Molecular interactions in the assembly of coronaviruses. *Adv Virus Res.,* 64**,** 165-230.

DECROLY, E., DEBARNOT, C., FERRON, F., BOUVET, M., COUTARD, B., IMBERT, I., GLUAIS, L., PAPAGEORGIOU, N., SHARFF, A., BRICOGNE, G., ORTIZ-LOMBARDIA, M., LESCAR, J. & CANARD, B. 2011. Crystal structure and functional analysis of the SARS-coronavirus RNA cap 2'-O-methyltransferase nsp10/nsp16 complex. *PLoS Pathog,* 7**,** e1002059.

DOMINGUEZ ANDRES, A., FENG, Y., CAMPOS, A. R., YIN, J., YANG, C. C., JAMES, B., MURAD, R., KIM, H., DESHPANDE, A. J., GORDON, D. E., KROGAN, N., PIPPA, R. & RONAI, Z. A. 2020. SARS-CoV-2 ORF9c Is a Membrane-Associated Protein that Suppresses Antiviral Responses in Cells. *bioRxiv*.

References

DONG, E., DU, H. & GARDNER, L. 2020a. An interactive web-based dashboard to track COVID-19 in real time. *The Lancet Infectious Diseases,* 20**,** 533-534.

DONG, R., PEI, S., YIN, C., HE, R. L. & YAU, S. S. 2020b. Analysis of the Hosts and Transmission Paths of SARS-CoV-2 in the COVID-19 Outbreak. *Genes (Basel),* 11.

DRAKE, J. W. & HOLLAND, J. J. 1999. Mutation rates among RNA viruses. *Proc Natl Acad Sci U S A,* 96**,** 13910-3.

DREIER, E., MALFERTHEINER, M. V., DIENEMANN, T., FISSER, C., FOLTAN, M., GEISMANN, F., GRAF, B., LUNZ, D., MAIER, L. S., MULLER, T., OFFNER, R., PETERHOFF, D., PHILIPP, A., SALZBERGER, B., SCHMIDT, B., SINNER, B. & LUBNOW, M. 2021. ECMO in COVID-19-prolonged therapy needed? A retrospective analysis of outcome and prognostic factors. *Perfusion,* 36**,** 582-591.

DREXLER, J. F., CORMAN, V. M. & DROSTEN, C. 2014. Ecology, evolution and classification of bat coronaviruses in the aftermath of SARS. *Antiviral Res,* 101**,** 45-56.

DU TOIT, A. 2020. Coronavirus replication factories. *Nat Rev Microbiol,* 18**,** 411.

DUAN, L., ZHENG, Q., ZHANG, H., NIU, Y., LOU, Y. & WANG, H. 2020. The SARS-CoV-2 Spike Glycoprotein Biosynthesis, Structure, Function, and Antigenicity: Implications for the Design of Spike-Based Vaccine Immunogens. *Front Immunol,* 11**,** 576622.

DYSON, L., HILL, E. M., MOORE, S., CURRAN-SEBASTIAN, J., TILDESLEY, M. J., LYTHGOE, K. A., HOUSE, T., PELLIS, L. & KEELING, M. J. 2021. Possible future waves of SARS-CoV-2 infection generated by variants of concern with a range of characteristics. *Nature Communications,* 12.

EA, J. A. & JONES, I. M. 2019. Membrane binding proteins of coronaviruses. *Future Virol,* 14**,** 275-286.

ELIAS, C., SEKRI, A., LEBLANC, P., CUCHERAT, M. & VANHEMS, P. 2021. The incubation period of COVID-19: A meta-analysis. *Int J Infect Dis,* 104**,** 708-710.

FADHILAH, A. S., KAI, T. H., LOKMAN, H. I., YASMIN, N. A. R., HAFANDI, A., HASLIZA, A. H., TENGKU RINALFI, T. A. & HEZMEE, M. N. M. 2020. Molecular and pathogenicity of infectious bronchitis virus (Gammacoronavirus) in Japanese quail (Coturnix japonica). *Poult Sci,* 99**,** 2937-2943.

FAGRE, A., LEWIS, J., ECKLEY, M., ZHAN, S., ROCHA, S. M., SEXTON, N. R., BURKE, B., GEISS, B., PEERSEN, O., BASS, T., KADING, R., ROVNAK, J., EBEL, G. D., TJALKENS, R. B., ABOELLAIL, T. & SCHOUNTZ, T. 2021. SARS-CoV-2 infection, neuropathogenesis and transmission among deer mice: Implications for spillback to New World rodents. *PLoS Pathog,* 17**,** e1009585.

FAN, B. E., UMAPATHI, T., CHUA, K., CHIA, Y. W., WONG, S. W., TAN, G. W. L., CHANDRASEKAR, S., LUM, Y. H., VASOO, S. & DALAN, R. 2021. Delayed catastrophic thrombotic events in young and asymptomatic post COVID-19 patients. *J Thromb Thrombolysis,* 51**,** 971-977.

FAN, Y., ZHAO, K., SHI, Z. L. & ZHOU, P. 2019. Bat Coronaviruses in China. *Viruses,* 11.

FANG, X., GAO, J., ZHENG, H., LI, B., KONG, L., ZHANG, Y., WANG, W., ZENG, Y. & YE, L. 2007. The membrane protein of SARS-CoV suppresses NF-kappaB activation. *J Med Virol,* 79**,** 1431-9.

FAO, F. A. A. O. O. T. U. N. 2010. *Global distribution of cattle in 2010* [Online]. Available: http://www.fao.org/livestock-systems/global-distributions/cattle/fr/ [Accessed 01.10.2021].

FDA, F. A. D. A. 2021. *Vaccine Development – 101* [Online]. Available: https://www.fda.gov/vaccines-blood-biologics/development-approval-process-cber/vaccine-development-101 [Accessed 01.10.2021].

FEHR, A. R. & PERLMAN, S. 2015. Coronaviruses: an overview of their replication and pathogenesis. *Methods Mol Biol,* 1282**,** 1-23.

FINKEL, Y., MIZRAHI, O., NACHSHON, A., WEINGARTEN-GABBAY, S., MORGENSTERN, D., YAHALOM-RONEN, Y., TAMIR, H., ACHDOUT, H., STEIN, D., ISRAELI, O., BETH-DIN, A., MELAMED, S., WEISS, S., ISRAELY, T., PARAN, N., SCHWARTZ, M. & STERN-GINOSSAR, N. 2021. The coding capacity of SARS-CoV-2. *Nature,* 589**,** 125-130.

FOGERON, M.-L., MONTSERRET, R., ZEHNDER, J., NGUYEN, M.-H., DUJARDIN, M., BRIGANDAT, L., COLE, L., NINOT-PEDROSA, M., LECOQ, L., MEIER, B. H. & BÖCKMANN, A. 2021. SARS-CoV-2 ORF7b: is a bat virus protein homologue a major cause of COVID-19 symptoms? *bioRxiv,* 2021.02.05.428650.

FOKAS, A. S. & KASTIS, G. A. 2021. SARS-CoV-2: The Second Wave in Europe. *J Med Internet Res,* 23**,** e22431.

FRANCIS, M. E., GONCIN, U., KROEKER, A., SWAN, C., RALPH, R., LU, Y., ETZIONI, A. L., FALZARANO, D., GERDTS, V., MACHTALER, S., KINDRACHUK, J. & KELVIN, A. A. 2021. SARS-CoV-2 infection in the Syrian hamster model causes inflammation as well as type I interferon dysregulation in both respiratory and non-respiratory tissues including the heart and kidney. *PLoS Pathog,* 17**,** e1009705.

FREEMAN, B., LESTER, S., MILLS, L., RASHEED, M. A. U., MOYE, S., ABIONA, O., HUTCHINSON, G. B., MORALES-BETOULLE, M., KRAPINUNAYA, I., GIBBONS, A., CHIANG, C. F., CANNON, D., KLENA, J., JOHNSON, J. A., OWEN, S. M., GRAHAM, B. S., CORBETT, K. S. & THORNBURG, N. J. 2020. Validation of a SARS-CoV-2 spike protein ELISA for use in contact investigations and serosurveillance. *bioRxiv*.

FUNG, T. S. & LIU, D. X. 2018. Post-translational modifications of coronavirus proteins: roles and function. *Future Virol,* 13**,** 405-430.

GAN, E. S., SYENINA, A., LINSTER, M., NG, B., ZHANG, S. L., WATANABE, S., RAJARETHINAM, R., TAN, H. C., SMITH, G. J. & OOI, E. E. 2021. A mouse model of lethal respiratory dysfunction for SARS-CoV-2 infection. *Antiviral Res,* 193**,** 105138.

GANDHI, M., YOKOE, D. S. & HAVLIR, D. V. 2020. Asymptomatic Transmission, the Achilles' Heel of Current Strategies to Control Covid-19. *N Engl J Med,* 382**,** 2158-2160.

GAO, Y., YAN, L., HUANG, Y., LIU, F., ZHAO, Y., CAO, L., WANG, T., SUN, Q., MING, Z., ZHANG, L., GE, J., ZHENG, L., ZHANG, Y., WANG, H., ZHU, Y., ZHU, C., HU, T., HUA, T., ZHANG, B., YANG, X., LI, J., YANG, H., LIU, Z., XU, W., GUDDAT, L. W., WANG, Q., LOU, Z. & RAO, Z. 2020. Structure of the RNA-dependent RNA polymerase from COVID-19 virus. *Science,* 368**,** 779-782.

GAVIN, R. J. H. J. A. H. A. Z. N. J. A. J. K. D. & DABRERA 2021. Impact of vaccination on household transmission of SARS-COV-2 in England.

GE, X. Y., LI, J. L., YANG, X. L., CHMURA, A. A., ZHU, G., EPSTEIN, J. H., MAZET, J. K., HU, B., ZHANG, W., PENG, C., ZHANG, Y. J., LUO, C. M., TAN, B., WANG, N., ZHU, Y., CRAMERI, G., ZHANG, S. Y., WANG, L. F., DASZAK, P. & SHI, Z. L. 2013. Isolation and characterization of a bat SARS-like coronavirus that uses the ACE2 receptor. *Nature,* 503**,** 535-8.

GHIMIRE, S., SHARMA, S., PATEL, A., BUDHATHOKI, R., CHAKINALA, R., KHAN, H., LINCOLN, M. & GEORGESTON, M. 2021. Diarrhea Is Associated with Increased Severity of Disease in COVID-19: Systemic Review and Metaanalysis. *SN Compr Clin Med***,** 1-8.

GHOSH, S., DELLIBOVI-RAGHEB, T. A., KERVIEL, A., PAK, E., QIU, Q., FISHER, M., TAKVORIAN, P. M., BLECK, C., HSU, V. W., FEHR, A. R., PERLMAN, S., ACHAR, S. R., STRAUS, M. R., WHITTAKER, G. R., DE HAAN, C. A. M., KEHRL, J., ALTAN-BONNET, G. & ALTAN-BONNET, N. 2020. beta-Coronaviruses Use Lysosomes for Egress Instead of the Biosynthetic Secretory Pathway. *Cell,* 183**,** 1520-1535 e14.

GORBALENYA, A. E., ENJUANES, L., ZIEBUHR, J. & SNIJDER, E. J. 2006. Nidovirales: evolving the largest RNA virus genome. *Virus Res,* 117**,** 17-37.

GORDON, D. E., JANG, G. M., BOUHADDOU, M., XU, J., OBERNIER, K., WHITE, K. M., O'MEARA, M. J., REZELJ, V. V., GUO, J. Z., SWANEY, D. L., TUMMINO, T. A., HUTTENHAIN, R., KAAKE, R. M., RICHARDS, A. L., TUTUNCUOGLU, B., FOUSSARD, H., BATRA, J., HAAS, K., MODAK, M., KIM, M., HAAS, P., POLACCO, B. J., BRABERG, H., FABIUS, J. M., ECKHARDT, M., SOUCHERAY, M., BENNETT, M. J., CAKIR, M., MCGREGOR, M. J., LI, Q., MEYER, B., ROESCH, F., VALLET, T., MAC KAIN, A., MIORIN, L., MORENO, E., NAING, Z. Z. C., ZHOU, Y., PENG, S., SHI, Y., ZHANG, Z., SHEN, W., KIRBY, I. T., MELNYK, J. E., CHORBA, J. S., LOU, K., DAI, S. A., BARRIO-HERNANDEZ, I., MEMON, D., HERNANDEZ-ARMENTA, C., LYU, J., MATHY, C. J. P., PERICA, T., PILLA, K. B., GANESAN, S. J., SALTZBERG, D. J., RAKESH, R., LIU, X., ROSENTHAL, S. B., CALVIELLO, L., VENKATARAMANAN, S., LIBOY-LUGO, J., LIN, Y., HUANG, X. P., LIU, Y., WANKOWICZ, S. A., BOHN, M., SAFARI, M., UGUR, F. S., KOH, C., SAVAR, N. S., TRAN, Q. D., SHENGJULER, D., FLETCHER, S. J., O'NEAL, M. C., CAI, Y., CHANG, J. C. J., BROADHURST, D. J., KLIPPSTEN, S., SHARP, P. P., WENZELL, N. A., KUZUOGLU-OZTURK, D., WANG, H. Y., TRENKER, R., YOUNG, J. M., CAVERO, D. A., HIATT, J., ROTH, T. L., RATHORE, U., SUBRAMANIAN, A., NOACK, J., HUBERT, M., STROUD, R. M., FRANKEL, A. D., ROSENBERG, O. S., VERBA, K. A., AGARD, D. A., OTT, M.,

EMERMAN, M., JURA, N., et al. 2020. A SARS-CoV-2 protein interaction map reveals targets for drug repurposing. *Nature,* 583**,** 459-468.

GOUILH, M. A., PUECHMAILLE, S. J., GONZALEZ, J. P., TEELING, E., KITTAYAPONG, P. & MANUGUERRA, J. C. 2011. SARS-Coronavirus ancestor's foot-prints in South-East Asian bat colonies and the refuge theory. *Infect Genet Evol,* 11**,** 1690-702.

GRAHAM, R. L. & BARIC, R. S. 2010. Recombination, reservoirs, and the modular spike: mechanisms of coronavirus cross-species transmission. *J Virol,* 84**,** 3134-46.

GREEN, M. S., NITZAN, D., SCHWARTZ, N., NIV, Y. & PEER, V. 2021. Sex differences in the case-fatality rates for COVID-19-A comparison of the age-related differences and consistency over seven countries. *PLoS One,* 16**,** e0250523.

GRIBBLE, J., STEVENS, L. J., AGOSTINI, M. L., ANDERSON-DANIELS, J., CHAPPELL, J. D., LU, X., PRUIJSSERS, A. J., ROUTH, A. L. & DENISON, M. R. 2021. The coronavirus proofreading exoribonuclease mediates extensive viral recombination. *PLoS Pathog,* 17**,** e1009226.

GRIFFIN, B. D., CHAN, M., TAILOR, N., MENDOZA, E. J., LEUNG, A., WARNER, B. M., DUGGAN, A. T., MOFFAT, E., HE, S., GARNETT, L., TRAN, K. N., BANADYGA, L., ALBIETZ, A., TIERNEY, K., AUDET, J., BELLO, A., VENDRAMELLI, R., BOESE, A. S., FERNANDO, L., LINDSAY, L. R., JARDINE, C. M., WOOD, H., POLIQUIN, G., STRONG, J. E., DREBOT, M., SAFRONETZ, D., EMBURY-HYATT, C. & KOBASA, D. 2021. SARS-CoV-2 infection and transmission in the North American deer mouse. *Nat Commun,* 12**,** 3612.

GUPTA, M. K., VEMULA, S., DONDE, R., GOUDA, G., BEHERA, L. & VADDE, R. 2021. In-silico approaches to detect inhibitors of the human severe acute respiratory syndrome coronavirus envelope protein ion channel. *J Biomol Struct Dyn,* 39**,** 2617-2627.

HABTEMARIAM, S., NABAVI, S. F., BANACH, M., BERINDAN-NEAGOE, I., SARKAR, K., SIL, P. C. & NABAVI, S. M. 2020. Should We Try SARS-CoV-2 Helicase Inhibitors for COVID-19 Therapy? *Arch Med Res,* 51**,** 733-735.

HACHIM, A., KAVIAN, N., COHEN, C. A., CHIN, A. W. H., CHU, D. K. W., MOK, C. K. P., TSANG, O. T. Y., YEUNG, Y. C., PERERA, R., POON, L. L. M., PEIRIS, J. S. M. & VALKENBURG, S. A. 2020. ORF8 and ORF3b antibodies are accurate serological markers of early and late SARS-CoV-2 infection. *Nat Immunol,* 21**,** 1293-1301.

HACKBART, M., DENG, X. & BAKER, S. C. 2020. Coronavirus endoribonuclease targets viral polyuridine sequences to evade activating host sensors. *Proc Natl Acad Sci U S A,* 117**,** 8094-8103.

HALPIN, S. J., MCIVOR, C., WHYATT, G., ADAMS, A., HARVEY, O., MCLEAN, L., WALSHAW, C., KEMP, S., CORRADO, J., SINGH, R., COLLINS, T., O'CONNOR, R. J. & SIVAN, M. 2021. Postdischarge symptoms and rehabilitation needs in survivors of COVID-19 infection: A cross-sectional evaluation. *J Med Virol,* 93**,** 1013-1022.

HARRIS, R. J., HALL, J. A., ZAIDI, A., ANDREWS, N. J., DUNBAR, J. K. & DABRERA, G. 2021. Effect of Vaccination on Household Transmission of SARS-CoV-2 in England. *N Engl J Med,* 385**,** 759-760.

HASSAN, S. S., CHOUDHURY, P. P., BASU, P. & JANA, S. S. 2020. Molecular conservation and differential mutation on ORF3a gene in Indian SARS-CoV2 genomes. *Genomics,* 112**,** 3226-3237.

HODGSON, S. H., MANSATTA, K., MALLETT, G., HARRIS, V., EMARY, K. R. W. & POLLARD, A. J. 2021. What defines an efficacious COVID-19 vaccine? A review of the challenges assessing the clinical efficacy of vaccines against SARS-CoV-2. *The Lancet Infectious Diseases,* 21**,** e26-e35.

HODGSON, T., BRITTON, P. & CAVANAGH, D. 2006. Neither the RNA nor the proteins of open reading frames 3a and 3b of the coronavirus infectious bronchitis virus are essential for replication. *J Virol,* 80**,** 296-305.

HOFFMANN, M., KLEINE-WEBER, H., SCHROEDER, S., KRUGER, N., HERRLER, T., ERICHSEN, S., SCHIERGENS, T. S., HERRLER, G., WU, N. H., NITSCHE, A., MULLER, M. A., DROSTEN, C. & POHLMANN, S. 2020. SARS-CoV-2 Cell Entry Depends on ACE2 and TMPRSS2 and Is Blocked by a Clinically Proven Protease Inhibitor. *Cell,* 181**,** 271-280 e8.

HOLMES, E. C., GOLDSTEIN, S. A., RASMUSSEN, A. L., ROBERTSON, D. L., CRITS-CHRISTOPH, A., WERTHEIM, J. O., ANTHONY, S. J., BARCLAY, W. S., BONI, M. F., DOHERTY, P. C., FARRAR, J., GEOGHEGAN, J. L., JIANG, X., LEIBOWITZ, J. L., NEIL, S. J. D., SKERN, T., WEISS, S. R., WOROBEY,

M., ANDERSEN, K. G., GARRY, R. F. & RAMBAUT, A. 2021. The origins of SARS-CoV-2: A critical review. *Cell,* 184**,** 4848-4856.

HOPFER, H., HERZIG, M. C., GOSERT, R., MENTER, T., HENCH, J., TZANKOV, A., HIRSCH, H. H. & MILLER, S. E. 2021. Hunting coronavirus by transmission electron microscopy - a guide to SARS-CoV-2-associated ultrastructural pathology in COVID-19 tissues. *Histopathology,* 78**,** 358-370.

HOULIHAN, C. F. & BEALE, R. 2020. The complexities of SARS-CoV-2 serology. *The Lancet Infectious Diseases,* 20**,** 1350-1351.

HUANG, C., WANG, Y., LI, X., REN, L., ZHAO, J., HU, Y., ZHANG, L., FAN, G., XU, J., GU, X., CHENG, Z., YU, T., XIA, J., WEI, Y., WU, W., XIE, X., YIN, W., LI, H., LIU, M., XIAO, Y., GAO, H., GUO, L., XIE, J., WANG, G., JIANG, R., GAO, Z., JIN, Q., WANG, J. & CAO, B. 2020a. Clinical features of patients infected with 2019 novel coronavirus in Wuhan, China. *The Lancet,* 395**,** 497-506.

HUANG, Y., YANG, C., XU, X. F., XU, W. & LIU, S. W. 2020b. Structural and functional properties of SARS-CoV-2 spike protein: potential antivirus drug development for COVID-19. *Acta Pharmacol Sin,* 41**,** 1141-1149.

HUSTON, N. C., WAN, H., DE CESARIS ARAUJO TAVARES, R., WILEN, C. & PYLE, A. M. 2020. Comprehensive in-vivo secondary structure of the SARS-CoV-2 genome reveals novel regulatory motifs and mechanisms. *bioRxiv*.

ICTV, I. C. O. T. O. V. 2021. *Virus Taxonomy: 2020 Release* [Online]. Available: https://talk.ictvonline.org/taxonomy/ [Accessed 01.10.2021].

IMBERT, I., SNIJDER, E. J., DIMITROVA, M., GUILLEMOT, J. C., LECINE, P. & CANARD, B. 2008. The SARS-Coronavirus PLnc domain of nsp3 as a replication/transcription scaffolding protein. *Virus Res,* 133**,** 136-48.

J. G. KECK, G. K. M., S. MAKINO, J. O. FLEMING, D. M. VANNIER, S. A. STOHLMAN, M. M.C. LAI 1988. In vivo RNA-RNA recombination of coronavirus in mouse brain. *Journal of virology,* 62**,** 1810-1813.

JACKWOOD, M. W. 2012. Review of infectious bronchitis virus around the world. *Avian Dis,* 56**,** 634-41.

JAIMES, J. A., MILLET, J. K. & WHITTAKER, G. R. 2020. Proteolytic Cleavage of the SARS-CoV-2 Spike Protein and the Role of the Novel S1/S2 Site. *iScience,* 23**,** 101212.

JANG, K. J., JEONG, S., KANG, D. Y., SP, N., YANG, Y. M. & KIM, D. E. 2020. A high ATP concentration enhances the cooperative translocation of the SARS coronavirus helicase nsP13 in the unwinding of duplex RNA. *Sci Rep,* 10**,** 4481.

JIN, Y., YANG, H., JI, W., WU, W., CHEN, S., ZHANG, W. & DUAN, G. 2020. Virology, Epidemiology, Pathogenesis, and Control of COVID-19. *Viruses,* 12.

JOHANSSON, M. A., QUANDELACY, T. M., KADA, S., PRASAD, P. V., STEELE, M., BROOKS, J. T., SLAYTON, R. B., BIGGERSTAFF, M. & BUTLER, J. C. 2021. SARS-CoV-2 Transmission From People Without COVID-19 Symptoms. *JAMA Netw Open,* 4**,** e2035057.

JONES, B. A., GRACE, D., KOCK, R., ALONSO, S., RUSHTON, J., SAID, M. Y., MCKEEVER, D., MUTUA, F., YOUNG, J., MCDERMOTT, J. & PFEIFFER, D. U. 2013. Zoonosis emergence linked to agricultural intensification and environmental change. *Proc Natl Acad Sci U S A,* 110**,** 8399-404.

JUNG, K., SAIF, L. J. & WANG, Q. 2020. Porcine epidemic diarrhea virus (PEDV): An update on etiology, transmission, pathogenesis, and prevention and control. *Virus Res,* 286**,** 198045.

JUNGREIS, I., SEALFON, R. & KELLIS, M. 2021. SARS-CoV-2 gene content and COVID-19 mutation impact by comparing 44 Sarbecovirus genomes. *Nat Commun,* 12**,** 2642.

KATO, K., IKLIPTIKAWATI, D. K., KOBAYASHI, A., KONDO, H., LIM, K., HAZAWA, M. & WONG, R. W. 2021. Overexpression of SARS-CoV-2 protein ORF6 dislocates RAE1 and NUP98 from the nuclear pore complex. *Biochem Biophys Res Commun,* 536**,** 59-66.

KE, Z., OTON, J., QU, K., CORTESE, M., ZILA, V., MCKEANE, L., NAKANE, T., ZIVANOV, J., NEUFELDT, C. J., CERIKAN, B., LU, J. M., PEUKES, J., XIONG, X., KRAUSSLICH, H. G., SCHERES, S. H. W., BARTENSCHLAGER, R. & BRIGGS, J. A. G. 2020. Structures and distributions of SARS-CoV-2 spike proteins on intact virions. *Nature,* 588**,** 498-502.

KHADE, S. M., YABAJI, S. M. & SRIVASTAVA, J. 2021. An update on COVID-19: SARS-CoV-2 life cycle, immunopathology, and BCG vaccination. *Prep Biochem Biotechnol,* 51**,** 650-658.

KHAILANY, R. A., SAFDAR, M. & OZASLAN, M. 2020. Genomic characterization of a novel SARS-CoV-2. *Gene Rep,* 19**,** 100682.

KIM, D., LEE, J. Y., YANG, J. S., KIM, J. W., KIM, V. N. & CHANG, H. 2020. The Architecture of SARS-CoV-2 Transcriptome. *Cell,* 181**,** 914-921 e10.

KIRTIPAL, N., BHARADWAJ, S. & KANG, S. G. 2020. From SARS to SARS-CoV-2, insights on structure, pathogenicity and immunity aspects of pandemic human coronaviruses. *Infect Genet Evol,* 85**,** 104502.

KLEIN, S., CORTESE, M., WINTER, S. L., WACHSMUTH-MELM, M., NEUFELDT, C. J., CERIKAN, B., STANIFER, M. L., BOULANT, S., BARTENSCHLAGER, R. & CHLANDA, P. 2020. SARS-CoV-2 structure and replication characterized by in situ cryo-electron tomography. *Nat Commun,* 11**,** 5885.

KNOOPS, K., KIKKERT, M., WORM, S. H., ZEVENHOVEN-DOBBE, J. C., VAN DER MEER, Y., KOSTER, A. J., MOMMAAS, A. M. & SNIJDER, E. J. 2008. SARS-coronavirus replication is supported by a reticulovesicular network of modified endoplasmic reticulum. *PLoS Biol,* 6**,** e226.

KONG, X., LIU, F., WANG, H., YANG, R., CHEN, D., WANG, X., LU, F., RAO, H. & CHEN, H. 2021. Prevention and control measures significantly curbed the SARS-CoV-2 and influenza epidemics in China. *J Virus Erad,* 7**,** 100040.

KONNO, Y., KIMURA, I., URIU, K., FUKUSHI, M., IRIE, T., KOYANAGI, Y., SAUTER, D., GIFFORD, R. J., CONSORTIUM, U.-C., NAKAGAWA, S. & SATO, K. 2020. SARS-CoV-2 ORF3b Is a Potent Interferon Antagonist Whose Activity Is Increased by a Naturally Occurring Elongation Variant. *Cell Rep,* 32**,** 108185.

KORBER, B., FISCHER, W. M., GNANAKARAN, S., YOON, H., THEILER, J., ABFALTERER, W., HENGARTNER, N., GIORGI, E. E., BHATTACHARYA, T., FOLEY, B., HASTIE, K. M., PARKER, M. D., PARTRIDGE, D. G., EVANS, C. M., FREEMAN, T. M., DE SILVA, T. I., SHEFFIELD, C.-G. G., MCDANAL, C., PEREZ, L. G., TANG, H., MOON-WALKER, A., WHELAN, S. P., LABRANCHE, C. C., SAPHIRE, E. O. & MONTEFIORI, D. C. 2020. Tracking Changes in SARS-CoV-2 Spike: Evidence that D614G Increases Infectivity of the COVID-19 Virus. *Cell,* 182**,** 812-827 e19.

KRAEMER, M. U. G., HILL, V., RUIS, C., DELLICOUR, S., BAJAJ, S., MCCRONE, J. T., BAELE, G., PARAG, K. V., BATTLE, A. L., GUTIERREZ, B., JACKSON, B., COLQUHOUN, R., O'TOOLE, A., KLEIN, B., VESPIGNANI, A., CONSORTIUM, C.-G. U., VOLZ, E., FARIA, N. R., AANENSEN, D. M., LOMAN, N. J., DU PLESSIS, L., CAUCHEMEZ, S., RAMBAUT, A., SCARPINO, S. V. & PYBUS, O. G. 2021. Spatiotemporal invasion dynamics of SARS-CoV-2 lineage B.1.1.7 emergence. *Science,* 373**,** 889-895.

KRAHLING, V., HALWE, S., ROHDE, C., BECKER, D., BERGHOFER, S., DAHLKE, C., EICKMANN, M., ERCANOGLU, M. S., GIESELMANN, L., HERWIG, A., KUPKE, A., MULLER, H., NEUBAUER-RADEL, P., KLEIN, F., KELLER, C. & BECKER, S. 2021. Development and characterization of an indirect ELISA to detect SARS-CoV-2 spike protein-specific antibodies. *J Immunol Methods,* 490**,** 112958.

KUMAR S., NYODU R., MAURYA V.K. & S.K., S. 2020. *Morphology, Genome Organization, Replication, and Pathogenesis of Severe Acute Respiratory Syndrome Coronavirus 2 (SARS-CoV-2).*

KUMARI, P., ROTHAN, H. A., NATEKAR, J. P., STONE, S., PATHAK, H., STRATE, P. G., ARORA, K., BRINTON, M. A. & KUMAR, M. 2021. Neuroinvasion and Encephalitis Following Intranasal Inoculation of SARS-CoV-2 in K18-hACE2 Mice. *Viruses,* 13.

LAM, T. T., JIA, N., ZHANG, Y. W., SHUM, M. H., JIANG, J. F., ZHU, H. C., TONG, Y. G., SHI, Y. X., NI, X. B., LIAO, Y. S., LI, W. J., JIANG, B. G., WEI, W., YUAN, T. T., ZHENG, K., CUI, X. M., LI, J., PEI, G. Q., QIANG, X., CHEUNG, W. Y., LI, L. F., SUN, F. F., QIN, S., HUANG, J. C., LEUNG, G. M., HOLMES, E. C., HU, Y. L., GUAN, Y. & CAO, W. C. 2020. Identifying SARS-CoV-2-related coronaviruses in Malayan pangolins. *Nature,* 583**,** 282-285.

LANCET, T. 2020. Facing up to long COVID. *The Lancet,* 396.

LATINNE, A., HU, B., OLIVAL, K. J., ZHU, G., ZHANG, L., LI, H., CHMURA, A. A., FIELD, H. E., ZAMBRANA-TORRELIO, C., EPSTEIN, J. H., LI, B., ZHANG, W., WANG, L. F., SHI, Z. L. & DASZAK, P. 2020. Origin and cross-species transmission of bat coronaviruses in China. *Nat Commun,* 11**,** 4235.

LECHIEN, J. R., CHIESA-ESTOMBA, C. M., PLACE, S., VAN LAETHEM, Y., CABARAUX, P., MAT, Q., HUET, K., PLZAK, J., HOROI, M., HANS, S., ROSARIA BARILLARI, M., CAMMAROTO, G., FAKHRY, N., MARTINY, D., AYAD, T., JOUFFE, L., HOPKINS, C., SAUSSEZ, S. & YO-IFOS, C.-T. F. O. 2020. Clinical and epidemiological characteristics of 1420 European patients with mild-to-moderate coronavirus disease 2019. *J Intern Med,* 288**,** 335-344.

LEE, T. Y., LEE, H., KIM, N., JEON, P., KIM, J. W., LIM, H. Y., YANG, J. S., KIM, K. C. & LEE, J. Y. 2021. Comparison of SARS-CoV-2 variant lethality in human angiotensin-converting enzyme 2 transgenic mice. *Virus Res,* 305**,** 198563.

LEI, J., KUSOV, Y. & HILGENFELD, R. 2018. Nsp3 of coronaviruses: Structures and functions of a large multi-domain protein. *Antiviral Res,* 149**,** 58-74.

LI, B., DENG, A., LI, K., HU, Y., LI, Z., XIONG, Q., LIU, Z., GUO, Q., ZOU, L., ZHANG, H., ZHANG, M., OUYANG, F., SU, J., SU, W., XU, J., LIN, H., SUN, J., PENG, J., JIANG, H., ZHOU, P., HU, T., LUO, M., ZHANG, Y., ZHENG, H., XIAO, J., LIU, T., CHE, R., ZENG, H., ZHENG, Z., HUANG, Y., YU, J., YI, L., WU, J., CHEN, J., ZHONG, H., DENG, X., KANG, M., PYBUS, O. G., HALL, M., LYTHGOE, K. A., LI, Y., YUAN, J., HE, J. & LU, J. 2021a. Viral infection and transmission in a large, well-traced outbreak caused by the SARS-CoV-2 Delta variant. *medRxiv***,** 2021.07.07.21260122.

LI, L.-L., WANG, J.-L., MA, X.-H., LI, J.-S., YANG, X.-F., SHI, W.-F. & DUAN, Z.-J. 2021b. A novel SARS-CoV-2 related virus with complex recombination isolated from bats in Yunnan province, China. *bioRxiv* 2021.03.17.435823.

LI, Q., GUAN, X., WU, P., WANG, X., ZHOU, L., TONG, Y., REN, R., LEUNG, K. S. M., LAU, E. H. Y., WONG, J. Y., XING, X., XIANG, N., WU, Y., LI, C., CHEN, Q., LI, D., LIU, T., ZHAO, J., LIU, M., TU, W., CHEN, C., JIN, L., YANG, R., WANG, Q., ZHOU, S., WANG, R., LIU, H., LUO, Y., LIU, Y., SHAO, G., LI, H., TAO, Z., YANG, Y., DENG, Z., LIU, B., MA, Z., ZHANG, Y., SHI, G., LAM, T. T. Y., WU, J. T., GAO, G. F., COWLING, B. J., YANG, B., LEUNG, G. M. & FENG, Z. 2020a. Early Transmission Dynamics in Wuhan, China, of Novel Coronavirus-Infected Pneumonia. *N Engl J Med,* 382**,** 1199-1207.

LI, X. Y., DAI, W. J., WU, S. N., YANG, X. Z. & WANG, H. G. 2020b. The occurrence of diarrhea in COVID-19 patients. *Clin Res Hepatol Gastroenterol,* 44**,** 284-285.

LIAO, Y., YUAN, Q., TORRES, J., TAM, J. P. & LIU, D. X. 2006. Biochemical and functional characterization of the membrane association and membrane permeabilizing activity of the severe acute respiratory syndrome coronavirus envelope protein. *Virology,* 349**,** 264-75.

LIU, D. X., FUNG, T. S., CHONG, K. K., SHUKLA, A. & HILGENFELD, R. 2014. Accessory proteins of SARS-CoV and other coronaviruses. *Antiviral Res,* 109**,** 97-109.

LIU, L., WANG, P., NAIR, M. S., YU, J., RAPP, M., WANG, Q., LUO, Y., CHAN, J. F., SAHI, V., FIGUEROA, A., GUO, X. V., CERUTTI, G., BIMELA, J., GORMAN, J., ZHOU, T., CHEN, Z., YUEN, K. Y., KWONG, P. D., SODROSKI, J. G., YIN, M. T., SHENG, Z., HUANG, Y., SHAPIRO, L. & HO, D. D. 2020. Potent neutralizing antibodies against multiple epitopes on SARS-CoV-2 spike. *Nature,* 584**,** 450-456.

LIU, R., AMERICO, J. L., COTTER, C. A., EARL, P. L., EREZ, N., PENG, C. & MOSS, B. 2021a. One or two injections of MVA-vectored vaccine shields hACE2 transgenic mice from SARS-CoV-2 upper and lower respiratory tract infection. *Proc Natl Acad Sci U S A,* 118.

LIU, R., WU, P., OGRODZKI, P., MAHMOUD, S., LIANG, K., LIU, P., FRANCIS, S. S., KHALAK, H., LIU, D., LI, J., MA, T., CHEN, F., LIU, W., HUANG, X., HE, W., YUAN, Z., QIAO, N., MENG, X., ALQARNI, B., QUILEZ, J., KUSUMA, V., LIN, L., JIN, X., YANG, C., ANTON, X., KOSHY, A., YANG, H., XU, X., WANG, J., XIAO, P., AL KAABI, N., FASIHUDDIN, M. S., SELVARAJ, F. A., WEBER, S., AL HOSANI, F. I., LIU, S. & ZAHER, W. A. 2021b. Genomic epidemiology of SARS-CoV-2 in the UAE reveals novel virus mutation, patterns of co-infection and tissue specific host immune response. *Sci Rep,* 11**,** 13971.

LU, R., ZHAO, X., LI, J., NIU, P., YANG, B., WU, H., WANG, W., SONG, H., HUANG, B., ZHU, N., BI, Y., MA, X., ZHAN, F., WANG, L., HU, T., ZHOU, H., HU, Z., ZHOU, W., ZHAO, L., CHEN, J., MENG, Y., WANG, J., LIN, Y., YUAN, J., XIE, Z., MA, J., LIU, W. J., WANG, D., XU, W., HOLMES, E. C., GAO, G. F., WU, G., CHEN, W., SHI, W. & TAN, W. 2020. Genomic characterisation and epidemiology of 2019 novel coronavirus: implications for virus origins and receptor binding. *The Lancet,* 395**,** 565-574.

LU, X., PAN, J., TAO, J. & GUO, D. 2011. SARS-CoV nucleocapsid protein antagonizes IFN-beta response by targeting initial step of IFN-beta induction pathway, and its C-terminal region is critical for the antagonism. *Virus Genes,* 42**,** 37-45.

LUCHINI, A., MICCIULLA, S., CORUCCI, G., BATCHU, K. C., SANTAMARIA, A., LAUX, V., DARWISH, T., RUSSELL, R. A., THEPAUT, M., BALLY, I., FIESCHI, F. & FRAGNETO, G. 2021. Lipid bilayer degradation induced by SARS-CoV-2 spike protein as revealed by neutron reflectometry. *Sci Rep,* 11**,** 14867.

LUKASSEN, S., CHUA, R. L., TREFZER, T., KAHN, N. C., SCHNEIDER, M. A., MULEY, T., WINTER, H., MEISTER, M., VEITH, C., BOOTS, A. W., HENNIG, B. P., KREUTER, M., CONRAD, C. & EILS, R. 2020. SARS-CoV-2 receptor ACE2 and TMPRSS2 are primarily expressed in bronchial transient secretory cells. *EMBO J,* 39**,** e105114.

LUNDSTROM, K., SEYRAN, M., PIZZOL, D., ADADI, P., MOHAMED ABD EL-AZIZ, T., HASSAN, S. S., SOARES, A., KANDIMALLA, R., TAMBUWALA, M. M., ALJABALI, A. A. A., KUMAR AZAD, G., PAL CHOUDHURY, P., UVERSKY, V. N., SHERCHAN, S. P., UHAL, B. D., REZAEI, N. & BRUFSKY, A. M. 2020. Viewpoint: Origin of SARS-CoV-2. *Viruses,* 12.

LYTHGOE, K. A., HALL, M., FERRETTI, L., DE CESARE, M., MACINTYRE-COCKETT, G., TREBES, A., ANDERSSON, M., OTECKO, N., WISE, E. L., MOORE, N., LYNCH, J., KIDD, S., CORTES, N., MORI, M., WILLIAMS, R., VERNET, G., JUSTICE, A., GREEN, A., NICHOLLS, S. M., ANSARI, M. A., ABELER-DORNER, L., MOORE, C. E., PETO, T. E. A., EYRE, D. W., SHAW, R., SIMMONDS, P., BUCK, D., TODD, J. A., OXFORD VIRUS SEQUENCING ANALYSIS, G., CONNOR, T. R., ASHRAF, S., DA SILVA FILIPE, A., SHEPHERD, J., THOMSON, E. C., CONSORTIUM, C.-G. U., BONSALL, D., FRASER, C. & GOLUBCHIK, T. 2021. SARS-CoV-2 within-host diversity and transmission. *Science,* 372.

MA, Y., WU, L., SHAW, N., GAO, Y., WANG, J., SUN, Y., LOU, Z., YAN, L., ZHANG, R. & RAO, Z. 2015. Structural basis and functional analysis of the SARS coronavirus nsp14-nsp10 complex. *Proc Natl Acad Sci U S A,* 112**,** 9436-41.

MACMULLAN, M. A., IBRAYEVA, A., TRETTNER, K., DEMING, L., DAS, S., TRAN, F., MORENO, J. R., CASIAN, J. G., CHELLAMUTHU, P., KRAFT, J., KOZAK, K., TURNER, F. E., SLEPNEV, V. I. & LE PAGE, L. M. 2020. ELISA detection of SARS-CoV-2 antibodies in saliva. *Sci Rep,* 10**,** 20818.

MALLAPATY, S. 2021a. After the WHO report: what's next in the search for COVID's origins. *Nature,* 592**,** 337-338.

MALLAPATY, S. 2021b. The search for animals harbouring coronavirus - and why it matters. *Nature,* 591**,** 26-28.

MANCERA GRACIA, J. C., PEARCE, D. S., MASIC, A. & BALASCH, M. 2020. Influenza A Virus in Swine: Epidemiology, Challenges and Vaccination Strategies. *Front Vet Sci,* 7**,** 647.

MARIANO, G., FARTHING, R. J., LALE-FARJAT, S. L. M. & BERGERON, J. R. C. 2020. Structural Characterization of SARS-CoV-2: Where We Are, and Where We Need to Be. *Front Mol Biosci,* 7**,** 605236.

MASTERS, P. S. 2006. The Molecular Biology of Coronaviruses. *Advances in Virus Research* 66**,** 193-292.

MASTERS, P. S. 2019. Coronavirus genomic RNA packaging. *Virology,* 537**,** 198-207.

MCBRIDE, R., VAN ZYL, M. & FIELDING, B. C. 2014. The coronavirus nucleocapsid is a multifunctional protein. *Viruses,* 6**,** 2991-3018.

MENDONCA, L., HOWE, A., GILCHRIST, J. B., SHENG, Y., SUN, D., KNIGHT, M. L., ZANETTI-DOMINGUES, L. C., BATEMAN, B., KREBS, A. S., CHEN, L., RADECKE, J., LI, V. D., NI, T., KOUNATIDIS, I., KORONFEL, M. A., SZYNKIEWICZ, M., HARKIOLAKI, M., MARTIN-FERNANDEZ, M. L., JAMES, W. & ZHANG, P. 2021. Correlative multi-scale cryo-imaging unveils SARS-CoV-2 assembly and egress. *Nat Commun,* 12**,** 4629.

MIAO, G., ZHAO, H., LI, Y., JI, M., CHEN, Y., SHI, Y., BI, Y., WANG, P. & ZHANG, H. 2021a. ORF3a of the COVID-19 virus SARS-CoV-2 blocks HOPS complex-mediated assembly of the SNARE complex required for autolysosome formation. *Dev Cell,* 56, 427-442 e5.

MIAO, Z., TIDU, A., ERIANI, G. & MARTIN, F. 2021b. Secondary structure of the SARS-CoV-2 5'-UTR. *RNA Biol,* 18**,** 447-456.

MILLET, J. K. & WHITTAKER, G. R. 2018. Physiological and molecular triggers for SARS-CoV membrane fusion and entry into host cells. *Virology,* 517**,** 3-8.

MINSKAIA, E., HERTZIG, T., GORBALENYA, A. E., CAMPANACCI, V., CAMBILLAU, C., CANARD, B. & ZIEBUHR, J. 2006. Discovery of an RNA virus 3'->5' exoribonuclease that is critically involved in coronavirus RNA synthesis. *Proc Natl Acad Sci U S A,* 103**,** 5108-13.

MIORIN, L., KEHRER, T., SANCHEZ-APARICIO, M. T., ZHANG, K., COHEN, P., PATEL, R. S., CUPIC, A., MAKIO, T., MEI, M., MORENO, E., DANZIGER, O., WHITE, K. M., RATHNASINGHE, R., UCCELLINI, M., GAO, S., AYDILLO, T., MENA, I., YIN, X., MARTIN-SANCHO, L., KROGAN, N. J., CHANDA, S. K., SCHOTSAERT, M., WOZNIAK, R. W., REN, Y., ROSENBERG, B. R., FONTOURA, B. M. A. & GARCIA-SASTRE, A. 2020. SARS-CoV-2 Orf6 hijacks Nup98 to block STAT nuclear import and antagonize interferon signaling. *Proc Natl Acad Sci U S A,* 117**,** 28344-28354.

MITTAL, A., MANJUNATH, K., RANJAN, R. K., KAUSHIK, S., KUMAR, S. & VERMA, V. 2020. COVID-19 pandemic: Insights into structure, function, and hACE2 receptor recognition by SARS-CoV-2. *PLoS Pathog,* 16**,** e1008762.

MOHANDAS, S., YADAV, P. D., SHETE, A., NYAYANIT, D., SAPKAL, G., LOLE, K. & GUPTA, N. 2021. SARS-CoV-2 Delta Variant Pathogenesis and Host Response in Syrian Hamsters. *Viruses,* 13.

MOK, B. W., LIU, H., DENG, S., LIU, J., ZHANG, A. J., LAU, S. Y., LIU, S., TAM, R. C., CREMIN, C. J., NG, T. T., LEUNG, J. S., LEE, L. K., WANG, P., TO, K. K., CHAN, J. F., CHAN, K. H., YUEN, K. Y., SIU, G. K. & CHEN, H. 2021. Low dose inocula of SARS-CoV-2 Alpha variant transmits more efficiently than earlier variants in hamsters. *Commun Biol,* 4**,** 1102.

MORENS, D. M., DASZAK, P., MARKEL, H. & TAUBENBERGER, J. K. 2020. Pandemic COVID-19 Joins History's Pandemic Legion. *mBio,* 11.

MURGOLO, N., THERIEN, A. G., HOWELL, B., KLEIN, D., KOEPLINGER, K., LIEBERMAN, L. A., ADAM, G. C., FLYNN, J., MCKENNA, P., SWAMINATHAN, G., HAZUDA, D. J. & OLSEN, D. B. 2021. SARS-CoV-2 tropism, entry, replication, and propagation: Considerations for drug discovery and development. *PLoS Pathog,* 17**,** e1009225.

NADEAU, S. A., VAUGHAN, T. G., SCIRE, J., HUISMAN, J. S. & STADLER, T. 2021. The origin and early spread of SARS-CoV-2 in Europe. *Proc Natl Acad Sci U S A,* 118.

NALBANDIAN, A., SEHGAL, K., GUPTA, A., MADHAVAN, M. V., MCGRODER, C., STEVENS, J. S., COOK, J. R., NORDVIG, A. S., SHALEV, D., SEHRAWAT, T. S., AHLUWALIA, N., BIKDELI, B., DIETZ, D., DER-NIGOGHOSSIAN, C., LIYANAGE-DON, N., ROSNER, G. F., BERNSTEIN, E. J., MOHAN, S., BECKLEY, A. A., SERES, D. S., CHOUEIRI, T. K., URIEL, N., AUSIELLO, J. C., ACCILI, D., FREEDBERG, D. E., BALDWIN, M., SCHWARTZ, A., BRODIE, D., GARCIA, C. K., ELKIND, M. S. V., CONNORS, J. M., BILEZIKIAN, J. P., LANDRY, D. W. & WAN, E. Y. 2021. Post-acute COVID-19 syndrome. *Nat Med,* 27**,** 601-615.

NAQVI, A. A. T., FATIMA, K., MOHAMMAD, T., FATIMA, U., SINGH, I. K., SINGH, A., ATIF, S. M., HARIPRASAD, G., HASAN, G. M. & HASSAN, M. I. 2020. Insights into SARS-CoV-2 genome, structure, evolution, pathogenesis and therapies: Structural genomics approach. *Biochim Biophys Acta Mol Basis Dis,* 1866**,** 165878.

NEUMAN, B. W. & BUCHMEIER, M. J. 2016. Supramolecular Architecture of the Coronavirus Particle. *Adv Virus Res,* 96**,** 1-27.

NEUMAN, B. W., KISS, G., KUNDING, A. H., BHELLA, D., BAKSH, M. F., CONNELLY, S., DROESE, B., KLAUS, J. P., MAKINO, S., SAWICKI, S. G., SIDDELL, S. G., STAMOU, D. G., WILSON, I. A., KUHN, P. & BUCHMEIER, M. J. 2011. A structural analysis of M protein in coronavirus assembly and morphology. *J Struct Biol,* 174**,** 11-22.

NIETO-TORRES, J. L., DEDIEGO, M. L., VERDIA-BAGUENA, C., JIMENEZ-GUARDENO, J. M., REGLA-NAVA, J. A., FERNANDEZ-DELGADO, R., CASTANO-RODRIGUEZ, C., ALCARAZ, A., TORRES, J., AGUILELLA, V. M. & ENJUANES, L. 2014. Severe acute respiratory syndrome coronavirus envelope protein ion channel activity promotes virus fitness and pathogenesis. *PLoS Pathog,* 10**,** e1004077.

NIH, N. I. O. H. 2021. *Clinical Spectrum of SARS-CoV-2 Infection* [Online]. Available: https://www.covid19treatmentguidelines.nih.gov/overview/clinical-spectrum/ [Accessed 01.10.2021].

NIKOLAI, L. A., MEYER, C. G., KREMSNER, P. G. & VELAVAN, T. P. 2020. Asymptomatic SARS Coronavirus 2 infection: Invisible yet invincible. *Int J Infect Dis,* 100**,** 112-116.

NOGRADY, B. 2020. What the data say about asymptomatic COVID infections. *Nature,* 587**,** 534-535.

NOGUEIRA, P. J., DE ARAUJO NOBRE, M., COSTA, A., RIBEIRO, R. M., FURTADO, C., BACELAR NICOLAU, L., CAMARINHA, C., LUIS, M., ABRANTES, R. & VAZ CARNEIRO, A. 2020. The Role of Health Preconditions on COVID-19 Deaths in Portugal: Evidence from Surveillance Data of the First 20293 Infection Cases. *J Clin Med,* 9.

OIE, W. O. F. A. H. 2021. *One Health* [Online]. Available: https://www.oie.int/en/what-we-do/global-initiatives/one-health/ [Accessed 01.10.2021].

OKBA, N. M. A., MULLER, M. A., LI, W., WANG, C., GEURTSVANKESSEL, C. H., CORMAN, V. M., LAMERS, M. M., SIKKEMA, R. S., DE BRUIN, E., CHANDLER, F. D., YAZDANPANAH, Y., LE HINGRAT, Q., DESCAMPS, D., HOUHOU-FIDOUH, N., REUSKEN, C., BOSCH, B. J., DROSTEN, C., KOOPMANS, M. P. G. & HAAGMANS, B. L. 2020. Severe Acute Respiratory Syndrome Coronavirus 2-Specific Antibody Responses in Coronavirus Disease Patients. *Emerg Infect Dis,* 26**,** 1478-1488.

OLADUNNI, F. S., PARK, J. G., PINO, P. A., GONZALEZ, O., AKHTER, A., ALLUE-GUARDIA, A., OLMO-FONTANEZ, A., GAUTAM, S., GARCIA-VILANOVA, A., YE, C., CHIEM, K., HEADLEY, C., DWIVEDI, V., PARODI, L. M., ALFSON, K. J., STAPLES, H. M., SCHAMI, A., GARCIA, J. I., WHIGHAM, A., PLATT, R. N., 2ND, GAZI, M., MARTINEZ, J., CHUBA, C., EARLEY, S., RODRIGUEZ, O. H., MDAKI, S. D., KAVELISH, K. N., ESCALONA, R., HALLAM, C. R. A., CHRISTIE, C., PATTERSON, J. L., ANDERSON, T. J. C., CARRION, R., JR., DICK, E. J., JR., HALL-URSONE, S., SCHLESINGER, L. S., ALVAREZ, X., KAUSHAL, D., GIAVEDONI, L. D., TURNER, J., MARTINEZ-SOBRIDO, L. & TORRELLES, J. B. 2020. Lethality of SARS-CoV-2 infection in K18 human angiotensin-converting enzyme 2 transgenic mice. *Nat Commun,* 11**,** 6122.

ORAN, D. P. & TOPOL, E. J. 2020. Prevalence of Asymptomatic SARS-CoV-2 Infection : A Narrative Review. *Ann Intern Med,* 173**,** 362-367.

ORD, M., FAUSTOVA, I. & LOOG, M. 2020. The sequence at Spike S1/S2 site enables cleavage by furin and phospho-regulation in SARS-CoV2 but not in SARS-CoV1 or MERS-CoV. *Sci Rep,* 10**,** 16944.

OUDE MUNNINK, B. B., SIKKEMA, R. S., NIEUWENHUIJSE, D. F., MOLENAAR, R. J., MUNGER, E., MOLENKAMP, R., VAN DER SPEK, A., TOLSMA, P., RIETVELD, A., BROUWER, M., BOUWMEESTER-VINCKEN, N., HARDERS, F., HAKZE-VAN DER HONING, R., WEGDAM-BLANS, M. C. A., BOUWSTRA, R. J., GEURTSVANKESSEL, C., VAN DER EIJK, A. A., VELKERS, F. C., SMIT, L. A. M., STEGEMAN, A., VAN DER POEL, W. H. M. & KOOPMANS, M. P. G. 2021. Transmission of SARS-CoV-2 on mink farms between humans and mink and back to humans. *Science,* 371**,** 172-177.

PAK, A., ADEGBOYE, O. A., ADEKUNLE, A. I., RAHMAN, K. M., MCBRYDE, E. S. & EISEN, D. P. 2020. Economic Consequences of the COVID-19 Outbreak: the Need for Epidemic Preparedness. *Front Public Health,* 8**,** 241.

PALMER, M. V., MARTINS, M., FALKENBERG, S., BUCKLEY, A., CASERTA, L. C., MITCHELL, P. K., CASSMANN, E. D., ROLLINS, A., ZYLICH, N. C., RENSHAW, R. W., GUARINO, C., WAGNER, B., LAGER, K. & DIEL, D. G. 2021. Susceptibility of white-tailed deer (Odocoileus virginianus) to SARS-CoV-2. *J Virol*.

PANCER, K., MILEWSKA, A., OWCZAREK, K., DABROWSKA, A., KOWALSKI, M., LABAJ, P. P., BRANICKI, W., SANAK, M. & PYRC, K. 2020. The SARS-CoV-2 ORF10 is not essential in vitro or in vivo in humans. *PLoS Pathog,* 16**,** e1008959.

PAUL, S. & LORIN, E. 2021. Distribution of incubation periods of COVID-19 in the Canadian context. *Sci Rep,* 11**,** 12569.

PAWLOWSKI, C., VENKATAKRISHNAN, A. J., RAMUDU, E., KIRKUP, C., PURANIK, A., KAYAL, N., BERNER, G., ANAND, A., BARVE, R., O'HORO, J. C., BADLEY, A. D. & SOUNDARARAJAN, V. 2021. Pre-existing conditions are associated with COVID-19 patients' hospitalization, despite confirmed clearance of SARS-CoV-2 virus. *EClinicalMedicine,* 34**,** 100793.

PECKHAM, H., DE GRUIJTER, N. M., RAINE, C., RADZISZEWSKA, A., CIURTIN, C., WEDDERBURN, L. R., ROSSER, E. C., WEBB, K. & DEAKIN, C. T. 2020. Male sex identified by global COVID-19 meta-analysis as a risk factor for death and ITU admission. *Nat Commun,* 11**,** 6317.

PERLMAN, S. & NETLAND, J. 2009. Coronaviruses post-SARS: update on replication and pathogenesis. *Nat Rev Microbiol,* 7**,** 439-50.

PFEFFERLE, S., HUANG, J., NORZ, D., INDENBIRKEN, D., LUTGEHETMANN, M., OESTEREICH, L., GUNTHER, T., GRUNDHOFF, A., AEPFELBACHER, M. & FISCHER, N. 2020. Complete Genome Sequence of a SARS-CoV-2 Strain Isolated in Northern Germany. *Microbiol Resour Announc,* 9.

PLANAS, D., VEYER, D., BAIDALIUK, A., STAROPOLI, I., GUIVEL-BENHASSINE, F., RAJAH, M. M., PLANCHAIS, C., PORROT, F., ROBILLARD, N., PUECH, J., PROT, M., GALLAIS, F., GANTNER, P., VELAY, A., LE GUEN, J., KASSIS-CHIKHANI, N., EDRISS, D., BELEC, L., SEVE, A., COURTELLEMONT, L., PERE, H., HOCQUELOUX, L., FAFI-KREMER, S., PRAZUCK, T., MOUQUET, H., BRUEL, T., SIMON-LORIERE, E., REY, F. A. & SCHWARTZ, O. 2021. Reduced sensitivity of SARS-CoV-2 variant Delta to antibody neutralization. *Nature,* 596**,** 276-280.

PLANT, E. P., PEREZ-ALVARADO, G. C., JACOBS, J. L., MUKHOPADHYAY, B., HENNIG, M. & DINMAN, J. D. 2005. A three-stemmed mRNA pseudoknot in the SARS coronavirus frameshift signal. *PLoS Biol,* 3**,** e172.

PLESCIA, C. B., DAVID, E. A., PATRA, D., SENGUPTA, R., AMIAR, S., SU, Y. & STAHELIN, R. V. 2021. SARS-CoV-2 viral budding and entry can be modeled using BSL-2 level virus-like particles. *J Biol Chem,* 296**,** 100103.

POLACK, F. P., THOMAS, S. J., KITCHIN, N., ABSALON, J., GURTMAN, A., LOCKHART, S., PEREZ, J. L., PEREZ MARC, G., MOREIRA, E. D., ZERBINI, C., BAILEY, R., SWANSON, K. A., ROYCHOUDHURY, S., KOURY, K., LI, P., KALINA, W. V., COOPER, D., FRENCK, R. W., JR., HAMMITT, L. L., TURECI, O., NELL, H., SCHAEFER, A., UNAL, S., TRESNAN, D. B., MATHER, S., DORMITZER, P. R., SAHIN, U., JANSEN, K. U., GRUBER, W. C. & GROUP, C. C. T. 2020. Safety and Efficacy of the BNT162b2 mRNA Covid-19 Vaccine. *N Engl J Med,* 383**,** 2603-2615.

PORT, J. R., YINDA, C. K., AVANZATO, V. A., SCHULZ, J. E., HOLBROOK, M. G., VAN DOREMALEN, N., SHAIA, C., FISCHER, R. J. & MUNSTER, V. J. 2021. Increased aerosol transmission for B.1.1.7 (alpha variant) over lineage A variant of SARS-CoV-2. *bioRxiv*.

PUSTERLA, N., VIN, R., LEUTENEGGER, C., MITTEL, L. D. & DIVERS, T. J. 2016. Equine coronavirus: An emerging enteric virus of adult horses. *Equine Vet Educ,* 28**,** 216-223.

QUESADA, J. A., LOPEZ-PINEDA, A., GIL-GUILLEN, V. F., ARRIERO-MARIN, J. M., GUTIERREZ, F. & CARRATALA-MUNUERA, C. 2021. Incubation period of COVID-19: A systematic review and meta-analysis. *Rev Clin Esp (Barc),* 221**,** 109-117.

RAMBAUT, A., HOLMES, E. C., O'TOOLE, A., HILL, V., MCCRONE, J. T., RUIS, C., DU PLESSIS, L. & PYBUS, O. G. 2020. A dynamic nomenclature proposal for SARS-CoV-2 lineages to assist genomic epidemiology. *Nat Microbiol,* 5**,** 1403-1407.

RAMOS-CASALS, M., BRITO-ZERON, P. & MARIETTE, X. 2021. Systemic and organ-specific immune-related manifestations of COVID-19. *Nat Rev Rheumatol,* 17**,** 315-332.

RANGAN, R., ZHELUDEV, I. N. & DAS, R. 2020. RNA genome conservation and secondary structure in SARS-CoV-2 and SARS-related viruses. *bioRxiv*.

REARDON, S. 2021. How the Delta variant achieves its ultrafast spread. *Nature*.

REDONDO, N., ZALDIVAR-LOPEZ, S., GARRIDO, J. J. & MONTOYA, M. 2021. SARS-CoV-2 Accessory Proteins in Viral Pathogenesis: Knowns and Unknowns. *Front Immunol,* 12**,** 708264.

REN, Y., SHU, T., WU, D., MU, J., WANG, C., HUANG, M., HAN, Y., ZHANG, X. Y., ZHOU, W., QIU, Y. & ZHOU, X. 2020. The ORF3a protein of SARS-CoV-2 induces apoptosis in cells. *Cell Mol Immunol,* 17**,** 881-883.

RICHARDSON, S., HIRSCH, J. S., NARASIMHAN, M., CRAWFORD, J. M., MCGINN, T., DAVIDSON, K. W., THE NORTHWELL, C.-R. C., BARNABY, D. P., BECKER, L. B., CHELICO, J. D., COHEN, S. L., COOKINGHAM, J., COPPA, K., DIEFENBACH, M. A., DOMINELLO, A. J., DUER-HEFELE, J., FALZON, L., GITLIN, J., HAJIZADEH, N., HARVIN, T. G., HIRSCHWERK, D. A., KIM, E. J., KOZEL, Z. M., MARRAST, L. M., MOGAVERO, J. N., OSORIO, G. A., QIU, M. & ZANOS, T. P. 2020. Presenting Characteristics, Comorbidities, and Outcomes Among 5700 Patients Hospitalized With COVID-19 in the New York City Area. *JAMA,* 323**,** 2052-2059.

ROMANO, M., RUGGIERO, A., SQUEGLIA, F., MAGA, G. & BERISIO, R. 2020. A Structural View of SARS-CoV-2 RNA Replication Machinery: RNA Synthesis, Proofreading and Final Capping. *Cells,* 9.

ROSSMAN, H., SHILO, S., MEIR, T., GORFINE, M., SHALIT, U. & SEGAL, E. 2021. COVID-19 dynamics after a national immunization program in Israel. *Nat Med,* 27**,** 1055-1061.

ROY, V., FISCHINGER, S., ATYEO, C., SLEIN, M., LOOS, C., BALAZS, A., LUEDEMANN, C., ASTUDILLO, M. G., YANG, D., WESEMANN, D. R., CHARLES, R., LAFRATE, A. J., FELDMAN, J., HAUSER, B., CARADONNA, T., MILLER, T. E., MURALI, M. R., BADEN, L., NILLES, E., RYAN, E., LAUFFENBURGER, D., BELTRAN, W. G. & ALTER, G. 2020. SARS-CoV-2-specific ELISA development. *J Immunol Methods,* 484-485**,** 112832.

SAIF, L. J. 2010. Bovine respiratory coronavirus. *Vet Clin North Am Food Anim Pract,* 26**,** 349-64.

SAIF, L. J., VAN COTT, J. L. & BRIM, T. A. 1994. Immunity to transmissible gastroenteritis virus and porcine respiratory coronavirus infections in swine. *Veterinary Immunology and Immunopathology,* 43**,** 89-97.

SAMRAT, S. K., THARAPPEL, A. M., LI, Z. & LI, H. 2020. Prospect of SARS-CoV-2 spike protein: Potential role in vaccine and therapeutic development. *Virus Res,* 288**,** 198141.

SATARKER, S. & NAMPOOTHIRI, M. 2020. Structural Proteins in Severe Acute Respiratory Syndrome Coronavirus-2. *Arch Med Res,* 51**,** 482-491.

SAYAMPANATHAN, A. A., HENG, C. S., PIN, P. H., PANG, J., LEONG, T. Y. & LEE, V. J. 2021. Infectivity of asymptomatic versus symptomatic COVID-19. *The Lancet,* 397**,** 93-94.

SCHLOTTAU, K., RISSMANN, M., GRAAF, A., SCHÖN, J., SEHL, J., WYLEZICH, C., HÖPER, D., METTENLEITER, T. C., BALKEMA-BUSCHMANN, A., HARDER, T., GRUND, C., HOFFMANN, D., BREITHAUPT, A. & BEER, M. 2020. SARS-CoV-2 in fruit bats, ferrets, pigs, and chickens: an experimental transmission study. *The Lancet Microbe,* 1**,** e218-e225.

SCHOEMAN, D. & FIELDING, B. C. 2019. Coronavirus envelope protein: current knowledge. *Virol J,* 16**,** 69.

SCHONFELD, D., ARIAS, S., BOSSIO, J. C., FERNANDEZ, H., GOZAL, D. & PEREZ-CHADA, D. 2021. Clinical presentation and outcomes of the first patients with COVID-19 in Argentina: Results of 207079 cases from a national database. *PLoS One,* 16**,** e0246793.

SCHUBERT, K., KAROUSIS, E. D., JOMAA, A., SCAIOLA, A., ECHEVERRIA, B., GURZELER, L. A., LEIBUNDGUT, M., THIEL, V., MUHLEMANN, O. & BAN, N. 2020. SARS-CoV-2 Nsp1 binds the ribosomal mRNA channel to inhibit translation. *Nat Struct Mol Biol,* 27**,** 959-966.

SHAH, A. S. V., GRIBBEN, C., BISHOP, J., HANLON, P., CALDWELL, D., WOOD, R., REID, M., MCMENAMIN, J., GOLDBERG, D., STOCKTON, D., HUTCHINSON, S., ROBERTSON, C., MCKEIGUE, P. M., COLHOUN, H. M. & MCALLISTER, D. A. 2021. Effect of Vaccination on Transmission of SARS-CoV-2. *N Engl J Med*.

SHEPLEY-MCTAGGART, A., SAGUM, C. A., OLIVA, I., RYBAKOVSKY, E., DIGUILIO, K., LIANG, J., BEDFORD, M. T., CASSEL, J., SUDOL, M., MULLIN, J. M. & HARTY, R. N. 2021. SARS-CoV-2 Envelope (E) protein interacts with PDZ-domain-2 of host tight junction protein ZO1. *PLoS One,* 16**,** e0251955.

SHI, C. S., QI, H. Y., BOULARAN, C., HUANG, N. N., ABU-ASAB, M., SHELHAMER, J. H. & KEHRL, J. H. 2014. SARS-coronavirus open reading frame-9b suppresses innate immunity by targeting mitochondria and the MAVS/TRAF3/TRAF6 signalosome. *J Immunol,* 193**,** 3080-9.

SHI, J., DENG, G., MA, S., ZENG, X., YIN, X., LI, M., ZHANG, B., CUI, P., CHEN, Y., YANG, H., WAN, X., LIU, L., CHEN, P., JIANG, Y., GUAN, Y., LIU, J., GU, W., HAN, S., SONG, Y., LIANG, L., QU, Z., HOU, Y., WANG, X., BAO, H., TIAN, G., LI, Y., JIANG, L., LI, C. & CHEN, H. 2018. Rapid Evolution of H7N9 Highly Pathogenic Viruses that Emerged in China in 2017. *Cell Host Microbe,* 24**,** 558-568 e7.

SHI, J., WEN, Z., ZHONG, G., YANG, H., WANG, C., HUANG, B., LIU, R., HE, X., SHUAI, L., SUN, Z., ZHAO, Y., LIU, P., LIANG, L., CUI, P., WANG, J., ZHANG, X., GUAN, Y., TAN, W., WU, G., CHEN, H. & BU, Z. 2020. Susceptibility of ferrets, cats, dogs, and other domesticated animals to SARS-coronavirus 2. *Science,* 368**,** 1016-1020.

SHI, Q., HU, Y., PENG, B., TANG, X. J., WANG, W., SU, K., LUO, C., WU, B., ZHANG, F., ZHANG, Y., ANDERSON, B., ZHONG, X. N., QIU, J. F., YANG, C. Y. & HUANG, A. L. 2021. Effective control of SARS-CoV-2 transmission in Wanzhou, China. *Nat Med,* 27**,** 86-93.

SIDDELL, S., WEGE, H. & TER MEULEN, V. 1982. The structure and replication of coronaviruses. *Curr Top Microbiol Immunol,* 99**,** 131-63.

SILVAS, J. A., VASQUEZ, D. M., PARK, J. G., CHIEM, K., ALLUE-GUARDIA, A., GARCIA-VILANOVA, A., PLATT, R. N., MIORIN, L., KEHRER, T., CUPIC, A., GONZALEZ-REICHE, A. S., BAKEL, H. V., GARCIA-

SASTRE, A., ANDERSON, T., TORRELLES, J. B., YE, C. & MARTINEZ-SOBRIDO, L. 2021. Contribution of SARS-CoV-2 Accessory Proteins to Viral Pathogenicity in K18 Human ACE2 Transgenic Mice. *J Virol,* 95**,** e0040221.

SIMMONS, G., ZMORA, P., GIERER, S., HEURICH, A. & POHLMANN, S. 2013. Proteolytic activation of the SARS-coronavirus spike protein: cutting enzymes at the cutting edge of antiviral research. *Antiviral Res,* 100**,** 605-14.

SNIJDER, E. J., LIMPENS, R., DE WILDE, A. H., DE JONG, A. W. M., ZEVENHOVEN-DOBBE, J. C., MAIER, H. J., FAAS, F., KOSTER, A. J. & BARCENA, M. 2020. A unifying structural and functional model of the coronavirus replication organelle: Tracking down RNA synthesis. *PLoS Biol,* 18**,** e3000715.

SOLA, I., ALMAZAN, F., ZUNIGA, S. & ENJUANES, L. 2015. Continuous and Discontinuous RNA Synthesis in Coronaviruses. *Annu Rev Virol,* 2**,** 265-88.

SPRATT, A. N., GALLAZZI, F., QUINN, T. P., LORSON, C. L., SONNERBORG, A. & SINGH, K. 2021. Coronavirus helicases: attractive and unique targets of antiviral drug-development and therapeutic patents. *Expert Opin Ther Pat,* 31**,** 339-350.

STOLTZ, M., SUNDSTROM, K. B., HIDMARK, A., TOLF, C., VENE, S., AHLM, C., LINDBERG, A. M., LUNDKVIST, A. & KLINGSTROM, J. 2011. A model system for in vitro studies of bank vole borne viruses. *PLoS One,* 6**,** e28992.

SU, S., WONG, G., SHI, W., LIU, J., LAI, A. C. K., ZHOU, J., LIU, W., BI, Y. & GAO, G. F. 2016. Epidemiology, Genetic Recombination, and Pathogenesis of Coronaviruses. *Trends Microbiol,* 24**,** 490-502.

SUBISSI, L., POSTHUMA, C. C., COLLET, A., ZEVENHOVEN-DOBBE, J. C., GORBALENYA, A. E., DECROLY, E., SNIJDER, E. J., CANARD, B. & IMBERT, I. 2014. One severe acute respiratory syndrome coronavirus protein complex integrates processive RNA polymerase and exonuclease activities. *Proc Natl Acad Sci U S A,* 111**,** E3900-9.

SUN, H., XIAO, Y., LIU, J., WANG, D., LI, F., WANG, C., LI, C., ZHU, J., SONG, J., SUN, H., JIANG, Z., LIU, L., ZHANG, X., WEI, K., HOU, D., PU, J., SUN, Y., TONG, Q., BI, Y., CHANG, K. C., LIU, S., GAO, G. F. & LIU, J. 2020a. Prevalent Eurasian avian-like H1N1 swine influenza virus with 2009 pandemic viral genes facilitating human infection. *Proc Natl Acad Sci U S A,* 117**,** 17204-17210.

SUN, S. H., CHEN, Q., GU, H. J., YANG, G., WANG, Y. X., HUANG, X. Y., LIU, S. S., ZHANG, N. N., LI, X. F., XIONG, R., GUO, Y., DENG, Y. Q., HUANG, W. J., LIU, Q., LIU, Q. M., SHEN, Y. L., ZHOU, Y., YANG, X., ZHAO, T. Y., FAN, C. F., ZHOU, Y. S., QIN, C. F. & WANG, Y. C. 2020b. A Mouse Model of SARS-CoV-2 Infection and Pathogenesis. *Cell Host Microbe,* 28**,** 124-133 e4.

TEKES, G. & THIEL, H. J. 2016. Feline Coronaviruses: Pathogenesis of Feline Infectious Peritonitis. *Adv Virus Res,* 96**,** 193-218.

TEMMAM, S., VONGPHAYLOTH, K., SALAZAR, E. B., MUNIER, S., BONOMI, M., RÉGNAULT, B., DOUANGBOUBPHA, B., KARAMI, Y., CHRETIEN, D., SANAMXAY, D., XAYAPHET, V., PAPHAPHANH, P., LACOSTE, V., SOMLOR, S., LAKEOMANY, K., PHOMMAVANH, N., PÉROT, P., DONATI, F., BIGOT, T., NILGES, M., REY, F., WERF, S. V. D., BREY, P. & ELOIT, M. 2021. Coronaviruses with a SARS-CoV-2-like receptor-binding domain allowing ACE2-mediated entry into human cells isolated from bats of Indochinese peninsula. *Research Square*.

TO, J., SURYA, W., FUNG, T. S., LI, Y., VERDIA-BAGUENA, C., QUERALT-MARTIN, M., AGUILELLA, V. M., LIU, D. X. & TORRES, J. 2017. Channel-Inactivating Mutations and Their Revertant Mutants in the Envelope Protein of Infectious Bronchitis Virus. *J Virol,* 91.

TONG, J. Y., WONG, A., ZHU, D., FASTENBERG, J. H. & THAM, T. 2020. The Prevalence of Olfactory and Gustatory Dysfunction in COVID-19 Patients: A Systematic Review and Meta-analysis. *Otolaryngol Head Neck Surg,* 163**,** 3-11.

TSOI, H., LI, L., CHEN, Z. S., LAU, K. F., TSUI, S. K. & CHAN, H. Y. 2014. The SARS-coronavirus membrane protein induces apoptosis via interfering with PDK1-PKB/Akt signalling. *Biochem J,* 464**,** 439-47.

TURONOVA, B., SIKORA, M., SCHURMANN, C., HAGEN, W. J. H., WELSCH, S., BLANC, F. E. C., VON BULOW, S., GECHT, M., BAGOLA, K., HORNER, C., VAN ZANDBERGEN, G., LANDRY, J., DE AZEVEDO, N. T. D., MOSALAGANTI, S., SCHWARZ, A., COVINO, R., MUHLEBACH, M. D., HUMMER, G., KRIJNSE LOCKER, J. & BECK, M. 2020. In situ structural analysis of SARS-CoV-2 spike reveals flexibility mediated by three hinges. *Science,* 370**,** 203-208.

References

TWOHIG, K. A., NYBERG, T., ZAIDI, A., THELWALL, S., SINNATHAMBY, M. A., ALIABADI, S., SEAMAN, S. R., HARRIS, R. J., HOPE, R., LOPEZ-BERNAL, J., GALLAGHER, E., CHARLETT, A., DE ANGELIS, D., PRESANIS, A. M., DABRERA, G., KOSHY, C., ASH, A., WISE, E., MOORE, N., MORI, M., CORTES, N., LYNCH, J., KIDD, S., FAIRLEY, D., CURRAN, T., MCKENNA, J., ADAMS, H., FRASER, C., GOLUBCHIK, T., BONSALL, D., HASSAN-IBRAHIM, M., MALONE, C., COGGER, B., WANTOCH, M., REYNOLDS, N., WARNE, B., MAKSIMOVIC, J., SPELLMAN, K., MCCLUGGAGE, K., JOHN, M., BEER, R., AFIFI, S., MORGAN, S., MARCHBANK, A., PRICE, A., KITCHEN, C., GULLIVER, H., MERRICK, I., SOUTHGATE, J., GUEST, M., MUNN, R., WORKMAN, T., CONNOR, T., FULLER, W., BRESNER, C., SNELL, L., PATEL, A., CHARALAMPOUS, T., NEBBIA, G., BATRA, R., EDGEWORTH, J., ROBSON, S., BECKETT, A., AANENSEN, D., UNDERWOOD, A., YEATS, C., ABUDAHAB, K., TAYLOR, B., MENEGAZZO, M., CLARK, G., SMITH, W., KHAKH, M., FLEMING, V., LISTER, M., HOWSON-WELLS, H., BERRY, L., BOSWELL, T., JOSEPH, A., WILLINGHAM, I., JONES, C., HOLMES, C., BIRD, P., HELMER, T., FALLON, K., TANG, J., RAVIPRAKASH, V., CAMPBELL, S., SHERIFF, N., BLAKEY, V., WILLIAMS, L.-A., LOOSE, M., HOLMES, N., MOORE, C., CARLILE, M., WRIGHT, V., SANG, F., DEBEBE, J., COLL, F., SIGNELL, A., BETANCOR, G., et al. 2021. Hospital admission and emergency care attendance risk for SARS-CoV-2 delta (B.1.617.2) compared with alpha (B.1.1.7) variants of concern: a cohort study. *The Lancet Infectious Diseases*.

UJIKE, M. & TAGUCHI, F. 2015. Incorporation of spike and membrane glycoproteins into coronavirus virions. *Viruses,* 7**,** 1700-25.

ULASLI, M., VERHEIJE, M. H., DE HAAN, C. A. & REGGIORI, F. 2010. Qualitative and quantitative ultrastructural analysis of the membrane rearrangements induced by coronavirus. *Cell Microbiol,* 12**,** 844-61.

V'KOVSKI, P., KRATZEL, A., STEINER, S., STALDER, H. & THIEL, V. 2021. Coronavirus biology and replication: implications for SARS-CoV-2. *Nat Rev Microbiol,* 19**,** 155-170.

VALESANO, A. L., RUMFELT, K. E., DIMCHEFF, D. E., BLAIR, C. N., FITZSIMMONS, W. J., PETRIE, J. G., MARTIN, E. T. & LAURING, A. S. 2021. Temporal dynamics of SARS-CoV-2 mutation accumulation within and across infected hosts. *PLoS Pathog,* 17**,** e1009499.

VAN DEN BROM, R., VAN ENGELEN, E., ROEST, H. I., VAN DER HOEK, W. & VELLEMA, P. 2015. Coxiella burnetii infections in sheep or goats: an opinionated review. *Vet Microbiol,* 181**,** 119-29.

VANDELLI, A., MONTI, M., MILANETTI, E., ARMAOS, A., RUPERT, J., ZACCO, E., BECHARA, E., DELLI PONTI, R. & TARTAGLIA, G. G. 2020. Structural analysis of SARS-CoV-2 genome and predictions of the human interactome. *Nucleic Acids Res,* 48**,** 11270-11283.

VEGA, S., LORENZO-REBENAQUE, L., MARIN, C., DOMINGO, R. & FARINAS, F. 2020. Tackling the Threat of Rabies Reintroduction in Europe. *Front Vet Sci,* 7**,** 613712.

VENKATAKRISHNAN, A. J., PAWLOWSKI, C., ZEMMOUR, D., HUGHES, T., ANAND, A., BERNER, G., KAYAL, N., PURANIK, A., CONRAD, I., BADE, S., BARVE, R., SINHA, P., O'HORO, J. C., BADLEY, A. D., HALAMKA, J. & SOUNDARARAJAN, V. 2021. Mapping each pre-existing condition's association to short-term and long-term COVID-19 complications. *NPJ Digit Med,* 4**,** 117.

VICTORA, P. C., CASTRO, P. M. C., GURZENDA, S., MEDEIROS, A. C., FRANCA, G. V. A. & BARROS, P. 2021. Estimating the early impact of vaccination against COVID-19 on deaths among elderly people in Brazil: Analyses of routinely-collected data on vaccine coverage and mortality. *EClinicalMedicine,* 38**,** 101036.

VLASOVA, A. N. & SAIF, L. J. 2021. Bovine Coronavirus and the Associated Diseases. *Front Vet Sci,* 8**,** 643220.

WAGNER, R., MEISSNER, J., GRABSKI, E., SUN, Y., VIETHS, S. & HILDT, E. 2021. Regulatory concepts to guide and promote the accelerated but safe clinical development and licensure of COVID-19 vaccines in Europe. *Allergy*.

WALLS, A. C., PARK, Y. J., TORTORICI, M. A., WALL, A., MCGUIRE, A. T. & VEESLER, D. 2020. Structure, Function, and Antigenicity of the SARS-CoV-2 Spike Glycoprotein. *Cell,* 181**,** 281-292 e6.

WANG, H. Y., LI, X. L., YAN, Z. R., SUN, X. P., HAN, J. & ZHANG, B. W. 2020a. Potential neurological symptoms of COVID-19. *Ther Adv Neurol Disord,* 13**,** 1756286420917830.

WANG, J., ZHENG, X. & CHEN, J. 2021. Clinical progression and outcomes of 260 patients with severe COVID-19: an observational study. *Sci Rep,* 11**,** 3166.

WANG, L., BYRUM, B. & ZHANG, Y. 2014. Porcine coronavirus HKU15 detected in 9 US states, 2014. *Emerg Infect Dis,* 20**,** 1594-5.

WANG, Q., LI, C., ZHANG, Q., WANG, T., LI, J., GUAN, W., YU, J., LIANG, M. & LI, D. 2010. Interactions of SARS coronavirus nucleocapsid protein with the host cell proteasome subunit p42. *Virol J,* 7**,** 99.

WANG, Q., ZHANG, Y., WU, L., NIU, S., SONG, C., ZHANG, Z., LU, G., QIAO, C., HU, Y., YUEN, K. Y., WANG, Q., ZHOU, H., YAN, J. & QI, J. 2020b. Structural and Functional Basis of SARS-CoV-2 Entry by Using Human ACE2. *Cell,* 181**,** 894-904 e9.

WANG, Y., LU, X., LI, Y., CHEN, H., CHEN, T., SU, N., HUANG, F., ZHOU, J., ZHANG, B., YAN, F. & WANG, J. 2020c. Clinical Course and Outcomes of 344 Intensive Care Patients with COVID-19. *Am J Respir Crit Care Med,* 201**,** 1430-1434.

WEISS, S. R. & LEIBOWITZ, J. L. 2011. Coronavirus pathogenesis. *Adv Virus Res,* 81**,** 85-164.

WERNIKE, K., AEBISCHER, A., MICHELITSCH, A., HOFFMANN, D., FREULING, C., BALKEMA-BUSCHMANN, A., GRAAF, A., MULLER, T., OSTERRIEDER, N., RISSMANN, M., RUBBENSTROTH, D., SCHON, J., SCHULZ, C., TRIMPERT, J., ULRICH, L., VOLZ, A., METTENLEITER, T. & BEER, M. 2021. Multi-species ELISA for the detection of antibodies against SARS-CoV-2 in animals. *Transbound Emerg Dis,* 68**,** 1779-1785.

WHO, W. H. O. 2020a. Modes of transmission of virus causing COVID-19: implications for IPC precaution recommendations.

WHO, W. H. O. 2020b. *Naming the coronavirus disease (COVID-19) and the virus that causes it* [Online]. Available: https://www.who.int/emergencies/diseases/novel-coronavirus-2019/technical-guidance/naming-the-coronavirus-disease-(covid-2019)-and-the-virus-that-causes-it [Accessed 01.10.2021].

WHO, W. H. O. 2020c. Report of the WHO-China Joint Mission on Coronavirus Disease 2019 (COVID-19).

WHO, W. H. O. 2020d. *Transmission of SARS-CoV-2: implications for infection prevention precautions* [Online]. Available: https://www.who.int/news-room/commentaries/detail/transmission-of-sars-cov-2-implications-for-infection-prevention-precautions [Accessed 01.10.2021].

WHO, W. H. O. 2020e. *WHO Director-General's opening remarks at the media briefing on COVID-19 - 11 March 2020* [Online]. Available: https://www.who.int/director-general/speeches/detail/who-director-general-s-opening-remarks-at-the-media-briefing-on-covid-19---11-march-2020 [Accessed 01.10.2021].

WHO, W. H. O. 2021a. *Considerations for implementing and adjusting public health and social measures in the context of COVID-19: Interim guidance* [Online]. Available: https://apps.who.int/iris/handle/10665/341811 [Accessed 01.10.2021].

WHO, W. H. O. 2021b. *Tracking SARS-CoV-2 variants* [Online]. Available: https://www.who.int/en/activities/tracking-SARS-CoV-2-variants/ [Accessed 01.10.2021].

WHO, W. H. O. 2021c. *WHO announces simple, easy-to-say labels for SARS-CoV-2 Variants of Interest and Concern* [Online]. Available: https://www.who.int/news/item/31-05-2021-who-announces-simple-easy-to-say-labels-for-sars-cov-2-variants-of-interest-and-concern [Accessed 01.10.2021].

WIBMER, C. K., AYRES, F., HERMANUS, T., MADZIVHANDILA, M., KGAGUDI, P., OOSTHUYSEN, B., LAMBSON, B. E., DE OLIVEIRA, T., VERMEULEN, M., VAN DER BERG, K., ROSSOUW, T., BOSWELL, M., UECKERMANN, V., MEIRING, S., VON GOTTBERG, A., COHEN, C., MORRIS, L., BHIMAN, J. N. & MOORE, P. L. 2021. SARS-CoV-2 501Y.V2 escapes neutralization by South African COVID-19 donor plasma. *Nat Med,* 27**,** 622-625.

WILMES, P., ZIMMER, J., SCHULZ, J., GLOD, F., VEIBER, L., MOMBAERTS, L., RODRIGUES, B., AALTO, A., PASTORE, J., SNOECK, C. J., OLLERT, M., FAGHERAZZI, G., MOSSONG, J., GONCALVES, J., SKUPIN, A. & NEHRBASS, U. 2021. SARS-CoV-2 transmission risk from asymptomatic carriers: Results from a mass screening programme in Luxembourg. *Lancet Reg Health Eur,* 4**,** 100056.

WINKLER, E. S., BAILEY, A. L., KAFAI, N. M., NAIR, S., MCCUNE, B. T., YU, J., FOX, J. M., CHEN, R. E., EARNEST, J. T., KEELER, S. P., RITTER, J. H., KANG, L. I., DORT, S., ROBICHAUD, A., HEAD, R.,

HOLTZMAN, M. J. & DIAMOND, M. S. 2020. SARS-CoV-2 infection of human ACE2-transgenic mice causes severe lung inflammation and impaired function. *Nat Immunol,* 21**,** 1327-1335.

WOLFF, G., LIMPENS, R., ZEVENHOVEN-DOBBE, J. C., LAUGKS, U., ZHENG, S., DE JONG, A. W. M., KONING, R. I., AGARD, D. A., GRUNEWALD, K., KOSTER, A. J., SNIJDER, E. J. & BARCENA, M. 2020a. A molecular pore spans the double membrane of the coronavirus replication organelle. *Science,* 369**,** 1395-1398.

WOLFF, G., MELIA, C. E., SNIJDER, E. J. & BARCENA, M. 2020b. Double-Membrane Vesicles as Platforms for Viral Replication. *Trends Microbiol,* 28**,** 1022-1033.

WOLLENSTEIN-BETECH, S., CASSANDRAS, C. G. & PASCHALIDIS, I. C. 2020. Personalized predictive models for symptomatic COVID-19 patients using basic preconditions: Hospitalizations, mortality, and the need for an ICU or ventilator. *Int J Med Inform,* 142**,** 104258.

WOLLINA, U., KARADAG, A. S., ROWLAND-PAYNE, C., CHIRIAC, A. & LOTTI, T. 2020. Cutaneous signs in COVID-19 patients: A review. *Dermatol Ther,* 33**,** e13549.

WONG, A. C. P., LI, X., LAU, S. K. P. & WOO, P. C. Y. 2019. Global Epidemiology of Bat Coronaviruses. *Viruses,* 11.

WONG, C. H., NGAN, C. Y., GOLDFEDER, R. L., IDOL, J., KUHLBERG, C., MAURYA, R., KELLY, K., OMERZA, G., RENZETTE, N., DE ABREU, F., LI, L., BROWNE, F. A., LIU, E. T. & WEI, C.-L. 2021. Reduced subgenomic RNA expression is a molecular indicator of asymptomatic SARS-CoV-2 infection. *Communications Medicine,* 1.

WONG, H. H., FUNG, T. S., FANG, S., HUANG, M., LE, M. T. & LIU, D. X. 2018. Accessory proteins 8b and 8ab of severe acute respiratory syndrome coronavirus suppress the interferon signaling pathway by mediating ubiquitin-dependent rapid degradation of interferon regulatory factor 3. *Virology,* 515**,** 165-175.

WONGTANGMAN, K., SANTER, P., WACHTENDORF, L. J., AZIMARAGHI, O., BAEDORF KASSIS, E., TEJA, B., MURUGAPPAN, K. R., SIDDIQUI, S., EIKERMANN, M. & GROUP, S. O. M. T. 2021. Association of Sedation, Coma, and In-Hospital Mortality in Mechanically Ventilated Patients With Coronavirus Disease 2019-Related Acute Respiratory Distress Syndrome: A Retrospective Cohort Study. *Crit Care Med,* 49**,** 1524-1534.

WOO, P. C., LAU, S. K., LAM, C. S., LAU, C. C., TSANG, A. K., LAU, J. H., BAI, R., TENG, J. L., TSANG, C. C., WANG, M., ZHENG, B. J., CHAN, K. H. & YUEN, K. Y. 2012. Discovery of seven novel Mammalian and avian coronaviruses in the genus deltacoronavirus supports bat coronaviruses as the gene source of alphacoronavirus and betacoronavirus and avian coronaviruses as the gene source of gammacoronavirus and deltacoronavirus. *J Virol,* 86**,** 3995-4008.

WOOLHOUSE, M. & GAUNT, E. 2007. Ecological origins of novel human pathogens. *Crit Rev Microbiol,* 33**,** 231-42.

WOSTYN, P. 2021. COVID-19 and chronic fatigue syndrome: Is the worst yet to come? *Med Hypotheses,* 146**,** 110469.

WU, A., PENG, Y., HUANG, B., DING, X., WANG, X., NIU, P., MENG, J., ZHU, Z., ZHANG, Z., WANG, J., SHENG, J., QUAN, L., XIA, Z., TAN, W., CHENG, G. & JIANG, T. 2020a. Genome Composition and Divergence of the Novel Coronavirus (2019-nCoV) Originating in China. *Cell Host Microbe,* 27**,** 325-328.

WU, F., ZHAO, S., YU, B., CHEN, Y. M., WANG, W., SONG, Z. G., HU, Y., TAO, Z. W., TIAN, J. H., PEI, Y. Y., YUAN, M. L., ZHANG, Y. L., DAI, F. H., LIU, Y., WANG, Q. M., ZHENG, J. J., XU, L., HOLMES, E. C. & ZHANG, Y. Z. 2020b. A new coronavirus associated with human respiratory disease in China. *Nature,* 579**,** 265-269.

WUNSCH, H. 2020. Mechanical Ventilation in COVID-19: Interpreting the Current Epidemiology. *Am J Respir Crit Care Med,* 202**,** 1-4.

XIAO, X., NEWMAN, C., BUESCHING, C. D., MACDONALD, D. W. & ZHOU, Z. M. 2021. Animal sales from Wuhan wet markets immediately prior to the COVID-19 pandemic. *Sci Rep,* 11**,** 11898.

YADAV, R., CHAUDHARY, J. K., JAIN, N., CHAUDHARY, P. K., KHANRA, S., DHAMIJA, P., SHARMA, A., KUMAR, A. & HANDU, S. 2021. Role of Structural and Non-Structural Proteins and Therapeutic Targets of SARS-CoV-2 for COVID-19. *Cells,* 10.

YAN, X., HAO, Q., MU, Y., TIMANI, K. A., YE, L., ZHU, Y. & WU, J. 2006. Nucleocapsid protein of SARS-CoV activates the expression of cyclooxygenase-2 by binding directly to regulatory elements for nuclear factor-kappa B and CCAAT/enhancer binding protein. *Int J Biochem Cell Biol,* 38**,** 1417-28.

YANG, N. & SHEN, H. M. 2020. Targeting the Endocytic Pathway and Autophagy Process as a Novel Therapeutic Strategy in COVID-19. *Int J Biol Sci,* 16**,** 1724-1731.

YANG, W., KANDULA, S., HUYNH, M., GREENE, S. K., VAN WYE, G., LI, W., CHAN, H. T., MCGIBBON, E., YEUNG, A., OLSON, D., FINE, A. & SHAMAN, J. 2021. Estimating the infection-fatality risk of SARS-CoV-2 in New York City during the spring 2020 pandemic wave: a model-based analysis. *The Lancet Infectious Diseases,* 21**,** 203-212.

YANG, Y. & DU, L. 2021. SARS-CoV-2 spike protein: a key target for eliciting persistent neutralizing antibodies. *Signal Transduct Target Ther,* 6**,** 95.

YANG, Y., PENG, F., WANG, R., YANGE, M., GUAN, K., JIANG, T., XU, G., SUN, J. & CHANG, C. 2020. The deadly coronaviruses: The 2003 SARS pandemic and the 2020 novel coronavirus epidemic in China. *J Autoimmun,* 109**,** 102434.

YAO, H., SONG, Y., CHEN, Y., WU, N., XU, J., SUN, C., ZHANG, J., WENG, T., ZHANG, Z., WU, Z., CHENG, L., SHI, D., LU, X., LEI, J., CRISPIN, M., SHI, Y., LI, L. & LI, S. 2020. Molecular Architecture of the SARS-CoV-2 Virus. *Cell,* 183**,** 730-738 e13.

YASSINE, H. M., LEE, C. W. & SAIF, Y. M. 2013. Interspecies transmission of influenza a viruses between Swine and poultry. *Curr Top Microbiol Immunol,* 370**,** 227-40.

YE, Y. & HOGUE, B. G. 2007. Role of the coronavirus E viroporin protein transmembrane domain in virus assembly. *J Virol,* 81**,** 3597-607.

YE, Z. W., YUAN, S., YUEN, K. S., FUNG, S. Y., CHAN, C. P. & JIN, D. Y. 2020. Zoonotic origins of human coronaviruses. *Int J Biol Sci,* 16**,** 1686-1697.

YINDA, C. K., PORT, J. R., BUSHMAKER, T., OFFEI OWUSU, I., PURUSHOTHAM, J. N., AVANZATO, V. A., FISCHER, R. J., SCHULZ, J. E., HOLBROOK, M. G., HEBNER, M. J., ROSENKE, R., THOMAS, T., MARZI, A., BEST, S. M., DE WIT, E., SHAIA, C., VAN DOREMALEN, N. & MUNSTER, V. J. 2021. K18-hACE2 mice develop respiratory disease resembling severe COVID-19. *PLoS Pathog,* 17**,** e1009195.

YOSHIMOTO, F. K. 2020. The Proteins of Severe Acute Respiratory Syndrome Coronavirus-2 (SARS CoV-2 or n-COV19), the Cause of COVID-19. *Protein J,* 39**,** 198-216.

YOSHIMOTO, F. K. 2021. A Biochemical Perspective of the Nonstructural Proteins (NSPs) and the Spike Protein of SARS CoV-2. *Protein J,* 40**,** 260-295.

YUE, Y., NABAR, N. R., SHI, C. S., KAMENYEVA, O., XIAO, X., HWANG, I. Y., WANG, M. & KEHRL, J. H. 2018. SARS-Coronavirus Open Reading Frame-3a drives multimodal necrotic cell death. *Cell Death Dis,* 9**,** 904.

ZAKI, N. & MOHAMED, E. A. 2021. The estimations of the COVID-19 incubation period: A scoping reviews of the literature. *J Infect Public Health,* 14**,** 638-646.

ZANDI, M. & SOLTANI, S. 2021. Hemagglutinin-esterase cannot be considered as a candidate for designing drug against COVID-19. *Mol Divers,* 25**,** 1999-2000.

ZELLER, M., GANGAVARAPU, K., ANDERSON, C., SMITHER, A. R., VANCHIERE, J. A., ROSE, R., SNYDER, D. J., DUDAS, G., WATTS, A., MATTESON, N. L., ROBLES-SIKISAKA, R., MARSHALL, M., FEEHAN, A. K., SABINO-SANTOS, G., JR., BELL-KAREEM, A. R., HUGHES, L. D., ALKUZWENY, M., SNARSKI, P., GARCIA-DIAZ, J., SCOTT, R. S., MELNIK, L. I., KLITTING, R., MCGRAW, M., BELDA-FERRE, P., DEHOFF, P., SATHE, S., MAROTZ, C., GRUBAUGH, N., NOLAN, D. J., DROUIN, A. C., GENEMARAS, K. J., CHAO, K., TOPOL, S., SPENCER, E., NICHOLSON, L., AIGNER, S., YEO, G. W., FARNAES, L., HOBBS, C. A., LAURENT, L. C., KNIGHT, R., HODCROFT, E. B., KHAN, K., FUSCO, D. N., COOPER, V. S., LEMEY, P., GARDNER, L., LAMERS, S. L., KAMIL, J. P., GARRY, R. F., SUCHARD, M. A. & ANDERSEN, K. G. 2021. Emergence of an early SARS-CoV-2 epidemic in the United States. *medRxiv*.

ZENG, Y., YE, L., ZHU, S., ZHENG, H., ZHAO, P., CAI, W., SU, L., SHE, Y. & WU, Z. 2008. The nucleocapsid protein of SARS-associated coronavirus inhibits B23 phosphorylation. *Biochem Biophys Res Commun,* 369**,** 287-91.

References

ZHANG, H. & ZHANG, H. 2021. Entry, egress and vertical transmission of SARS-CoV-2. *J Mol Cell Biol,* 13**,** 168-174.

ZHANG, J., LAN, Y. & SANYAL, S. 2020a. Membrane heist: Coronavirus host membrane remodeling during replication. *Biochimie,* 179**,** 229-236.

ZHANG, Q., CHEN, C. Z., SWAROOP, M., XU, M., WANG, L., LEE, J., WANG, A. Q., PRADHAN, M., HAGEN, N., CHEN, L., SHEN, M., LUO, Z., XU, X., XU, Y., HUANG, W., ZHENG, W. & YE, Y. 2020b. Heparan sulfate assists SARS-CoV-2 in cell entry and can be targeted by approved drugs in vitro. *Cell Discov,* 6**,** 80.

ZHANG, Y. Z. & HOLMES, E. C. 2020. A Genomic Perspective on the Origin and Emergence of SARS-CoV-2. *Cell,* 181**,** 223-227.

ZHOU, H.-Y., CHENG, Y.-X., XU, L., LI, J.-Y., TAO, C.-Y., JI, C.-Y., HAN, N., YANG, R., LI, Y. & WU, A. 2021a. Genomic evidence for divergent co-infections of SARS-CoV-2 lineages. *bioRxiv*.

ZHOU, L., AYEH, S. K., CHIDAMBARAM, V. & KARAKOUSIS, P. C. 2021b. Modes of transmission of SARS-CoV-2 and evidence for preventive behavioral interventions. *BMC Infect Dis,* 21**,** 496.

ZHOU, P., YANG, X. L., WANG, X. G., HU, B., ZHANG, L., ZHANG, W., SI, H. R., ZHU, Y., LI, B., HUANG, C. L., CHEN, H. D., CHEN, J., LUO, Y., GUO, H., JIANG, R. D., LIU, M. Q., CHEN, Y., SHEN, X. R., WANG, X., ZHENG, X. S., ZHAO, K., CHEN, Q. J., DENG, F., LIU, L. L., YAN, B., ZHAN, F. X., WANG, Y. Y., XIAO, G. F. & SHI, Z. L. 2020. A pneumonia outbreak associated with a new coronavirus of probable bat origin. *Nature,* 579**,** 270-273.

ZHOU, Z., HUANG, C., ZHOU, Z., HUANG, Z., SU, L., KANG, S., CHEN, X., CHEN, Q., HE, S., RONG, X., XIAO, F., CHEN, J. & CHEN, S. 2021c. Structural insight reveals SARS-CoV-2 ORF7a as an immunomodulating factor for human CD14(+) monocytes. *iScience,* 24**,** 102187.

ZHU, N., ZHANG, D., WANG, W., LI, X., YANG, B., SONG, J., ZHAO, X., HUANG, B., SHI, W., LU, R., NIU, P., ZHAN, F., MA, X., WANG, D., XU, W., WU, G., GAO, G. F., TAN, W., CHINA NOVEL CORONAVIRUS, I. & RESEARCH, T. 2020. A Novel Coronavirus from Patients with Pneumonia in China, 2019. *N Engl J Med,* 382**,** 727-733.

CHAPTER VIII: APPENDIX

VIII. APPENDIX

1. LIST OF FIGURES

Figure 1: Virion structure of SARS-CoV-2.

Figure 2: SARS-CoV-2 genome organization and annotation of ORFs.

Figure 3: Illustration of the set of sub-genomic RNAs in a SARS-CoV-2 diagnostic sample and their frequency.

Figure 4: Overview of SARS-CoV-2 cellular entry, replication, and egress.

2. LEGAL PERMISSIONS

Figure 1: Permission for reuse was granted under license no. 5155561007410 from Copyright Clearance Center.

Figure 2: Permission for reuse was granted under license no. 5155830931333 from Copyright Clearance Center.

Figure 3: Reuse is licensed under the Creative Commons Attribution 4.0 International License

Figure 4: Permission for reuse was granted under license no. 5155561007410 from Copyright Clearance Center.

Review article: Permission for reuse by the author was granted under license no. 5158610889476 from Copyright Clearance Center.

Publication I & II: The Centers for Disease Control and Prevention, publisher of *Emerging Infectious Diseases*, are a U.S. governmental institution and content are in public domain. Reuse does not require permission.

Publication III: Springer Nature grants permission for reproduction to the author.

Publication IV: Reuse is licensed under a Creative Commons Attribution 4.0 International License (http://creativecommons.org/licenses/by/4.0/).

Publication V: Reuse is licensed under a Creative Commons Attribution 4.0 International License (http://creativecommons.org/licenses/by/4.0/).

3. LIST OF ABBREVIATIONS

Abs.	Absatz
ACE2	angiotensin - converting enzyme 2
BCoV	bovine coronavirus
CoV	coronavirus
COVID-19	coronavirus disease-2019
COX-2	cyclooxygenase-2
cq	quantification cycle
CT	computed tomography
D	aspartic acid
DMV	double membrane vesicle
doi	digital object identifier
E	envelope protein
ECMO	extracorporeal membrane oxygenation
e.g.	exempli gratia
ERGIC	ER-Golgi intermediate compartment
et al.	et alii / et aliae
FAO	Food and Agriculture Organization of the United Nations
G	glycine
HCoV	human coronavirus
ICTV	International Committee on Taxonomy of Viruses
K18	keratin 18 promoter
kb	kilobase
M	membrane glycoprotein
MERS-CoV	Middle East respiratory syndrome–related coronavirus
N	nucleocapsid protein
nsp	non-structural protein
NTD	N-terminal domain
OIE	Office international des epizooties
ORF	open reading frame
pH	potential hydrogenii

pp	polyprotein
RBD	receptor binding domain
(r)ER	(rough) endoplasmic reticulum
(m)RNA	(messenger) ribonucleic acid
RTC	replication–transcription complex
S	spike protein
S1	spike protein subunit 1
S2	spike protein subunit 2
SARS-CoV	Severe acute respiratory syndrome coronavirus
SARS-CoV-2	severe acute respiratory syndrome coronavirus 2
TMPRSS2	transmembrane protease serine subtype 2
UTR	untranslated region
VOC	variant of concern
VOI	variant of interest
WHO	World Health Organization

CHAPTER IX: ACKNOWLEDGMENTS

IX. ACKNOWLEDGMENTS